



5-2011

Fluorescent Receptors for Biomolecules

Chi-Linh Do-Thanh
cdothanh@utk.edu

Recommended Citation

Do-Thanh, Chi-Linh, "Fluorescent Receptors for Biomolecules." PhD diss., University of Tennessee, 2011.
https://trace.tennessee.edu/utk_graddiss/960

This Dissertation is brought to you for free and open access by the Graduate School at Trace: Tennessee Research and Creative Exchange. It has been accepted for inclusion in Doctoral Dissertations by an authorized administrator of Trace: Tennessee Research and Creative Exchange. For more information, please contact trace@utk.edu.

To the Graduate Council:

I am submitting herewith a dissertation written by Chi-Linh Do-Thanh entitled "Fluorescent Receptors for Biomolecules." I have examined the final electronic copy of this dissertation for form and content and recommend that it be accepted in partial fulfillment of the requirements for the degree of Doctor of Philosophy, with a major in Chemistry.

Michael D. Best, Major Professor

We have read this dissertation and recommend its acceptance:

Shawn R. Campagna, Bin Zhao, Gregory R. Armel

Accepted for the Council:

Dixie L. Thompson

Vice Provost and Dean of the Graduate School

(Original signatures are on file with official student records.)

Fluorescent Receptors for Biomolecules

A Dissertation Presented for
the Doctor of Philosophy
Degree
The University of Tennessee, Knoxville

Chi-Linh Do-Thanh
May 2011

Acknowledgements

I would first like to thank my parents for their continuing love, inspiration, and patience. Secondly, I would like to acknowledge my advisor Dr. Michael Best for being an excellent mentor throughout my time in graduate school. Your enthusiasm and knowledge helped me learn and accomplish more things about chemistry than I could possibly have imagined when I first entered this program. I also want to thank my committee members Dr. Shawn Campagna, Dr. Bin Zhao, and Dr. Gregory Armel for their guidance in writing this dissertation.

And of course, I would like to express my thanks to my labmates, past and present, from The Best Group, including Dr. Denghuang Gong, Dr. Matthew Smith, Erin Losey, Meng Rowland, Manpreet Cheema, Leah Cuthriell, Heidi Bostic, Paul Petersen, Ashdeep Kaur, Ritu Nandal, Andrew Bayer, Benjamin Smith, Sammy Eni-Eni, and Yilin Wang for being constant sources of motivation and entertainment throughout the years, whether intentional or unintentional. I wish you all the best in your future endeavors.

I would also like to thank Dr. Samson Francis from the Baker group for his help on molecular modeling, Vitali Coltuclu from the Kabalka group for his assistance with boron NMR spectra, and Dr. David C. Baker for occasional entertaining stories and helpful discussions on experimental setups and reversed-phase purifications. And finally, I want to acknowledge Heidi, Ashdeep, Ritu, Ben, and Dr. Baker for supporting the fact that not all left-handed people are evil.

Abstract

The development of synthetic receptors capable of high-affinity complexation of biologically relevant analytes in competitive solvent systems represents an ongoing challenge in molecular recognition. Anion recognition is particularly problematic, which is significant since numerous biological processes are regulated by anions, such as those resulting from phosphorylation. In this dissertation, we present the design and synthesis of a fluorescent sensor containing two cyclen groups that are preorganized to form a binding cleft for anion complexation. The receptor design includes a rigid acridine backbone, which is also exploited for fluorescence signal transduction. Furthermore, click chemistry is employed to facilitate receptor synthesis, and binding studies with various phosphorylated guest molecules are described.

Additionally, the development of boronic acid-based carbohydrate receptors is presented. Carbohydrates play important roles in a large number of biochemical processes such as signal transduction and cell surface recognition events. The receptors will be used to study carbohydrate binding through Förster resonance energy transfer (FRET) and surface enhanced Raman spectroscopy (SERS).

Another project involves the synthesis of aromatic compounds that can act as auxin herbicides. Auxins are plant hormones that play a major role in the regulation of plant growth and development. A modular synthetic strategy is employed to access a library of small molecules that will be tested for herbicidal activity on a variety of weeds.

Finally, the work on the design and synthesis of molecular building blocks to generate covalently-bonded ordered organic frameworks is discussed.

Table of Contents

| | |
|--|------------|
| Chapter 1: Introduction to Molecular Recognition | 1 |
| 1.1 Molecular Interactions | 1 |
| 1.2 Thermodynamics of Binding..... | 3 |
| 1.3 Cooperativity | 6 |
| 1.4 Preorganization and Complementarity | 8 |
| 1.5 Common Core Scaffolds | 9 |
| 1.6 Detection of Binding | 14 |
| 1.7 Characterization of Binding | 17 |
| Chapter 2: A Fluorescent Bis-Cyclen Tweezer Receptor for Inositol (1,4,5)- Trisphosphate Employing Click Chemistry for Convenient Synthesis | 22 |
| 2.1 Introduction..... | 22 |
| 2.2 Inositol (1,4,5)-Trisphosphate Guest Background..... | 23 |
| 2.3 Receptors for Inositol (1,4,5)-Trisphosphate..... | 24 |
| 2.4 Receptor Design | 26 |
| 2.5 Bis-Cyclen Tweezer Synthesis | 29 |
| 2.6 Guest Binding Studies | 31 |
| 2.7 Initial Receptor Design..... | 39 |
| 2.8 Alkyne Scaffold Synthesis | 42 |
| 2.9 Azide-Tagged Polyammonium Macrocycle Synthesis | 45 |
| 2.10 Experimental..... | 52 |
| Chapter 3: Design and Synthesis of Boronic Acid-Based Carbohydrate Receptors | 117 |
| 3.1 Introduction..... | 117 |
| 3.2 Boronic Acid-Based Receptors | 120 |
| 3.3 FRET-Based Detection..... | 123 |
| 3.4 Synthesis of Fluorophore-Tagged Boronic Acid Receptors | 125 |
| 3.5 SERS-Based Detection | 128 |
| 3.6 Synthesis of Thiol-Tagged Boronic Acid Receptor..... | 129 |
| 3.7 Experimental..... | 132 |
| Chapter 4: Evaluation of Novel Auxin Herbicides through the Synthesis and Screening of a Small Molecule Library..... | 152 |
| 4.1 Introduction..... | 152 |

| | |
|--|------------|
| 4.2 Synthesis of Aromatic Compounds..... | 155 |
| 4.3 Growth Control Testing..... | 157 |
| 4.4 Experimental..... | 159 |
| Chapter 5: Synthesis and Assembly of Geometrically Defined Building Blocks for Dynamic Covalent Synthesis of Robust Higher Order Organic Frameworks | 212 |
| 5.1 Introduction..... | 212 |
| 5.2 Assembly Strategy..... | 213 |
| 5.3 Synthesis of Building Blocks..... | 214 |
| 5.4 Experimental..... | 221 |
| List of References | 251 |
| Vita..... | 271 |

List of Figures

| | |
|--|-----|
| Figure 1.1. Receptors containing polyamine, calixarene, pyrrole, triazole, and triethylbenzene groups..... | 11 |
| Figure 1.2. Steroid-based host 1.6, zinc(II) complex 1.7, and boronic acid 1.8. | 13 |
| Figure 1.3. General design of a molecular sensor..... | 14 |
| Figure 1.4. Molecular sensors with signal transduction through PET, MLCT, and IDA. | 16 |
| Figure 1.5. Typical Job plot for a 1:1 host–guest complex. | 20 |
| Figure 2.1. Inositol (1,4,5)-trisphosphate (InsP ₃). | 23 |
| Figure 2.2. Examples of receptors for inositol 1,4,5-trisphosphate..... | 25 |
| Figure 2.3. Molecular model of tweezer receptor 2.5. | 27 |
| Figure 2.4. Plots exhibiting the decrease in emission of host 2.5 upon addition of guest 2.1..... | 32 |
| Figure 2.5. Binding curves for guests studied in titrations of host 2.5. | 33 |
| Figure 2.6. Structures of guests used for binding studies..... | 34 |
| Figure 2.7. Plots exhibiting the decrease in emission of host 2.16 upon addition of guest 2.1..... | 36 |
| Figure 2.8. Binding curves for guests studied in titrations of host 2.16. | 37 |
| Figure 2.9. Modular structure for anion-binding tweezer receptors. | 40 |
| Figure 3.1. Tetramethylrhodamine-boronic acid 3.3 and polyphenylboronic acid monolayer 3.4. | 122 |
| Figure 3.2. FRET-based assay for the detection of carbohydrate clustering on surfaces. | 124 |
| Figure 3.3. Phenylboronic acid-based receptors derivatized with FRET pairs. | 125 |
| Figure 4.1. Structures of natural and synthetic auxins..... | 152 |
| Figure 4.2. Commercial herbicides used as controls in testing auxin activities. | 154 |
| Figure 4.3. Growth control data for synthetic compounds and commercial herbicides. | 158 |

List of Schemes

| | |
|---|-----|
| Scheme 2.1. Design of tweezer receptor 2.5 and hypothetical binding complex with InsP_3 | 26 |
| Scheme 2.2. Synthetic route to bis-cyclen tweezer host 2.5. | 30 |
| Scheme 2.3. Hypothetical binding complex of receptor 2.16 with InsP_3 and synthesis of 2.16..... | 35 |
| Scheme 2.4. Preorganization of polyammonium macrocycles in tweezer structure. | 39 |
| Scheme 2.5. Late-stage scaffold–macrocycle linkage via azide–alkyne cycloaddition. | 41 |
| Scheme 2.6. Synthesis of alkyne scaffolds. | 42 |
| Scheme 2.7. Attempted cycloaddition between 2.19 and various azides. | 44 |
| Scheme 2.8. Synthetic approach to polyammonium macrocyclization step to produce azide-tagged polyamines such as heptaazamacrocycle 2.24. | 45 |
| Scheme 2.9. Synthetic route to triamine intermediate 2.32. | 46 |
| Scheme 2.10. Syntheses of <i>N</i> -nosylaziridine 2.33 and bis(mesylate) 2.36. | 48 |
| Scheme 2.11. Azide-tagged cyclen 2.43 and planned synthetic route towards macrocycle 2.24. | 50 |
| Scheme 2.12. Synthesis of azide-tagged cyclen 2.43. | 50 |
| Scheme 3.1. Equilibria involved in phenylboronate binding of a diol..... | 118 |
| Scheme 3.2. Equilibria for <i>ortho</i> -aminomethylphenylboronic acids. | 119 |
| Scheme 3.3. Binding between boronic acid 3.1 and glycoconjugates, and glucopyranoside structure 3.2..... | 121 |
| Scheme 3.4. Synthesis of NBD-tagged boronic acid 3.5..... | 126 |
| Scheme 3.5. Synthesis of rhodamine-tagged amine 3.12. | 126 |
| Scheme 3.6. Synthetic routes from amine 3.12 to rhodamine-tagged boronic acid 3.6. | 127 |
| Scheme 3.7. Synthesis of phenylboronic acid disulfide 3.13..... | 130 |
| Scheme 4.1. General synthetic route to aromatic acid targets. | 155 |
| Scheme 4.2. Synthesis of various aromatic acid targets. | 156 |
| Scheme 4.3. Additional aromatic acid and <i>N</i> -acetyl compounds..... | 157 |
| Scheme 5.1. Strategy for the assembly of ordered crystalline organic frameworks using DCC. | 213 |
| Scheme 5.2. Example of reversible imine formation between vertex and edge pieces. | 214 |

| | |
|---|-----|
| Scheme 5.3. General synthetic route to vertex structure 5.1..... | 214 |
| Scheme 5.4. Synthesis of <i>N</i> -protected ethynylanilines 5.6 and 5.9..... | 216 |
| Scheme 5.5. Synthetic approaches to tertiary alcohol building block 5.2..... | 218 |
| Scheme 5.6. Attempts of vertex and imine bond formations. | 219 |

Abbreviations

| | |
|---------------------------------|---|
| 1-NAA | 1-naphthalene acetic acid |
| 2,4-D | 2,4-dichlorophenoxyacetic acid |
| 4-Cl-IAA | 4-chloroindole-3-acetic acid |
| acac | acetylacetonate |
| AcCl | acetyl chloride |
| AcOH | acetic acid |
| AcSH | thiolacetic acid |
| ADP | adenosine diphosphate |
| ATP | adenosine triphosphate |
| Boc | <i>tert</i> -butoxycarbonyl |
| Boc ₂ O | di- <i>tert</i> -butyl dicarbonate |
| DCC | dynamic combinatorial chemistry |
| DCL | dynamic combinatorial library |
| DMF | <i>N,N</i> -dimethylformamide |
| DMSO | dimethyl sulfoxide |
| DNA | deoxyribonucleic acid |
| EDC | 1-(3-dimethylaminopropyl)-3-ethylcarbodiimide |
| Et ₃ N | triethylamine |
| EtOAc | ethyl acetate |
| EtOH | ethanol |
| FBP | fructose 1,6-bisphosphate |
| FRET | Förster resonance energy transfer |
| GPI | glycosylphosphatidylinositol |
| HOBt | 1-hydroxybenzotriazole |
| IAA | indole-3-acetic acid |
| IBA | indole-3-butyric acid |
| IDA | indicator–displacement assay |
| InsP ₃ | inositol 1,4,5-trisphosphate |
| InsP ₆ | inositol hexaphosphate; phytate |
| <i>i</i> -Pr ₂ NEt | <i>N,N</i> -diisopropylethylamine |
| ITC | isothermal titration calorimetry |
| MCPA | 2-methyl-4-chlorophenoxyacetic acid |
| Me ₂ CO ₃ | dimethyl carbonate |
| MeCN | acetonitrile |
| MeOH | methanol |
| MLCT | metal-to-ligand charge transfer |
| MOF | metal organic framework |
| Ms | methanesulfonyl |
| NADPH | nicotinamide adenine dinucleotide phosphate, reduced form |

| | |
|------------------|--|
| NBD | 7-nitrobenzofurazan |
| <i>n</i> -BuLi | <i>n</i> -butyllithium |
| NMR | nuclear magnetic resonance |
| Nos | 4-nitrobenzenesulfonyl |
| NPhth | <i>N</i> -phthaloyl |
| <i>n</i> -PrOH | <i>n</i> -propyl alcohol; 1-propanol |
| Ns | 2-nitrobenzenesulfonyl |
| PAA | phenylacetic acid |
| PET | photoinduced electron transfer |
| PH | pleckstrin homology |
| PhSH | thiophenol |
| PLC | phospholipase C |
| PMB | <i>para</i> -methoxybenzyl |
| PPh ₃ | triphenylphosphine |
| pyr | pyridine |
| RNA | ribonucleic acid |
| rt | room temperature |
| SAM | self-assembled monolayer |
| SERS | surface enhanced Raman spectroscopy |
| STABASE | 1,1,4,4-tetramethyldisilyl azacyclopentane |
| TBAF | tetrabutylammonium fluoride |
| TBS | <i>tert</i> -butyldimethylsilyl |
| <i>t</i> -BuLi | <i>tert</i> -butyllithium |
| TFA | trifluoroacetic acid |
| THF | tetrahydrofuran |
| TsOH | <i>para</i> -toluenesulfonic acid |

Chapter 1: Introduction to Molecular Recognition

Molecular recognition, the specific, non-covalent association between a host molecule and a particular guest, is present in nature at many different levels. Various biologically important processes involve specific interactions between a receptor and a substrate. As a result, chemists have pursued the design and synthesis of artificial receptor molecules for target guests in order to emulate the degree of selectivity and specificity from the biological world. Molecular recognition forms the basis of supramolecular chemistry, the chemistry of molecular systems beyond individual molecules, because the entire field of supramolecular chemistry is centered on how molecules are recognized and influenced and how specific functions occur due to molecular interactions.

1.1 Molecular Interactions

Molecular recognition involves the specific binding of a guest molecule to a complementary host through various non-covalent interactions. It is important to understand these binding forces in order to design a synthetic receptor that can selectively recognize its intended guest. A cooperative enhancement in binding can often be seen when several types of forces act together. Therefore, utilizing the right combination of interactions is crucial to an efficient molecular recognition system.

One type of attraction consists of electrostatic interactions that occur between charged molecules. Oppositely charged molecules attract due to charge–charge interactions. Electrostatic forces are relatively large in magnitude compared to other non-covalent interactions. Therefore, the contributions from these attractions in

molecular recognition systems cannot usually be ignored. The strength of electrostatic forces is inversely proportional to the dielectric constant of the surrounding medium. Thus, the interaction is stronger in a more hydrophobic environment with a smaller dielectric constant.

Hydrogen bonding can also have important roles in molecular recognition, even though the interaction is weaker than an electrostatic force. The hydrogen bonding between two functional groups is a crucial interaction in many cases because bonding only occurs when the interacting groups are in the correct orientation. For example, highly specific hydrogen bonding takes place between nucleobases that form base pairs in DNA strands. Hydrogen bonding is a dipole–dipole interaction involving positively polarized hydrogen atoms from donor groups such as amino and hydroxyl groups. A small, polarized hydrogen can interact with other electron-rich atoms in proximity, such as an oxygen from a carbonyl group or a nitrogen from a nitrile group. This results in a relatively strong hydrogen bond in which two functional groups specifically interact with one hydrogen atom.

Another type of attractive force is coordinate bonding between metal ions and electron-rich atoms. In this case, a metal can either be a binding site as part of the host, or it can be the guest analyte. For successful work, it is essential to understand the properties of the metal ion used, such as ionization state, coordination geometry, and ligand affinities. Transition metal cations can also be involved in cation– π interactions by forming complexes with alkenes or aromatic hydrocarbons. The energies of these forces can be of the same order of magnitude as hydrogen bonds.¹

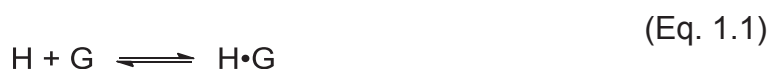
Aromatic groups also interact via π - π stacking, often when one group is relatively electron-rich and the other is electron-poor. Their π -electron orbitals overlap as the aromatic rings interact via either face-to-face or edge-to-face geometries. This is observed in the double helix structure of DNA, part of which is stabilized by π - π stacking between the aromatic rings of the base pairs. And finally, hydrophobic effects play important roles in aqueous solutions. Non-polar, hydrophobic molecules tend to aggregate in aqueous media, as seen in the formation of micelles and cell membranes from lipids.

When using the aforementioned binding interactions to design a host molecule that selectively targets a guest analyte, it is important to consider the polarity of the solvent. The magnitude of the binding forces between species in solution can heavily depend on the solvent. Highly polar solvents such as water and methanol compete effectively for hydrogen bonding sites, decreasing the hydrogen bond affinities between host and guest. This is accompanied by an increased hydrophobic effect that causes non-polar molecules to aggregate in solution due to repulsions with the polar solvent. Additionally, the pH of the solution needs to be taken into account. Functional groups can have different charges and protonation states, depending on the acidity of the solution. Therefore, it is essential to control the pH so that these groups are properly charged or protonated for successful binding.

1.2 Thermodynamics of Binding

The affinity of a host for a particular guest can be assessed by its binding constant K , which is also known as the association constant K_a . The constant itself is

dimensionless but is often calculated using concentrations and therefore has units of inverse concentration. In biological systems, it is common to use the dissociation constant K_d , which is the reciprocal of the association constant. The K_d value can be useful in drug design because it measures the concentration below which a drug–receptor complex will dissociate. The binding equilibrium between a host (H) and a guest (G) to form the complex (H•G) can be expressed using K_a , K_d , and the Gibbs free energy (ΔG°) in the following equations:



$$K_a = \frac{[H \cdot G]}{[H][G]} \quad (\text{Eq. 1.2})$$

$$K_d = \frac{[H][G]}{[H \cdot G]} \quad (\text{Eq. 1.3})$$

$$\Delta G^\circ = -RT \ln(K_a) \quad (\text{Eq. 1.4})$$

Even though the solvent can have a profound effect on the magnitude of the binding forces, it is not explicitly written as part of these equations. This is because ΔG° indicates the stability of solvated host and guest molecules relative to the solvated host–guest complex and released solvent.

There are three major challenges in host design. First, strong binding needs to be achieved in a competitive solvent such as an aqueous solution, where the solvent can out-compete non-covalent host–guest interactions. Second, an easily detectable signaling mechanism is required to observe the binding event. Furthermore, it is necessary to accomplish selectivity by differentiating between different guests.

Hemoglobin, the iron heme transport protein in blood, can selectively take up oxygen in the presence of nitrogen, water, and carbon dioxide, all of which typically bind strongly to iron. Using thermodynamic terms, selectivity is the ratio of the binding constant for one guest over another:

$$\text{Selectivity} = \frac{K_{\text{Guest1}}}{K_{\text{Guest2}}} \quad (\text{Eq. 1.5})$$

However, a distinction should be made between guest selectivity and inter-guest discrimination. Thermodynamic selectivity involves the magnitudes of binding constants while discrimination relates to other observed results from often highly specific host–guest interactions. For example, in molecular recognition systems using colorimetric or fluorescence changes, the guest analyte that is bound most strongly is not necessarily the one that exhibits the largest change in color or emission intensity. Instead of being directly proportional to binding affinity, changes in light absorption and emission may come from a particular host–guest interaction. Consequently, a host may be able to discriminate between two different guests by showing different intensity changes even if their binding constants are close in value.²

When examining recognition events over a variety of conditions, it is often observed that as binding becomes more enthalpically favorable, it gets more entropically unfavorable. As the binding interactions become stronger, favoring the enthalpic component of the Gibbs free energy. At the same time, the host binds to the guest more tightly, thereby restricting movement of both molecules. As a result, entropy becomes less favorable. It is important to consider this “enthalpy–entropy compensation” when designing stronger receptors. Isothermal titration calorimetry (ITC)

is a technique that can directly measure the thermodynamic parameters of interactions in solution. Studies have been done in molecular recognition systems containing cyclodextrins,³ cyclophanes,⁴ and guanidiniums⁵ to determine the contributions of enthalpy and entropy to the stability of host–guest complexes.

1.3 Cooperativity

A large part in the construction of supramolecular host molecules involves forming multiple interactions in a molecular recognition event. It is possible to build a stable host–guest complex using weaker non-covalent interactions if the number of these interactions is maximized. Combined binding forces can lead to significant affinity between two molecules. When added to all the small stabilizations from the other interactions, the small amount of stabilizing energy gained by one interaction results in substantial binding energy and complex stability. In some cases, the interaction of the system is greater than the sum of the parts. When two or more binding sites on a host cooperate in this way to bind a guest, the interaction is called cooperativity. Positive cooperativity occurs when the Gibbs free energy of binding is more negative than the sum of all the Gibbs free energy changes for each individual binding interaction. Negative cooperativity arises when the Gibbs free energy of binding is more positive than the sum of the individual parts.¹

The cooperativity from the interaction of a two-binding-site guest (A–B) with a host can be expressed in terms of the overall Gibbs free energy of binding (ΔG_{AB}°), which is equal to the sum of the intrinsic binding free energies of each component A and B (ΔG_A^i and ΔG_B^i) plus a factor known as the connection Gibbs free energy (ΔG^S) (Eq.

1.6). The connection Gibbs free energy is the extent to which the binding of guest A–B differs from the sum of the individual interactions of A and B.

$$\Delta G_{AB}^{\circ} = \Delta G_A^i + \Delta G_B^i + \Delta G^S \quad (\text{Eq. 1.6})$$

$$\Delta G_A^i = \Delta G_{AB}^{\circ} - \Delta G_B^{\circ} \quad (\text{Eq. 1.7})$$

$$\Delta G_B^i = \Delta G_{AB}^{\circ} - \Delta G_A^{\circ} \quad (\text{Eq. 1.8})$$

$$\Delta G^S = \Delta G_A^{\circ} + \Delta G_B^{\circ} - \Delta G_{AB}^{\circ} \quad (\text{Eq. 1.9})$$

The intrinsic binding energy represents the energy group A or B imparts to the binding of the rest of the molecule if no differences in strain or entropy result from the interaction of the group with the host (Eq. 1.7 and 1.8). Substituting these expressions into Eq. 1.6 shows that the connection Gibbs free energy is equal to the sum of the separate affinities of isolated parts A and B minus the binding free energy of A–B (Eq. 1.9).

Since the equilibrium constants (K) for the binding of A, B, and A–B by a host can be determined and related to the Gibbs free energy according to $\Delta G^{\circ} = -RT \ln K$, Eq. 1.9 can be used to give an empirical measure of the cooperativity. If ΔG^S is positive, then the binding sites A and B display favorable positive cooperativity. A negative ΔG^S value implies unfavorable negative cooperativity.

One of the best known examples of cooperativity in biology is the allosteric oxygenation of hemoglobin.⁶ This protein binds four individual oxygen molecules with increasing affinity until all four of its binding sites are occupied. Another form of cooperativity is called multivalency, which is the simultaneous binding of multiple ligands on one entity to multiple receptors on another.⁷ These multivalent binding

interactions tend to be much stronger than the analogous monovalent ones and are known to occur throughout biological systems. For example, the influenza virus attaches to the surface of a bronchial epithelial cell through interactions between multiple trimers of hemagglutinin, a lectin that is densely packed on the surface of the virus, and multiple units of sialic acid, a sugar that is arranged densely on the surface of the target cell.⁸

1.4 Preorganization and Complementarity

Many host–guest complexes are more stable than expected from the effects of functional groups on the hosts alone. For example, Fischer’s lock and key concept⁹ described that the guest has a geometric shape that complements the host, as seen in receptor–substrate binding by enzymes. Various hosts are large ring-shaped ligands that chelate their guests using multiple binding moieties. This macrocyclic effect provides additional stabilization to the complex due to not only the presence of numerous binding sites, but also the preorganization of those sites in space. As a result, host–guest interactions can take place without undergoing high energy conformational changes. Moreover, the enthalpic costs involved in bringing lone electron pairs from donor atoms closer to each other have been “paid in advance” during the synthesis of the macrocyclic host.

Preorganization of the host is a crucial concept because it signifies a major enhancement to the overall free energy of host–guest complexation. The principle of preorganization states that —the more highly hosts and guests are organized for binding and low solvation prior to their complexation, the more stable will be their complexes.”¹⁰

Disregarding solvent effects, the binding process between a receptor and its target can be loosely divided into two parts. First, the host adjusts to arrange its binding functionalities to fit the guest while simultaneously minimizing unfavorable repulsions between one binding site and another. This is an energetically disfavored step, and the receptor must maintain its binding conformation throughout the lifetime of the host–guest complex. Then, the binding event that follows is energetically favored due to the mutual attraction between complementary binding sites of receptor and target. The overall free energy of complexation corresponds to the difference between the unfavorable rearrangement energy and the favorable binding energy. As a result, a preorganized host requires only a small amount of energy to reorganize, leading to an increase in overall free energy, which stabilizes the complex.

Even though it is desirable to design a receptor with preorganized binding sites for ideal affinities, it may not always be advantageous. For example, if the optimal binding conformation of the host is not reached, then the system’s rigidity could actually hinder the ability of the host to bind to the guest. Therefore, it may be beneficial to have flexible systems that follow the induced fit model¹¹ by allowing the receptor and target to move more freely into the proper binding geometry. The amount of flexibility versus rigidity required for ideal binding would depend on each individual system.

1.5 Common Core Scaffolds

Supramolecular hosts for all types of guests come in a wide variety of designs. There are numerous common frameworks that provide particular preorganized binding functionalities on host compounds. One such type is a class of cyclic hosts called the

macrocyclic polyamines. They are structural analogs of crown ethers, with the oxygen atoms in the ethers being replaced by nitrogens. The presence of amine groups in these molecules results in unique host properties. The amine can act as a hydrogen bond donor or a positively charged binding site when protonated. Furthermore, amine moieties exist in the recognition processes of many anionic species by biological substrates. For example, X-ray crystal structures of proteins with bound phosphates revealed that glycine residues allow a loop of amino acids to wrap around the bound phosphate in a near-macrocyclic conformation to hydrogen bond with backbone NH amino acidic residues.¹²

Following nature, protonated forms of synthetic polyamine macrocycles have been shown to wrap around anions based on their ring size and adapt to the stereochemical requirements of the guests to form optimize hydrogen bonding. One example is the cyclic hexaamine **1.1** (Figure 1.1) which, along with *N*-methylated and larger ring size analogs, has been studied for its capability of binding inorganic phosphate-type anions.¹³ Receptor **1.1** was found to bind phosphate or sulfate selectively, depending on the pH of the solution. Sulfate was selectively bound in the presence of phosphate in alkaline solutions (pH > 8.5) while an inversion in selectivity took place in more acidic solutions (pH < 7.0). As a result, selective recognition of phosphate over sulfate occurs with increased protonation states of phosphate, mimicking the actions of phosphate binding proteins in nature.¹⁴

Another type of host frameworks consists of the calixarenes.¹⁵ These macrocycles are prepared by linking several *para*-substituted phenol residues through

methylene moieties. Calixarenes with different cavity sizes have been designed, and their phenolic hydroxyl groups have often been modified. They can also exist as conformational isomers in which the phenol groups point in the same or opposite direction.

Calix[4]arene derivative **1.2** was developed, which contains an amide-linked disulfonoanthracene group.¹⁶ This molecule displayed significant affinity and selectivity for the dihydrogen phosphate anion. Fluorescence enhancement was used to signal the binding event, and a 1:2 host to guest stoichiometry for the complex was determined. The same authors also prepared a related calix[4]arene that was selective for acetate.¹⁷

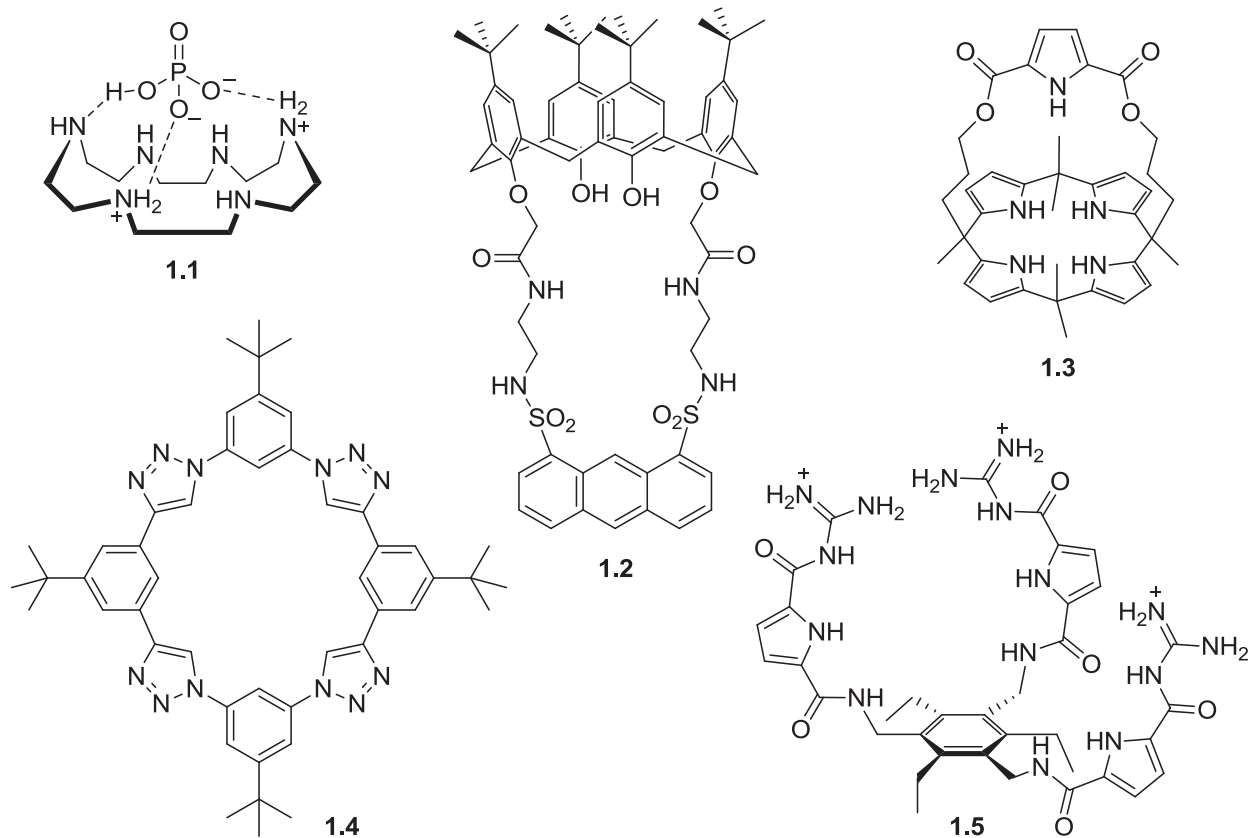


Figure 1.1. Receptors containing polyamine, calixarene, pyrrole, triazole, and triethylbenzene groups.

Pyrrole-based structures are also commonly used as a receptor platform.¹⁸ The pyrrole units contain NH hydrogen bond donor groups and no hydrogen bond acceptors, as opposed to other amine groups that are both hydrogen bond donors and acceptors. Therefore, intramolecular hydrogen bonding, which may occur in amide or urea groups, can be avoided. One example is the strapped calix[4]pyrrole system **1.3**, which binds to chloride anion.¹⁹ It was used to determine chloride concentrations in deuterated dimethylsulfoxide (DMSO- d_6)/water mixtures via ^1H NMR spectroscopy.²⁰ Furthermore, the calix[4]pyrrole core structure has been shown to extract cesium bromide and chloride salts from an aqueous environment into nitrobenzene.²¹

There are also hosts containing 1,2,3-triazole moieties that have recently been reported. They bind guest species by using only hydrogen bonding interactions between neutral CH groups and the anion target. The affinity of receptor **1.4** to chloride was studied through ^1H NMR and UV-vis spectroscopy.²² A 1:1 binding stoichiometry was found, and other derivatives were examined to compare hydrogen bonding strengths by CH groups.²³

Another class of scaffolds is the 1,3,5-tris-functionalized 2,4,6-triethylbenzene core.²⁴ In this system, the ethyl groups alternate with the binding functional groups on the benzene ring. This allows the three binding moieties to exist primarily on the same face of the ring, forming a binding cavity. One example is host **1.5**, which binds citrate and other tricarboxylates with association constants (K_a) above 10^5 M^{-1} in water.²⁵ Binding is strong enough that the complex stability is only marginally affected by the presence of a large excess amount of competing anions or buffer salts.

Steroids represent another series of receptor structures, using binding functionalities based on the cholesterol backbone made from bile acids such as cholic acid.²⁶ The scaffold is very rigid and stereochemically well-defined, resulting in highly asymmetrical but uniquely designed receptors that can potentially differentiate between enantiomeric guests. Cholapod **1.6** (Figure 1.2) features a long hydrocarbon tail for solubility in organic solvents and binds chloride anion in chloroform with a binding constant (K_a) above 10^{11} M^{-1} .²⁷ This demonstrates a near ideal combination of hydrogen bonding sites that are preorganized in a relatively uncompetitive solvent.

Finally, receptor scaffolds can contain cationic metal centers as Lewis acidic binding sites. Since water is a relatively poor Lewis base, it is less likely to interfere with systems that rely on anion coordination to Lewis acidic metal cations.²⁸ The most

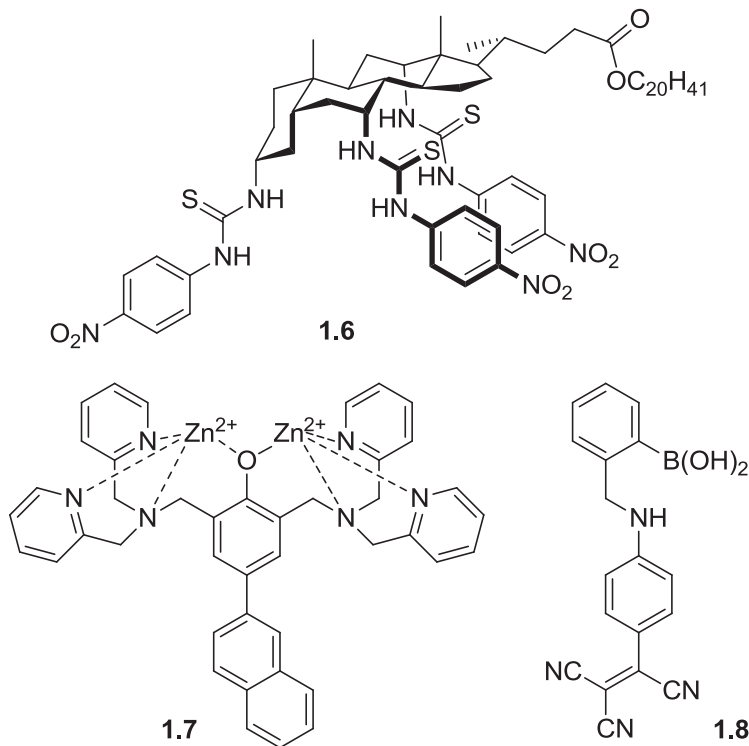


Figure 1.2. Steroid-based host **1.6**, zinc(II) complex **1.7**, and boronic acid **1.8**.

commonly used metals in this type of hosts are copper(II) and zinc(II). A very recent study used binuclear zinc(II) complex **1.7** and boronic acid **1.8** to distinguish between pyrophosphate and nucleoside triphosphates.²⁹ In a mixture of **1.7** and **1.8**, a fluorescence enhancement is only observed with pyrophosphate. This is due to the boronic acid binding to the ribose diol group in the nucleoside, thereby quenching the fluorescence signal. Additionally, this sensing system was used for the direct quantification of RNA polymerase activity.

1.6 Detection of Binding

One of the major areas of application for synthetic receptors is in molecular sensor devices. These compounds can perform both molecular recognition and detection of binding. The basic concept of a molecular sensor (Figure 1.3) is as follows: The target analyte is attracted to the receptor part of the sensor, which can be any of the host systems previously discussed. Binding should be selective for the guest in the presence of other potential substrates. The receptor also needs to be connected to a signaling moiety that responds to the binding event.³⁰ The generated signal can be a form of an emission of electromagnetic radiation, an electric current, or an externally

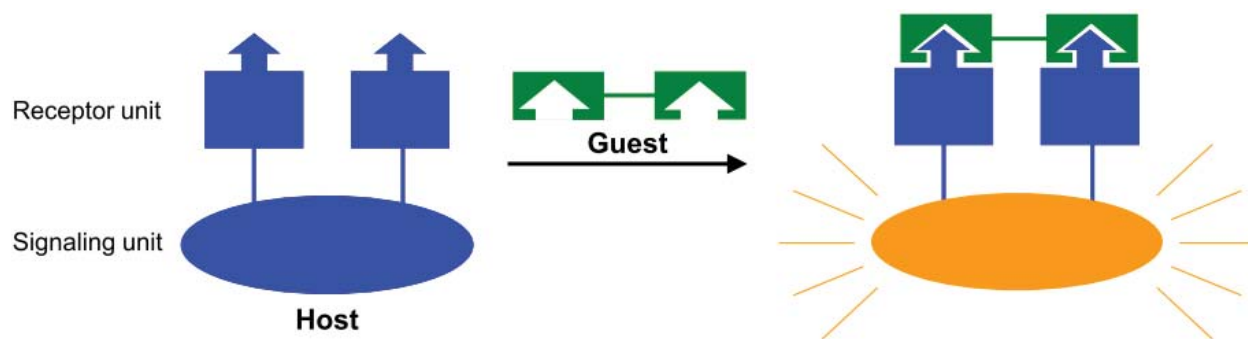


Figure 1.3. General design of a molecular sensor.

detectable change such as color or pH. This transduction indicates that the recognition event must trigger a change in properties of the host–guest complex compared to the free receptor, which generates the signal.

One sensitive method of signal transduction is the emission of visible light. This can either be visible to the human eye or to a detector such as a fluorescence spectrophotometer. Fluorescence is a property that can be detected and measured in real time by using often as little as nanomolar concentrations of the analyte and instrumentation that is not too expensive and can be miniaturized for field applications. Fluorescent sensors can be made by simply covalently attaching a known fluorescent dye to a receptor at a position where the properties are expected to change upon complex formation. Examples of this type of sensor include the aforementioned calixarene **1.2**, which contains anthracene, and zinc-chelated host **1.7**, which has an attached naphthyl group.

A related principle is photoinduced electron transfer (PET),³¹ which involves the quenching of the excited state of a fluorescent molecule by transferring an electron to the vacant lower energy level from a donor group nearby. Fluorescent sensor **1.9** (Figure 1.4) was developed to bind glucosamine via two binding sites.³² The monoaza-18-crown-6 ether binds to the ammonium group while the boronic acid interacts with the diol motif. Without binding, the fluorescent signal of the anthracene group is quenched via PET from the nitrogen lone pair of either binding unit. As a result, both sites have to bind to the guest in order to stop PET and enable the anthracene fluorescence.

An additional example is macrocyclic receptor **1.10** that was used to bind nucleotide polyphosphates such as ATP and NADPH. The intrinsic fluorescence is partially quenched due to an intramolecular interaction between the two acridine groups that leads to energy transfer. Upon complexation, the fluorescence is enhanced due to stacking interactions between the acridines and the aromatic groups on the nucleotides.

Another process is metal-to-ligand charge transfer (MLCT) in which an electron is transferred from a central metal ion to a ligand, resulting in the excitation of the ligand and charge transfer to the metal. The photon emission of this excited state intermediate then generates the signal. A well-known complex with MLCT excited states is tris(2,2'-bipyridyl)ruthenium(II). This species was incorporated into receptor **1.11** with amide and boronic acid functionalities for binding phosphorylated sugars.³³ Changes in emission intensity allowed for the detection of binding fructose-6-phosphate in water.

While many systems undergo subtle changes in emission upon guest binding, it is difficult for a single sensor to bring about a significant color change that is visible to

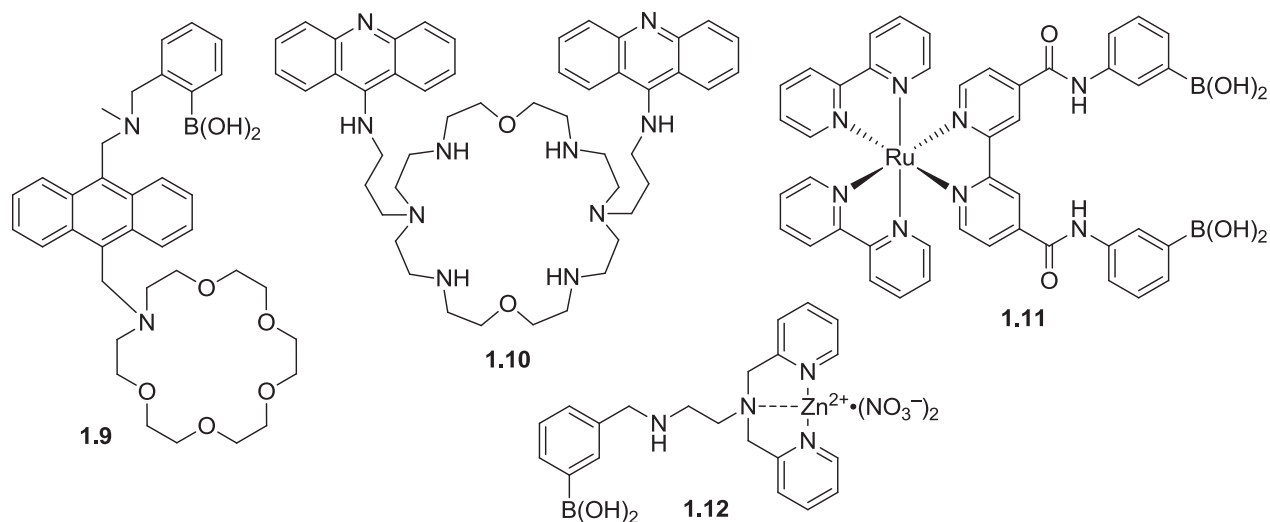


Figure 1.4. Molecular sensors with signal transduction through PET, MLCT, and IDA.

the human eye. One major disadvantage of attaching the signaling unit to the receptor is that it may require difficult syntheses. An alternative method that avoids this problem is the indicator–displacement assay (IDA),³⁴ which makes use of a guest molecule as an indicator. In this approach, the indicator is first reversibly bound by the receptor, which changes its optical properties. This indicator is chosen so that it binds to the host more weakly than the target analyte. Then, when the analyte is added, the indicator is released from the receptor and returns to its unbound state. This technique is especially convenient for an indicator whose color varies depending on whether it is bound to the host or free. Receptor **1.12** contains a boronic acid and a zinc complex that binds to an alizarin dye.³⁵ When pyrophosphate is added, the complex reorganizes, leading to an increase in fluorescence which is visible to the naked eye.

1.7 Characterization of Binding

Most experimental techniques that are used to measure binding constants for a reaction rely on the analysis of a binding isotherm, which is the theoretical change in the concentration of one component as a function of the concentration of another component at constant temperature.¹ A detailed discussion of this concept has been described.³⁶ Generally, the concentrations are determined through an experimental method such as NMR, UV-vis, or fluorescence spectroscopy, and the data is fit to the binding isotherm. The experiment is usually carried out by keeping the concentration of one component constant while varying the concentration of the other species.

In order to determine the concentration of the host–guest complex $H \cdot G$, the equilibrium needs to be expressed in terms that are measured in the laboratory.

Experimentally, the concentration of the host–guest complex, $[H\cdot G]$, can be determined as a function of the initial concentration of the guest, $[G]_0$. However, the association constant K_a is a function of the concentration of host, $[H]$, and guest, $[G]$, at equilibrium. As a result, to obtain $[H\cdot G]$ as a function of $[G]_0$, assumptions must be made because only the initial concentrations of host and guest, $[H]_0$ and $[G]_0$, are known in the experiment. First, an equilibrium approximation is made, stating that the initial host concentration $[H]_0$ is equivalent to the concentration of both the complex, $[H\cdot G]$, and host at equilibrium, $[H]$:

$$[H]_0 = [H\cdot G] + [H] \quad (\text{Eq. 1.10})$$

Solving for $[H]$ yields:

$$[H] = [H]_0 - [H\cdot G] \quad (\text{Eq. 1.11})$$

Eq. 1.11 can then be substituted into the original equilibrium equation (Eq. 1.2, page 4):

$$K_a = \frac{[H\cdot G]}{[H][G]} = \frac{[H\cdot G]}{([H]_0 - [H\cdot G])[G]} \quad (\text{Eq. 1.12})$$

Solving for $[H\cdot G]$ yields:

$$[H\cdot G] = \frac{[H]_0 K_a [G]}{1 + K_a [G]} \quad (\text{Eq. 1.13})$$

Another assumption is made by setting the initial guest concentration $[G]_0$ much higher than the initial host concentration $[H]_0$. Therefore, since $[G]_0 \gg [H]_0$, it can be assumed that $[G] = [G]_0$ because at all points in the isotherm, only a small fraction of G is converted to $H\cdot G$. With this assumption, $[H\cdot G]$ can be determined as a function of the initial concentrations of host and guest:

$$[H \cdot G] = \frac{[H]_0 K_a [G]_0}{1 + K_a [G]_0} \quad (\text{Eq. 1.14})$$

This forms the basis of many methods for determining binding constants, including the Benesi–Hildebrand method.³⁷

If the assumption is not valid, then $[G]$ and $[G]_0$ need to be related to each other. First, an equilibrium approximation similar to Eq. 1.10 is made, showing that the initial guest concentration $[G]_0$ is equal to the concentration of both the complex, $[H \cdot G]$, and the guest at equilibrium, $[G]$:

$$[G]_0 = [H \cdot G] + [G] \quad (\text{Eq. 1.15})$$

Solving for $[H \cdot G]$ yields:

$$[H \cdot G] = [G]_0 - [G] \quad (\text{Eq. 1.16})$$

Eq. 1.16 can then be substituted into Eq. 1.13:

$$\frac{[H]_0 K_a [G]}{1 + K_a [G]} = [G]_0 - [G] \quad (\text{Eq. 1.17})$$

Moving all terms to one side gives a quadratic equation that can be used to relate $[G]$ and $[G]_0$:

$$K_a [G]^2 + (K_a [H]_0 - K_a [G]_0 + 1)[G] - [G]_0 = 0 \quad (\text{Eq. 1.18})$$

For each value of $[G]_0$, this equation is solved to obtain $[G]$, and that particular $[G]$ value is then used in Eq. 1.13 to generate the isotherm. In order to calculate $[G]$, the value of K_a must first be known. Therefore, it is necessary to initially guess a value of K_a to calculate $[G]$ values for different $[G]_0$ values, and then repeatedly change K_a until the theoretical isotherm matches the experimental data. This —est fit” between theory and

experiment gives the appropriate K_a value for the system. In practice, the fitting is usually done via non-linear regression analysis of the plotted binding isotherm by means of a data analysis program.

When plotting the binding isotherm, a parameter related to the concentration of $H \cdot G$ is normally used for the y-axis, and controlled concentrations such as $[H]_0$ or $[G]$ are placed on the x-axis. Studies are commonly done for many different concentrations of G with $[H]_0$ kept constant. The binding curve is generated by plotting the experimentally measured $[H \cdot G]$ or related parameter values as a function of guest concentration.

Another aspect of characterizing a binding event is the determination of the stoichiometry of the host–guest complex. This is usually accomplished via the method of continuous variation by using a mole fraction plot called a Job plot.³⁸ A system's

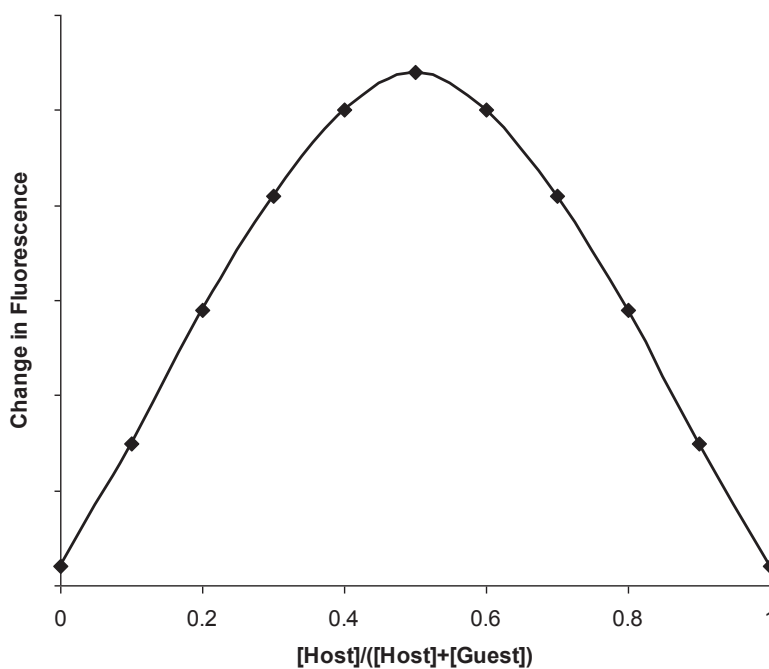


Figure 1.5. Typical Job plot for a 1:1 host–guest complex.

binding stoichiometry can be elucidated from most kinds of titrations in which the concentration of the complex can be determined by employing a series of solutions with varying host:guest ratios while the total concentration of host and guest stays constant. The concentration of the complex is generally related to an observable signal change such as the change in fluorescence emission. After monitoring the samples with different host and guest concentrations, a plot of signal change against the mole fraction of the host ($[H]/([H] + [G])$) can be made. In a 1:1 complex, a peak of maximal change would be observed at mole fraction 0.5 (Figure 1.5) while a peak at 0.66 would indicate a 2:1 host:guest stoichiometry.

Chapter 2: A Fluorescent Bis-Cyclen Tweezer Receptor for Inositol (1,4,5)-Trisphosphate Employing Click Chemistry for Convenient Synthesis

2.1 Introduction

Anions are ubiquitous in nature.³⁹ Chloride anions are present in large amounts in the oceans;⁴⁰ nitrate and sulfate are found in acid rain;⁴¹ and carbonates are key components of biomineralized materials.⁴² Phosphate and nitrates from agriculture and other human activities,⁴³ and pertechnetate,⁴⁴ a radioactive product of nuclear fuel reprocessing, are major environmental pollutants. Anions are also critical to regulating biological systems. Most biochemical processes consist of the recognition, transformation, or transportation of anions. As a result, the disruption of anion flux across cell membranes can be the main factor in many diseases such as Bartter syndrome,⁴⁵ cystic fibrosis,⁴⁶ Dent's disease,⁴⁷ Pendred syndrome,⁴⁸ and osteopetrosis.⁴⁹ Furthermore, anion transport through cell phospholipid bilayers is known to be regulated by various channels and anion transport systems with at least 14 mitochondrial anion transport systems having been identified to date.⁵⁰ These include systems controlling the trafficking of ADP, ATP, citrate, fumarate, glutamate, halide, maleate, oxaloacetate, phosphate, and sulfate anions. The importance of anion recognition in biology highlights the potential use of synthetic anion receptors.

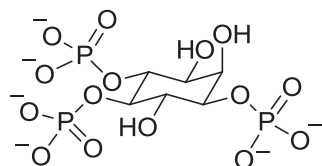
The development of molecular sensors that are effective for detecting important biomolecular targets in competitive media remains a significant challenge in the field of supramolecular chemistry.⁵¹ This process involves the design of a macromolecular host containing preorganized binding groups to instill geometric complementarity with a

target guest and therefore increase the affinity and selectivity of binding. In addition, a signal transduction element is installed for detection purposes, of which fluorescence is advantageous due to its high sensitivity.⁵²

Within the field of supramolecular chemistry, anion recognition has proven problematic due to inherent challenges, including the large and varying shapes of anions, their multiple pH-dependent charge states, and the difficulty in synthetically incorporating anion-binding moieties into receptors.^{52c,53} Despite these challenges, a number of receptor motifs have been developed for anion recognition, including polyammonium macrocycles,⁵⁴ porphyrins,¹⁸ the triethylbenzene system,²⁴ bimetallic hosts,²⁸ calixarenes,¹⁵ and steroidal constructs.⁵⁵ However, the generation of sensors capable of detecting anionic targets for real world applications remains a significant barrier due to the difficulty of achieving strong binding in competitive media.

2.2 Inositol (1,4,5)-Trisphosphate Guest Background

Anion sensing is critical as biological systems rely heavily on the manipulation of anionic functional groups as a regulatory means, mainly through the control of biomolecule phosphorylation. As a result, sensors for phosphorylated molecules are of particular interest.^{12c,56}



2.1

Figure 2.1. Inositol (1,4,5)-trisphosphate (InsP₃).

An important target for molecular sensing is the signaling molecule inositol (1,4,5)-trisphosphate (InsP₃, **2.1**, Figure 2.1). This is the quintessential biologically active inositol phosphate⁵⁷ due to its prominent role as a second messenger in calcium release, originally reported in 1983.⁵⁸ InsP₃ is produced through the hydrolysis of phosphatidylinositol (4,5)-bisphosphate by phospholipase C.⁵⁹ This soluble product then binds to its cognate receptors, the inositol triphosphate receptors (InsP₃R),⁶⁰ leading to the opening of these gated ion channels, which directly results in calcium release by gradient diffusion into the cytoplasm. InsP₃-mediated calcium release is critical due to the various physiological processes that are mediated by this ion, which includes cell proliferation, differentiation, secretion, muscular contraction, embryonic development, immune responses, and many others.^{60a,60d}

2.3 Receptors for Inositol (1,4,5)-Trisphosphate

Due to its important role in biological systems, InsP₃ has been a target for sensor design. Anslyn and co-workers initially reported hexa-guanidinium receptor **2.2** with a binding cavity engineered via the 1,3,5-triethylbenzene scaffold.⁶¹ A dye displacement assay was implemented for optical detection, and strong binding ($K_a = 2.2 \times 10^4 \text{ M}^{-1}$) was observed in aqueous solution. More recently, Kimura and co-workers assembled complex **2.3** by incorporating non-fluorescent receptors containing zinc–cyclen chelating groups into a ruthenium tris-bipyridyl system to achieve fluorescence signaling.⁶² In addition, Ahn and co-workers developed tris zinc–dipicolylamine receptor **2.4**, and again employed a dye displacement assay to achieve detection.⁶³ Matile, Prestwich, and co-workers used a synthetic multifunctional pore based on rigid *para*-octiphenyl rods

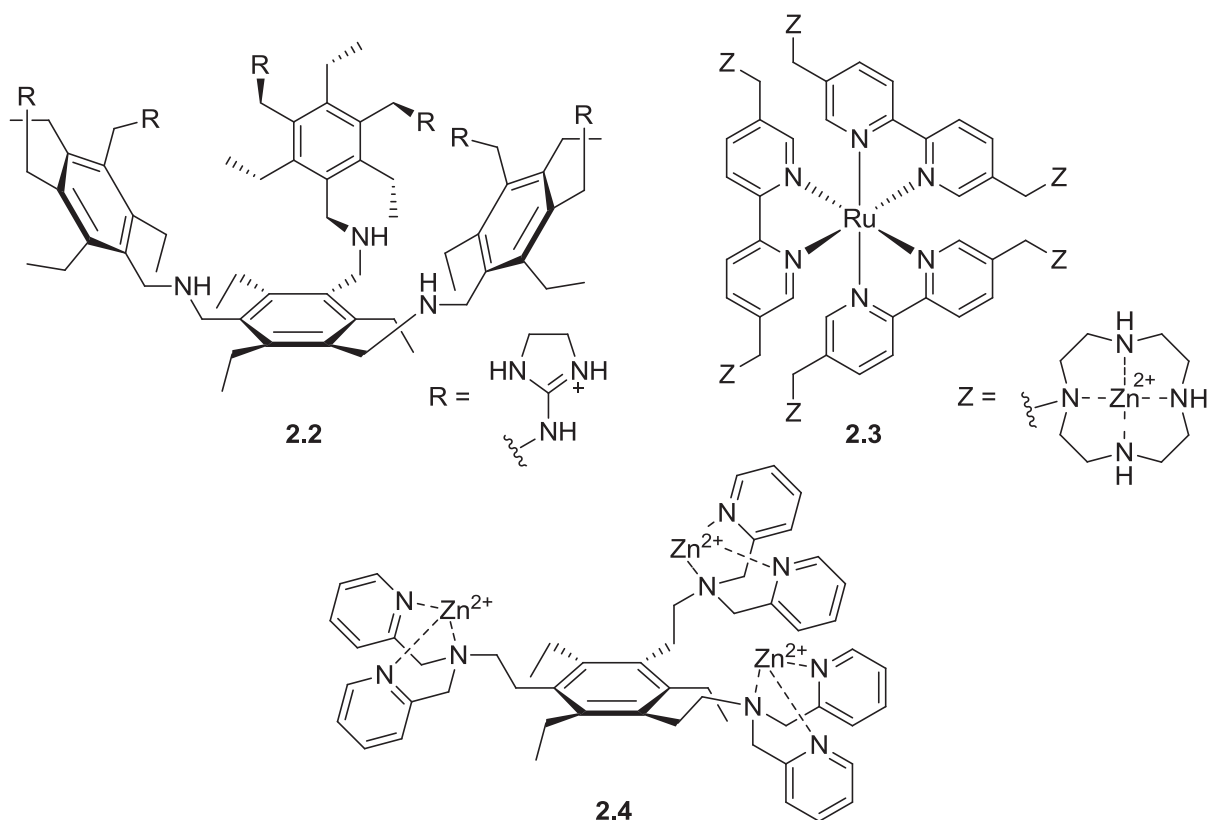


Figure 2.2. Examples of receptors for inositol 1,4,5-trisphosphate.

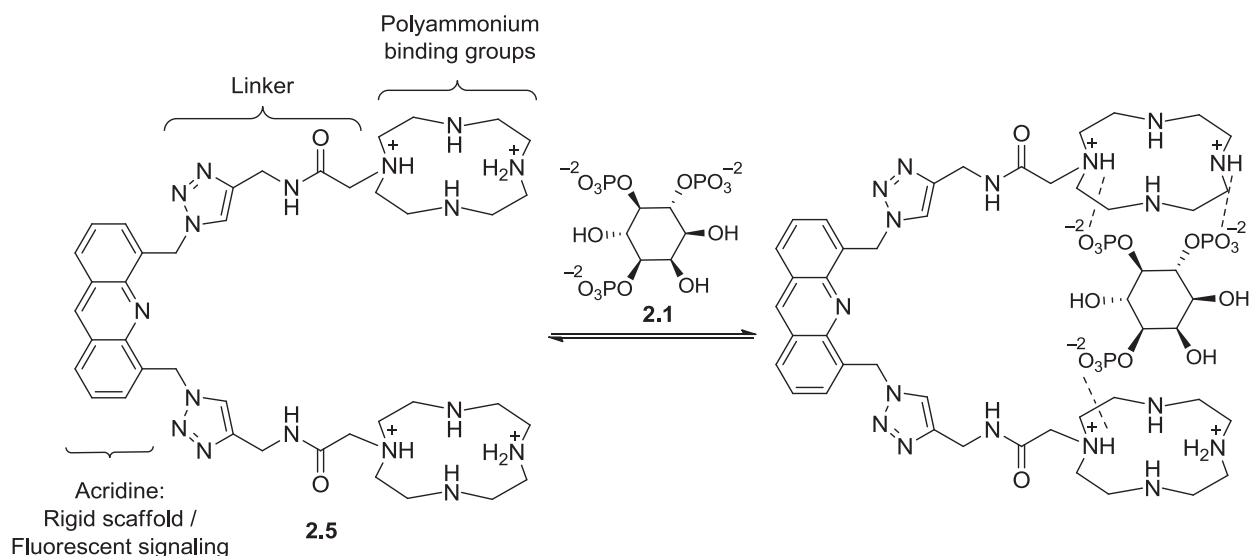
organized into a β -barrel. The fluorimetric detection of InsP_3 binding was transduced by pore opening and closing.⁶⁴

Approaches other than molecular receptors have also been successful for InsP_3 detection, particularly through using labeled or engineered protein receptors.⁶⁵ In one example, fluorophores were placed within the pleckstrin homology (PH) domain of phospholipase C (PLC) $\delta 1$ to create a variety of biosensors that can detect InsP_3 concentrations with a micromolar dissociation constant. One of the sensors showed a higher selectivity for InsP_3 over other inositol derivatives than the parent PH domain.^{65c} Finally, colorimetric sensors for phytate (InsP_6), another inositol phosphate isomer, have been reported as well.⁶⁶ One report used the triethylbenzene scaffold attached to three

copper(II)–dipicolylamine groups to bind InsP_6 through an indicator–displacement assay.^{66b}

2.4 Receptor Design

We set out to develop a host for InsP_3 **2.1** with built-in fluorescence signaling. This would bypass the problems associated with a dye displacement assay for which the host is required to first bind to the dye and then bind more strongly to the guest. While multiple host designs have been pursued, the design that was used for binding studies will be discussed first, and other approaches will be covered later in this chapter. The host design (**2.5**, Scheme 2.1) consists of a tweezer structure that incorporates an acridine scaffold connected to two macrocyclic polyammonium groups via triazole-based linkers to accommodate multiply phosphorylated biomolecules such as InsP_3 **2.1**. This creates an effective binding cavity in which the anion guest is sandwiched between the two macrocycle groups. A molecular model of the host



Scheme 2.1. Design of tweezer receptor **2.5** and hypothetical binding complex with InsP_3 .

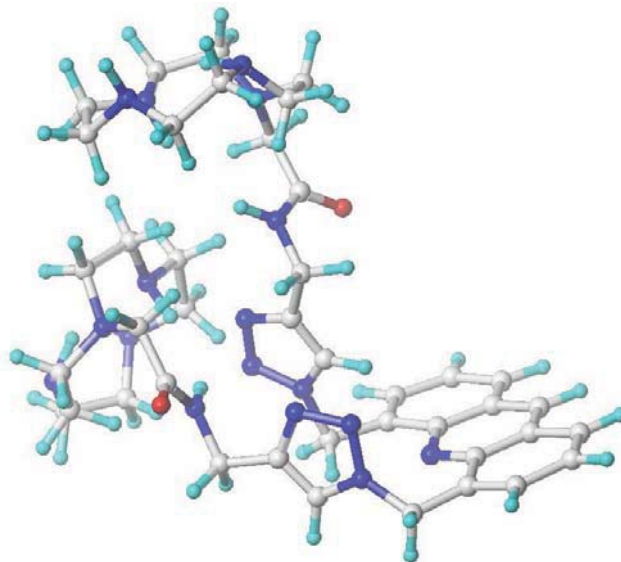


Figure 2.3. Molecular model of tweezer receptor **2.5**.

structure was generated in SYBYL 8.0 using the Powell minimization method (Figure 2.3). Before minimizing, the two CH₂ carbons attached to the acridine were rotated in opposite directions towards the left and right of the acridine to keep the macrocycles far apart. The minimized structure suggested that the polyammonium moieties do not rotate away from each other, thereby forming the desired binding cleft for the guest.

While the presence of multiple binding groups in the tweezer structure may cause concern over the possibility of multiple equilibria, precedence from the monomeric polyammonium macrocycles suggested that this would not occur. Even the largest macrocycles are known to form 1:1 complexes with both small (phosphate)¹³ and large (tricarboxylates) anions.⁶⁷ Therefore, with correct polyammonium preorganization in the tweezer, guest anions were expected to rest in a similar geometry, but now between two polyammoniums, yielding 1:1 complexes.

A key synthetic transformation is the attachment of the polyammonium macrocycles to the scaffold, which is best performed at a late stage in the synthesis to

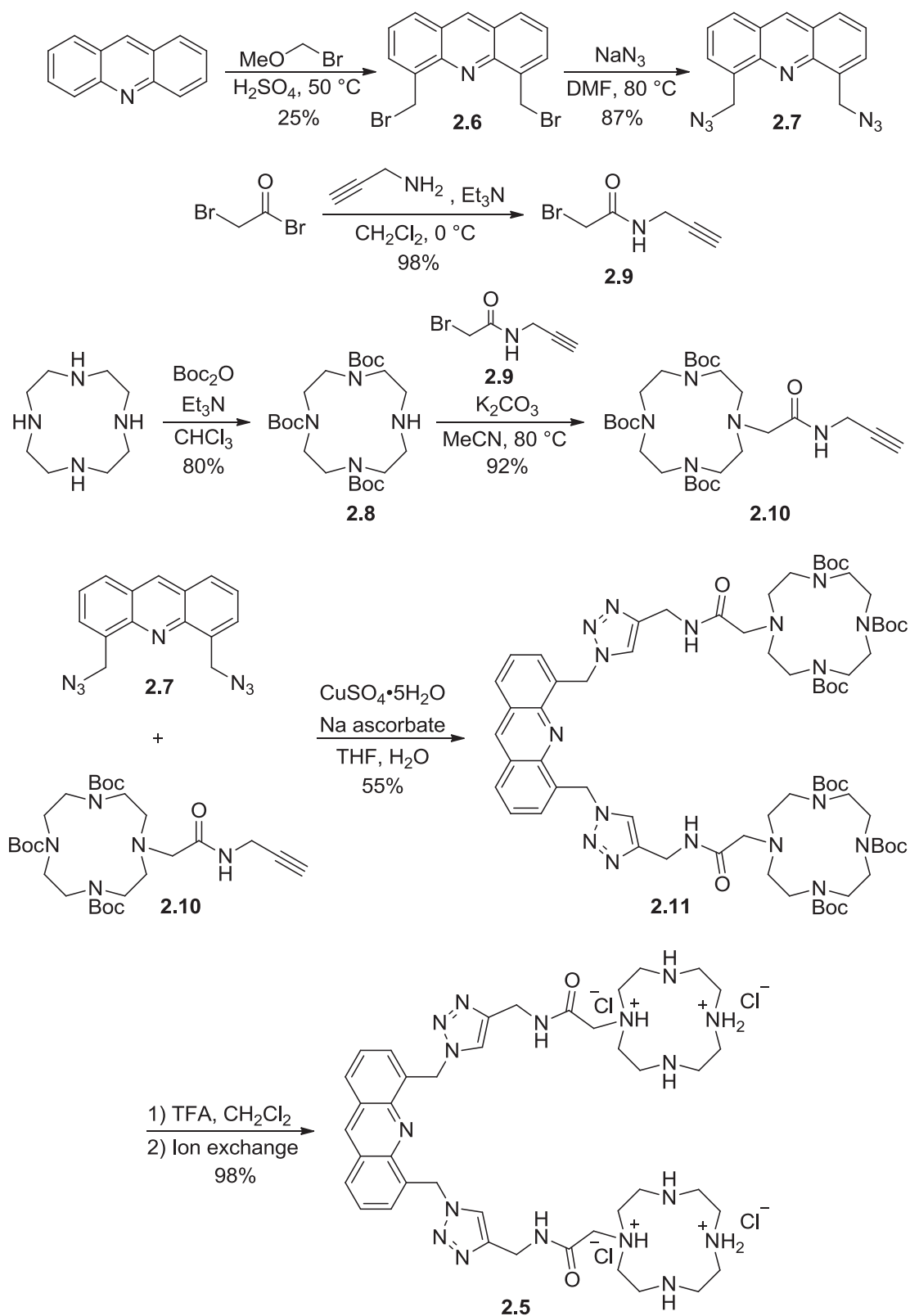
provide an efficient modular approach. Later, we will describe such a modular strategy for attaching different polyamines and scaffolds. However, direct functionalization of polyammonium macrocycles can be challenging due to the presence of multiple reactive amine functionalities. Thus, we chose to perform this attachment using the azide–alkyne Huisgen 1,3-dipolar cycloaddition (“click” chemistry) due to the beneficial functional group tolerance of this reaction.⁶⁸

Recently, the azide–alkyne 1,3-dipolar cycloaddition has proven effective for polyammonium macrocycle derivatization for MRI imaging⁶⁹ and luminescent metal binding studies.⁷⁰ The resulting triazole from this reaction is advantageous due to the rigidity it provides to the receptor scaffold. Furthermore, triazoles have been shown to be effective for forming hydrogen bonding interactions with anionic guests⁷¹ and therefore could contribute to the binding of phosphorylated analytes.

The acridine moiety in the receptor structure provides fluorescence signal transduction for the direct detection of a guest, as opposed to indicator displacement, and has previously been used in fluorescent sensors for phosphate⁷² and nucleotide polyphosphates such as ATP and NADPH.⁷³ The acridine has conveniently been derivatized at the 4- and 5-positions to preorganize two binding groups into an effective binding cavity. This allows for a convergent synthesis in which these groups could be conveniently merged using “click” chemistry. A bis-azide functionalized acridine intermediate exists in the literature⁷⁴ while an alkyne-tethered cyclen has also been reported.⁶⁹

2.5 Bis-Cyclen Tweezer Synthesis

The synthesis began with the 4,5-bis-bromomethylation of acridine to product **2.6** (Scheme 2.2),⁷⁵ followed by azide substitution to obtain bis(azidomethyl)acridine **2.7**. Commercially available cyclen was tris-*tert*-butoxycarbonyl (Boc) protected to **2.8**⁷⁶ and then coupled with alkyne **2.9**, which was synthesized from bromoacetyl bromide.⁷⁷ The resulting alkynyl cyclen **2.10** was then reacted with the bis-azide-tagged acridine in the key azide–alkyne cycloaddition to form tweezer structure **2.11** which was then deprotected with trifluoroacetic acid. Ion exchange was next performed to access precursor **2.5** with chloride counteranions, and it is estimated that four chlorides were associated with the cationic host structure. The exchange was done to facilitate purification via reversed-phase column chromatography.



Scheme 2.2. Synthetic route to bis-cyclen tweezer host **2.5**.

2.6 Guest Binding Studies

Following the completion of the synthesis, receptor **2.5** was employed as host for titration binding studies to evaluate the binding of InsP₃ (**2.1**) with concomitant fluorescence signal transduction. Guest **2.1** was synthesized by Meng Rowland in our lab using intermediates from previous group publications.⁷⁸ First, a UV scan of the host was performed, exhibiting an absorption peak centered around 355 nm, with excitation at this wavelength leading to a fluorescence emission signal located around 440 nm. Next, a solution containing host **2.5** and guest **2.1** was titrated into a solution of host **2.5** to keep the total host concentration constant. Here, dose-dependent decreases in the emission signal of host were observed upon guest addition. This was performed in a range of solvents varying from 0 to 100% methanol in water buffered at pH 7.4.

From these preliminary studies, a solvent mixture of 50% methanol/water was identified as a competitive solvent in which strong binding was observed. A representative plot shows the decrease in emission properties of host **2.5** upon addition of guest **2.1** in this solvent mixture (Figure 2.4). While the changes in emission properties were somewhat modest, dropping by 10–15%, these signals could still be reproducibly correlated to a binding curve for **2.1** (Figure 2.5). The absolute values of the changes in fluorescence intensities upon addition of **2.1** are shown as averaged values over several runs, with error bars depicting the standard error. From these results, an average association constant (K_a) of $1.0 \times 10^6 \text{ M}^{-1}$ with standard errors (Table 2.1) was calculated for the complex, indicating high-affinity binding in competitive media.

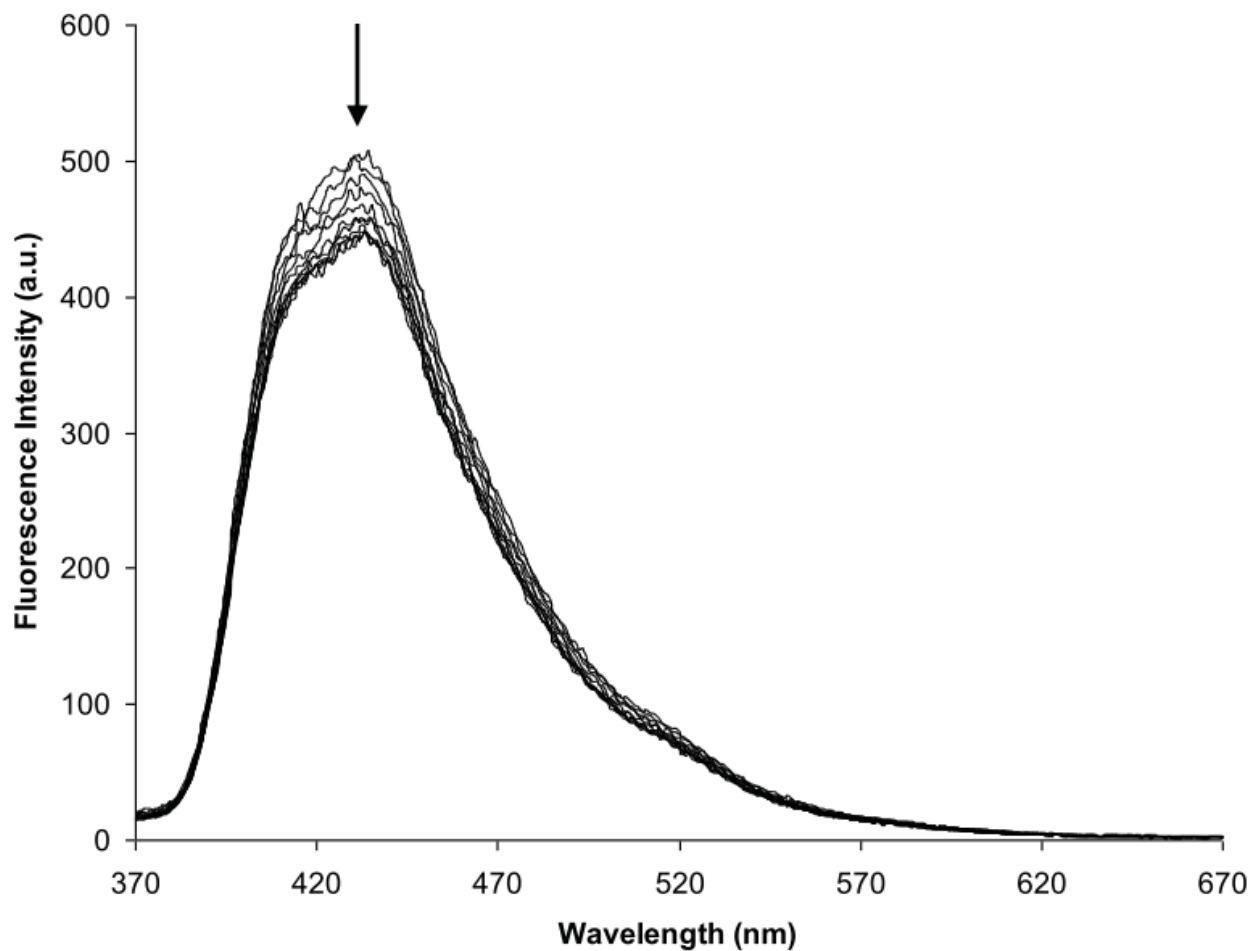


Figure 2.4. Plots exhibiting the decrease in emission of host **2.5** upon addition of guest **2.1**.

Table 2.1. Association constants calculated for the binding of host **2.5** to phosphorylated guests.

| Guest | K_a (M^{-1}) | Standard Error |
|---|--------------------|-----------------------|
| Inositol (1,4,5)-trisphosphate (2.1) | 1.0×10^6 | $\pm 1.6 \times 10^5$ |
| Fructose 1,6-bisphosphate (2.12) | 9.5×10^5 | $\pm 7.1 \times 10^4$ |
| Cyanoethyl phosphate (2.13) | 8.9×10^5 | $\pm 1.2 \times 10^5$ |
| Sodium dihydrogen phosphate (2.14) | 7.8×10^5 | $\pm 4.3 \times 10^4$ |

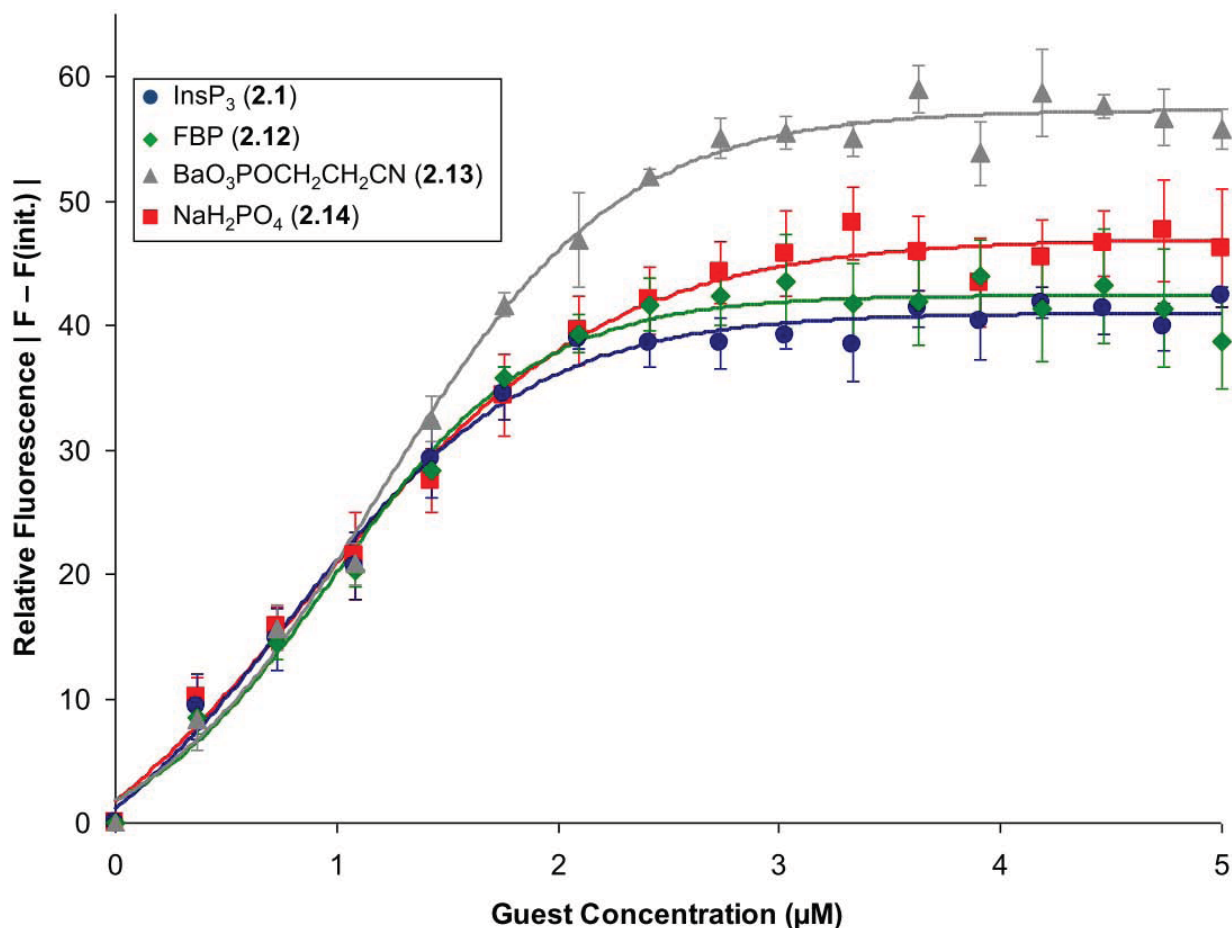


Figure 2.5. Binding curves for guests studied in titrations of host **2.5**.

Next, a series of related phosphorylated compounds were tested for binding studies to further investigate the recognition properties of host **2.5**. These included D-fructose 1,6-bisphosphate trisodium salt (FBP, **2.12**, Figure 2.6), cyanoethyl phosphate barium salt (**2.13**), and sodium dihydrogen phosphate (**2.14**). These molecules were selected due to their variation in the number of phosphate and alkyl groups, and as biomolecules that can compete for binding. The binding curves and the resulting association constants for these guests are displayed alongside those corresponding to **2.1** (Figure 2.5 and Table 2.1). In general, each of these guests displayed fairly strong

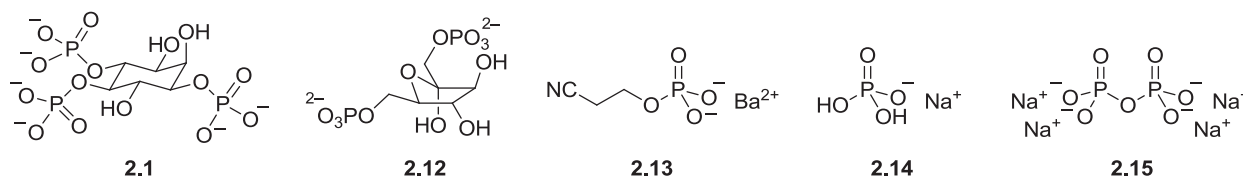
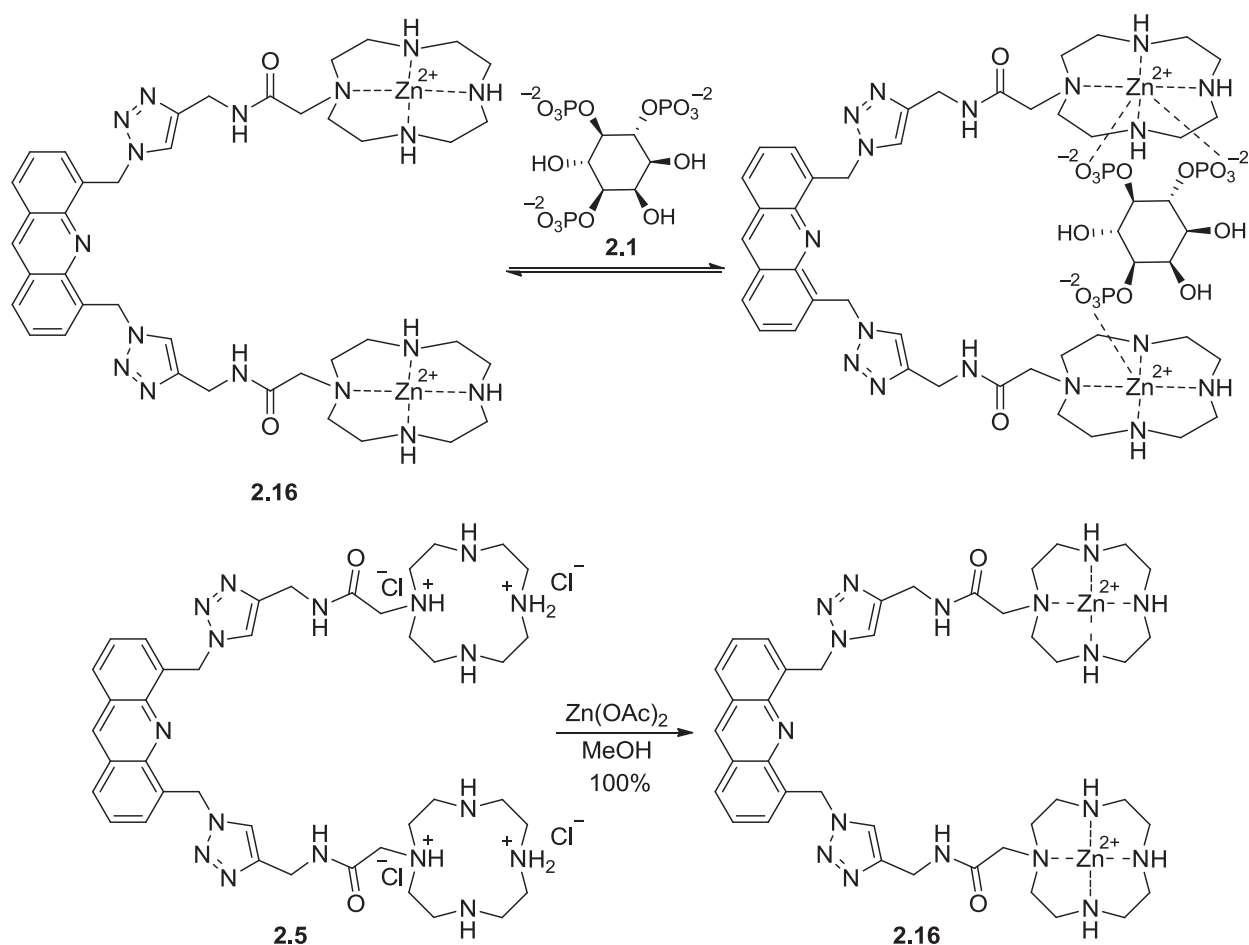


Figure 2.6. Structures of guests used for binding studies.

binding, showing that host **2.5** is generally effective at complexing a range of phosphorylated guest structures in competitive solvents. However, slight variations in binding affinity were observed in the order of **2.1** > **2.12** > **2.13** > **2.14**, according to numerical values. Statistical analysis of the association constants showed that they are not significantly different, with p values > 0.05 (F-test of equality of variances: $p = 0.12$ for **2.1** vs. **2.12**, $p = 0.06$ for **2.1** vs. **2.13**, $p = 0.23$ for **2.12** vs. **2.13**, $p = 0.08$ for **2.13** vs. **2.14**). Therefore, the results indicated very modest selectivity for InsP₃ (**2.1**), as well as for multiply phosphorylated guests (**2.1** and **2.12**) over singly phosphorylated guests (**2.13** and **2.14**) in the series. This is a common obstacle in anion binding as enhancing selectivity remains a significant challenge.

Following these modest results, we anticipated that with the addition of zinc, complex **2.16** (Scheme 2.3) would yield more promising results because metallic coordination complexes have shown strong binding of anions even in aqueous media.²⁸ In this case, the zinc cations would serve as electrophilic binding sites. The zinc-chelated host **2.16** was formed by treating receptor **2.5** with zinc(II) acetate.



Scheme 2.3. Hypothetical binding complex of receptor **2.16** with InsP₃ and synthesis of **2.16**.

The same fluorescence titration binding experiments were performed with host **2.16** in order to compare recognition properties to those of metal-free **2.5**. Once again, titration with **2.1** yielded a decrease in emission for **2.16**, for which a representative plot is shown (Figure 2.7). While still modest, the emission changes of **2.16** upon addition of **2.1** (20–25%) were greater than those of precursor **2.5**. Once again, receptor **2.16** exhibited strong binding of **2.1**, with an association constant of $5.1 \times 10^5 \text{ M}^{-1}$ (Table 2.2). Despite the enhanced fluctuation in emission properties upon guest addition, this binding affinity was slightly weaker than that of host **2.5**.

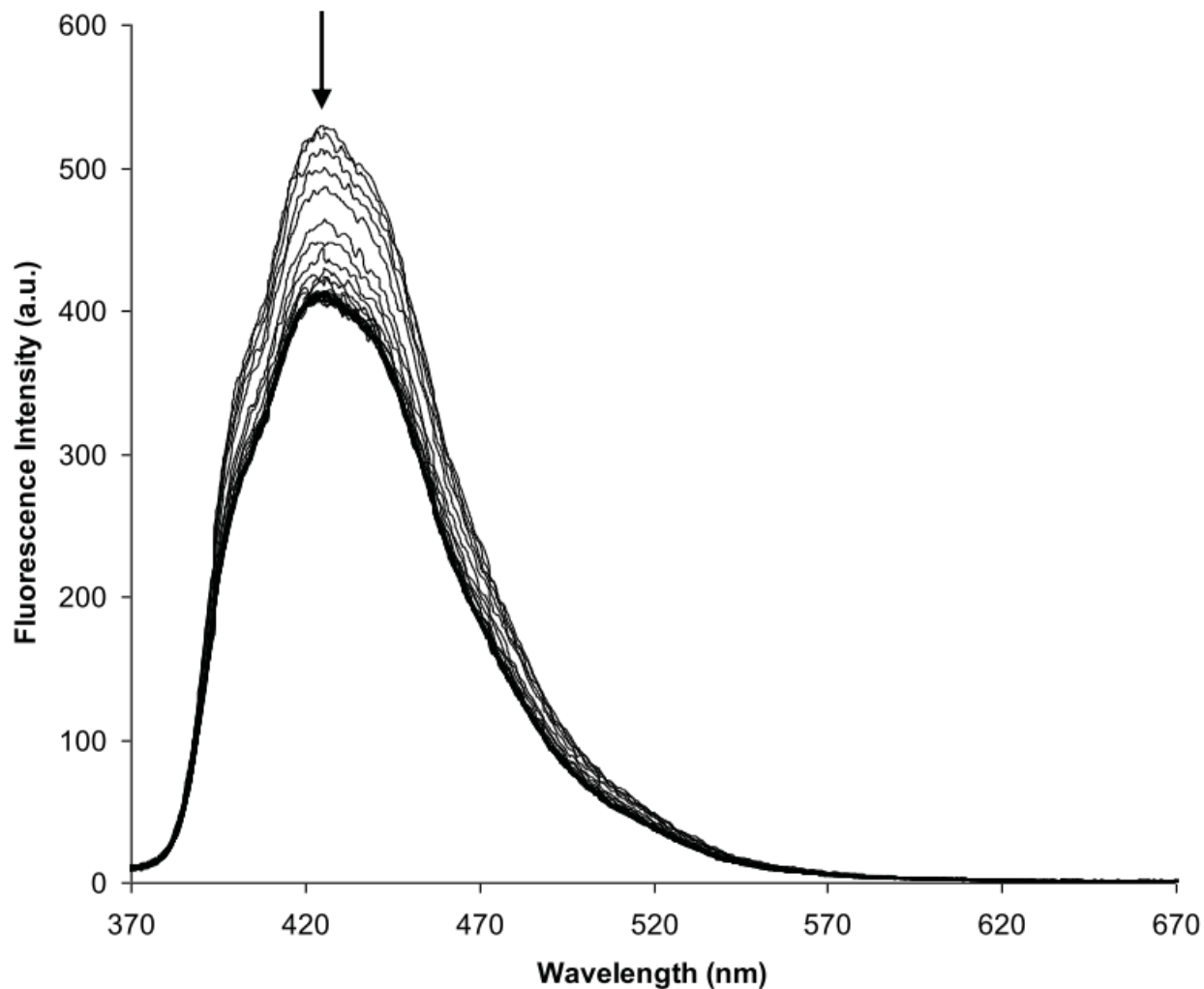


Figure 2.7. Plots exhibiting the decrease in emission of host **2.16** upon addition of guest **2.1**.

Table 2.2. Association constants calculated for the binding of host **2.16** to phosphorylated guests.

| Guest | K_a (M^{-1}) | Standard Error |
|---|--------------------|-----------------------|
| Inositol (1,4,5)-trisphosphate (2.1) | 5.1×10^5 | $\pm 4.3 \times 10^4$ |
| Fructose 1,6-bisphosphate (2.12) | 4.9×10^5 | $\pm 8.4 \times 10^4$ |
| Cyanoethyl phosphate (2.13) | 9.4×10^5 | $\pm 6.3 \times 10^4$ |
| Sodium dihydrogen phosphate (2.14) | 4.3×10^5 | $\pm 4.3 \times 10^4$ |
| Sodium pyrophosphate (2.15) | 4.7×10^5 | $\pm 3.3 \times 10^4$ |

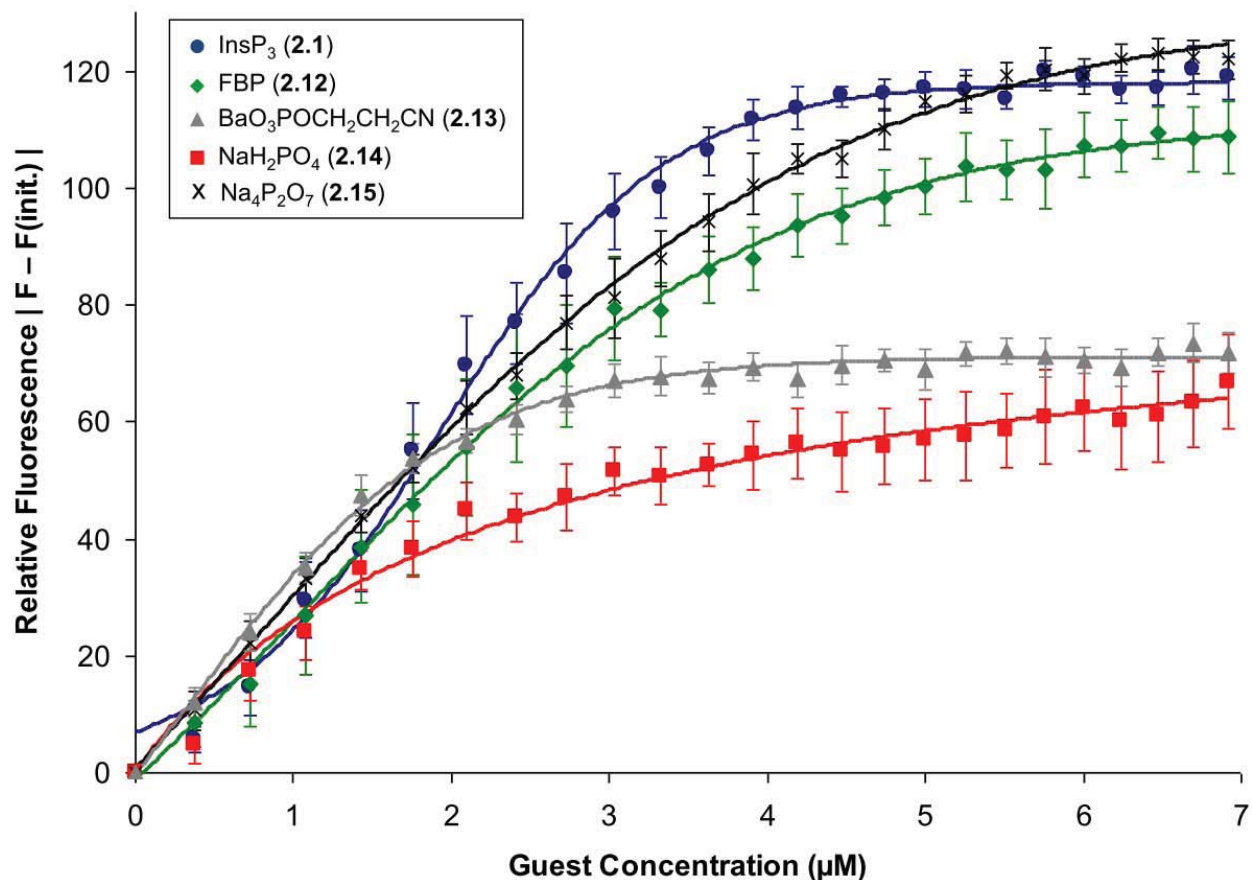


Figure 2.8. Binding curves for guests studied in titrations of host **2.16**.

Next, the same series of phosphorylated guests was analyzed for binding with **2.16**, along with the addition of sodium pyrophosphate (**2.15**, Figure 2.6). The binding curves for these guests and the resulting association constants are shown alongside those corresponding to **2.1** (Figure 2.8 and Table 2.2). Once again, each guest exhibited strong binding, and only slight variations in affinity were observed. In this case, cyanoethyl phosphate surprisingly yielded the strongest binding, and an ordering of **2.13** > **2.1** > **2.12** > **2.15** > **2.14** was observed. With the exception of **2.13**, comparison of the association constants again indicated that they do not differ significantly ($p = 0.15$ for **2.1** vs. **2.12**, $p = 0.37$ for **2.1** vs. **2.15**, $p = 0.46$ for **2.1** vs. **2.14**,

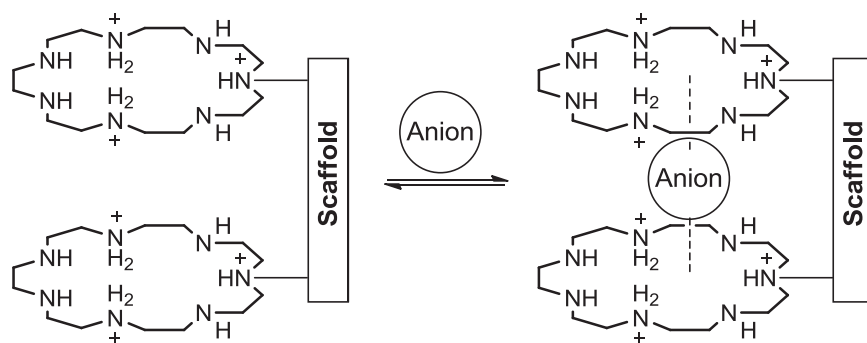
$p = 0.07$ for **2.12** vs. **2.15**, $p = 0.17$ for **2.12** vs. **2.14**, $p = 0.43$ for **2.15** vs. **2.14**). However, in these studies, multiply phosphorylated guests (**2.1**, **2.12**, and **2.15**) all produced higher changes in fluorescence emission than those analytes containing a single phosphate group (**2.13** and **2.14**). This provided evidence for variation in binding mode resulting from the presence of more than one phosphate in the guest structure and points to the benefits of preorganizing two phosphate binding groups into a cavity for complexation of multiply phosphorylated targets. As discussed in the previous chapter, there is a distinction between guest selectivity and inter-guest discrimination. Selectivity in binding affinity and the magnitude of signaling changes do not always match. Even though the binding constants for most of the guests were close in value (Table 2.2), the analytes with multiple phosphate groups showed higher fluorescence changes.

In order to obtain the binding stoichiometry, we sought to generate a Job plot for this system. However, since the fluorescence signal of the host decreased upon addition of guest, it was not possible to determine the stoichiometry via a Job plot. For a system in which emission increases with added guest, a plot of fluorescence intensity as a function of mole fraction of guest would show a peak of maximum signal. In our case with decreasing emission, the maximum would be where there is only host present and no guest, and the minimum would be in a solution containing only guest. This is particularly problematic due to a low signal change. Therefore, the fluorescence was expected to simply decrease as the mole fraction of guest increases, and this was confirmed with solutions of host **2.5** and guest **2.1**.

Overall, strong binding to various phosphorylated guests in competitive solvent was observed for the hosts. The low fluorescence emission changes may have been caused by the long distance between the acridine and polyamine units in the structure. This may be alleviated by shortening the alkyne linker attached to the macrocycles. The receptor was designed with a hypothetical cavity (Schemes 2.1 and 2.3) in mind, but the binding mode remains unknown. Other binding stoichiometries such as 2:1 host:guest complexes cannot be ruled out. In order to design receptors with enhanced selectivities, different structures with varying degrees of preorganization need to be tested. If a more rigid host were built, then the complementarity of the functional groups towards the guest would have to be very good. This would most likely require a modular approach similar to the one we initially attempted.

2.7 Initial Receptor Design

Our original host design involved the preorganization of two larger polyammonium macrocycle groups in a tweezer structure (Scheme 2.4). The general design represents a modular strategy in which multiple parts of the structure, including the identities of the macrocycles, the tweezer scaffold, and the tether between the two,



Scheme 2.4. Preorganization of polyammonium macrocycles in tweezer structure.

can be modified to tune the binding properties of the host.

The main characteristic that is regulated by varying the scaffold and the tethers is the rigidity of the receptor, a crucial property that controls binding group presentation. Generally, a rigid host structure can reach maximum affinity with perfect placement of binding functionalities, but errors in preorganization often result in severe affinity decreases. While host flexibility can lower the ceiling of binding affinity, it also provides more room for error in achieving strong complexation. Due to the significance of rigidity in receptor design, an approach that allows efficient fine-tuning of this property is beneficial. Therefore, variable rigid (scaffold) and flexible (tether) portions were incorporated into the receptor backbone (Figure 2.9) to maximize coordination properties.

Polyammonium macrocycles ranging from cyclen ($m = 1$) up to heptaazamacrocycles ($m = 4$) would provide receptors with varying anion selectivities due to the different cavity sizes and number of ammonium groups. One concern with

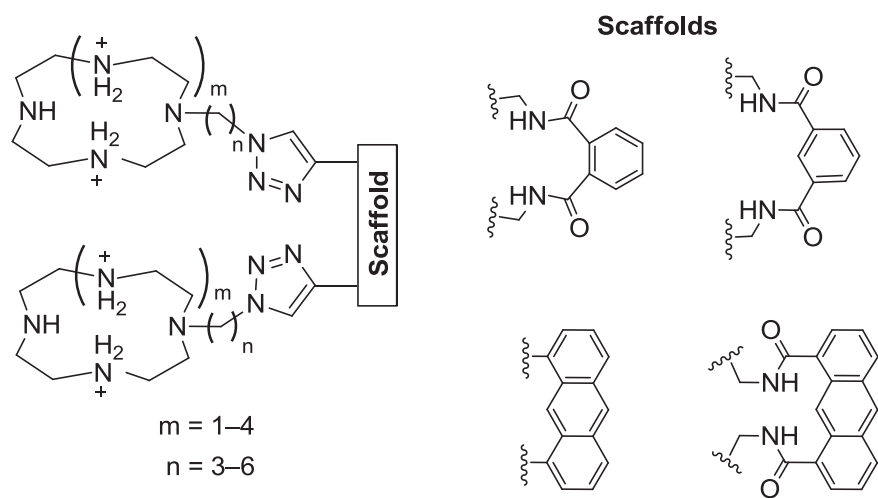
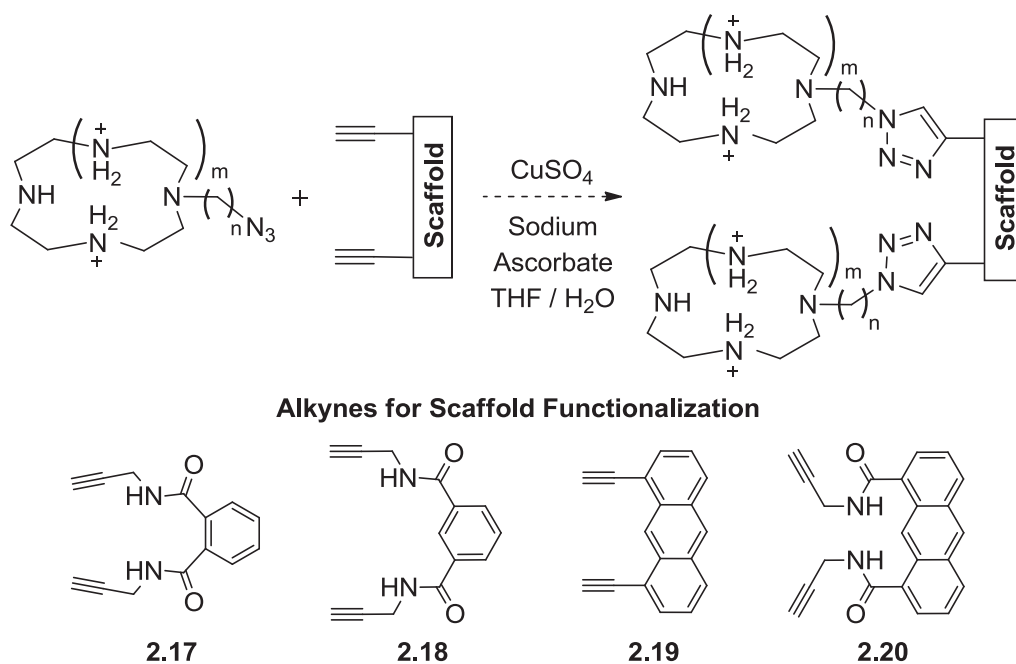


Figure 2.9. Modular structure for anion-binding tweezer receptors.

the tweezer scaffold was that bond rotation could result in conformations with the macrocycles facing away from each other. Therefore, several different scaffolds were investigated in order to find those that are most effective at preorganizing binding moieties. Possible dimeric scaffolds included *ortho*- and *meta*-diamides and anthracenes (Figure 2.9) to offer different binding group geometries. The amides could be favorable by participating in recognition through hydrogen bonding to the bound anion while the anthracenes are beneficial for generating fluorescence signal transduction of binding events. And finally, the length of the alkyl chain tether (n , Figure 2.9) connecting the macrocycles to the scaffold could also be modified.

Once again, the “click” chemistry approach was employed to attach the polyammonium macrocycles to the scaffold. This strategy is illustrated by the reaction of an azide-functionalized macrocycle with a generic bis-alkyne scaffold to access

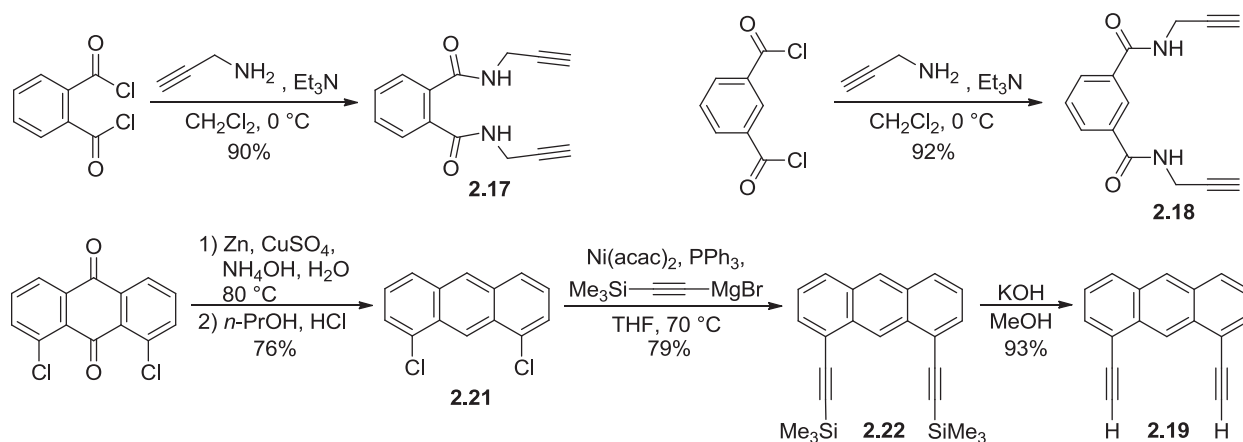


Scheme 2.5. Late-stage scaffold–macrocycle linkage via azide–alkyne cycloaddition.

various tweezers (Scheme 2.5). The bis-alkyne precursors used for scaffold introduction include difunctionalized benzenes (**2.17** and **2.18**) and anthracenes (**2.19** and **2.20**). The benzenes have recently been used in the synthesis of carbohydrate–triazole ligands.⁷⁹ Finally, azido-macrocycles could also be functionalized by other methods if necessary, such as the Staudinger ligation⁸⁰ or azide reduction and derivatization of the resulting amine.⁸¹

2.8 Alkyne Scaffold Synthesis

We first set out to synthesize the difunctionalized benzenes **2.17** and **2.18** from commercially available starting materials in one step using the exact same reaction conditions for both (Scheme 2.6). The dichlorides were reacted with propargylamine at cold temperature to form the corresponding alkynes in good yield. Next,

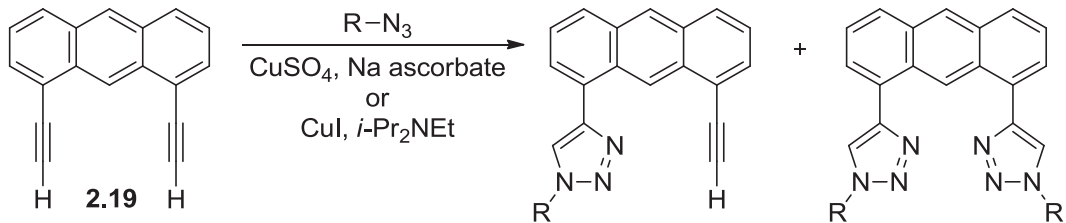


Scheme 2.6. Synthesis of alkyne scaffolds.

diethynylanthracene **2.19** was prepared using a series of known literature procedures. 1,8-dichloroanthraquinone was reduced with zinc to anthracene **2.21**,⁸² followed by Grignard addition of (trimethylsilyl)ethynyl groups to product **2.22**⁸³ which was then deprotected in base to give **2.19**.⁸⁴ This anthracene scaffold looked particularly

interesting to us because the resulting triazoles from the cycloaddition with azides would provide extra rigidity to the core. Furthermore, the triazoles would be in conjugation with the anthracene, which may lead to larger changes in fluorescence upon binding.

Consequently, diethynylantracene **2.19** was tested with various small azides in the azide–alkyne cycloaddition to form triazole adducts (Scheme 2.7). The reactions were performed in a variety of solvents, and copper(II) sulfate and copper(I) iodide were used as the copper catalyst source (Table 2.3). The results show that almost all attempts returned the alkyne starting material and failed to form any bis(triazole) product. Only a few reaction sets were able to form mono-triazole products in low yield. The collected mono products were then reacted again with more azide, but this resulted in no change. It is possible that steric hindrance could make it difficult for the second triazole unit to form, especially since the first triazole ring is conjugated to the anthracene system and most likely would have little freedom to rotate. Any plans to test the same sets of reactions on the benzene scaffolds **2.17** and **2.18** were later abandoned when our acridine host **2.5** became successful. While the cycloaddition reactions did not quite “click” so far, sufficient amounts of alkyne materials were synthesized, and we turned our attention towards the synthesis of the polyammonium macrocycles.



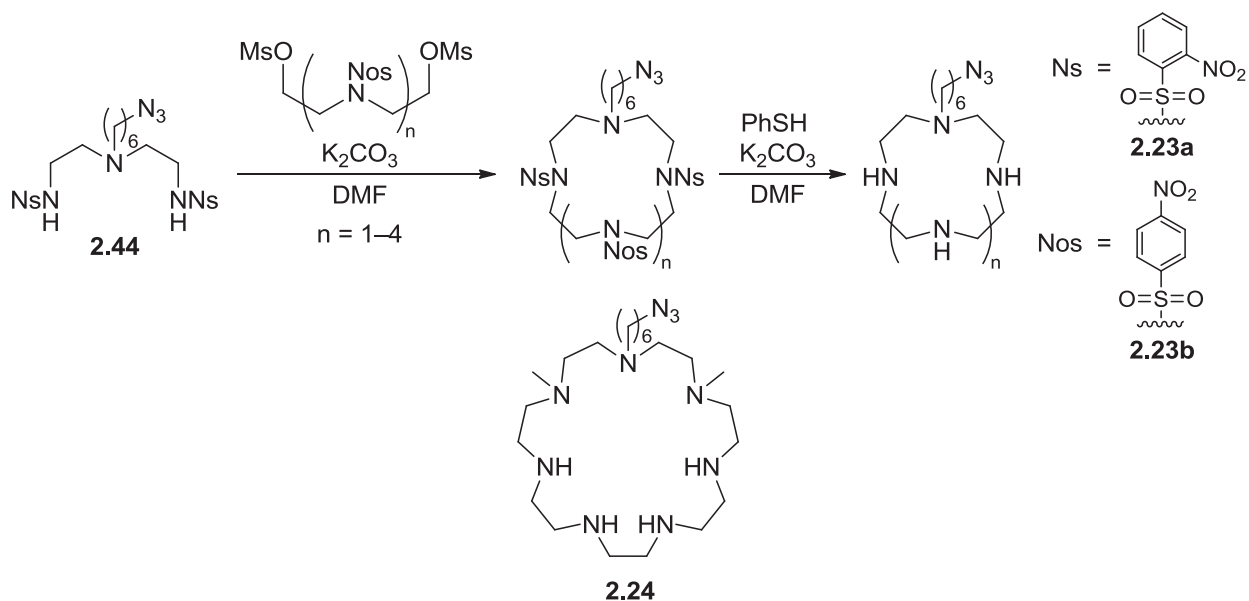
Scheme 2.7. Attempted cycloaddition between **2.19** and various azides.

Table 2.3. Results of azide–alkyne cycloaddition reactions.

| Azide | Copper source | Solvent(s) | Mono product | Bis product | 2.19 recovery |
|-------|-------------------|---|--------------|-------------|----------------------|
| | CuSO ₄ | THF/H ₂ O | 19% | 19% | no |
| | CuSO ₄ | THF/H ₂ O | - | - | yes |
| | CuSO ₄ | THF/H ₂ O | 31% | - | yes |
| | CuSO ₄ | MeCN/H ₂ O | - | - | yes |
| | CuSO ₄ | DMF/H ₂ O | - | - | no |
| | CuI | THF | - | - | yes |
| | CuI | MeCN | - | - | yes |
| | CuSO ₄ | THF/H ₂ O | 17% | - | yes |
| | CuSO ₄ | CH ₂ Cl ₂ /H ₂ O | 23% | - | yes |

2.9 Azide-Tagged Polyammonium Macrocycle Synthesis

A modular scaffold also requires the synthesis of the polyamine receptor units. While the field of polyammonium macrocycle chemistry has produced effective synthetic methods, these syntheses remain somewhat challenging due to the high amine content and the need for macrocyclization. Additionally, azide-labeled macrocycle development requires mild conditions due to the sensitivity of azide groups to, for example, reduction and acid. In previous work,⁸⁵ the tosyl group was frequently used as a protecting group for nitrogen, but it was removed under strongly acidic conditions, which makes its use not suitable for functionalized polyamines such as our azide-tagged structures. Therefore, an important aspect of polyammonium synthesis is the choice of protecting/activating group for nitrogen. We chose the nitrobenzenesulfonyl (nosyl) groups (**2.23a–b**, Scheme 2.8), as they are robust yet can be removed using mild conditions, and they promote high yields in cyclization reactions.⁸⁶ We were particularly

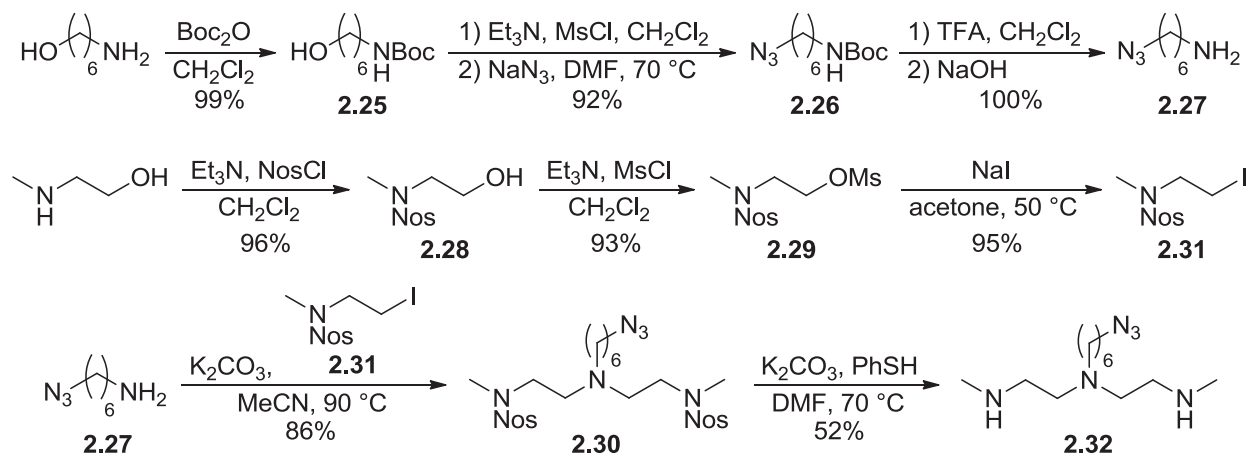


Scheme 2.8. Synthetic approach to polyammonium macrocyclization step to produce azide-tagged polyamines such as heptaazamacrocycle **2.24**.

interested in synthesizing a heptaazamacrocycle since such structures have been shown to strongly bind multiple phosphate groups.^{13b}

The modular building block approach to access azide-tagged polyammonium macrocycles started with the synthesis of azidohexyl heptaazamacrocycle **2.24**. This method involved a slight modification of the traditional Richman–Atkins cyclization protocol⁸⁷ by employing nosylamine alkylation (Scheme 2.8). A similar strategy was used to access numerous functionalized macrocycles by using tosylamine groups, although strongly acidic conditions were employed for tosyl deprotection.⁸⁸ Target **2.24** has two methylated nitrogen atoms in order to prevent multiple amine alkylations in the later stages of the synthesis.

The sequence started with the *tert*-butoxycarbonyl (Boc) protection of 6-aminohexanol (Scheme 2.9). Mesityl introduction to product **2.25** followed by direct azide substitution to **2.26** and Boc deprotection led to 6-azidohexylamine **2.27**. Next, 2-(methylamino)ethanol was protected using the nosyl group to form **2.28**, followed by *O*-mesylation to **2.29**. Initially, this mesylate was set to react with the trifluoroacetate salt

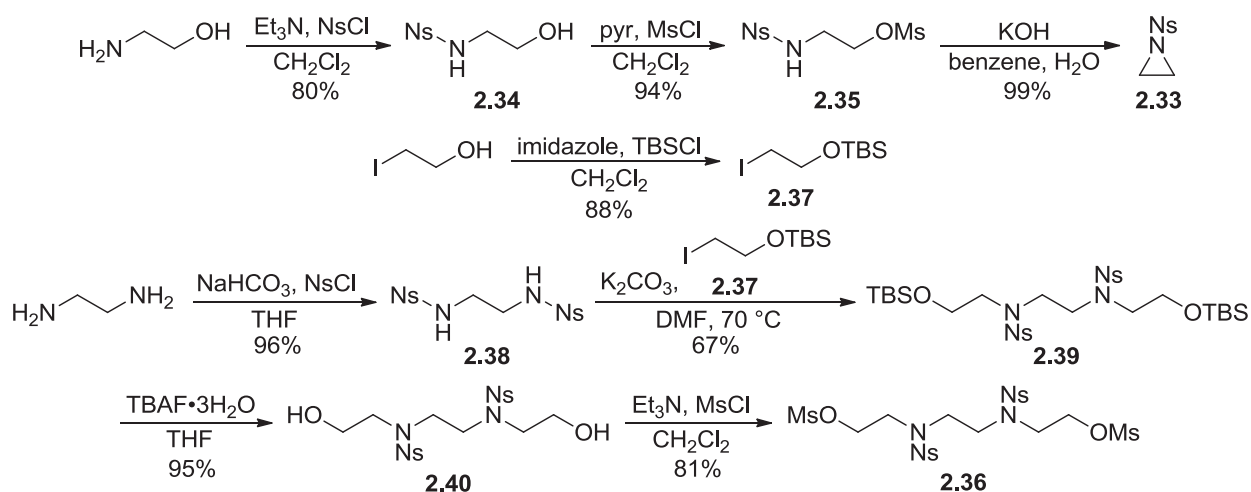


Scheme 2.9. Synthetic route to triamine intermediate **2.32**.

of amine **2.27** to yield adduct **2.30**. However, the reaction failed to give any clean product. Some mesylate starting material and precursor alcohol **2.28** were recovered. To improve the leaving group, sodium iodide and potassium carbonate were then added to the mesylate in order to form the iodide derivative **2.31** in situ, but still had no effect. After similar attempts of the reaction using the tosylate analog of **2.29** were still unsuccessful, iodide **2.31** was synthesized separately. The observed low reactivity may also have been due to the trifluoroacetate salt form of amine **2.27**. The salt could become hydrated, making alkylations more difficult. As a result, amine **2.27** was extracted in base to yield its more reactive free amine form. The reaction then finally succeeded after heating **2.27** and iodide **2.31** in acetonitrile at 90 °C for two days to afford **2.30**. The *N*-methyl groups were specifically included to avoid aziridine formation in **2.29** and **2.31** and limit the forthcoming triamine **2.32** to single alkylations.

The ensuing nosyl deprotection step proved to be fairly problematic. After initially choosing mercaptoacetic acid as the deprotecting thiol reagent turned out to be ineffective, using thiophenol instead led to formation of triamine unit **2.32**. Unfortunately, most attempts led to mixtures containing product, a partially deprotected byproduct, and unreacted thiophenol. While the thiophenol was removed using *N*-phenylmaleimide in basic solution, the partially deprotected byproduct could not be separated from the product on a C18 reversed-phase column with gradient elution from 0 to 100% methanol/water.

Having made small amounts of reasonably pure intermediate **2.32**, other building blocks for the alkylation and cyclization steps were synthesized (Scheme 2.10).

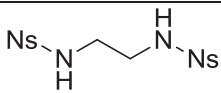
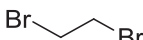
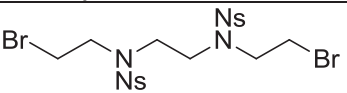
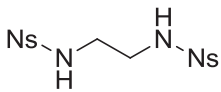
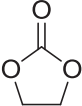
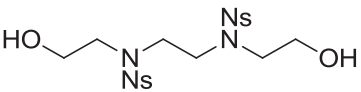
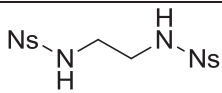
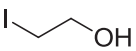
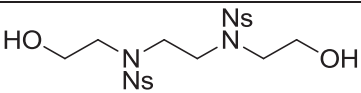


Scheme 2.10. Syntheses of *N*-nosylaziridine **2.33** and bis(mesylate) **2.36**.

Nosylaziridine **2.33** was accessed using a modified known sequence of procedures⁸⁹ starting with the *N*-nosylation of ethanolamine to **2.34**. *O*-mesylation to **2.35** followed where the choice of base was crucial. The literature report used triethylamine which in our case resulted in the mesylation of both the nitrogen and the oxygen in the major product. Changing the base to pyridine gave the intended *O*-mesylate in good yield. Finally, cyclization in base was expected to yield aziridine **2.33**. Initially, this reaction was ineffective due to apparent polymerization. To avoid this problem, catalytic amounts of 4-*tert*-butylcatechol, which had previously been used for *N*-tosylaziridine,⁹⁰ were added during workup to generate pure **2.33**.

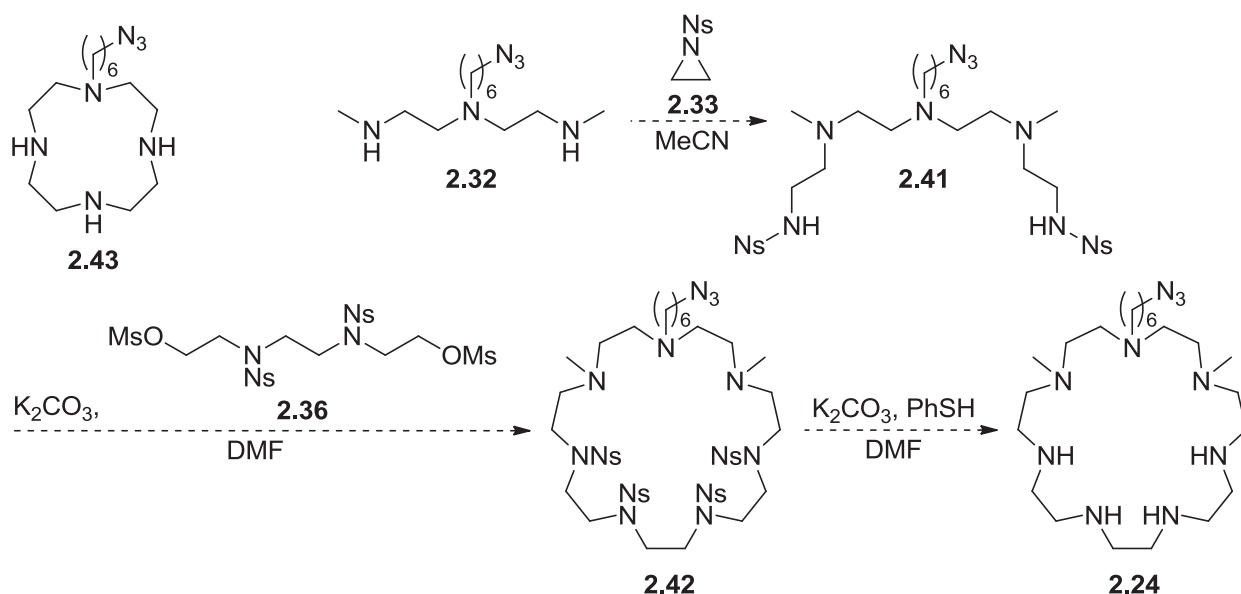
Next, the synthesis focused on cyclization piece **2.36**. Initially, various attempts were made without using protecting groups but were ineffective (Table 2.4). As a consequence, a protecting group seemed essential in this case. First, 2-iodoethanol was protected using the *tert*-butyldimethylsilyl (TBS) group to form **2.37**,⁹¹ and *N*-nosylation of ethylenediamine led to **2.38**.⁹² These two products were then combined to

Table 2.4. Alkylation attempts of diamine **2.38**.

| Diamine | Base | Electrophile | Expected Product | Result |
|---|--------------------------------|---|--|-------------------|
|  | K ₂ CO ₃ |  |  | Diamine recovered |
|  | K ₂ CO ₃ |  |  | Diamine recovered |
|  | K ₂ CO ₃ |  |  | Diamine recovered |

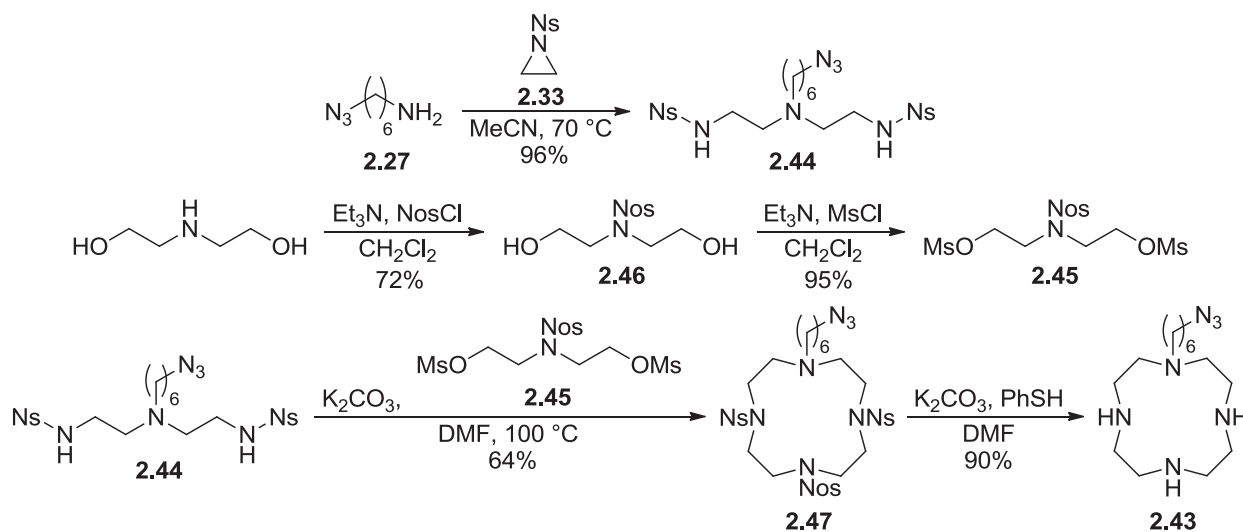
yield **2.39**, followed by deprotection of the silyl groups with tetrabutylammonium fluoride (TBAF) to diol **2.40**. Finally, O-mesylation gave product **2.36**.

The remainder of the proposed synthetic route to macrocycle **2.24** (Scheme 2.11) consisted of coupling of triamine **2.32** with aziridine **2.33** to form pentamine **2.41**, followed by cyclization with bis(mesyate) **2.36** to protected macrocycle **2.42**. Deprotection using thiophenol would then lead to final product **2.24**. Unfortunately, the triamine–aziridine coupling reaction failed to give any clean product. In repeated attempts, thin layer chromatography showed two to three spots that did not match the starting materials or the expected product based on the ¹H nuclear magnetic resonance (NMR) spectra. The secondary amine groups of triamine **2.32** appeared to be difficult to alkylate besides already causing purification problems earlier due to their high polarity. With no amounts of clean triamine precursor remaining, we tested this strategy on the synthesis of a smaller macrocycle, azide-tagged cyclen **2.43**.



Scheme 2.11. Azide-tagged cyclen **2.43** and planned synthetic route towards macrocycle **2.24**.

The synthesis of cyclen **2.43** (Scheme 2.12) started with the coupling of the previously made amine **2.27** with aziridine **2.33** to generate azide-labeled cyclization precursor **2.44**. Unlike the reaction to form pentamine **2.41**, there were no problems in alkylating the more reactive primary amine. The complementary cyclization component **2.45** was obtained according to a literature procedure⁹³ from *N*-nosylation of



Scheme 2.12. Synthesis of azide-tagged cyclen **2.43**.

diethanolamine to form **2.46**, followed by *O*-mesylation. The cyclization pieces were then combined to produce protected macrocycle **2.47**, followed by global deprotection using thiophenol to give azide-tagged cyclen **2.43**.

While pure samples of final product **2.43** have been successfully prepared, the deprotection step at the end suffered from low reproducibility. Mixtures of partially deprotected byproducts and low product yields were frequently encountered. Attempts to purify the mixtures on a C18 reversed-phase column with gradient elution from 0 to 100% methanol/water mostly failed to isolate the completely deprotected cyclen product. Consequently, an alternative synthetic strategy had to be pursued, as was described for our final host structure at the beginning of this chapter.

Even though we did not manage to form an azide-tagged heptaazamacrocycle, we did successfully synthesize the smaller cyclen analog. The crucial steps that were problematic turned out to be the nosyl group deprotections and the polyamine alkylations. These key reactions highlight the complexity that remains in the synthesis of functionalized polyammonium macrocycles. Based on our findings, we learned that it seemed better to introduce a functionalized tag such as an azide or alkyne during a later stage of the synthesis, as shown in our previously discussed acridine host.

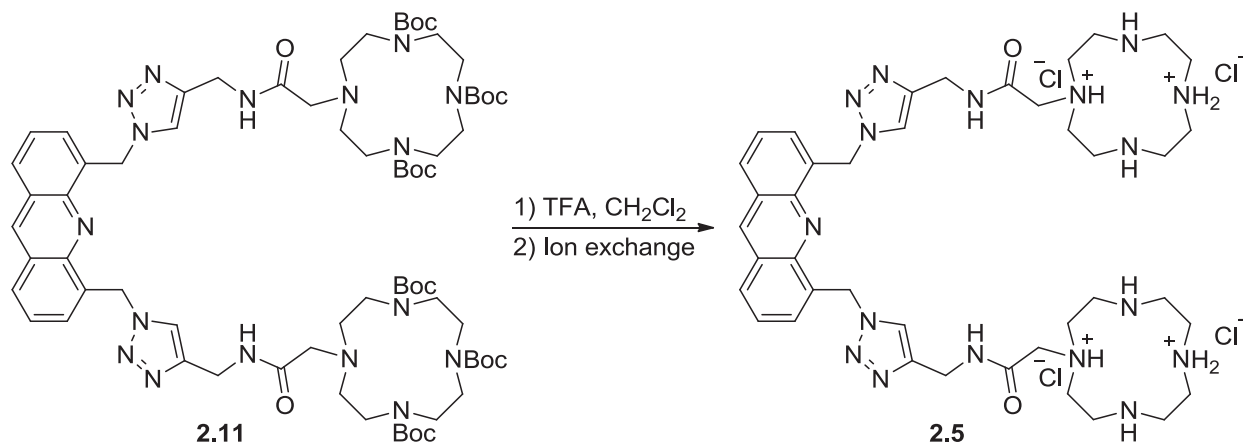
2.10 Experimental

General Considerations

Generally, reagents were purchased from Acros, Aldrich, or AK Scientific and used as received. Dry solvents were obtained from a Pure Solv solvent delivery system purchased from Innovative Technology, Inc. Grignard and organolithium reagent solutions were titrated with either 1,3-diphenylacetone *p*-tosylhydrazone⁹⁴ or *N*-benzylbenzamide⁹⁵ to assess concentration prior to use. Column chromatography was performed using 230–400 mesh silica gel purchased from Sorbent Technologies. Chloride counteranion ion exchange, as well as C18 reversed phase solid phase extraction (SPE) syringe columns were obtained from Silicycle. NMR spectra were obtained using a Bruker AC250 spectrometer updated with a Tecmag DSPECT data collection system, a Varian Mercury 300 spectrometer, a Bruker Avance 400 spectrometer, and a Varian 500 spectrometer. Mass spectra were obtained with a JEOL DART–AccuTOF spectrometer and an ABI Voyager DE Pro MALDI spectrometer with high resolution capabilities. UV–vis absorption spectra were obtained with a Thermo Evolution 600 UV–vis spectrophotometer, and fluorescence spectra were obtained with a Perkin Elmer LS 55 luminescence spectrometer. InsP₃ (**2.1**) used for binding studies was synthesized from protected inositol intermediates that we previously reported.⁷⁸

Procedures for Bis-Cyclen Tweezer Synthesis

N,N'-((1,1'-(acridine-4,5-diylbis(methylene))bis(1*H*-1,2,3-triazole-4,1-diyl))bis(methylene))bis(2-(1,4,7,10-tetraazacyclododecan-1-yl)acetamide) (**2.5**)



Trifluoroacetic acid (3 mL) was added dropwise to a solution of **2.11** (0.024 g, 0.017 mmol) in dichloromethane (3 mL) at rt. The reaction mixture was stirred at rt for 3 h, followed by concentration via rotary evaporation. The crude product was next dissolved in deionized water, loaded onto a chloride counteranion exchange column (0.5 g, Si-TMA chloride), and eluted with deionized water. Purification on a reversed-phase column (2 g, C18) with gradient elution from 0 to 50% methanol/water gave the product as a yellow solid (0.016 g, 98%).

¹H NMR (300 MHz, CD₃OD) δ 9.09 (s, 1H), 8.19 (d, *J* = 8.3 Hz, 2H), 8.04 (s, 2H), 7.78 (d, *J* = 6.6 Hz, 2H), 7.67–7.59 (m, 2H), 6.36 (s, 4H), 4.50 (s, 4H), 3.39 (s, 4H), 3.24–2.70 (m, 32H). ¹³C NMR (75 MHz, CD₃OD) δ 174.06, 147.03, 145.90, 138.48, 134.30, 132.21, 130.69, 127.88, 126.84, 124.95, 56.87, 51.73, 51.43, 47.85, 45.93, 44.25, 44.01, 35.76. MALDI–HRMS [*M*+HCl+H₂O+H]⁺ calcd: 878.5145, found: 878.5143.

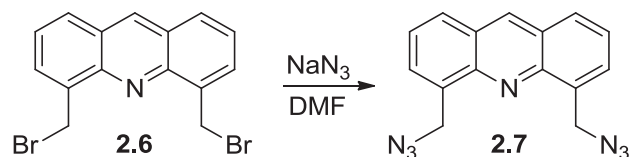
4,5-bis(bromomethyl)acridine (**2.6**)



Acridine (1.00 g, 5.49 mmol) was added to concentrated sulfuric acid (15 mL). The reaction mixture was heated to 50 °C, and bromomethyl methyl ether (1.99 mL, 21.97 mmol) was added. After stirring at 50 °C for 15 h, the reaction crude was poured into ice and stirred for 1 h. The mixture was then extracted with chloroform (2 × 40 mL), and the combined organic layers were dried over magnesium sulfate, filtered, and concentrated. Column chromatography over silica gel with gradient elution from 20 to 70% dichloromethane/hexanes gave the product as a light yellow solid (0.51 g, 25%). Characterizations matched those reported in the literature.⁷⁵

¹H NMR (300 MHz, CDCl₃) δ 8.77 (s, 1H), 7.96 (dd, *J* = 14.8, 7.7 Hz, 4H), 7.51 (dd, *J* = 8.5, 6.9 Hz, 2H), 5.43 (s, 4H). ¹³C NMR (63 MHz, CDCl₃) δ 145.77, 136.44, 131.09, 128.99, 126.80, 125.81, 119.96, 30.10.

4,5-bis(azidomethyl)acridine (**2.7**)

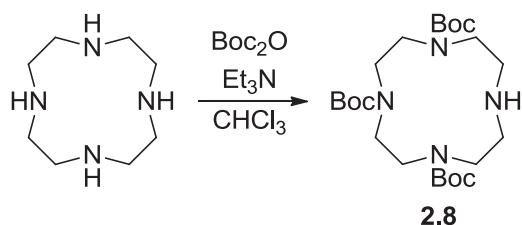


Sodium azide (0.51 g, 7.82 mmol) was added to a solution of **2.6** (0.48 g, 1.30 mmol) in *N,N*-dimethylformamide (20 mL) at rt. The reaction mixture was then heated to 80 °C and allowed to stir overnight. The reaction crude was then filtered, and the filtrate was

concentrated by rotary evaporation. Column chromatography over silica gel with gradient elution from 20 to 100% dichloromethane/hexanes gave the product as a light yellow solid (0.33 g, 87%).

^1H NMR (300 MHz, CDCl_3) δ 8.72 (s, 1H), 7.94 (d, J = 8.5 Hz, 2H), 7.78 (d, J = 6.8 Hz, 2H), 7.52 (dd, J = 8.5, 6.8 Hz, 2H), 5.20 (s, 4H). ^{13}C NMR (75 MHz, CDCl_3) δ 146.43, 136.59, 134.41, 129.77, 128.61, 126.60, 125.67, 51.49. DART-HRMS $[\text{M}+\text{H}]^+$ calcd: 290.1154, found: 290.1074.

1,4,7-tris(*tert*-butyloxycarbonyl)-1,4,7,10-tetraazacyclododecane (2.8)

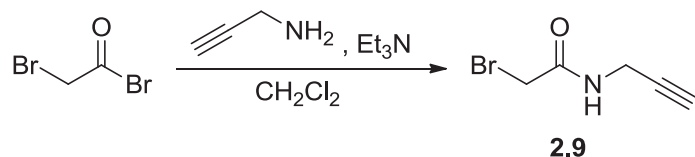


A solution of di-*tert*-butyl dicarbonate (1.77 g, 8.12 mmol) in chloroform (10 mL) was added slowly via addition funnel to a solution of cyclen (0.51 g, 2.90 mmol) and triethylamine (1.25 mL, 8.99 mmol) in chloroform (40 mL) at rt. The reaction mixture was stirred at rt overnight and then concentrated through rotary evaporation. The resulting residue was purified by column chromatography over silica gel with gradient elution from ethyl acetate to 5% methanol/dichloromethane to yield the product as a white solid (1.02 g, 80%).

Characterizations matched those reported in the literature.⁷⁶

^1H NMR (300 MHz, CDCl_3) δ 3.73–3.55 (m, 4H), 3.45–3.20 (m, 8H), 2.92–2.79 (m, 4H), 1.47 (s, 9H), 1.45 (s, 18H). ^{13}C NMR (63 MHz, CDCl_3) δ 155.69, 155.44, 79.40, 79.19, 50.97, 49.49, 45.95, 45.07, 28.69, 28.51.

2-bromo-*N*-(propargyl)acetamide (2.9)

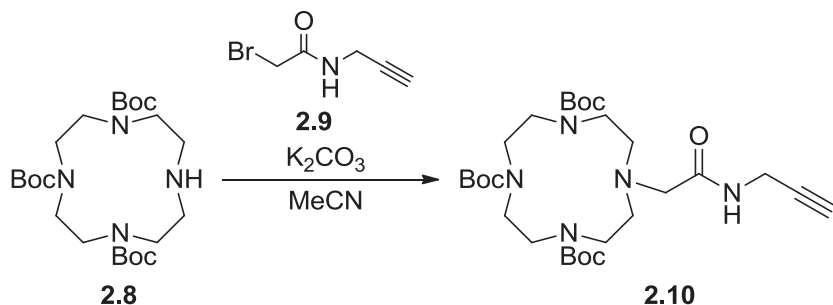


Propargylamine (0.36 mL, 5.61 mmol) and triethylamine (0.78 mL, 5.61 mmol) were added to a solution of bromoacetyl bromide (0.50 mL, 5.61 mmol) in dichloromethane (25 mL) at 0 °C. After stirring at 0 °C for 1 h, the reaction mixture was concentrated through rotary evaporation, resuspended in ethyl acetate (50 mL), and then filtered through a pad of silica gel. The filtrate was then concentrated to provide the product as a dark orange solid (0.96 g, 98%).

Characterizations matched those reported in the literature.⁷⁷

^1H NMR (300 MHz, CDCl_3) δ 6.70 (bs, 1H), 4.10 (dd, $J = 5.3, 2.6$ Hz, 2H), 3.91 (s, 2H), 2.29 (t, $J = 2.6$ Hz, 1H).

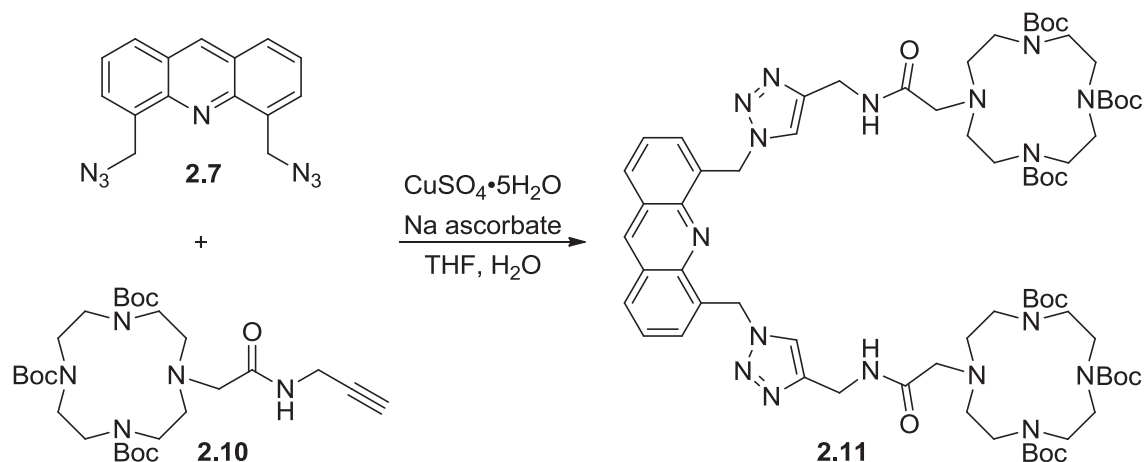
***N*-(propargyl)-1,4,7-tris(tert-butyloxycarbonyl)-1,4,7,10-tetraazacyclododecan-10-yl-acetamide (2.10)**



A solution of **2.9** (0.19 g, 1.06 mmol) in acetonitrile (5 mL) was added to a solution of **2.8** (0.34 g, 0.71 mmol) in acetonitrile (20 mL) at rt. Anhydrous potassium carbonate (0.15 g, 1.06 mmol) was then added, and the reaction mixture heated to 80 °C, at which it was stirred for 2 days. The mixture was then filtered, followed by concentration of the filtrate by rotary evaporation. Column chromatography over silica gel with gradient elution from 50 to 100% ethyl acetate/hexanes then provided the product as a white solid (0.37 g, 92%).

¹H NMR (300 MHz, CDCl₃) δ 7.16 (bs, 1H), 4.05–3.98 (m, 2H), 3.71–3.11 (m, 14H), 2.92–2.45 (m, 4H), 2.18 (s, 1H), 1.51–1.43 (m, 27H). ¹³C NMR (75 MHz, CDCl₃) δ 170.72, 155.52, 79.88, 79.18, 71.18, 58.19, 56.22, 50.95, 49.78, 28.50. DART–HRMS [M+H]⁺ calcd: 568.3710, found: 568.3605.

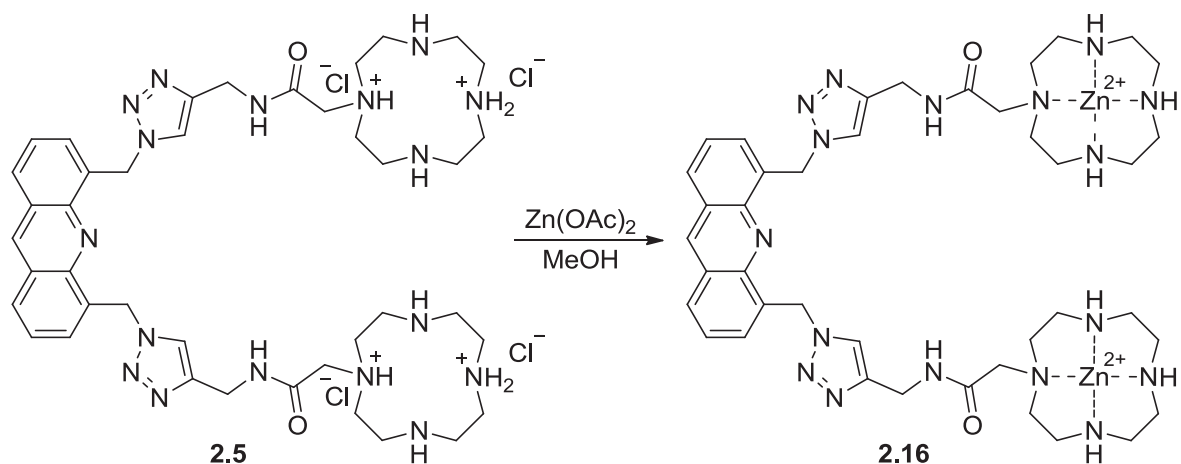
hexa-*tert*-butyl 10,10'-((((1,1'-(acridine-4,5-diylbis(methylene))bis(1*H*-1,2,3-triazole-4,1-diyl))bis(methylene))bis(azanediyl))bis(2-oxoethane-2,1-diyl))bis(1,4,7,10-tetraazacyclododecane-1,4,7-tricarboxylate) (**2.11**)



A solution of alkyne **2.10** (0.084 g, 0.15 mmol) in tetrahydrofuran (1 mL) was added to a solution of bis-azide **2.7** (0.021 g, 0.074 mmol) in tetrahydrofuran (1 mL) at rt. Copper sulfate pentahydrate (0.0092 g, 0.037 mmol), sodium ascorbate (0.037 g, 0.19 mmol), and water (2 mL) were then added, and the reaction mixture was stirred at rt overnight. After the addition of water (20 mL), the mixture was extracted with dichloromethane (2 × 20 mL). The combined organic layers were then dried over magnesium sulfate, filtered, and concentrated. Column chromatography over silica gel with gradient elution from 3 to 10% methanol/dichloromethane provided the product as a pale yellow solid (0.058 g, 55%).

^1H NMR (300 MHz, CDCl_3) δ 8.82 (s, 1H), 8.03 (d, $J = 8.5$ Hz, 2H), 7.82 (s, 2H), 7.71 (d, $J = 6.2$ Hz, 2H), 7.58–7.49 (m, 2H), 7.37 (s, 2H), 6.30 (s, 4H), 4.45 (d, $J = 5.0$ Hz, 4H), 3.52–3.00 (m, 28H), 2.62 (s, 8H), 1.52–1.30 (m, 54H). ^{13}C NMR (75 MHz, CDCl_3) δ 170.98, 167.27, 146.06, 137.11, 129.30, 126.60, 125.78, 79.80, 50.45, 47.88, 34.97, 28.43. MALDI–HRMS $[\text{M}+\text{Na}]^+$ calcd: 1446.8238, found: 1446.8245.

Zinc(II) complex (2.16)



Zinc acetate (0.008 g, 0.044 mmol) was added to a solution of **2.5** (0.021 g, 0.022 mmol) in methanol (5 mL). The reaction mixture was stirred at 50 °C overnight, followed by concentration via rotary evaporation to obtain the complex as a light yellow solid of tetraacetate salts (0.026 g, 100%).

^1H NMR (300 MHz, CD_3OD) δ 9.11 (s, 1H), 8.21 (d, J = 8.8 Hz, 2H), 8.06–7.90 (m, 2H), 7.90–7.76 (m, 2H), 7.69–7.60 (m, 2H), 6.34 (s, 4H), 4.49 (s, 4H), 3.45 (s, 4H), 3.04–2.62 (m, 32H). MALDI–HRMS $[\text{M}-3\text{H}]^+$ calcd: 952.3505, found: 952.3497.

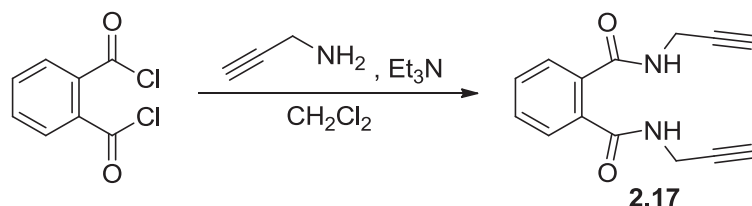
Procedure for Titration Binding Studies

All binding studies were conducted in a buffered solution of 50% methanol/water solution (50 mM Tris buffer, pH 7.4) formed by adding a 2X buffered aqueous solution to methanol. After obtaining an excitation spectrum of host (**2.5** or **2.16**), fluorescence experiments were performed through excitation at 355 nm at rt. In these studies, a 10 μM buffered solution of host (2 mL) was titrated stepwise with 25 μL aliquots of a buffered solution consisting of 10 μM host and 30 μM guest. After each addition, the

fluorescence spectra were recorded. The changes in fluorescence intensities at the emission λ_{max} (440 nm) were then plotted against the concentration of added guest. Binding constants were next determined by non-linear least squares analysis of the data using the SigmaPlot 11.0 data analysis and graphing program. Both a single-site saturation curve fit and a four-parameter sigmoidal curve fit were utilized, and both methods resulted in similar K_a values. It should be noted that binding curves exhibit some sigmoidal, or s-shaped, character in Figures 2.5 and 2.8. Sigmoidal properties typically indicate the presence of more than one equilibria or cooperativity.

Procedures for Alkyne Scaffold Synthesis

ortho-phthaloyl propargylamide (2.17)

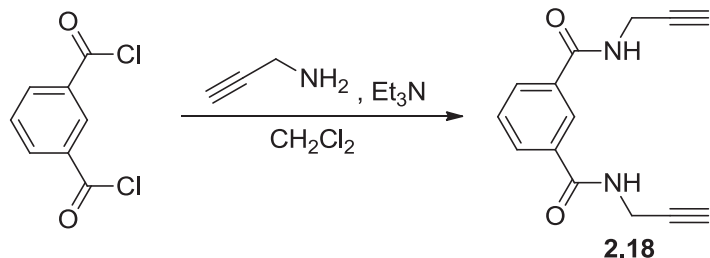


Propargylamine (0.14 mL, 2.19 mmol) and triethylamine (0.28 mL, 2.19 mmol) were added to a solution of *ortho*-phthaloyl chloride (0.16 mL, 0.99 mmol) in dichloromethane (10 mL) at 0 °C. The reaction mixture was stirred at 0 °C for 1 h and then concentrated. Column chromatography over silica gel with gradient elution from 3 to 7% methanol/dichloromethane provided the product as a white solid (0.21 g, 90%).

Characterizations matched those reported in the literature.⁷⁹

^1H NMR (300 MHz, CD_3OD) δ 7.56–7.53 (m, 4H), 4.12 (d, J = 2.6 Hz, 4H), 2.62 (t, J = 2.6 Hz, 2H).

isophthaloyl propargylamide (2.18)

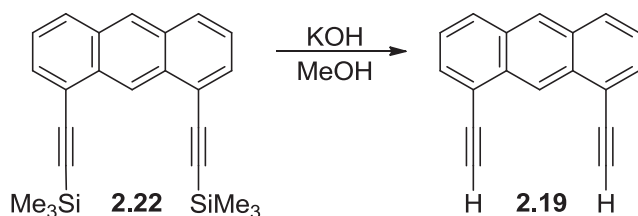


This compound was prepared, as described above, from isophthaloyl dichloride (0.21 g, 1.02 mmol), propargylamine (0.13 mL, 2.04 mmol), and triethylamine (0.28 mL, 2.00 mmol) as a white solid (0.22 g, 92%).

Characterizations matched those reported in the literature.^{79,96}

^1H NMR (300 MHz, CD_3OD) δ 8.33–8.27 (m, 1H), 7.99 (d, J = 7.8 Hz, 2H), 7.58 (t, J = 7.8 Hz, 1H), 4.17 (d, J = 2.5 Hz, 4H), 2.62 (t, J = 2.5 Hz, 2H).

1,8-diethynylantracene (2.19)

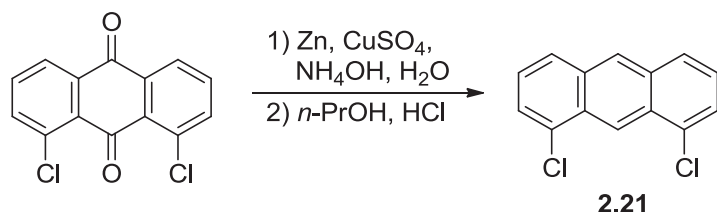


A 1 M aqueous potassium hydroxide solution (0.8 mL) was added to a solution of **2.22** (0.095 g, 0.26 mmol) in methanol (10 mL). The reaction mixture was stirred at rt overnight and then concentrated. Column chromatography over silica gel with gradient elution from 0 to 10% ethyl acetate/hexanes gave the product as a yellow solid (0.054 g, 93%).

Characterizations matched those reported in the literature.^{83a,84}

^1H NMR (300 MHz, CDCl_3) δ 9.43 (s, 1H), 8.44 (s, 1H), 8.02 (d, $J = 8.5$ Hz, 2H), 7.79 (d, $J = 6.9$ Hz, 2H), 7.45 (dd, $J = 8.5, 6.9$ Hz, 2H), 3.62 (s, 2H).

1,8-dichloroanthracene (2.21)



Zinc dust (26.96 g, 412.46 mmol) and copper(II) sulfate pentahydrate (0.14 g, 0.55 mmol) to a solution of 1,8-dichloroanthraquinone (8.02 g, 27.50 mmol) in water (216 mL) and ammonium hydroxide (84 mL). The reaction mixture was stirred at 80 °C for 6 h and then filtered. Acetone (200 mL) was added to the residue, and the mixture was stirred at rt for 30 min, followed by filtering and concentrating the filtrate. The residue was dissolved with hot 1-propanol (300 mL), and concentrated hydrochloric acid (1 mL) was added dropwise. The resulting precipitate was filtered and collected as yellow needles (5.19 g, 76%).

Characterizations matched those reported in the literature.^{82,97}

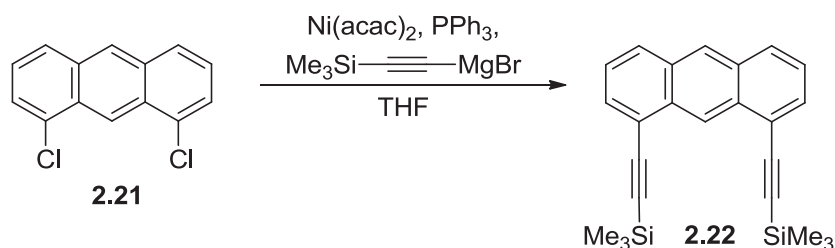
^1H NMR (300 MHz, CDCl_3) δ 9.24 (s, 1H), 8.46 (s, 1H), 7.93 (d, $J = 8.5$ Hz, 2H), 7.62 (d, $J = 7.2$ Hz, 2H), 7.41 (dd, $J = 8.5, 7.2$ Hz, 2H).

Titration of ethylmagnesium bromide with 1,3-diphenylacetone *p*-tosylhydrazone

Under argon, anhydrous tetrahydrofuran (10 mL) was added to 1,3-diphenylacetone *p*-tosylhydrazone (0.18 g, 0.47 mmol) via syringe. The solution was allowed to stir and

cooled to 0 °C. A solution of ethylmagnesium bromide in tetrahydrofuran was added via syringe dropwise until the mixture became consistently dark yellow. The volume of ethylmagnesium bromide solution added (0.70 mL) and the number of moles of titrating reagent were used to calculate the ethylmagnesium bromide solution concentration.

1,8-bis[(trimethylsilyl)ethynyl]anthracene (2.22)



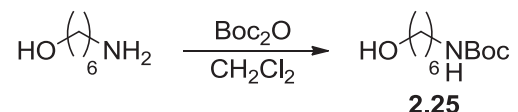
Under a nitrogen atmosphere, ethylmagnesium bromide (25.92 mL, 17.37 mmol, 0.67 M in tetrahydrofuran) was added to a solution of trimethylsilylacetylene (2.78 mL, 19.11 mmol) in anhydrous tetrahydrofuran (40 mL) at 0 °C. The mixture was stirred and allowed to warm up for 1.5 h. The resulting [(trimethylsilyl)ethynyl]magnesium bromide solution was then added to a solution of 1,8-dichloroanthracene (0.86 g, 3.47 mmol), nickel(II) acetylacetonate (0.009 g), and PPh_3 (0.018 g) in anhydrous tetrahydrofuran (10 mL). The reaction mixture was stirred at 70 °C for 2 days, after which it was extracted with chloroform (2 × 50 mL) from saturated ammonium chloride (50 mL). The combined organic layers were dried over magnesium sulfate, filtered, and concentrated. Column chromatography over silica gel with gradient elution from 5 to 20% dichloromethane/hexanes gave the product as a yellow solid (1.02 g, 79%).

Characterizations matched those reported in the literature.⁸³⁻⁸⁴

^1H NMR (300 MHz, CDCl_3) δ 9.33 (s, 1H), 8.42 (s, 1H), 7.98 (d, $J = 8.5$ Hz, 2H), 7.79 (d, $J = 6.9$ Hz, 2H), 7.42 (dd, $J = 8.5, 6.9$ Hz, 2H), 0.39 (s, 18H).

Procedures for Azide-Tagged Polyammonium Macrocycle Synthesis

tert-butyl (6-hydroxyhexyl)carbamate (**2.25**)

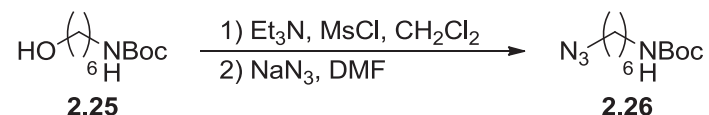


A solution of di-*tert*-butyl dicarbonate (2.72 g, 12.47 mmol) in dichloromethane (10 mL) was added slowly via addition funnel to a solution of 6-amino-1-hexanol (1.37 g, 11.34 mmol) in dichloromethane (30 mL) at rt. The reaction mixture was stirred at rt overnight and then extracted with dichloromethane (2 × 40 mL) from saturated aqueous ammonium chloride (40 mL). The combined organic layers were dried over magnesium sulfate, filtered, and concentrated to give the product as a yellow oil (2.43 g, 98%).

Characterizations matched those reported in the literature.⁹⁸

^1H NMR (300 MHz, CDCl_3) δ 4.55 (bs, 1H), 3.64 (q, $J = 6.3$ Hz, 2H), 3.12 (q, $J = 6.3$ Hz, 2H), 1.60–1.51 (m, 3H), 1.50–1.41 (m, 11H), 1.41–1.31 (m, 3H).

tert-butyl (6-azidohexyl)carbamate (**2.26**)



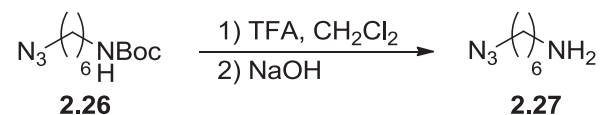
Methanesulfonyl chloride (0.22 mL, 2.79 mmol) was added to a solution of **2.25** (0.55 g, 2.54 mmol) and triethylamine (0.42 mL, 3.04 mmol) in dichloromethane (20 mL) at 0 °C.

After stirring at rt for 3 h, the reaction mixture was concentrated through rotary evaporation and resuspended in *N,N*-dimethylformamide (20 mL). Sodium azide (0.33 g, 5.07 mmol) was added to the mixture which was then heated to 70 °C and allowed to stir overnight. The reaction crude was then filtered, and the filtrate was concentrated by rotary evaporation. Column chromatography over silica gel with gradient elution from 15 to 30% ethyl acetate/hexanes gave the product as a colorless oil (0.57 g, 92%).

Characterizations matched those reported in the literature.^{98a}

¹H NMR (300 MHz, CDCl₃) δ 4.53 (bs, 1H), 3.27 (t, *J* = 6.9 Hz, 2H), 3.12 (q, *J* = 6.6 Hz, 2H), 1.67–1.54 (m, 2H), 1.54–1.41 (m, 12H), 1.41–1.28 (m, 3H).

6-azido-1-hexanamine (2.27)

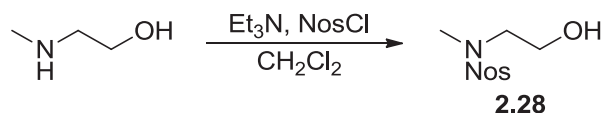


Trifluoroacetic acid (20 mL) was added dropwise to a solution of **2.26** (0.55 g, 2.26 mmol) in dichloromethane (20 mL) at rt. The reaction mixture was stirred at rt for 2 h, followed by concentration via rotary evaporation. The crude product was then extracted with dichloromethane (2 × 40 mL) from 1 M aqueous sodium hydroxide (40 mL). The combined organic layers were dried over magnesium sulfate, filtered, and concentrated to yield the product as a brown liquid (0.32 g, 100%).

Characterizations matched those reported in the literature.⁹⁹

¹H NMR (300 MHz, CDCl₃) δ 3.70 (bs, 2H), 3.27 (t, *J* = 6.9 Hz, 2H), 2.75 (t, *J* = 6.9 Hz, 2H), 1.66–1.46 (m, 4H), 1.45–1.33 (m, 4H).

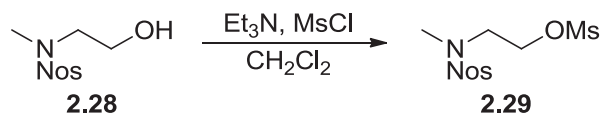
***N*-(2-hydroxyethyl)-*N*-methyl-4-nitrobenzenesulfonamide (2.28)**



A solution of 4-nitrobenzenesulfonyl chloride (1.05 g, 4.48 mmol) in dichloromethane (10 mL) was added dropwise to a solution of 2-(methylamino)ethanol (0.30 mL, 3.74 mmol) and triethylamine (0.63 mL, 4.48 mmol) in dichloromethane (20 mL) at 0 °C. The reaction mixture was stirred at rt overnight and then concentrated. Column chromatography over silica gel with gradient elution from 2 to 10% methanol/dichloromethane gave the product as a yellow solid (0.93 g, 96%).

¹H NMR (300 MHz, CDCl₃) δ 8.39 (d, *J* = 9.0 Hz, 2H), 8.01 (d, *J* = 9.0 Hz, 2H), 3.86–3.76 (m, 2H), 3.26 (t, *J* = 5.3 Hz, 2H), 2.92 (s, 3H), 2.06 (bs, 1H).

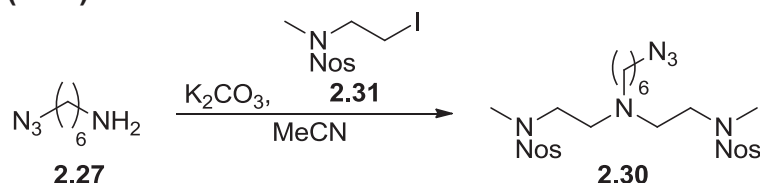
2-(*N*-methyl-4-nitrobenzenesulfonamido)ethyl methanesulfonate (2.29)



Methanesulfonyl chloride (0.71 mL, 8.92 mmol) was added to a solution of **2.28** (2.11 g, 8.10 mmol) and triethylamine (1.36 mL, 9.73 mmol) in dichloromethane (80 mL) at 0 °C. After stirring at rt for 3 h, the reaction mixture was extracted with dichloromethane (2 × 50 mL) from saturated aqueous sodium bicarbonate (50 mL). The combined organic layers were dried over magnesium sulfate, filtered, and concentrated. Column chromatography over silica gel with gradient elution from 3 to 10% methanol/dichloromethane gave the product as a yellow solid (2.54 g, 93%).

^1H NMR (300 MHz, CDCl_3) δ 8.41 (d, $J = 8.9$ Hz, 2H), 8.01 (d, $J = 8.9$ Hz, 2H), 4.40 (t, $J = 5.4$ Hz, 2H), 3.47 (t, $J = 5.4$ Hz, 2H), 3.08 (s, 3H), 2.94 (s, 3H).

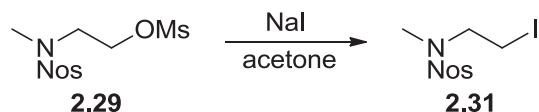
***N*-(6-azidohexyl)-*N,N*-bis[2-(*N*-methyl-4-nitrobenzenesulfonamido)ethyl]amine (2.30)**



Potassium carbonate (0.52 g, 3.76 mmol) and a solution of **2.27** (0.11 g, 0.75 mmol) in acetonitrile (5 mL) was added to a solution of **2.31** (0.70 g, 1.88 mmol) in acetonitrile (15 mL). The reaction mixture was stirred at 90 °C for 2 days and then concentrated. Column chromatography over silica gel with gradient elution from 1 to 5% methanol/dichloromethane gave the product as a yellow liquid (0.40 g, 86%).

^1H NMR (250 MHz, CDCl_3) δ 8.39 (d, $J = 8.7$ Hz, 4H), 8.00 (d, $J = 8.7$ Hz, 4H), 3.27 (t, $J = 6.7$ Hz, 2H), 3.15 (t, $J = 6.7$ Hz, 4H), 2.85 (s, 6H), 2.72 (t, $J = 6.7$ Hz, 4H), 2.50 (t, $J = 6.7$ Hz, 2H), 1.68–1.52 (m, 2H), 1.51–1.24 (m, 6H).

***N*-(2-iodoethyl)-*N*-methyl-4-nitrobenzenesulfonamide (2.31)**

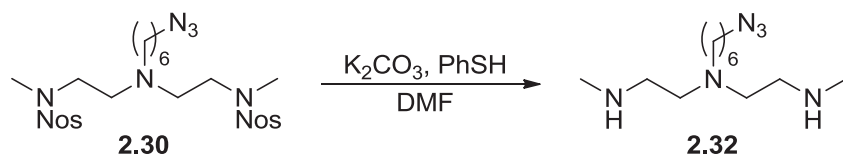


Sodium iodide (1.95 g, 13.02 mmol) was added to a solution of **2.29** (0.8811 g, 2.60 mmol) in acetone (80 mL). The reaction mixture was stirred at 50 °C overnight and then

concentrated. Column chromatography over silica gel with gradient elution from 25 to 35% ethyl acetate/hexanes gave the product as a light yellow solid (0.91 g, 95%).

^1H NMR (300 MHz, CDCl_3) δ 8.40 (d, $J = 9.0$ Hz, 2H), 8.01 (d, $J = 9.0$ Hz, 2H), 3.45 (t, $J = 7.5$ Hz, 2H), 3.27 (t, $J = 7.5$ Hz, 2H), 2.90 (s, 3H).

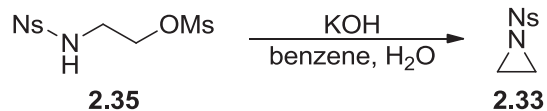
***N*-(6-azidohexyl)-*N,N*-bis(2-methylaminoethyl)amine (2.32)**



Potassium carbonate (0.39 g, 2.84 mmol) and thiophenol (0.10 mL, 0.95 mmol) were added to a solution of **2.30** (0.18 g, 0.28 mmol) in *N,N*-dimethylformamide (5 mL). The reaction mixture was stirred at 70 °C overnight and then concentrated by rotary evaporation. Glacial acetic acid (20 mL) was added, and the mixture was concentrated again. Purification on a reversed-phase column (2 g, C18) with gradient elution from 0 to 100% methanol/water yielded a crude product that was then extracted with chloroform (2 × 20 mL) from 1 M sodium hydroxide (20 mL). The combined organic layers were dried over magnesium sulfate, filtered, and concentrated to give the product as a yellow liquid (0.038 g, 52%).

^1H NMR (300 MHz, CDCl_3) δ 3.27 (t, $J = 6.9$ Hz, 2H), 2.66–2.52 (m, 6H), 2.48–2.36 (m, 8H), 2.06–1.86 (m, 2H), 1.68–1.53 (m, 2H), 1.50–1.25 (m, 6H).

***N*-(2-nitrobenzenesulfonyl)aziridine (2.33)**

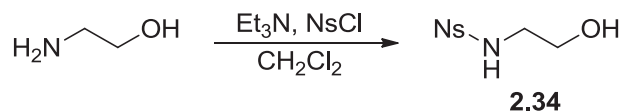


A solution of potassium hydroxide (0.78 g, 13.90 mmol) in water (10 mL) was added to a solution of **2.35** (0.90 g, 2.78 mmol) in benzene (30 mL). The reaction mixture was stirred at rt for 3 h and then extracted with dichloromethane (2 × 40 mL) from water (40 mL). The combined organic layers were dried over magnesium sulfate and filtered. A small amount of 4-*tert*-butylcatechol (0.25 g) was added to the filtrate which was then concentrated to yield the product as a yellow oil (0.63 g, 99%).

Characterizations matched those reported in the literature.⁸⁹

¹H NMR (300 MHz, CDCl₃) δ 8.25–8.17 (m, 1H), 7.83–7.71 (m, 3H), 2.63 (s, 4H).

***N*-(2-hydroxyethyl)-2-nitrobenzenesulfonamide (2.34)**

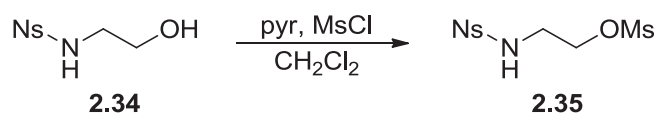


A solution of 2-nitrobenzenesulfonyl chloride (7.34 g, 33.14 mmol) in dichloromethane (10 mL) was added dropwise to a solution of ethanolamine (2.00 mL, 33.14 mmol) and triethylamine (1.57 mL, 11.30 mmol) in dichloromethane (40 mL) at 0 °C. The reaction mixture was stirred at rt overnight and then extracted with dichloromethane (2 × 40 mL) from 1 M hydrochloric acid (40 mL). The combined organic layers were dried over magnesium sulfate, filtered, and concentrated. Column chromatography over silica gel

with gradient elution from 3 to 10% methanol/dichloromethane gave the product as a light yellow solid (6.92 g, 80%).

^1H NMR (300 MHz, CDCl_3) δ 8.19–8.11 (m, 1H), 7.93–7.84 (m, 1H), 7.79–7.72 (m, 2H), 3.76 (q, $J = 5.1$ Hz, 2H), 3.27 (q, $J = 5.1$ Hz, 2H), 1.87 (t, $J = 5.1$ Hz, 1H).

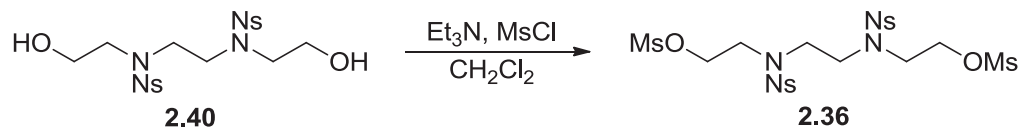
2-(2-nitrobenzenesulfonamido)ethyl methanesulfonate (2.35)



Methanesulfonyl chloride (0.63 mL, 8.16 mmol) was added to a solution of **2.34** (2.01 g, 8.16 mmol) and pyridine (0.79 mL, 9.79 mmol) in dichloromethane (80 mL) at 0 °C. After stirring at rt overnight, the reaction mixture was concentrated through rotary evaporation. Column chromatography over silica gel with gradient elution from 50 to 100% ethyl acetate/hexanes then provided the product as a white solid (2.49 g, 94%). Characterizations matched those reported in the literature.⁸⁹

^1H NMR (300 MHz, CDCl_3) δ 8.19–8.10 (m, 1H), 7.96–7.87 (m, 1H), 7.82–7.74 (m, 2H), 5.85 (t, $J = 5.9$ Hz, 1H), 4.31 (t, $J = 5.4$ Hz, 2H), 3.51 (q, $J = 5.4$ Hz, 2H), 3.03 (s, 1H).

1,2-bis[*N*-(2-methanesulfonyloxyethyl)-2-nitrobenzenesulfonamido]ethane (2.36)

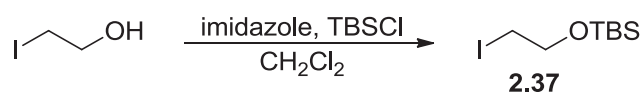


Methanesulfonyl chloride (0.061 mL, 0.77 mmol) was added to a solution of **2.40** (0.20 g, 0.39 mmol) and triethylamine (0.16 mL, 1.16 mmol) in dichloromethane (10 mL).

After stirring at rt for 3 h, the reaction mixture was concentrated by rotary evaporation. Column chromatography over silica gel with gradient elution from 2 to 5% methanol/dichloromethane gave the product (0.21 g, 81%).

^1H NMR (250 MHz, DMSO- d_6) δ 8.06–7.97 (m, 4H), 7.97–7.79 (m, 4H), 4.29 (t, J = 4.9 Hz, 4H), 3.69 (t, J = 4.9 Hz, 4H), 3.54 (s, 4H), 3.14 (s, 6H).

***tert*-butyl(2-iodoethoxy)dimethylsilane (2.37)**

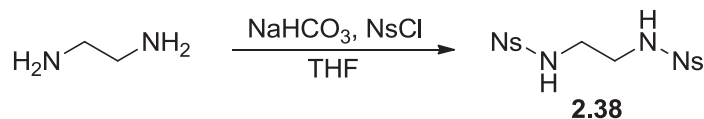


Imidazole (0.48 g, 7.05 mmol) and *tert*-butyldimethylsilyl chloride (1.08 g, 7.05 mmol) were added to a solution of 2-iodoethanol (0.50 mL, 6.41 mmol) in dichloromethane (15 mL). The reaction mixture was stirred at rt for 2 h and then extracted with dichloromethane (2 × 40 mL) from 0.5 M hydrochloric acid (40 mL). The combined organic layers were dried over magnesium sulfate, filtered, and concentrated to give the product as a colorless liquid (1.61 g, 88%).

Characterizations matched those reported in the literature.^{91,100}

^1H NMR (300 MHz, CDCl₃) δ 3.83 (t, J = 7.0 Hz, 2H), 3.20 (t, J = 7.0 Hz, 2H), 0.90 (s, 9H), 0.08 (s, 6H).

***N,N'*-bis(2-nitrobenzenesulfonyl)ethylenediamine (2.38)**

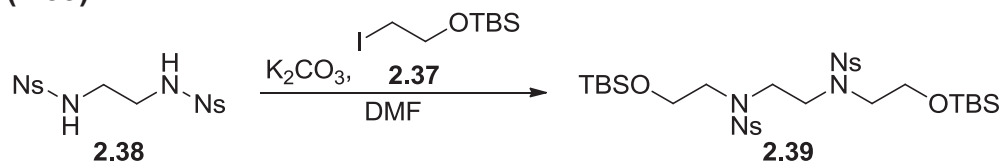


A solution of 2-nitrobenzenesulfonyl chloride (6.83 g, 29.88 mmol) in tetrahydrofuran (10 mL) was added to a solution of ethylenediamine (1.00 mL, 14.94 mmol) and sodium bicarbonate (2.64 g, 31.38 mmol) in tetrahydrofuran (40 mL). The reaction mixture was stirred at rt overnight and then extracted with dichloromethane (2 × 40 mL) from water (40 mL). The combined organic layers were dried over magnesium sulfate, filtered, and concentrated. Column chromatography over silica gel with gradient elution from 3 to 15% methanol/dichloromethane provided the product as a tan solid (6.15 g, 96%).

Characterizations matched those reported in the literature.⁹²

¹H NMR (300 MHz, DMSO-d₆) δ 8.14 (bs, 2H), 8.00–7.92 (m, 4H), 7.90–7.82 (m, 4H), 2.98 (s, 4H).

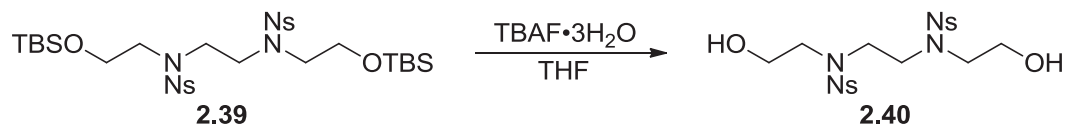
1,2-bis{N-[2-(tert-butyl dimethylsilyloxy)ethyl]-2-nitrobenzenesulfonamido}ethane (2.39)



Potassium carbonate (0.15 g, 1.06 mmol) and a solution of **2.37** (0.16 g, 0.54 mmol) in *N,N*-dimethylformamide (2 mL) were added to a solution of **2.38** (0.11 g, 0.25 mmol) in *N,N*-dimethylformamide (3 mL). The reaction mixture was stirred at 70 °C overnight and then concentrated. The residue was extracted with dichloromethane (2 × 20 mL) from water (20 mL), and the combined organic layers were dried over magnesium sulfate, filtered, and concentrated. Column chromatography over silica gel with gradient elution from 25 to 75% ethyl acetate/hexanes gave the product (0.12 g, 67%).

^1H NMR (300 MHz, CDCl_3) δ 8.08–8.00 (m, 2H), 7.73–7.60 (m, 6H), 3.73 (t, $J = 5.6$ Hz, 4H), 3.58 (s, 4H), 3.47 (t, $J = 5.6$ Hz, 4H), 0.83 (s, 18H), -0.01 (s, 12H).

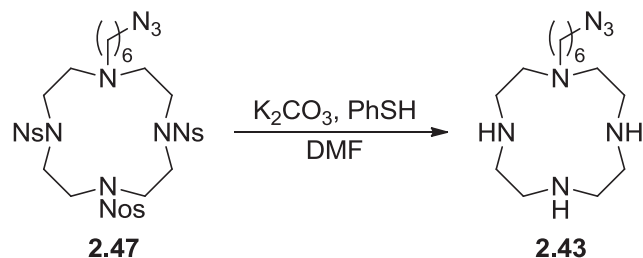
1,2-bis[*N*-(2-hydroxyethyl)-2-nitrobenzenesulfonylamido]ethane (**2.40**)



A solution of tetrabutylammonium fluoride trihydrate (0.62 g, 1.96 mmol) in tetrahydrofuran (5 mL) was added to a solution of **2.39** in tetrahydrofuran (10 mL). The reaction mixture was stirred at rt for 3 h and then extracted with dichloromethane (2 × 40 mL) from saturated aqueous ammonium chloride (40 mL). The combined organic layers were dried over magnesium sulfate, filtered, and concentrated. Column chromatography over silica gel with gradient elution from 2 to 10% methanol/dichloromethane provided the product (0.32 g, 95%).

^1H NMR (300 MHz, CDCl_3) δ 8.08–8.01 (m, 2H), 7.76–7.68 (m, 4H), 7.67–7.60 (m, 2H), 3.80 (t, $J = 5.0$ Hz, 4H), 3.65 (s, 4H), 3.51 (t, $J = 5.0$ Hz, 4H).

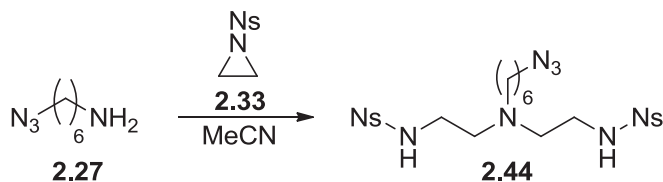
1-(6-azidoheptyl)-1,4,7,10-tetraazacyclododecane (**2.43**)



Potassium carbonate (0.15 g, 1.06 mmol) and thiophenol (0.11 mL, 1.06 mmol) were added to a solution of **2.47** (0.15 g, 0.18 mmol) in *N,N*-dimethylformamide (2 mL). After stirring at rt for 3 h, the reaction mixture was extracted with 2 M hydrochloric acid (30 mL) from dichloromethane (30 mL). The aqueous layer was basified with solid NaOH and then extracted with chloroform (2 × 30 mL). The combined organic layers were dried over magnesium sulfate, filtered, and concentrated to provide the product as a yellow oil (0.047 g, 90%).

¹H NMR (300 MHz, CDCl₃) δ 3.26–3.17 (m, 2H), 2.82–2.43 (m, 16H), 2.41 (t, *J* = 7.1 Hz, 2H), 1.61–1.50 (m, 2H), 1.49–1.24 (m, 6H).

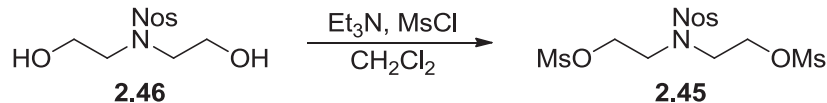
***N*-(6-azidohexyl)-*N,N*-bis[2-(2-nitrobenzenesulfonamido)ethyl]amine (2.44)**



A solution of **2.27** (0.10 g, 0.70 mmol) in acetonitrile (2 mL) was added to a solution of **2.33** (0.34 g, 1.48 mmol) in acetonitrile (8 mL). After stirring at 70 °C overnight, the reaction mixture was concentrated through rotary evaporation. Column chromatography over silica gel with gradient elution from 1 to 5% methanol/dichloromethane then yielded the product as a light brown oil (0.40 g, 96%).

¹H NMR (250 MHz, CDCl₃) δ 8.14–8.05 (m, 2H), 7.90–7.82 (m, 2H), 7.80–7.70 (m, 4H), 5.70 (bs, 2H), 3.25 (t, *J* = 6.8 Hz, 2H), 3.07 (t, *J* = 5.8 Hz, 4H), 2.58 (t, *J* = 5.8 Hz, 4H), 2.38–2.29 (m, 2H), 1.65–1.48 (m, 2H), 1.46–1.15 (m, 6H).

***N,N*-bis[(2-methanesulfonyloxy)ethyl]-4-nitrobenzenesulfonamide (2.45)**

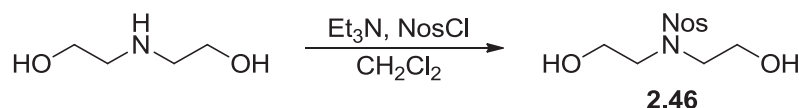


Methanesulfonyl chloride (0.58 mL, 7.47 mmol) was added to a solution of **2.46** (0.87 g, 2.99 mmol) and triethylamine (1.25 mL, 8.96 mmol) in dichloromethane (30 mL) at 0 °C. After stirring at rt for 5 h, the reaction mixture was extracted with dichloromethane (2 × 30 mL) from water (30 mL). The combined organic layers were dried over magnesium sulfate, filtered, and concentrated. Column chromatography over silica gel with gradient elution from 50 to 100% ethyl acetate/hexanes, then 5 to 7% methanol/dichloromethane gave the product as a white solid (1.26 g, 95%).

Characterizations matched those reported in the literature.⁹³

¹H NMR (300 MHz, DMSO-*d*₆) δ 8.40 (d, *J* = 8.9 Hz, 2H), 8.14 (d, *J* = 8.9 Hz, 2H), 4.31 (t, *J* = 5.5 Hz, 4H), 3.61 (t, *J* = 5.5 Hz, 4H), 3.17 (s, 6H).

***N,N*-bis(2-hydroxyethyl)-4-nitrobenzenesulfonamide (2.46)**



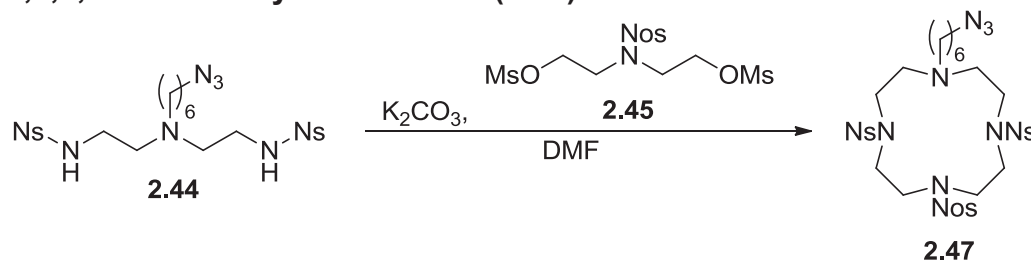
A solution of 4-nitrobenzenesulfonyl chloride (1.05 g, 4.75 mmol) in dichloromethane (10 mL) was added dropwise to a solution of diethanolamine (0.50 g, 4.75 mmol) and triethylamine (0.86 mL, 6.18 mmol) in dichloromethane (40 mL) at 0 °C. After stirring at rt overnight, the reaction mixture was concentrated through rotary evaporation. Column

chromatography over silica gel with gradient elution from 1 to 7% methanol/dichloro-
methane then gave the product as a white solid (0.98 g, 72%).

Characterizations matched those reported in the literature.⁹³

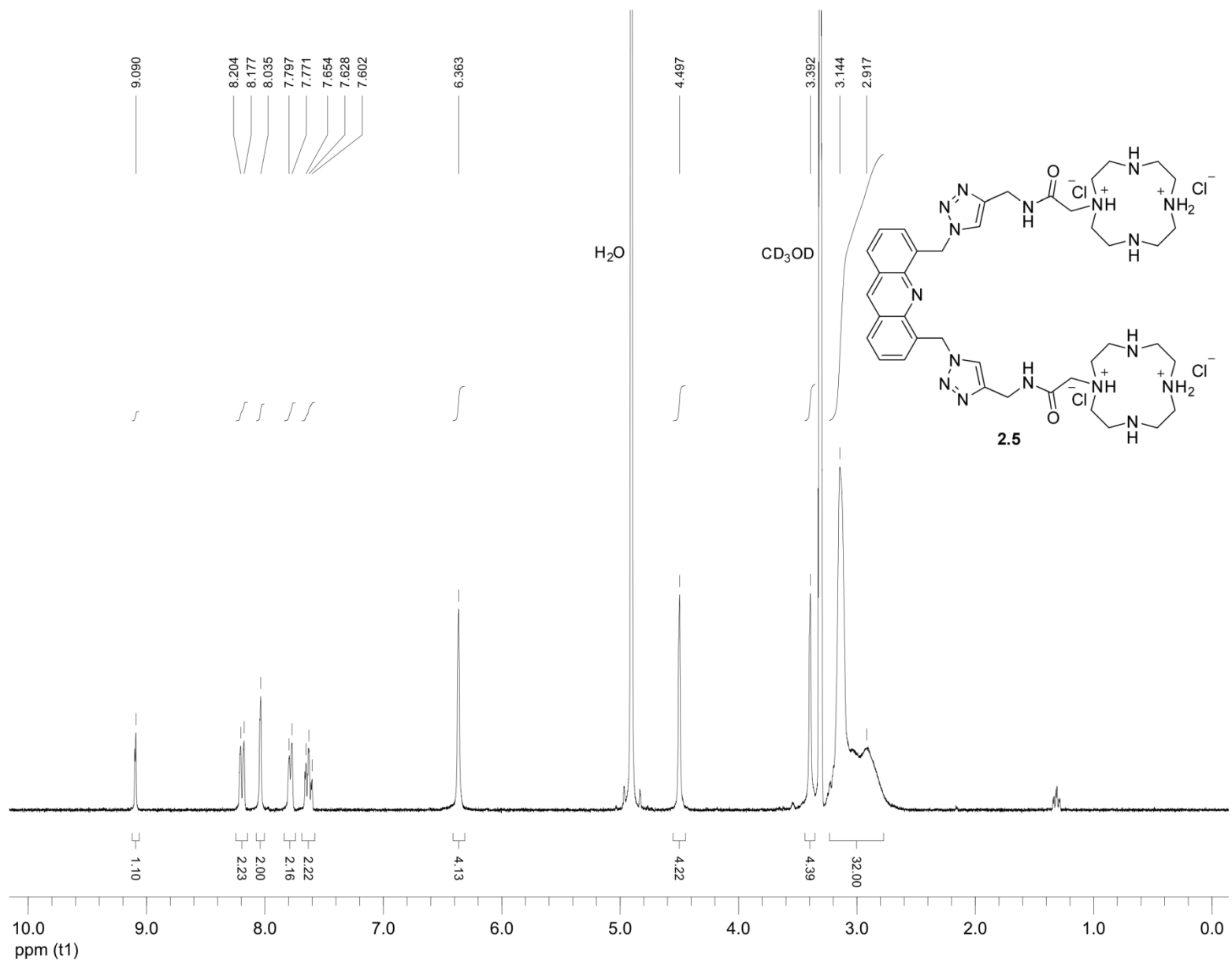
¹H NMR (300 MHz, DMSO-d₆) δ 8.39 (d, *J* = 9.0 Hz, 2H), 8.08 (d, *J* = 9.0 Hz, 2H), 4.84
(t, *J* = 5.4 Hz, 2H), 3.52 (q, *J* = 5.9 Hz, 4H), 3.24 (t, *J* = 6.2 Hz, 4H).

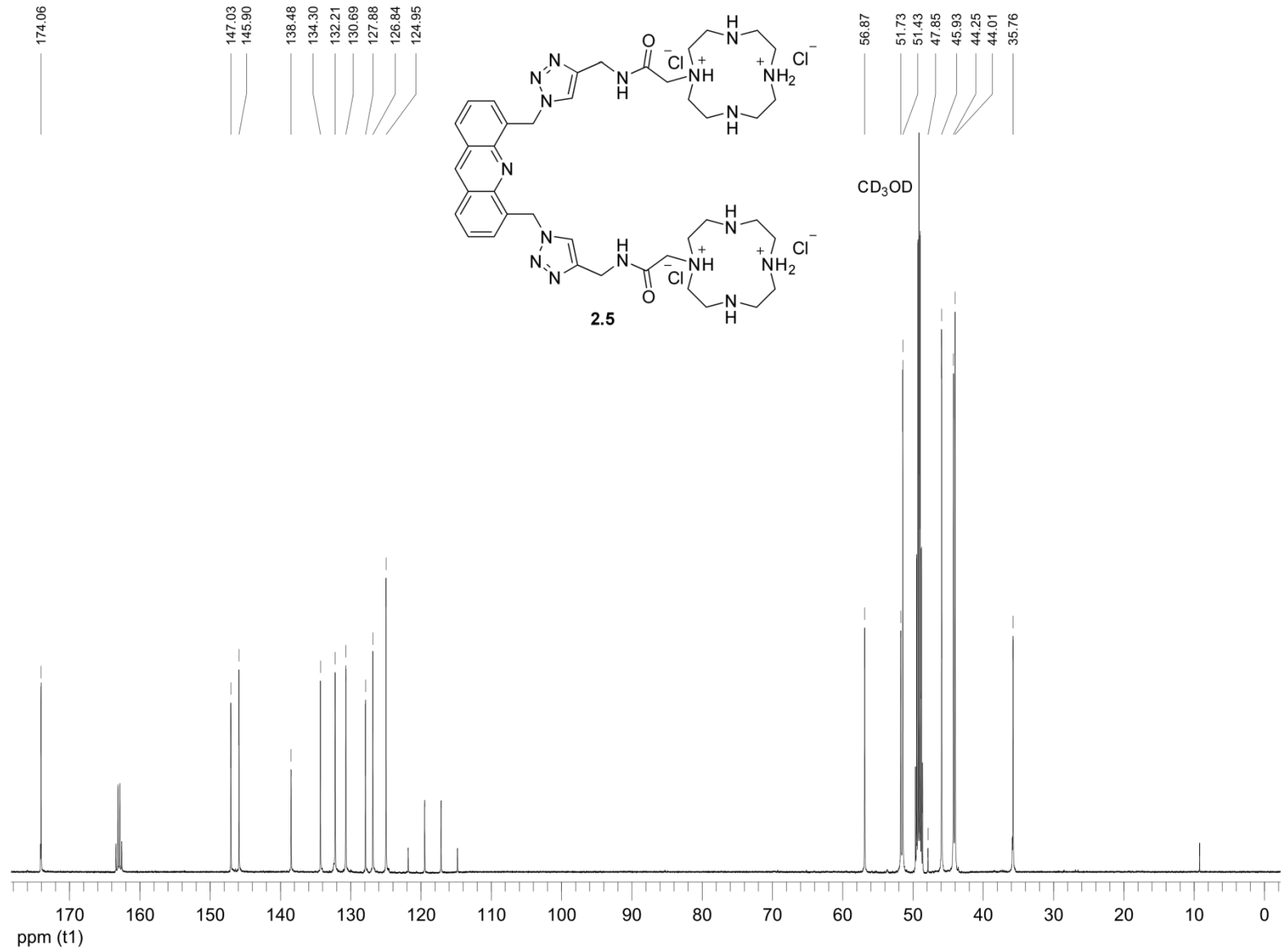
**1-(6-azidoheptyl)-4,10-bis(2-nitrobenzenesulfonyl)-7-(4-nitrobenzenesulfonyl)-
1,4,7,10-tetraazacyclododecane (2.47)**

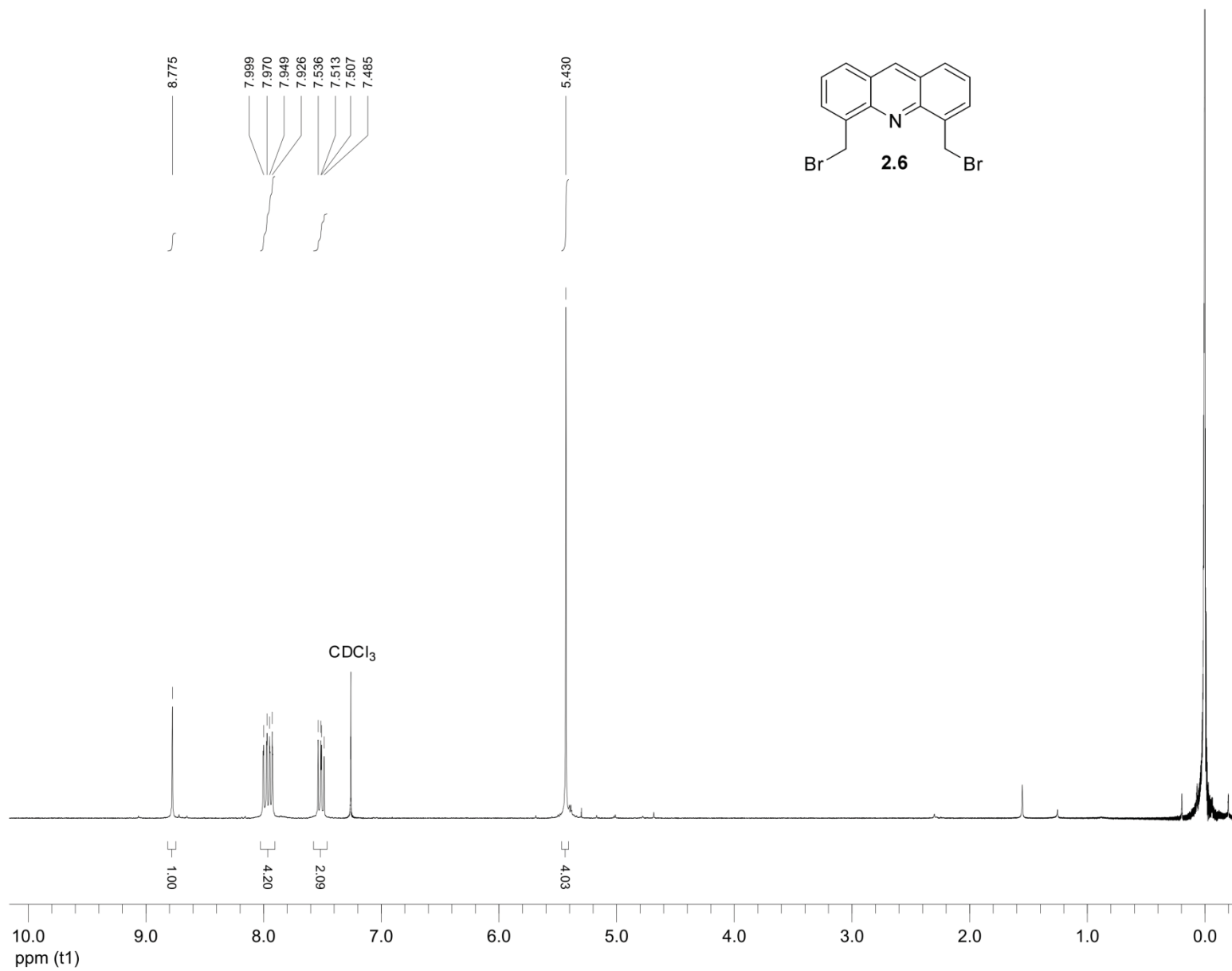


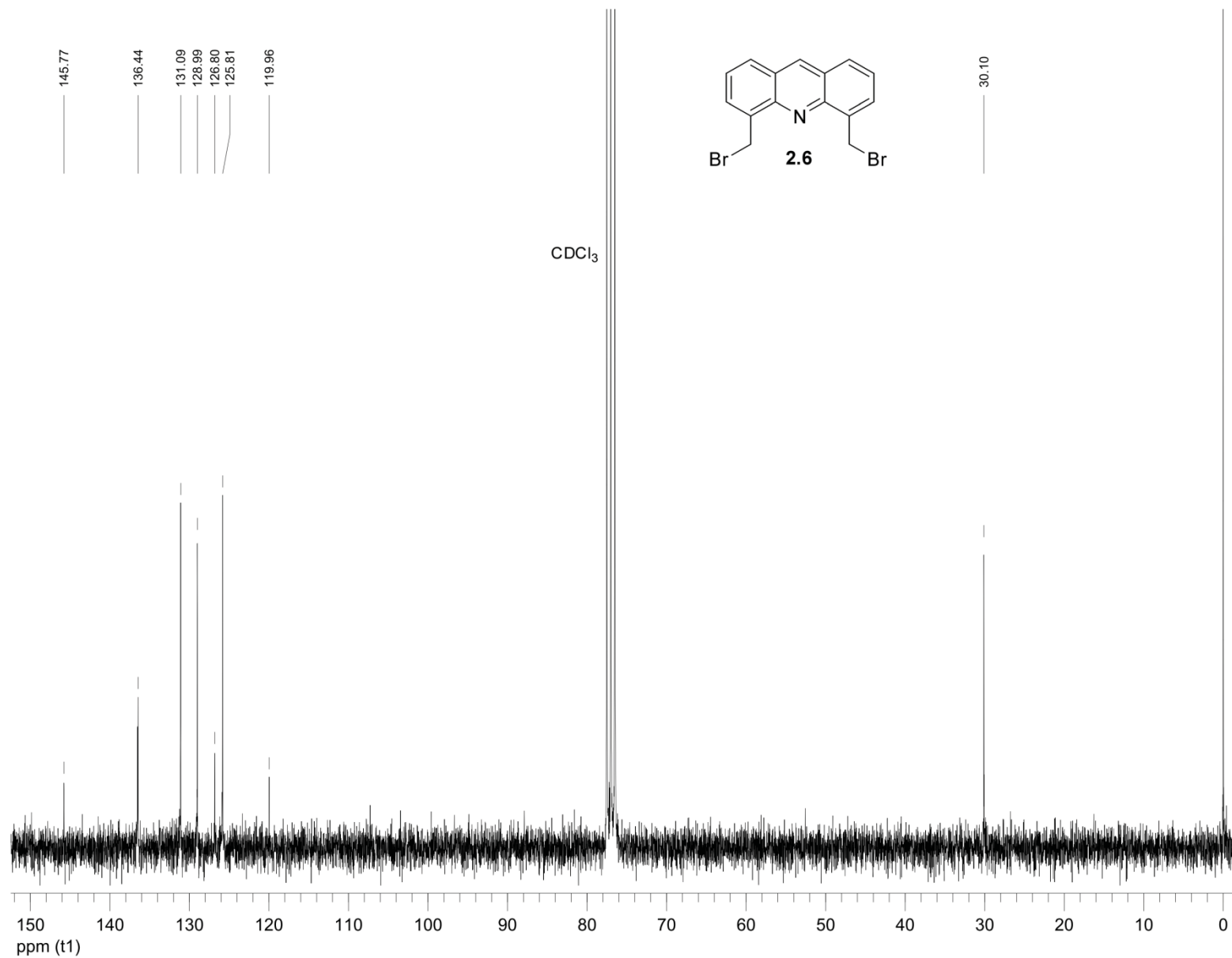
Mesylate **2.45** (0.042 g, 0.094 mmol) and potassium carbonate (0.065 g, 0.47 mmol) were added to a solution of **2.44** (0.056 g, 0.094 mmol) in *N,N*-dimethylformamide (5 mL). After stirring at 100 °C overnight, the reaction mixture was filtered and concentrated through rotary evaporation. Column chromatography over silica gel with gradient elution from 50 to 100% ethyl acetate/hexanes gave the product as a yellow solid (0.080 g, 64%).

¹H NMR (300 MHz, CDCl₃) δ 8.39 (d, *J* = 8.8 Hz, 2H), 8.07 (d, *J* = 8.8 Hz, 2H), 7.97–
7.89 (m, 2H), 7.77–7.69 (m, 4H), 7.66–7.59 (m, 2H), 3.78–3.68 (m, 4H), 3.58–3.48 (m,
4H), 3.39–3.30 (m, 4H), 3.26 (t, *J* = 6.6 Hz, 2H), 2.81–2.71 (m, 4H), 2.55–2.45 (m, 2H),
1.63–1.19 (m, 8H).

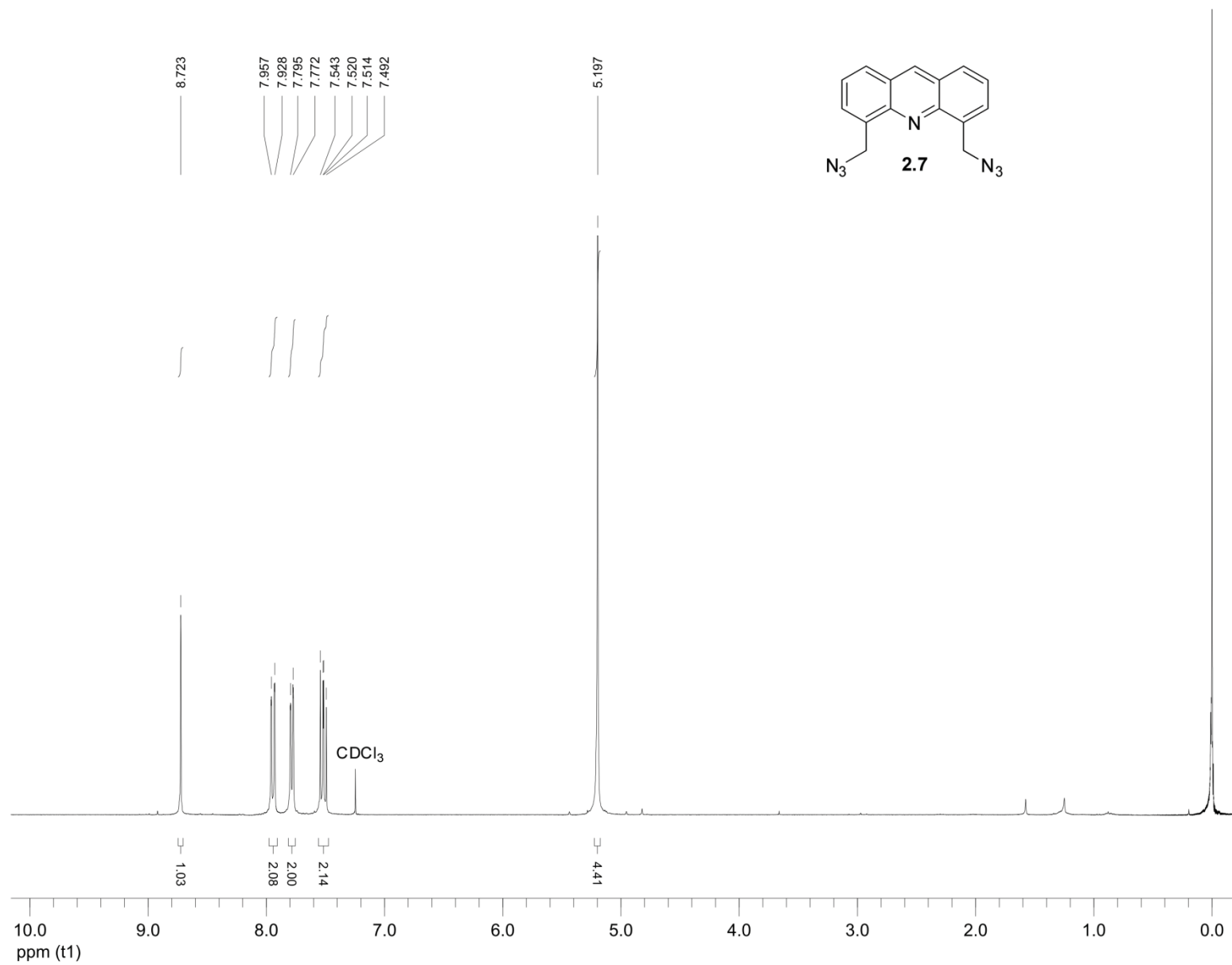


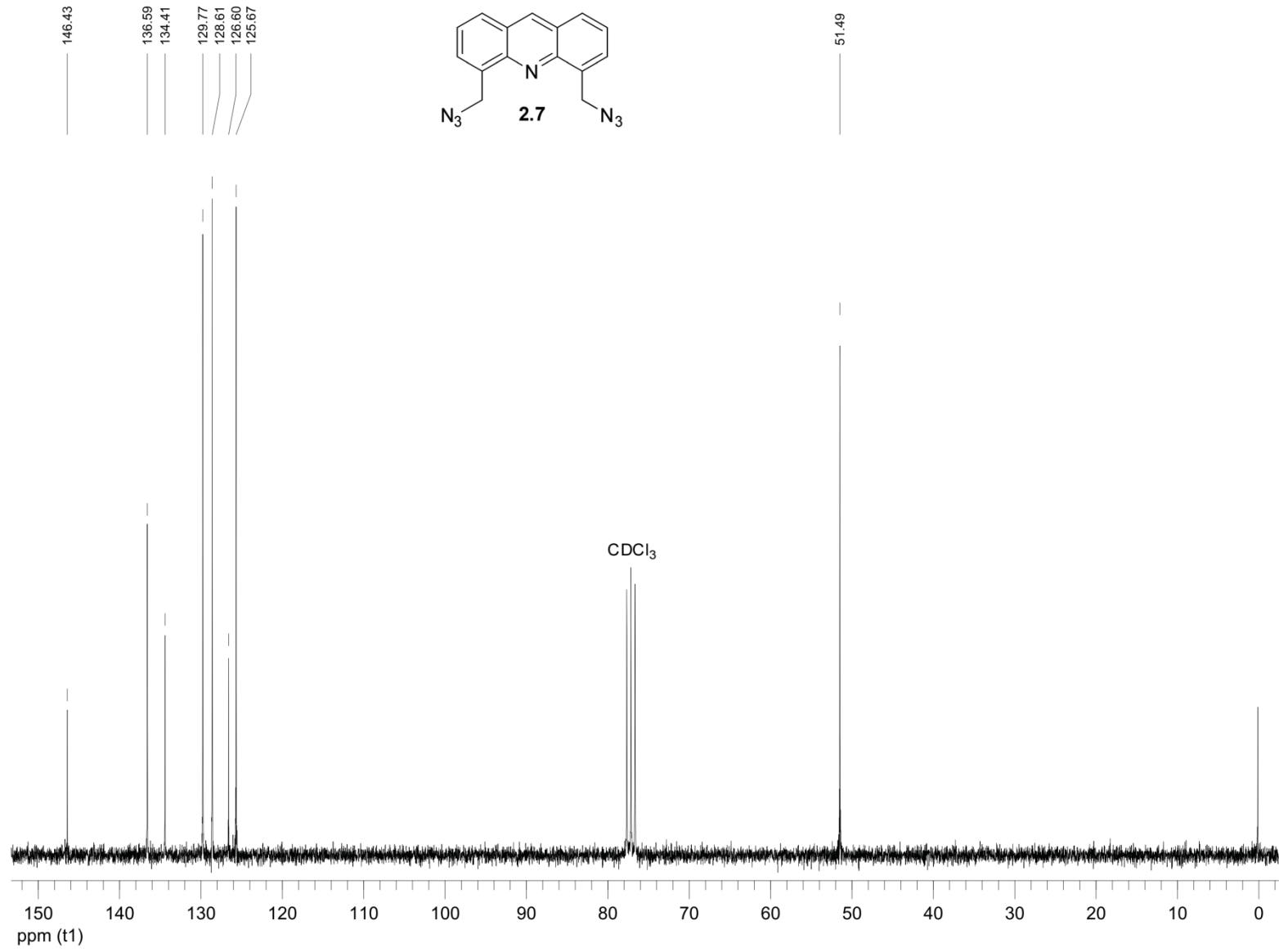


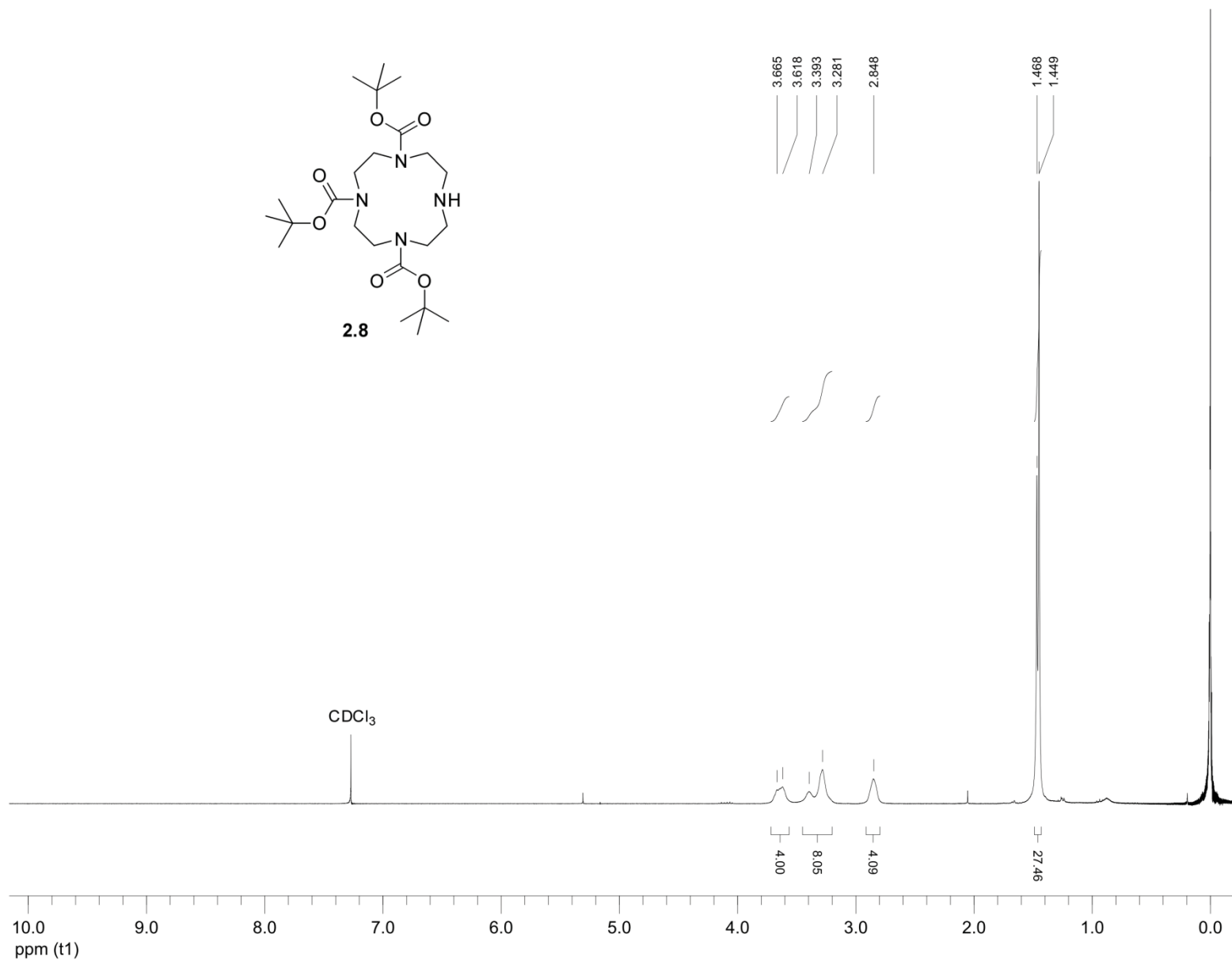
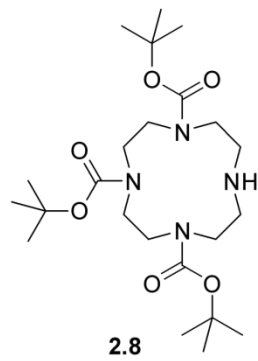


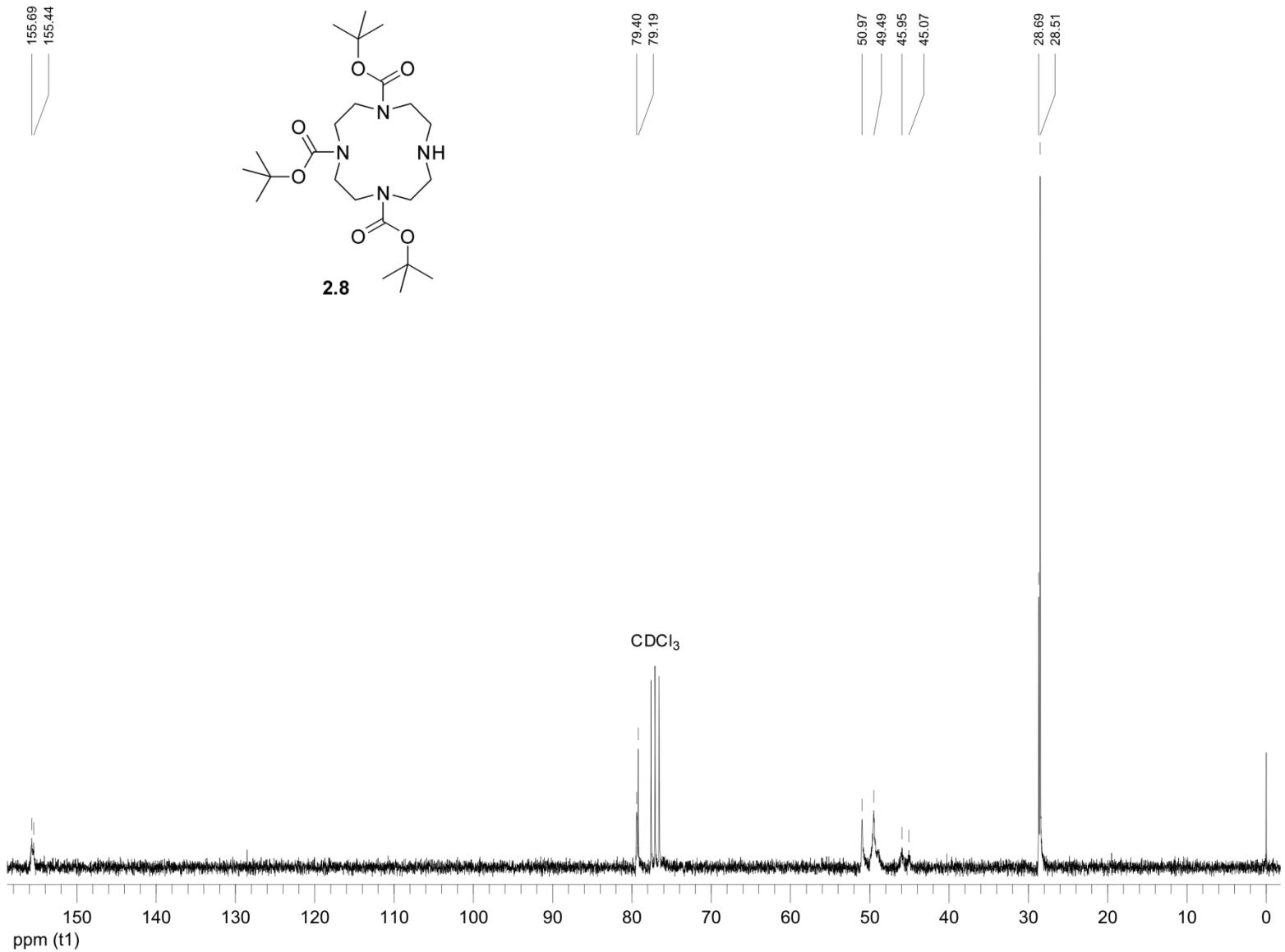


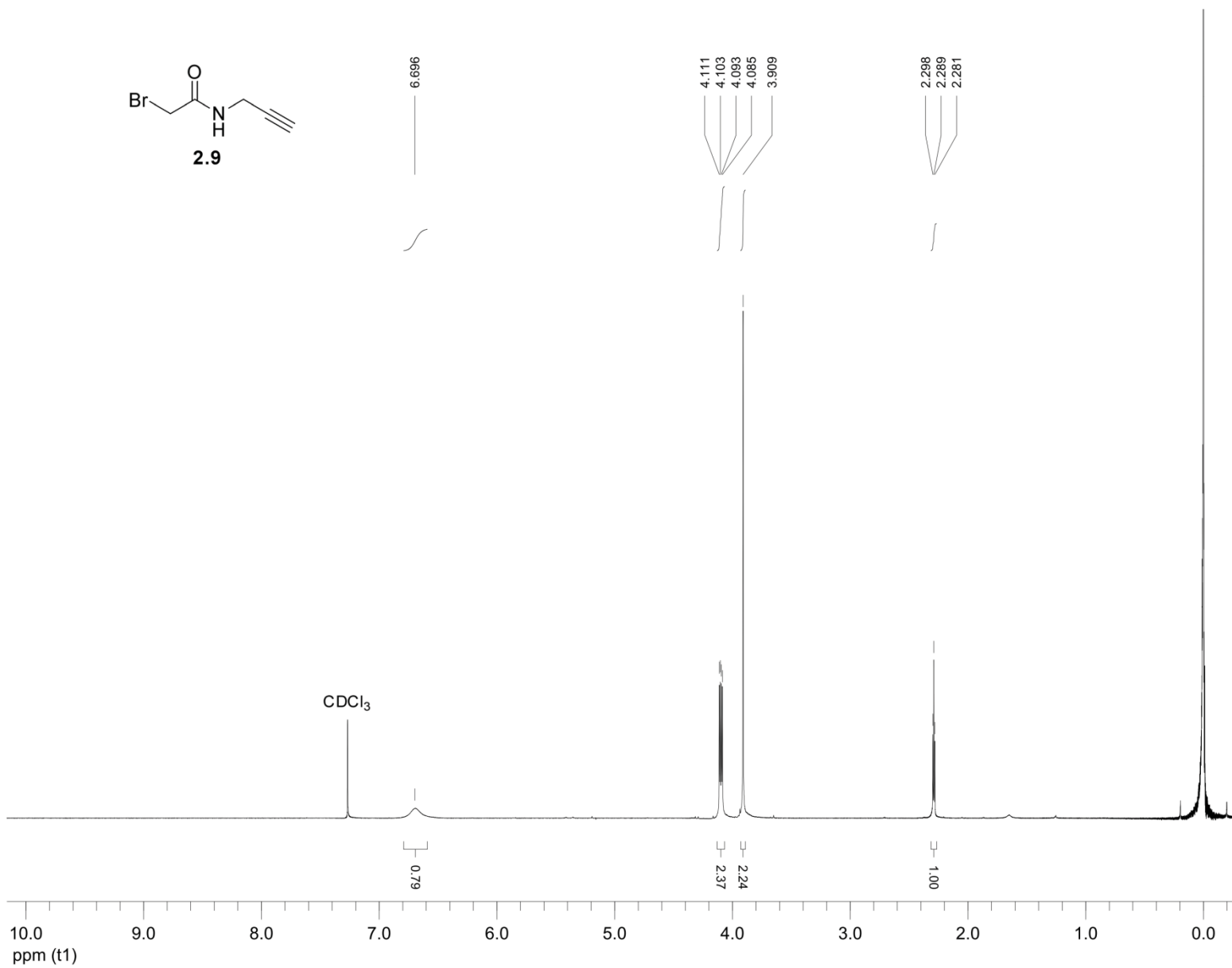
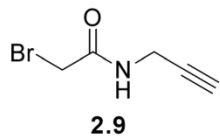
80

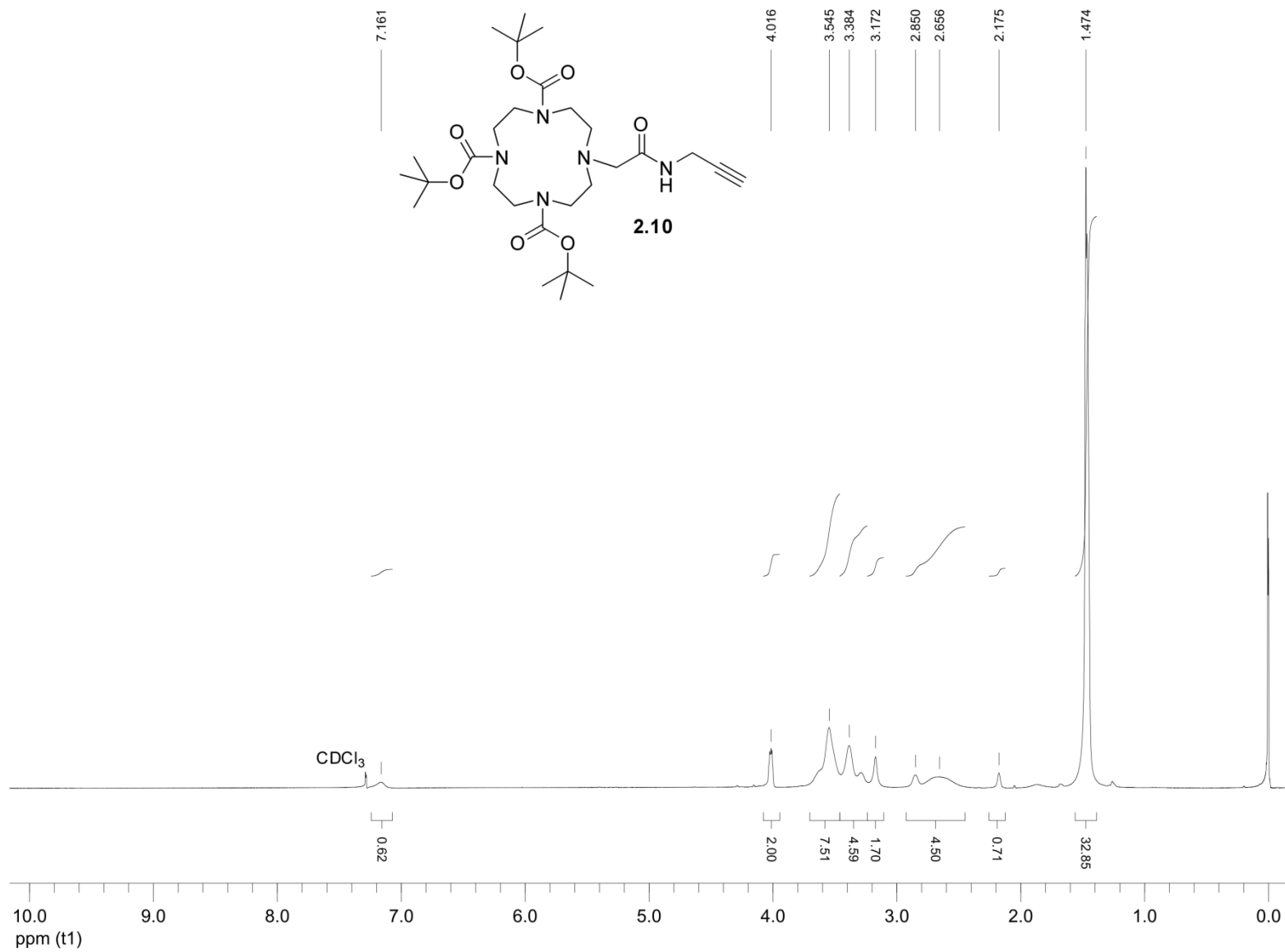




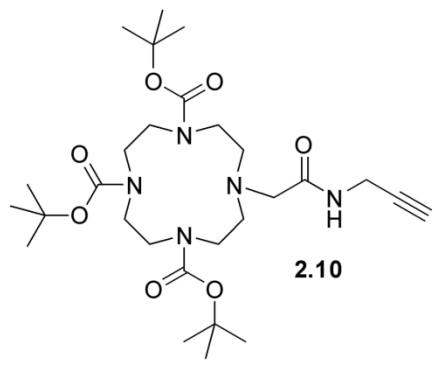




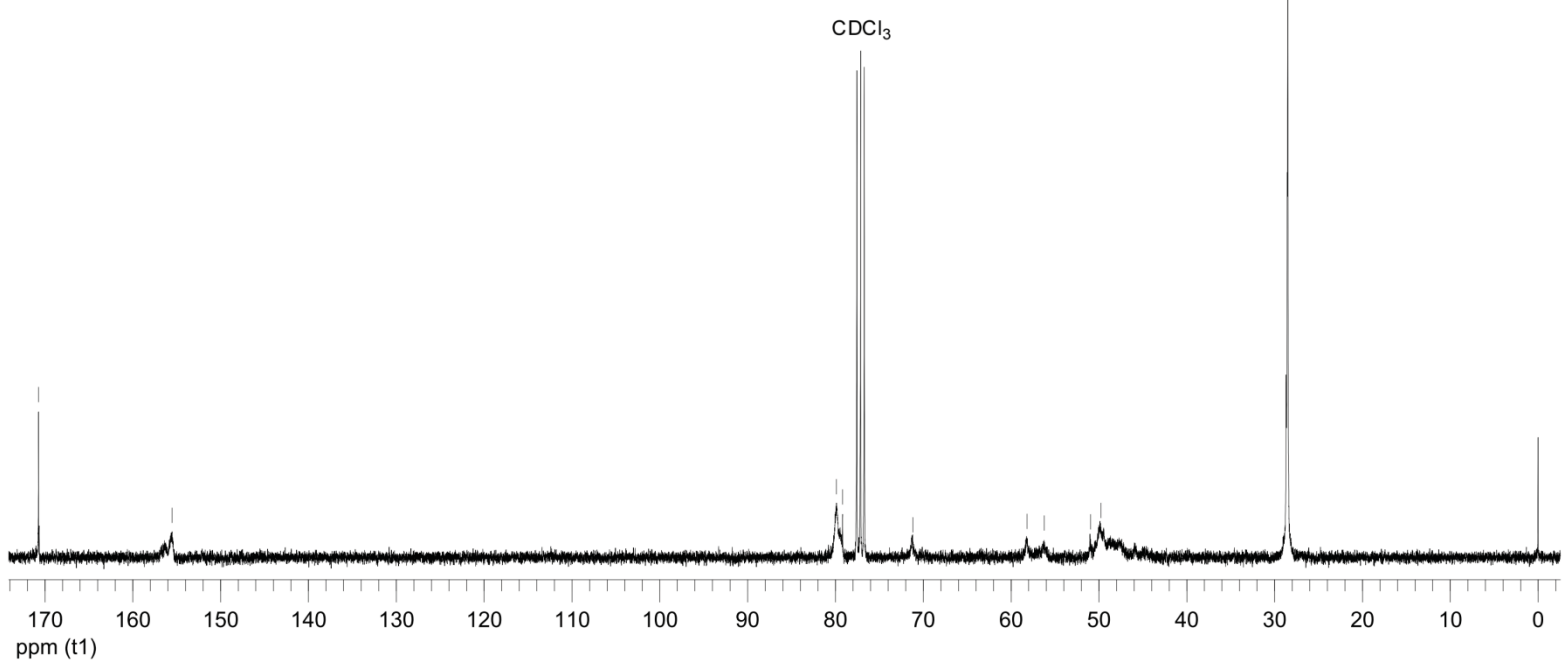


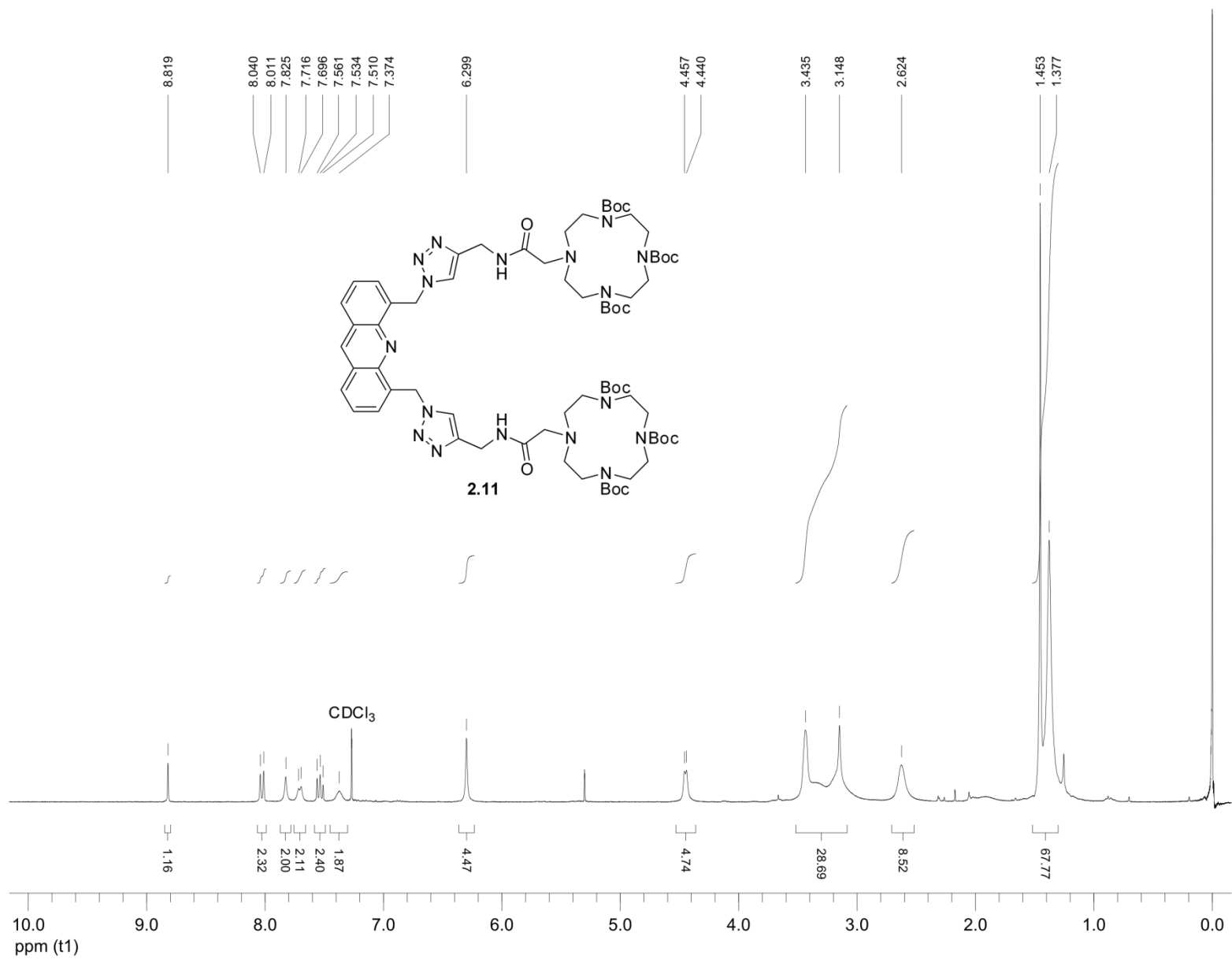


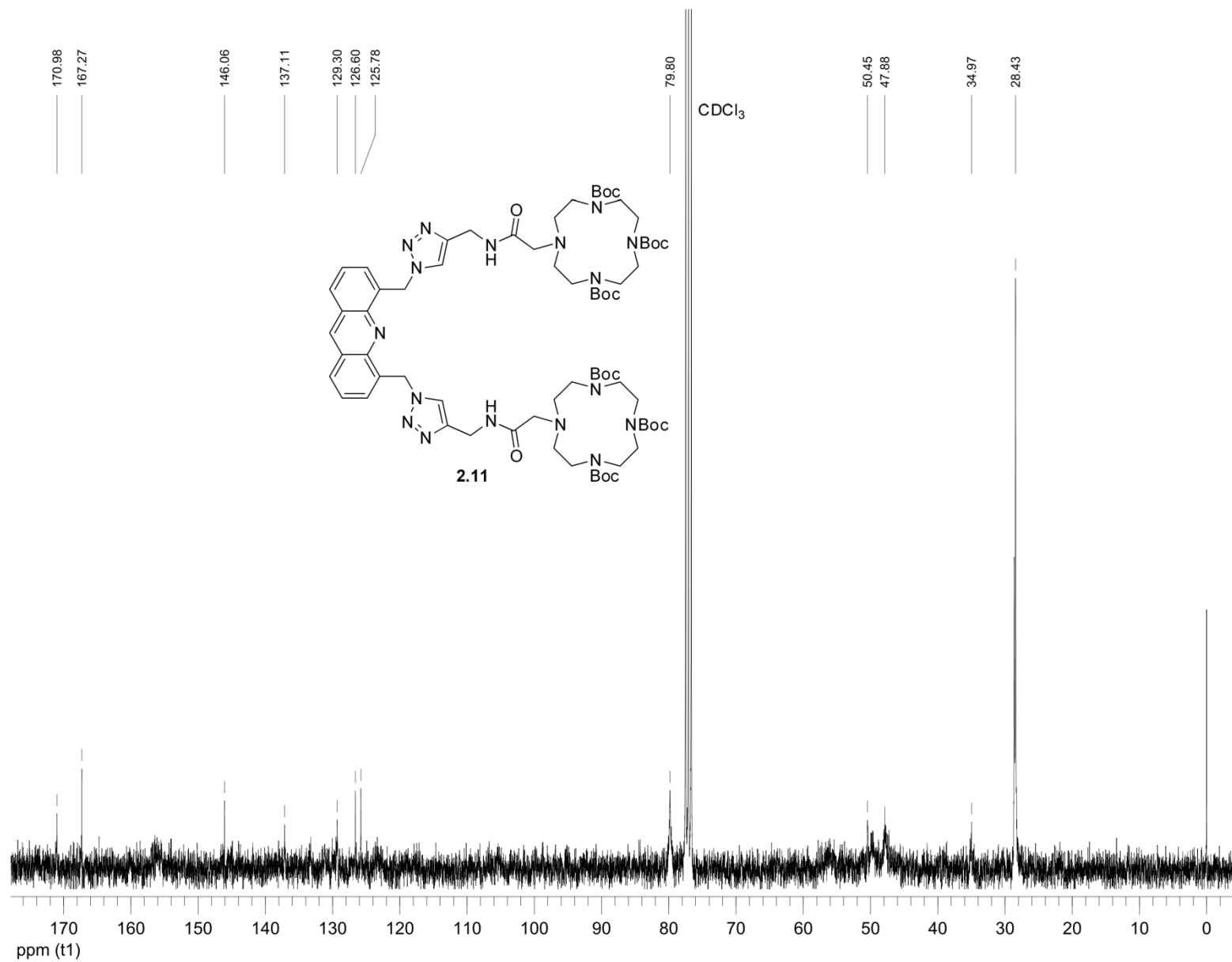
170.72
155.52

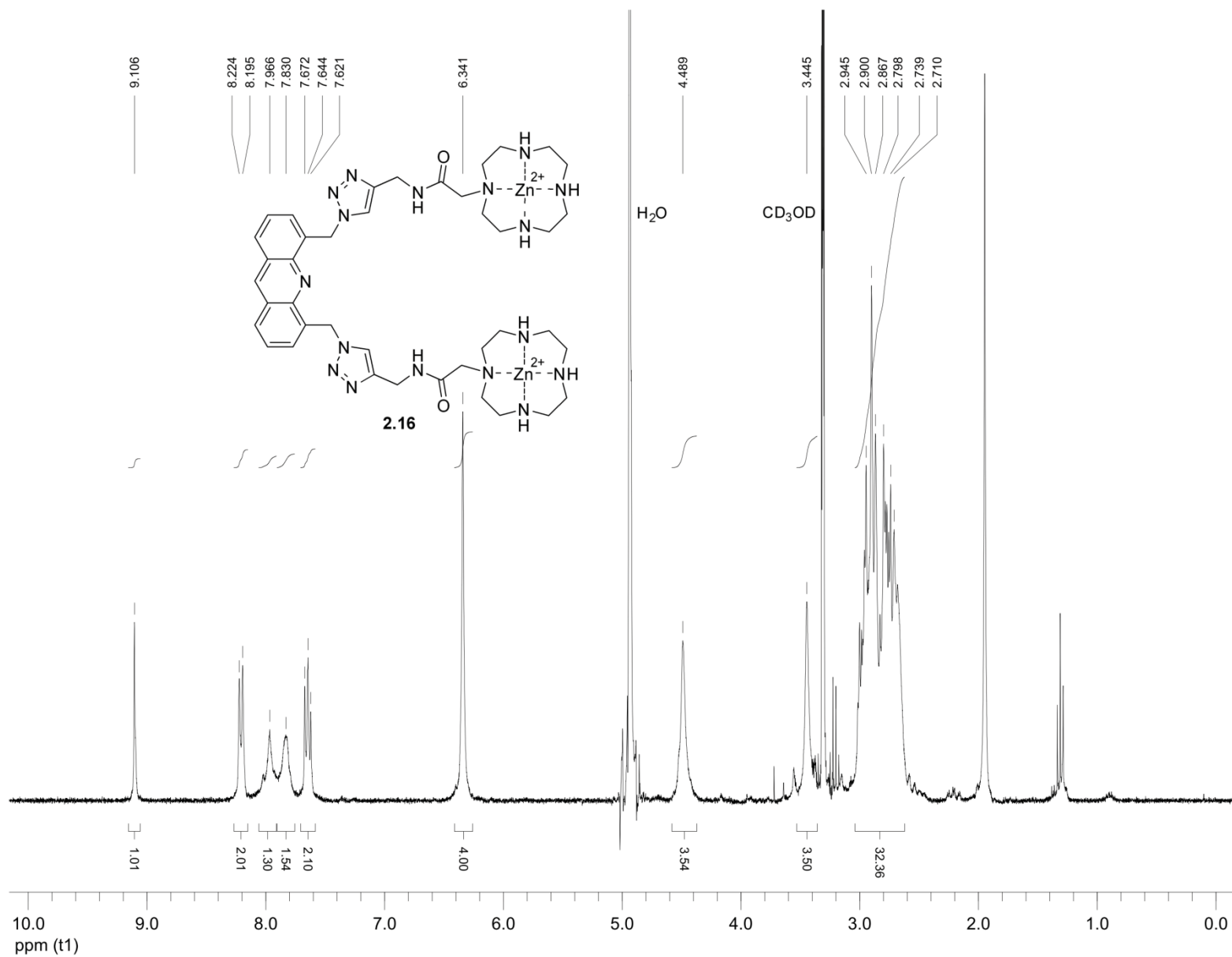


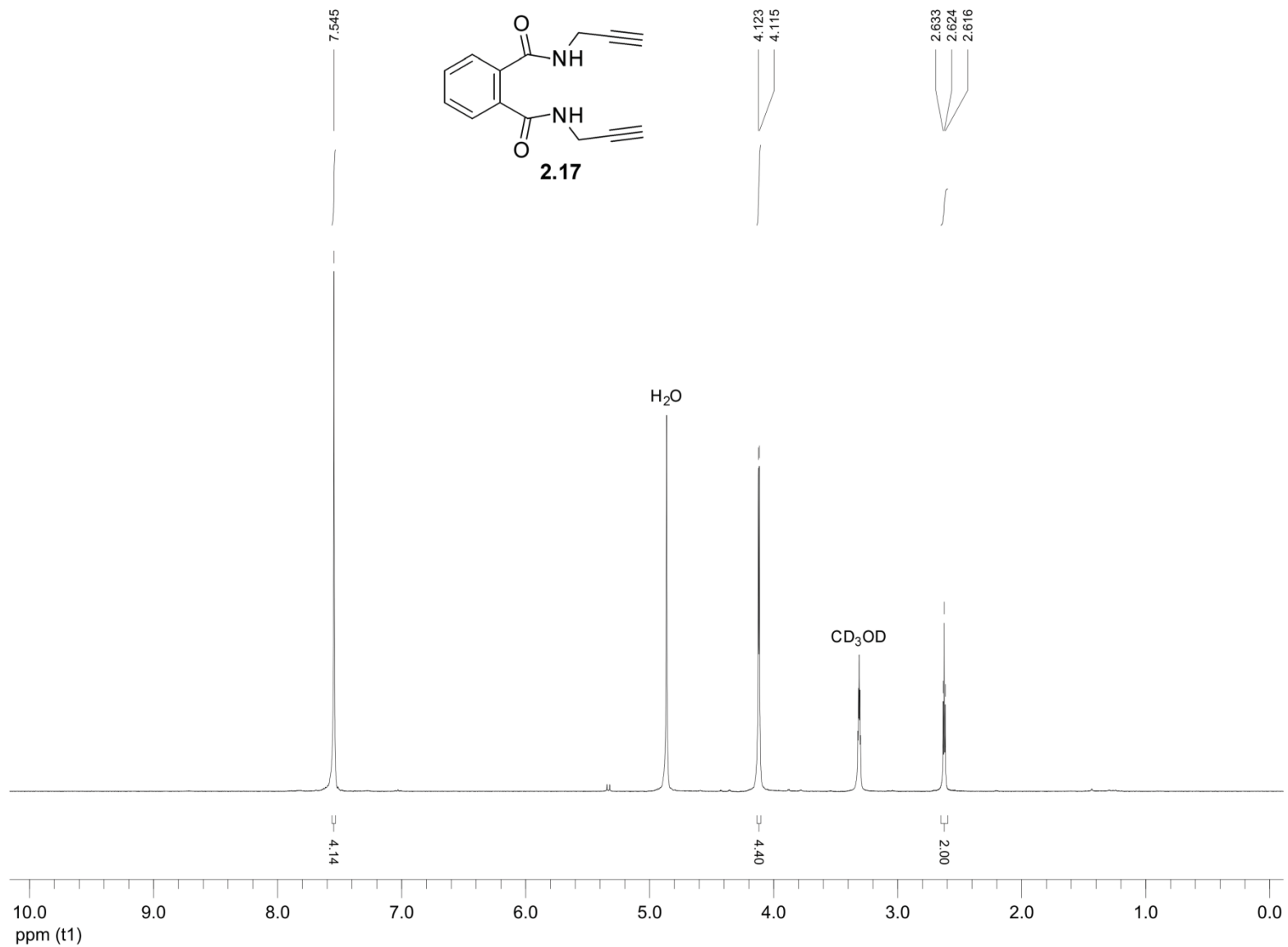
79.88
79.18
71.18
58.19
56.22
50.95
49.78
28.50

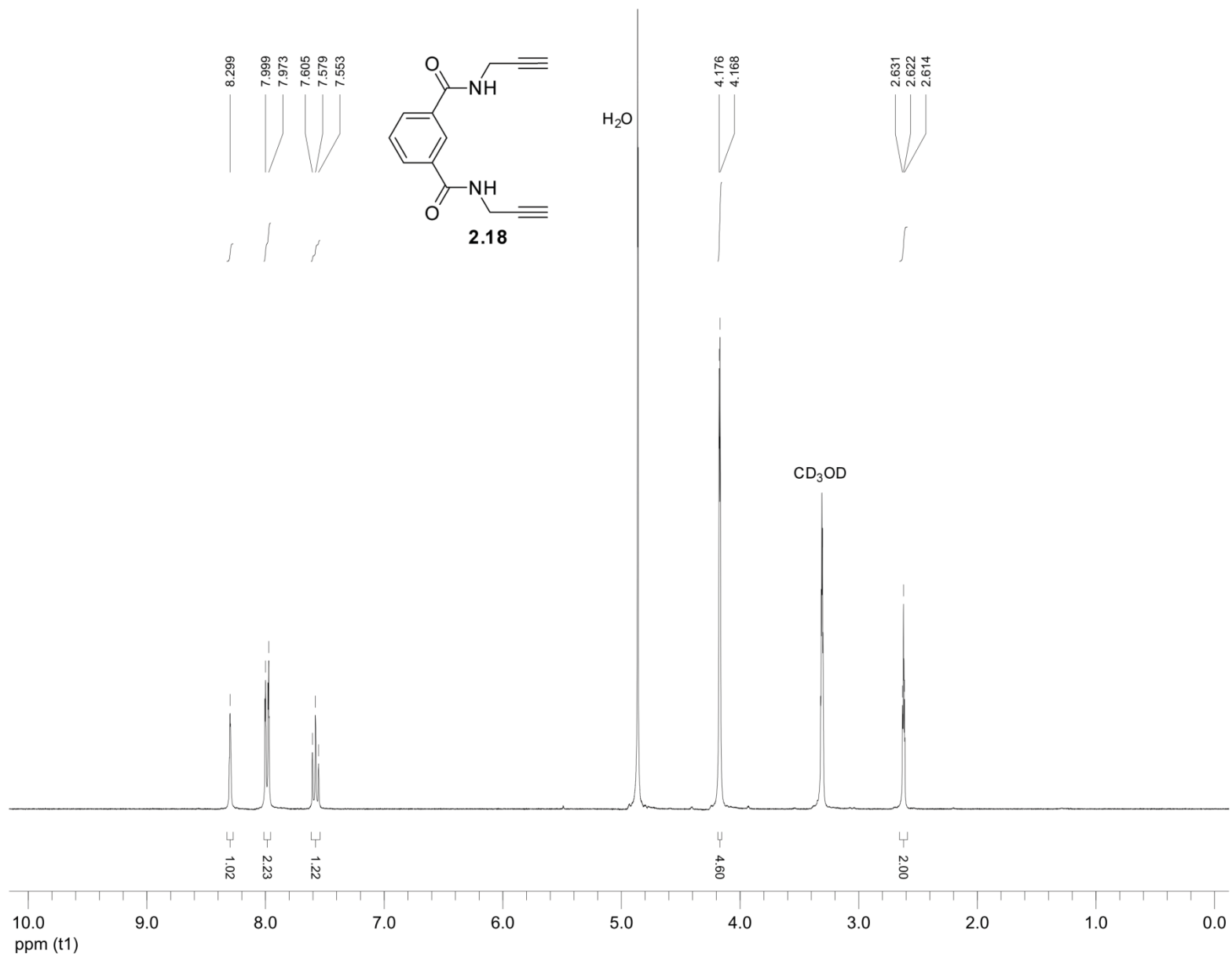


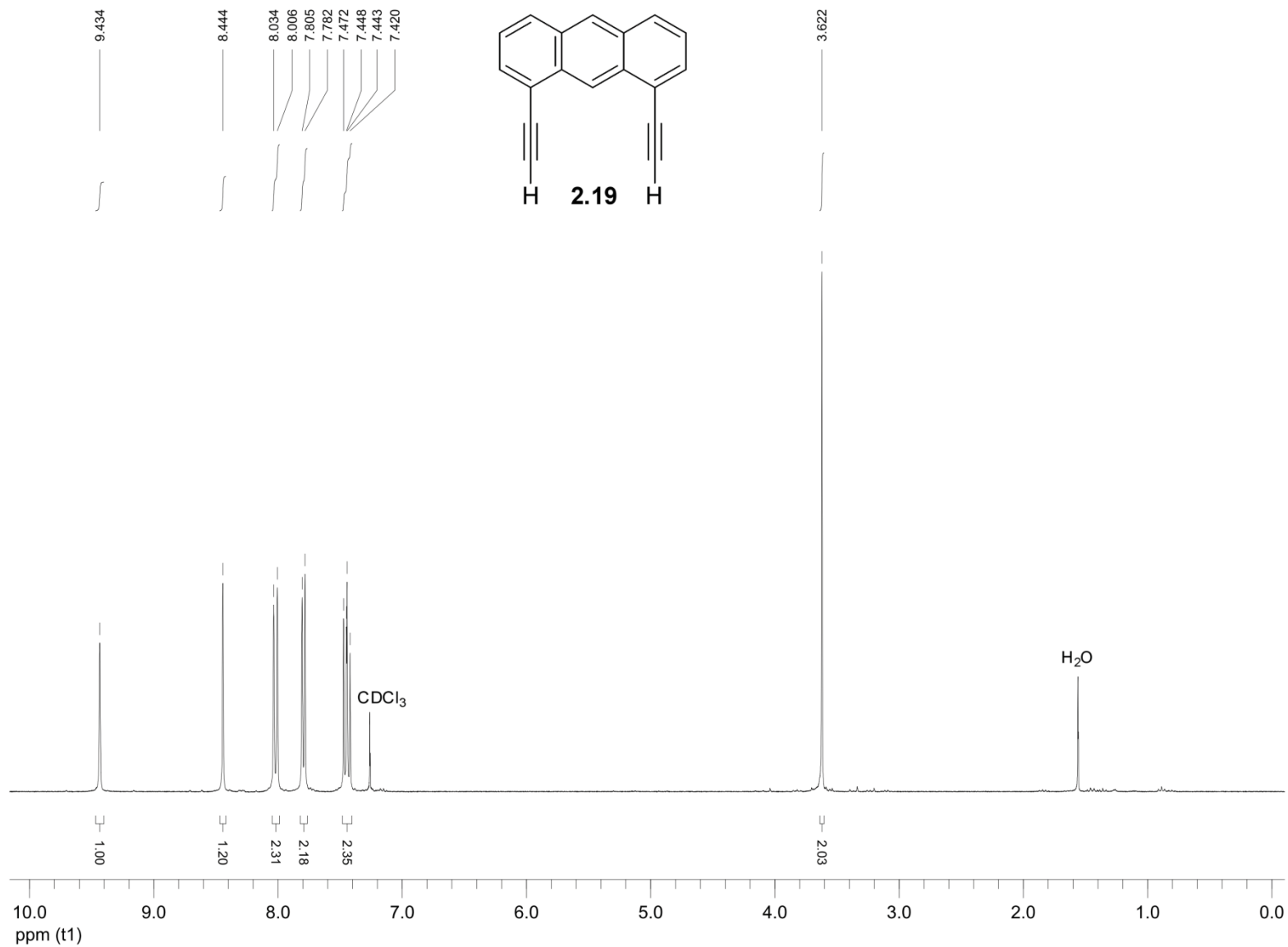


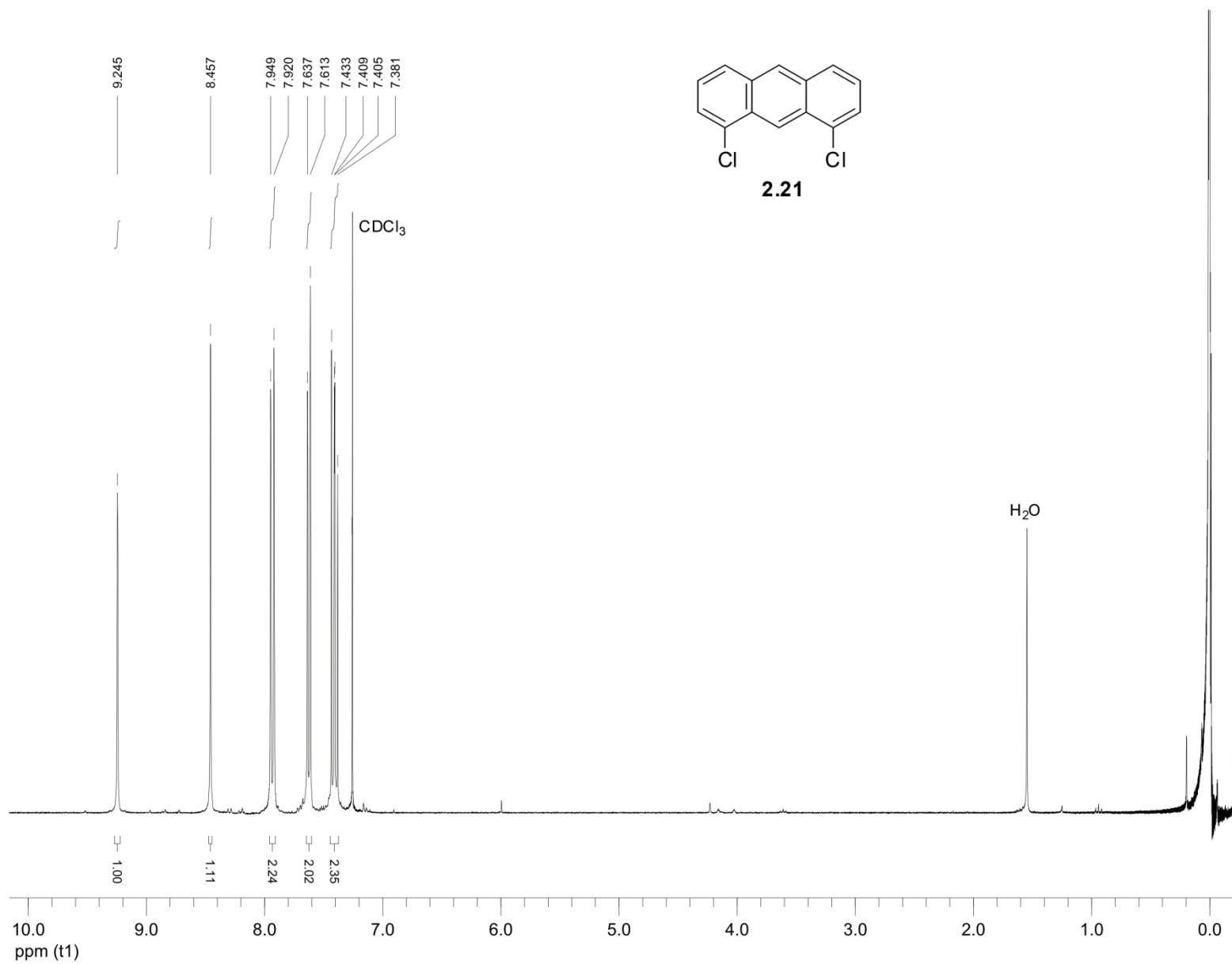


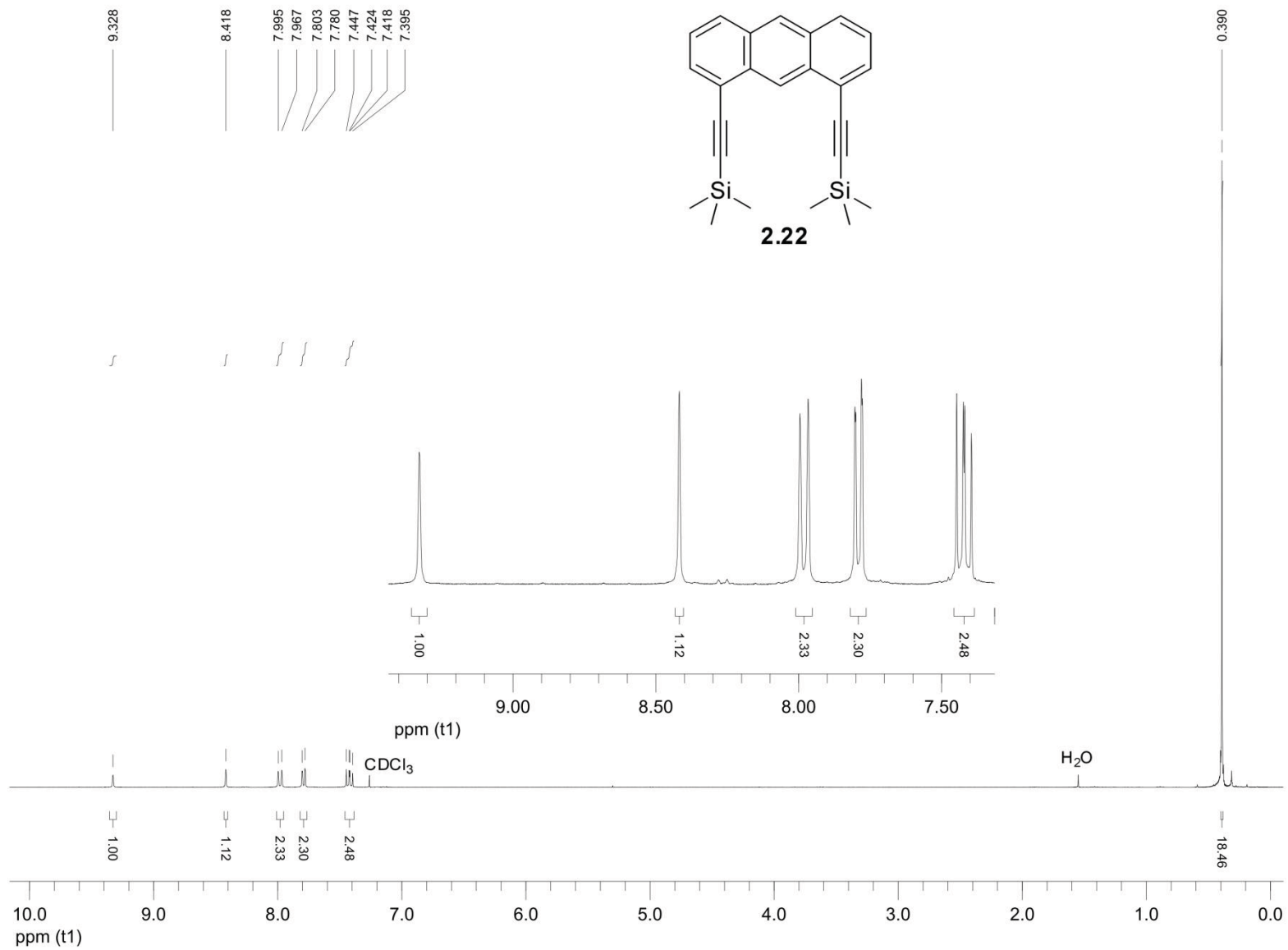


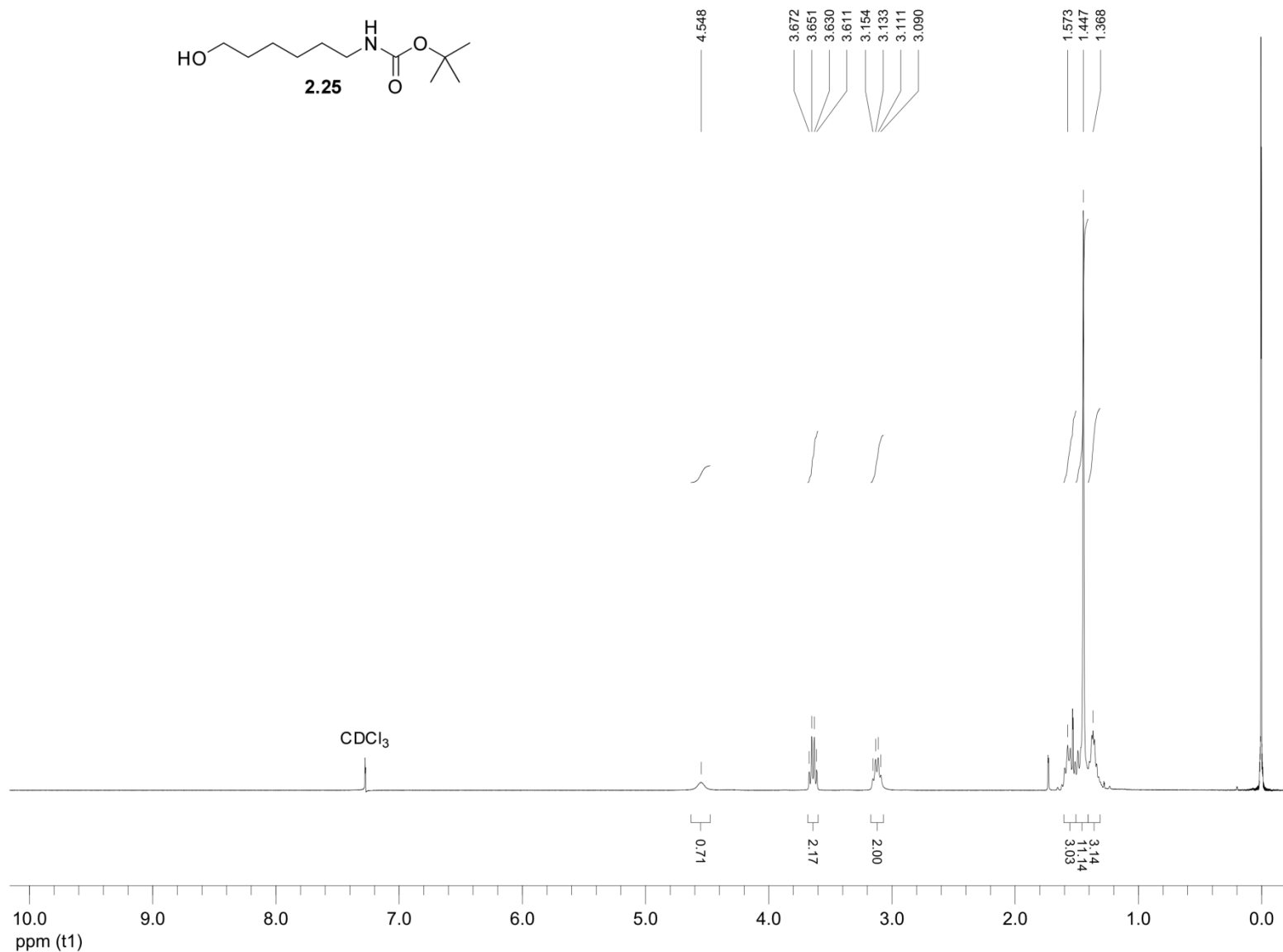
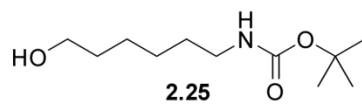


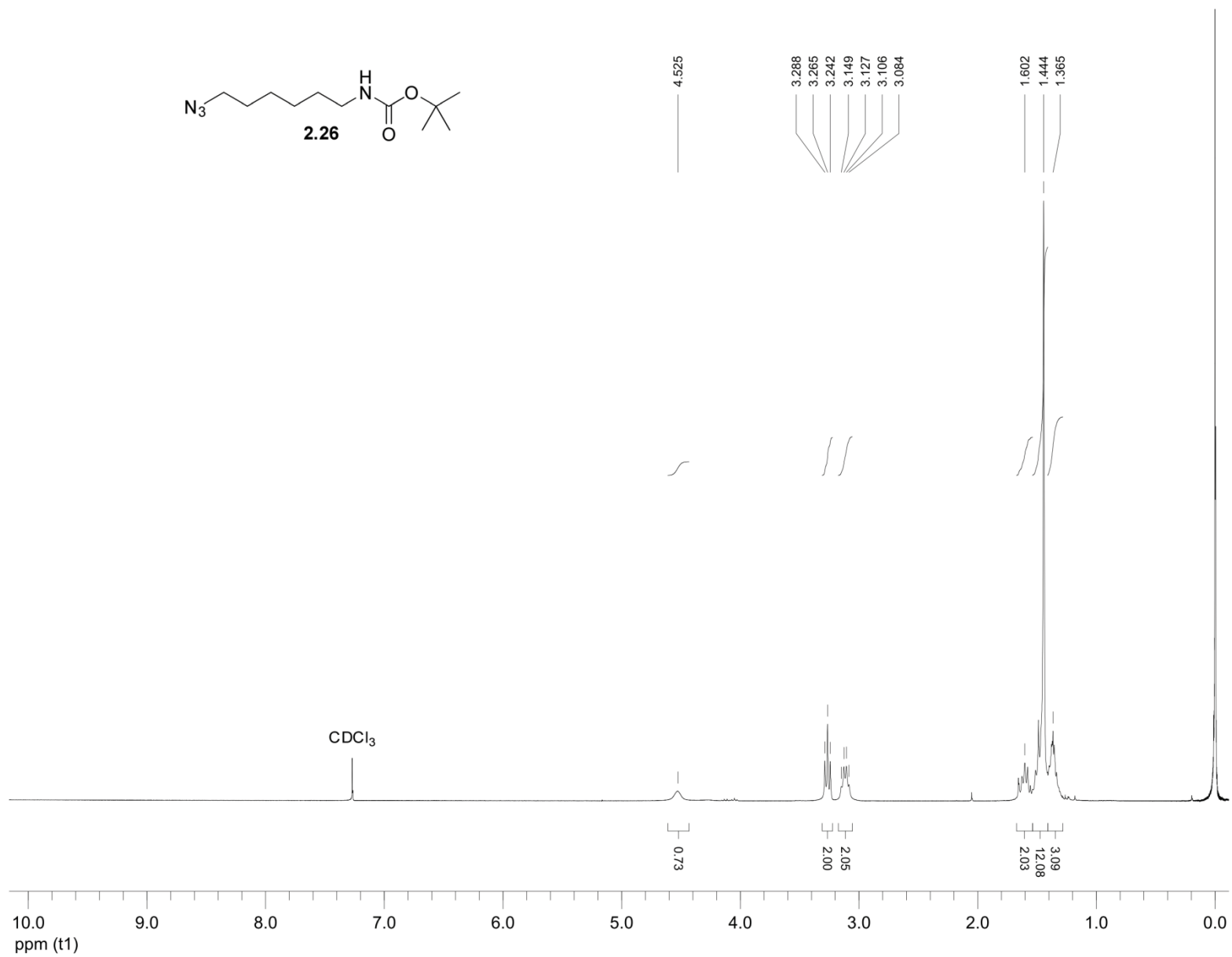
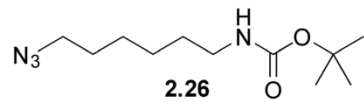


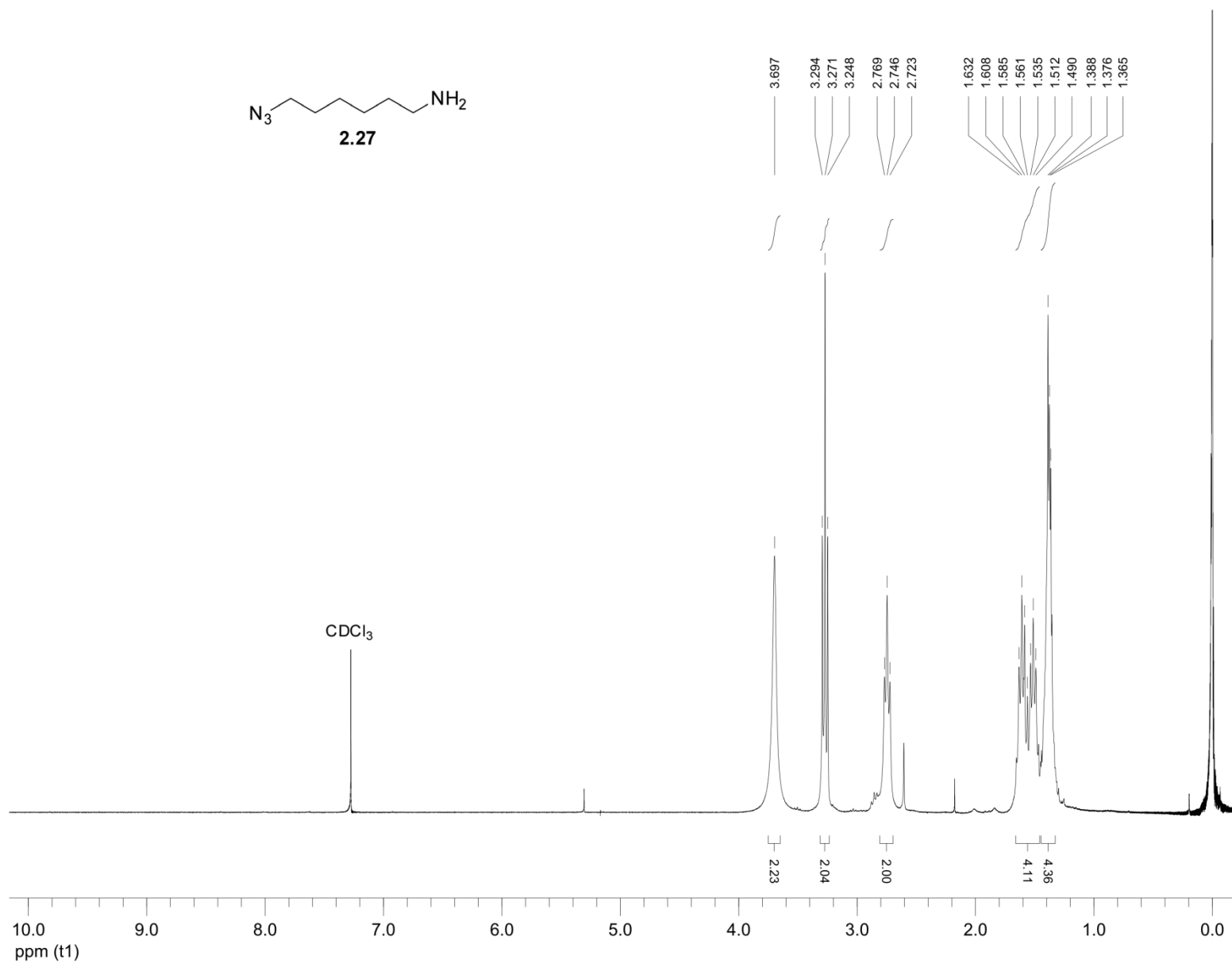
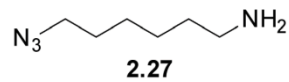


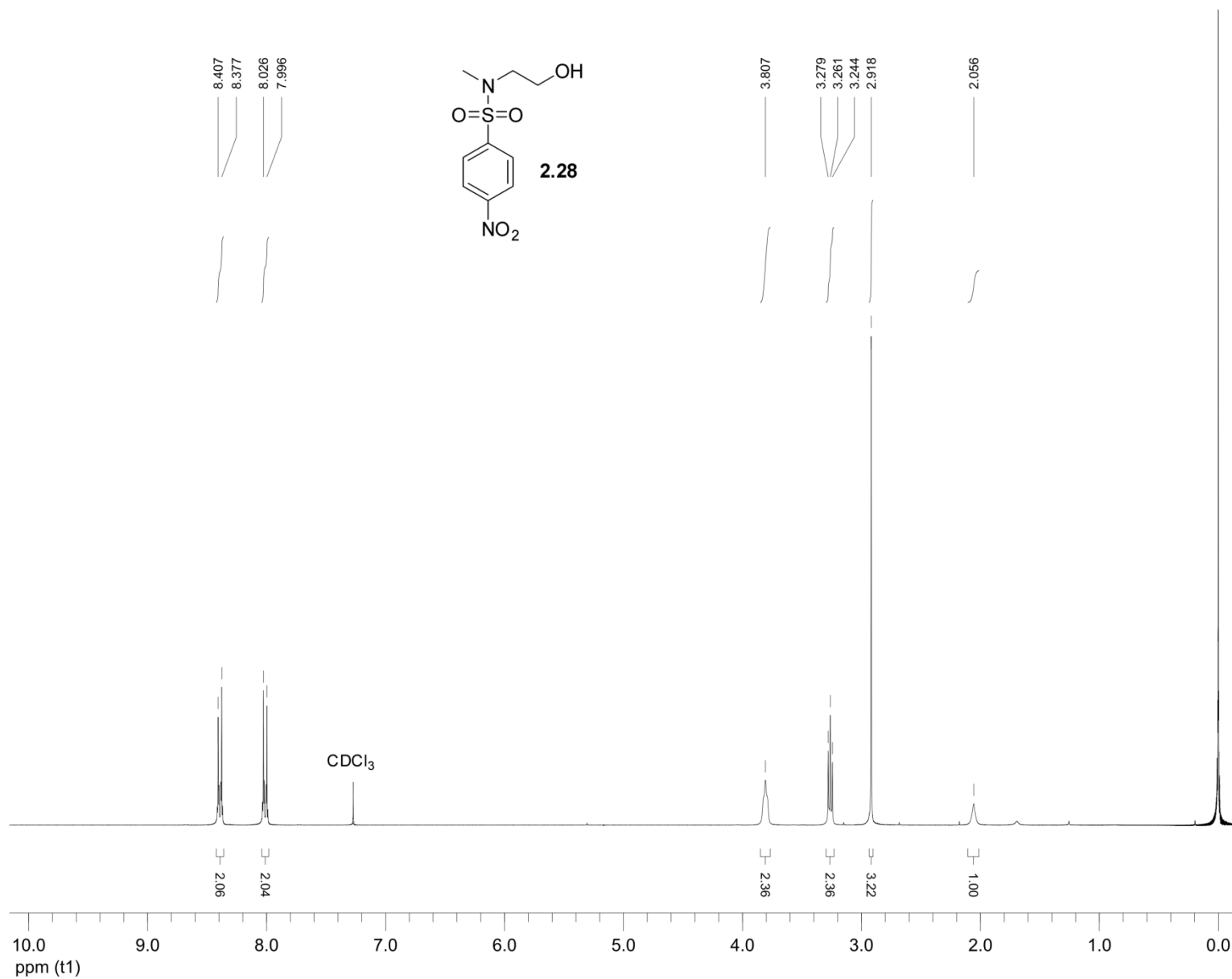


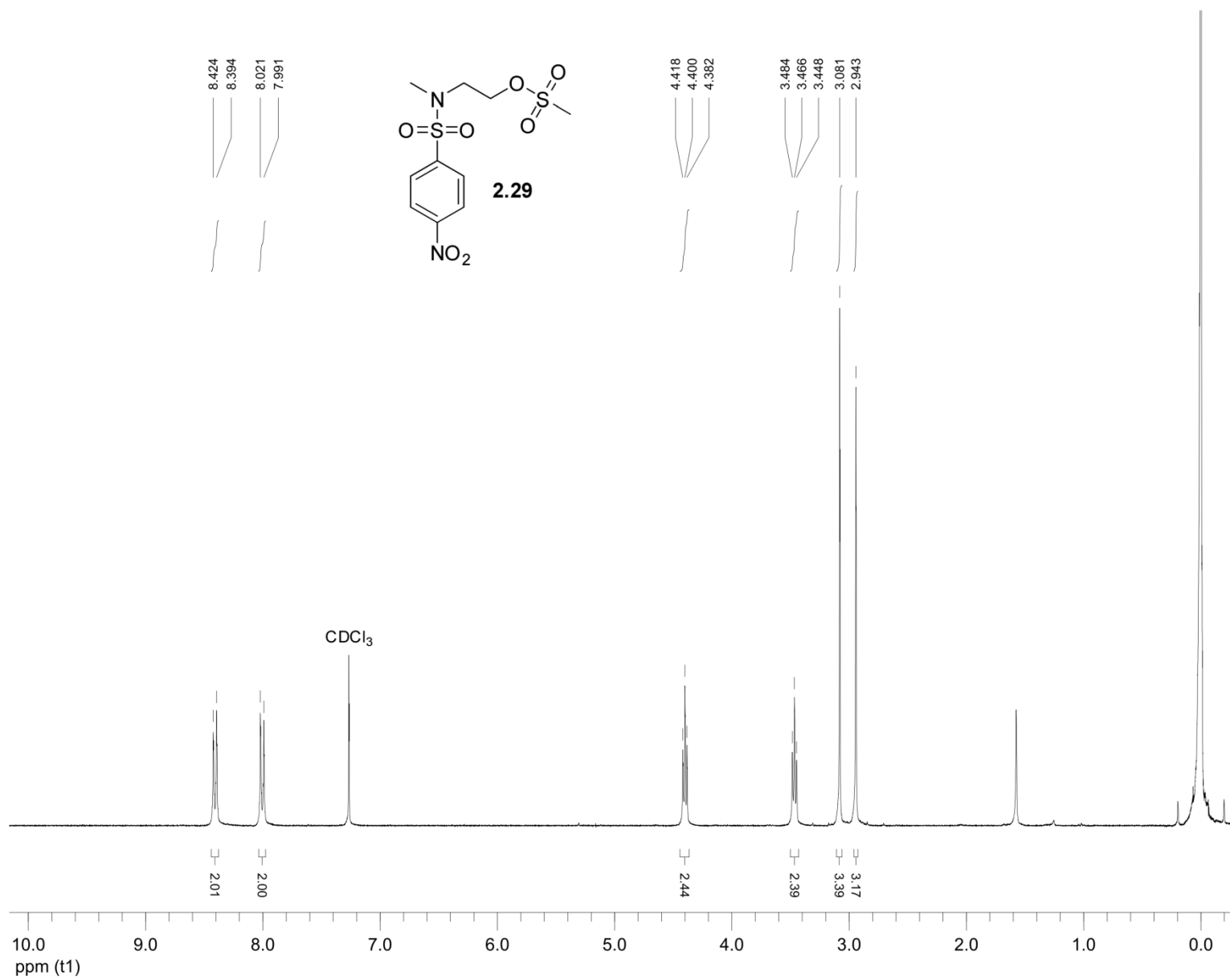


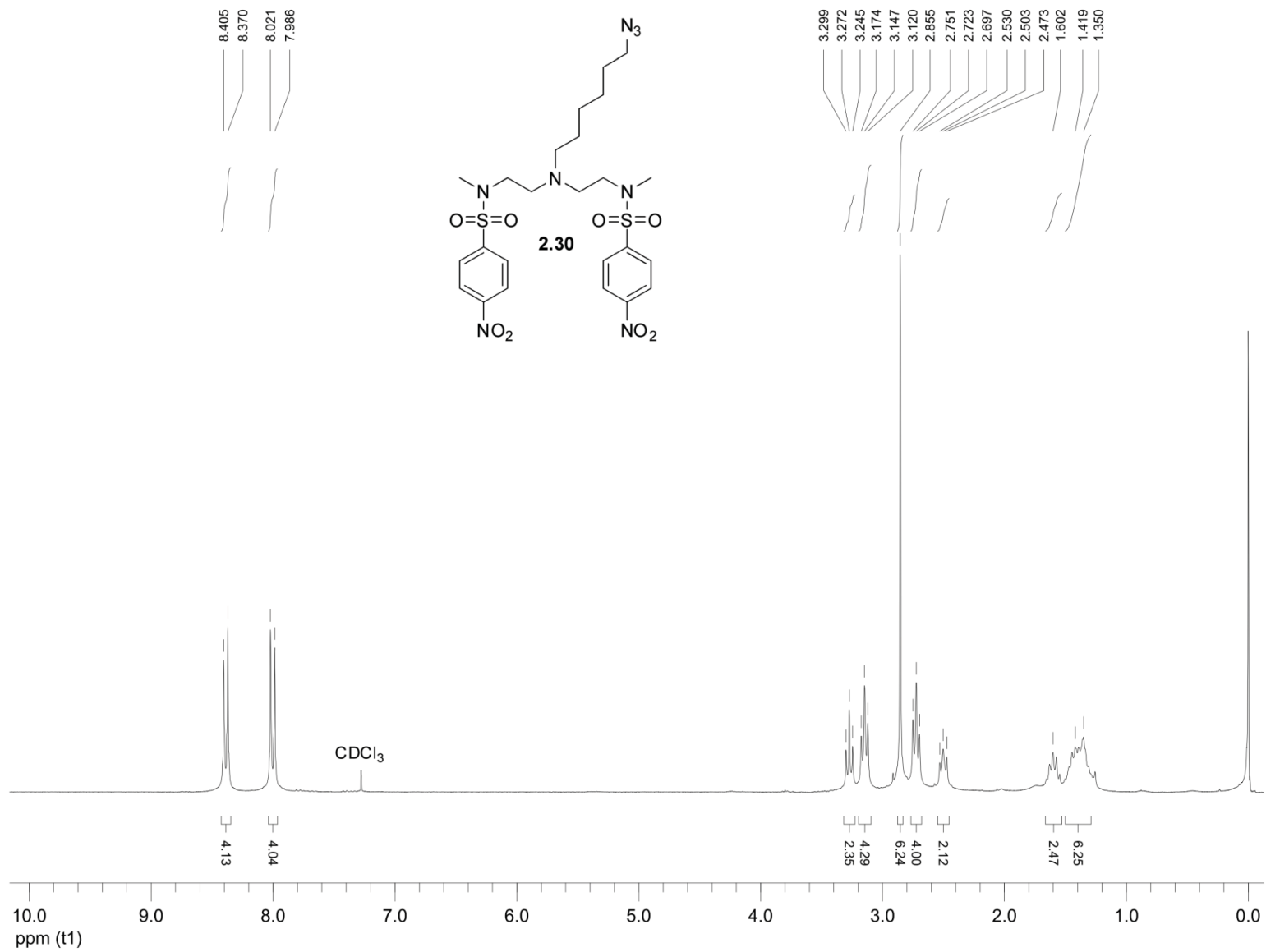


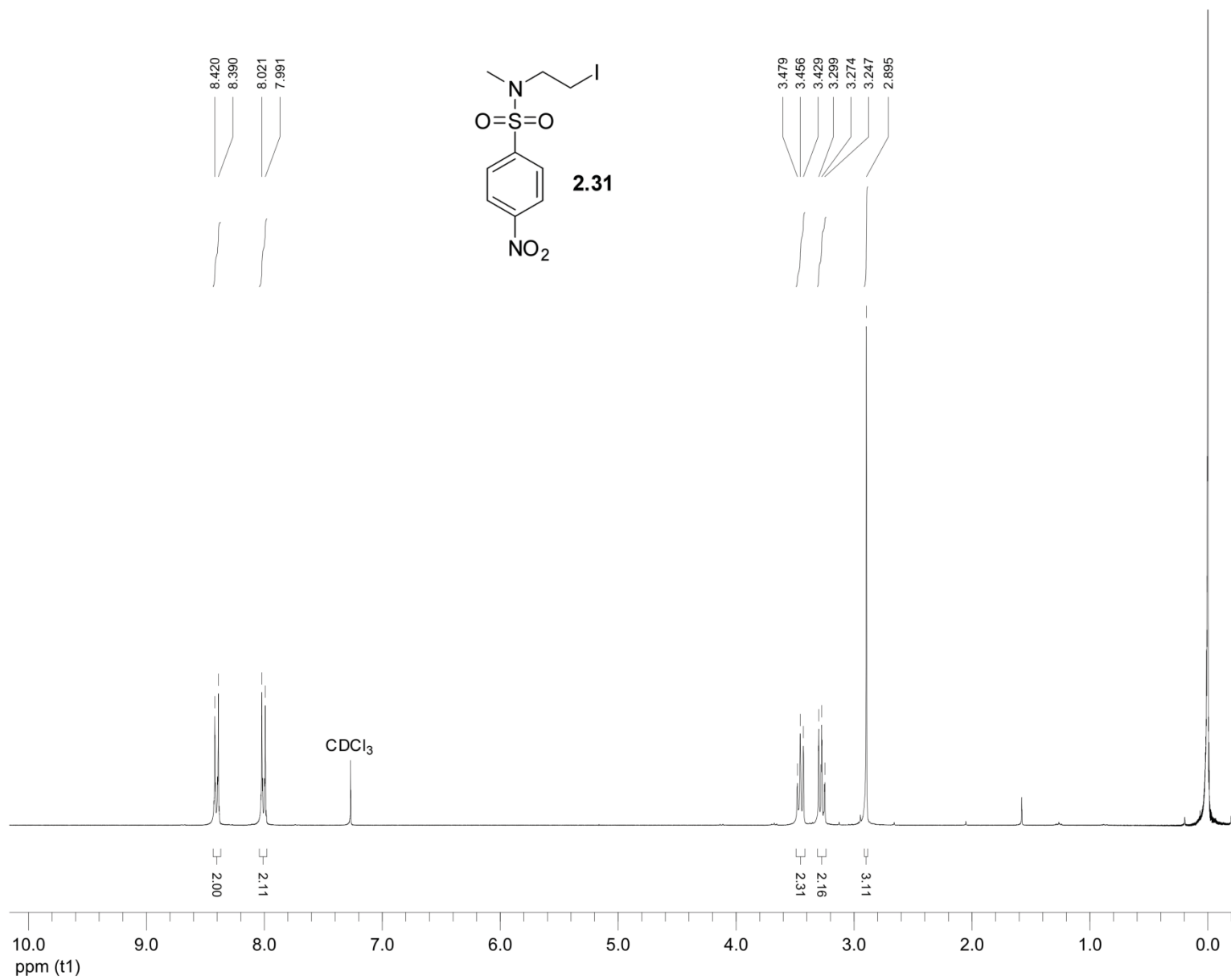


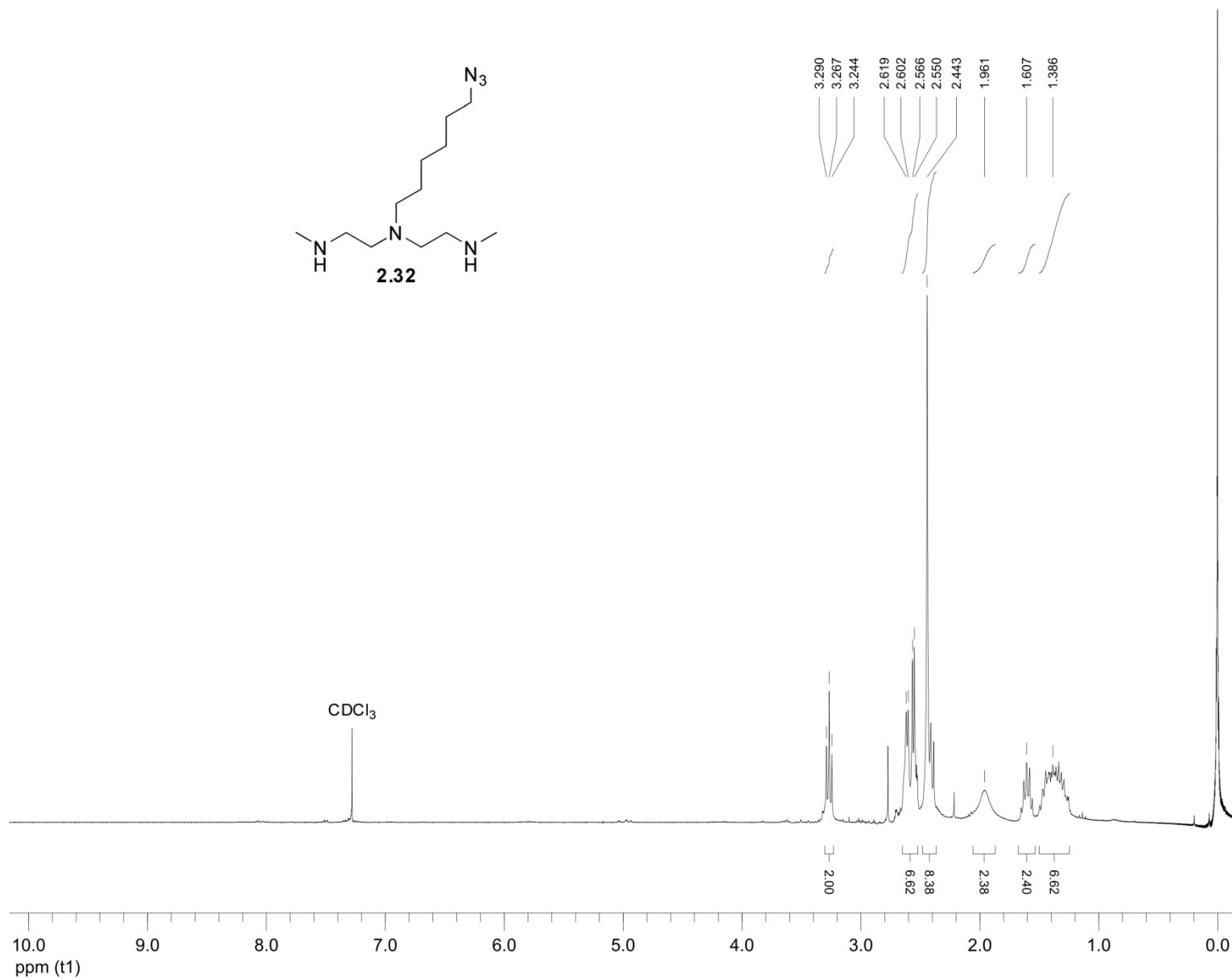
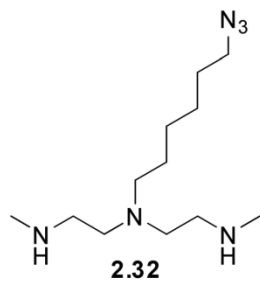


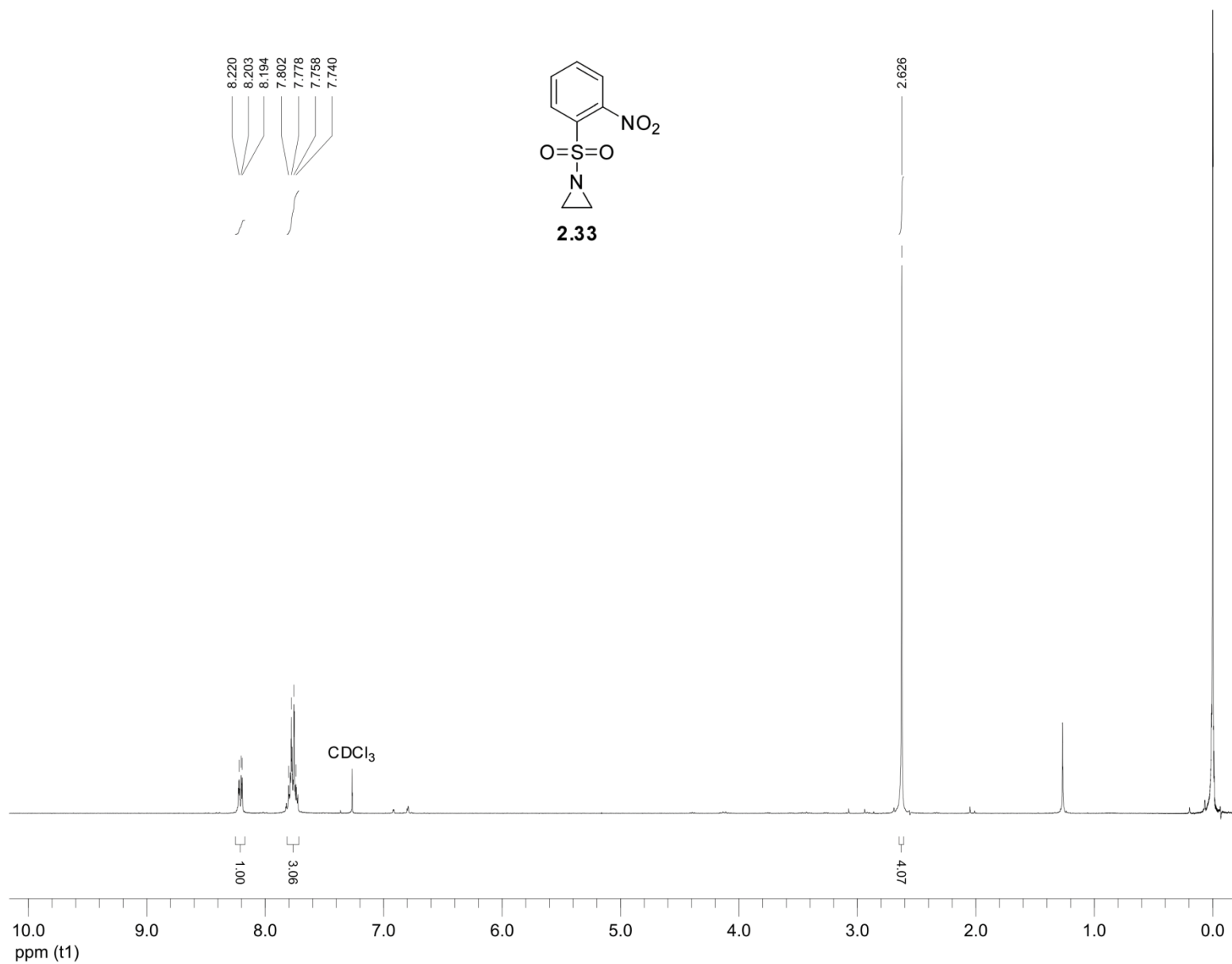


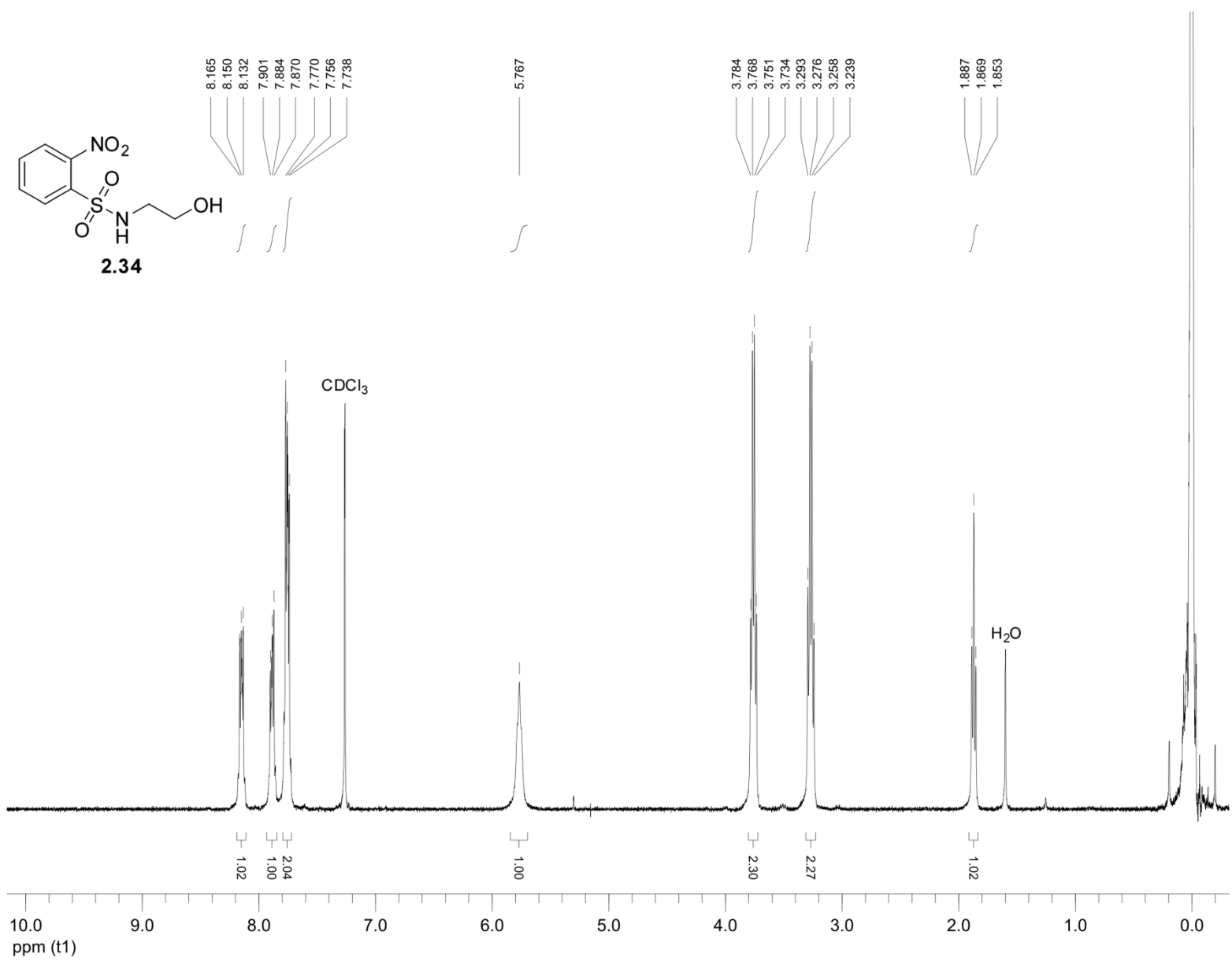


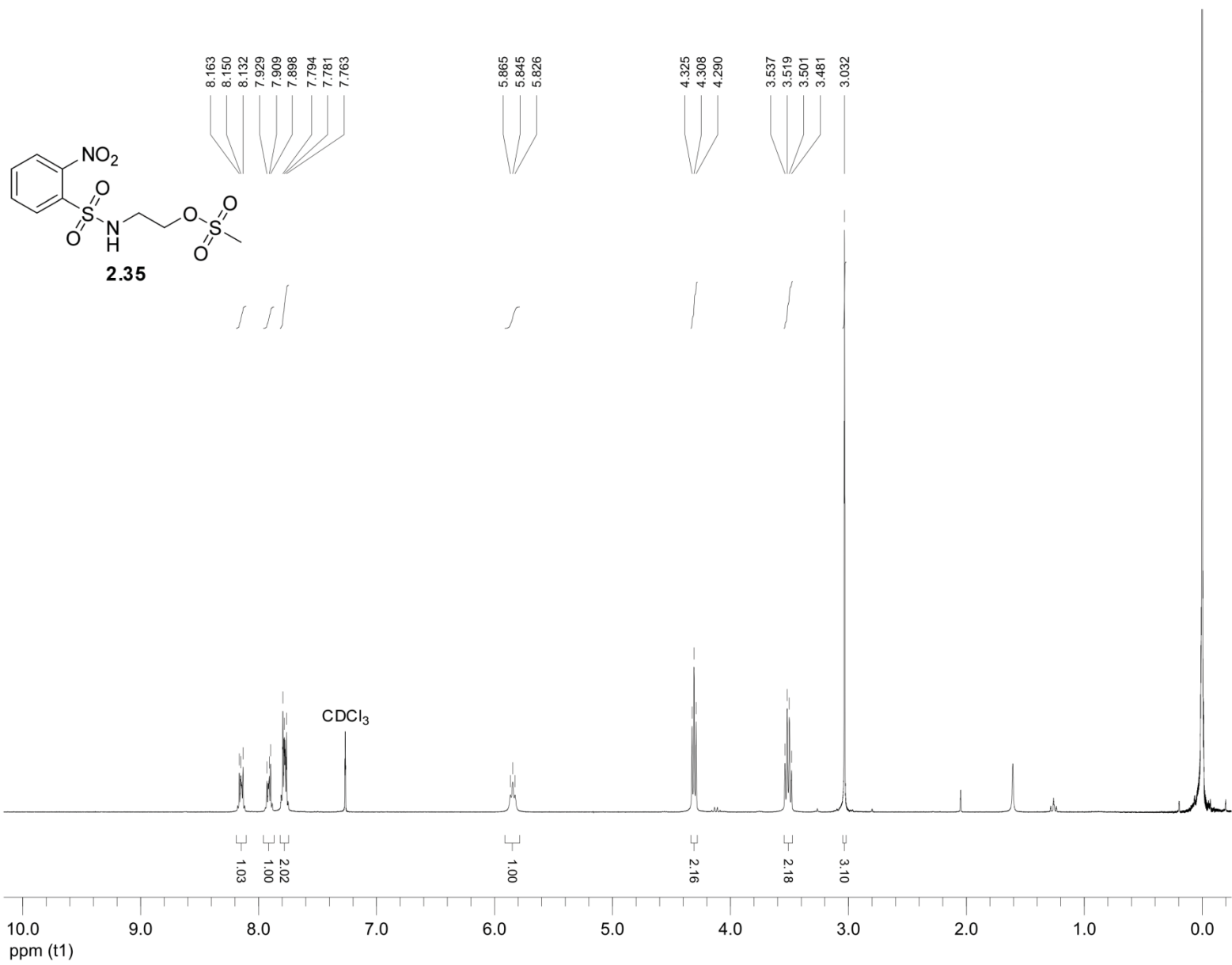


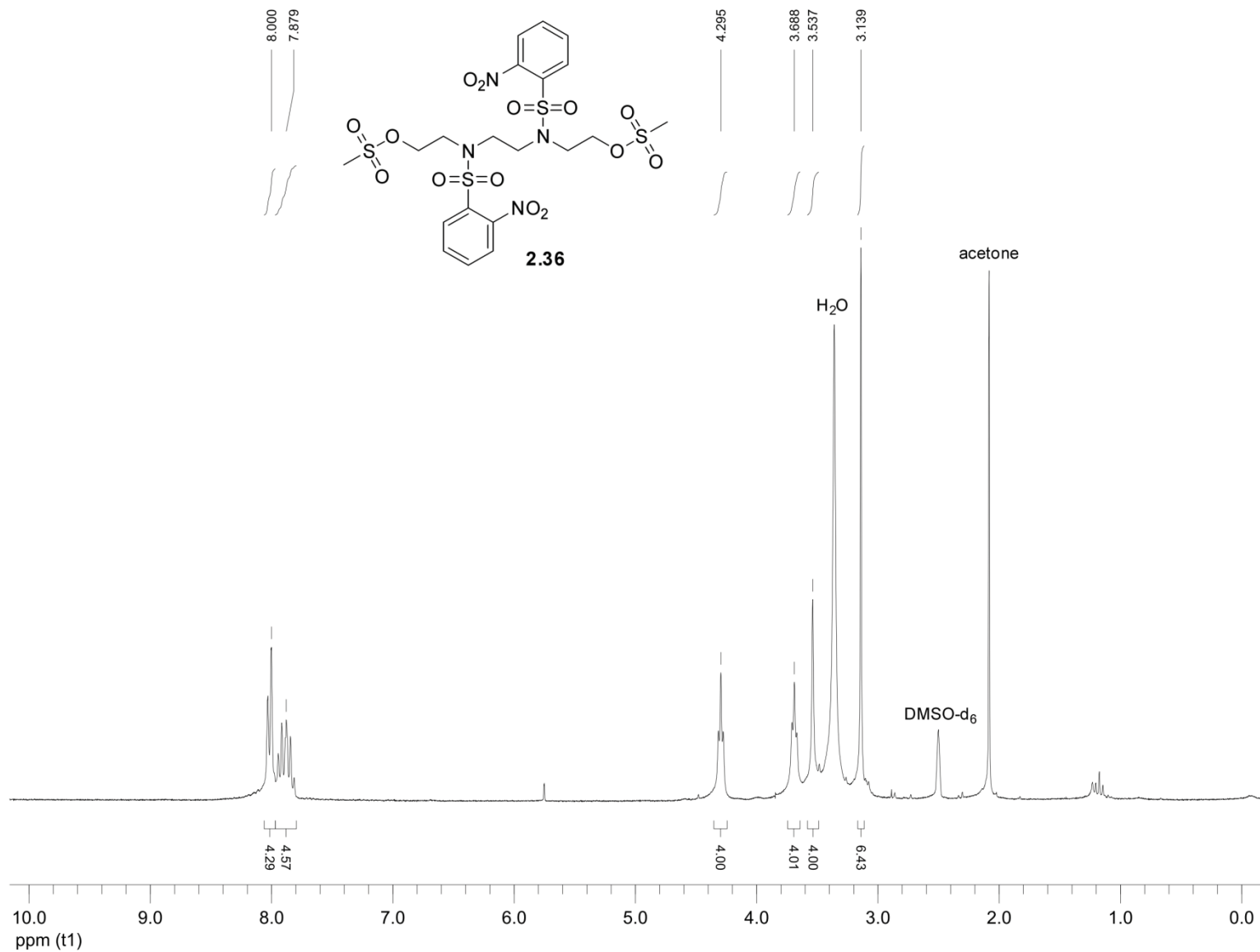


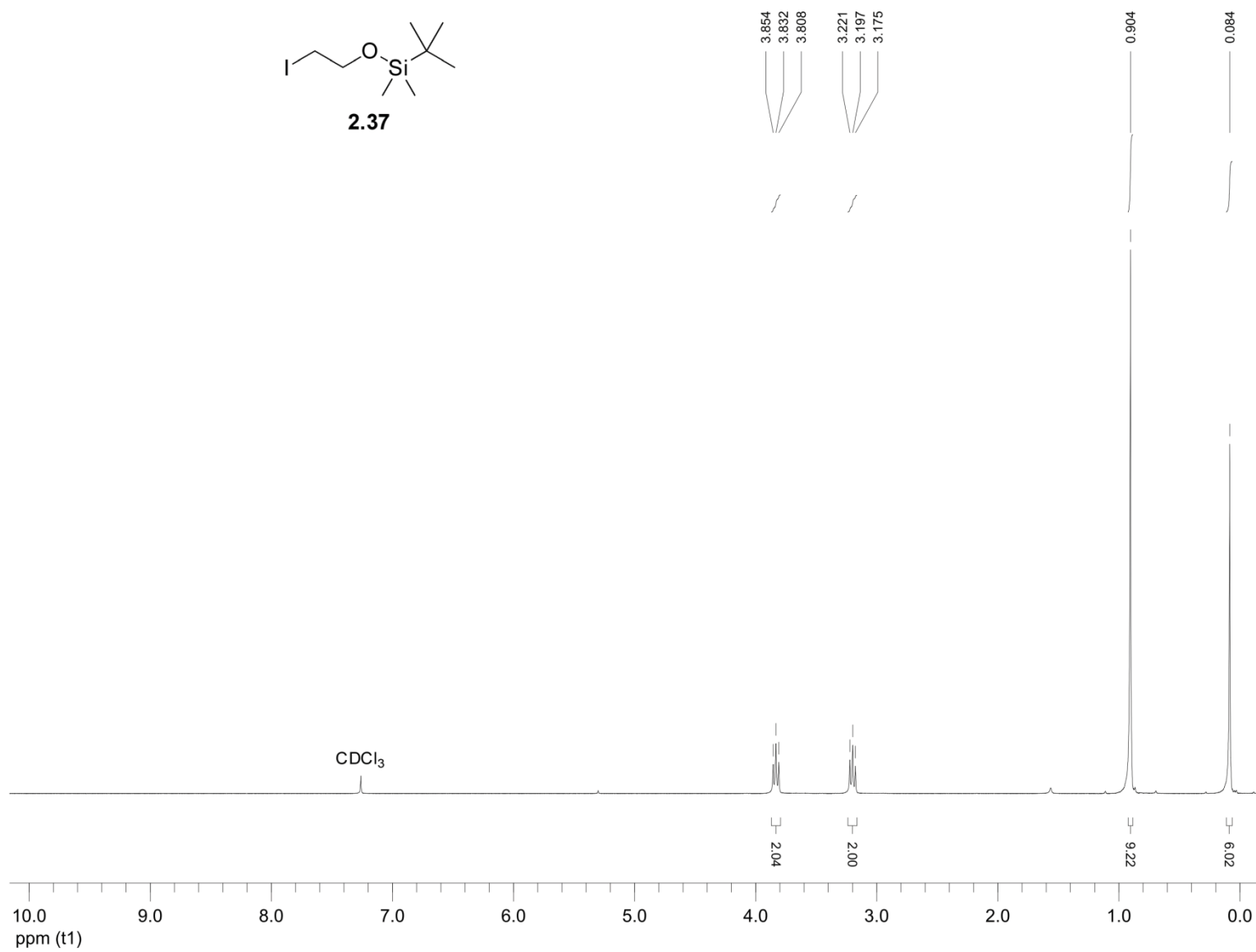
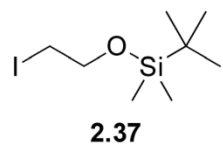


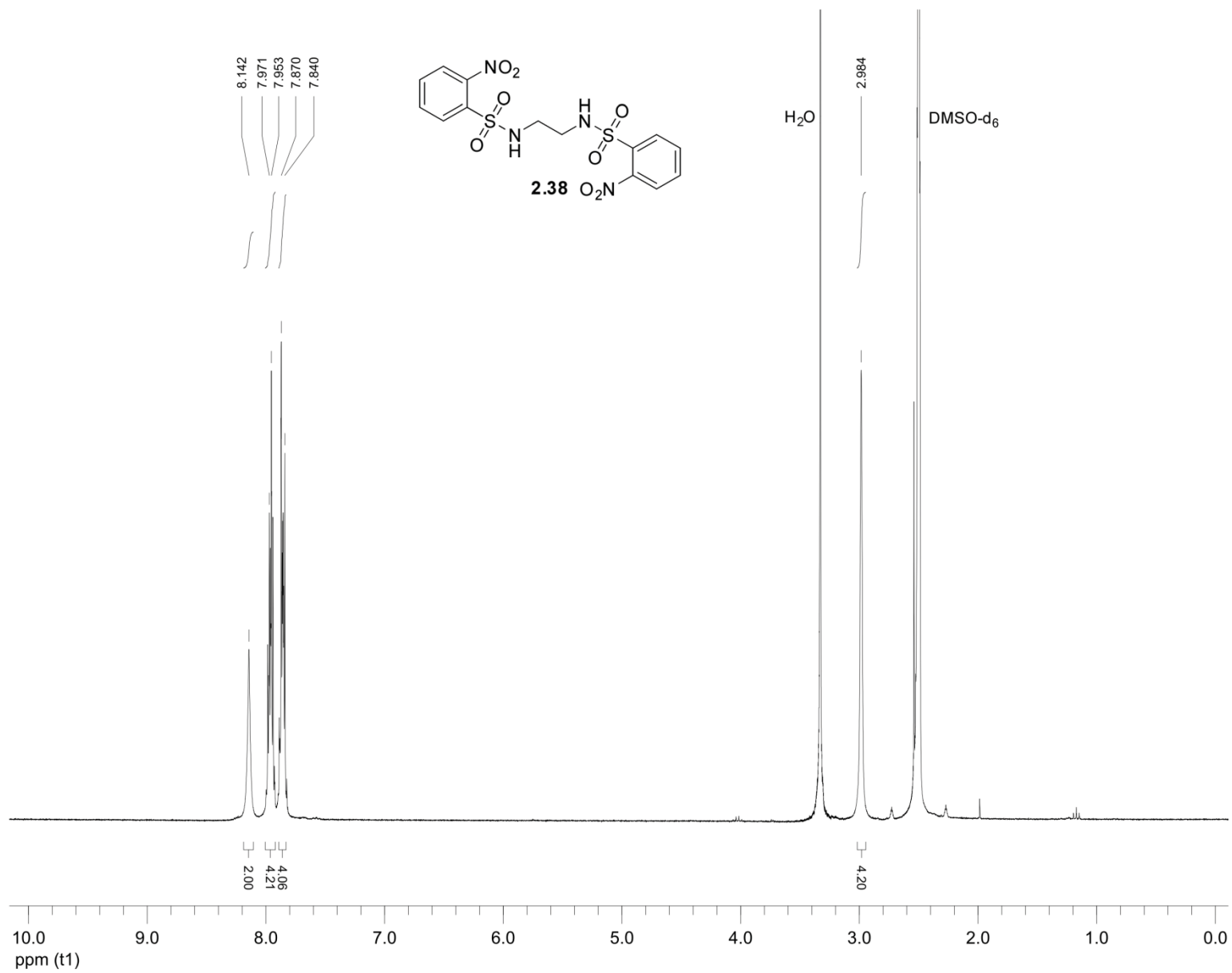


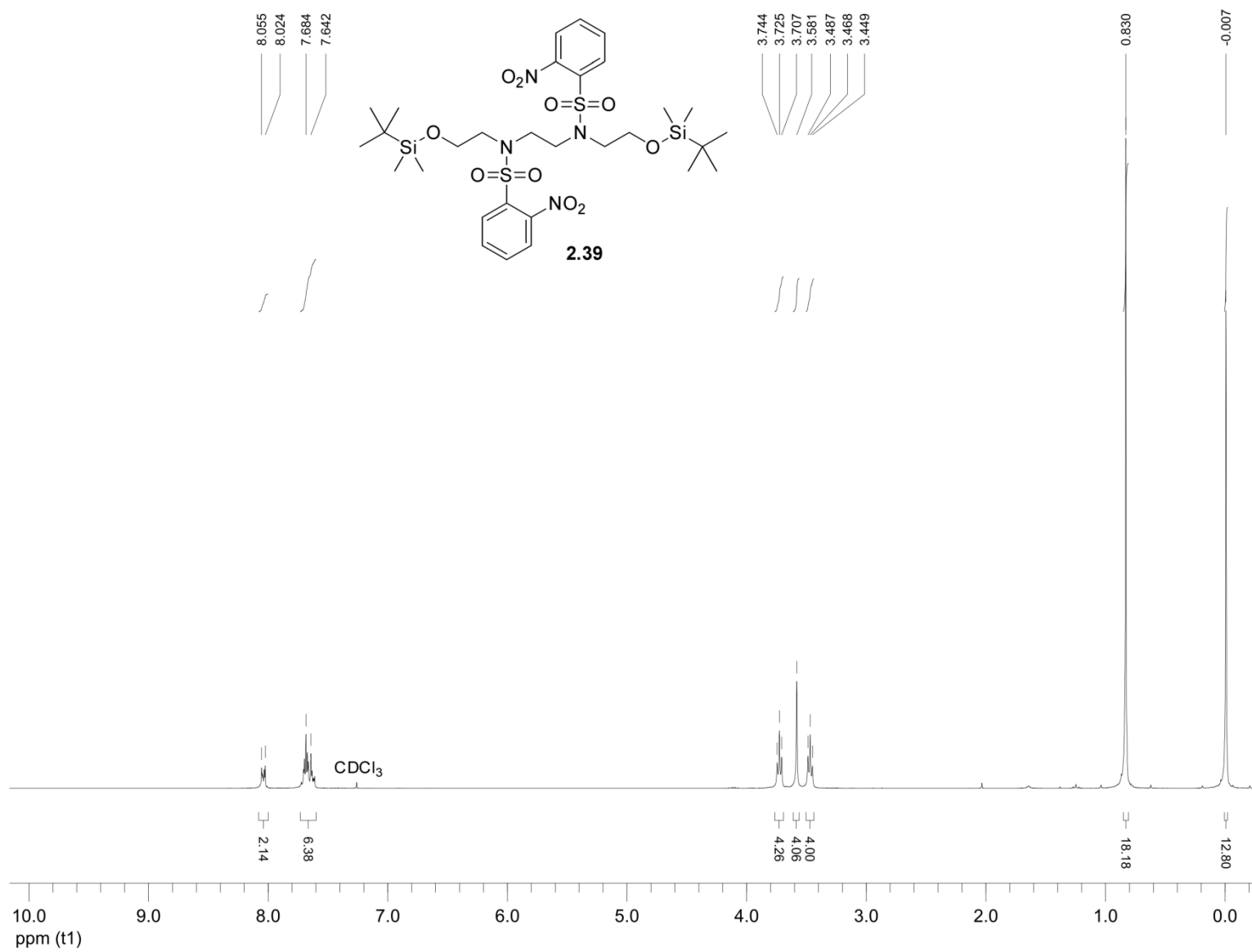


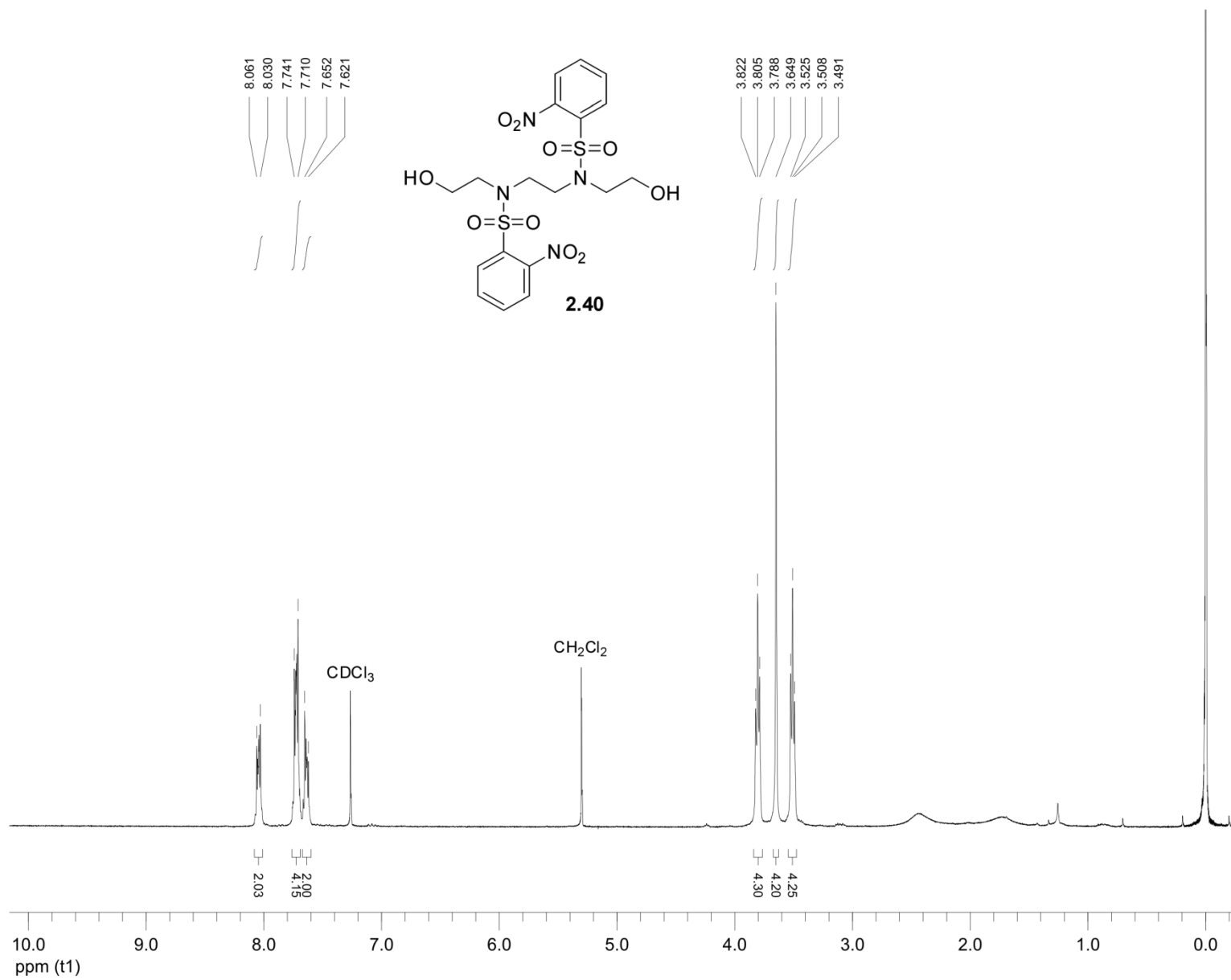


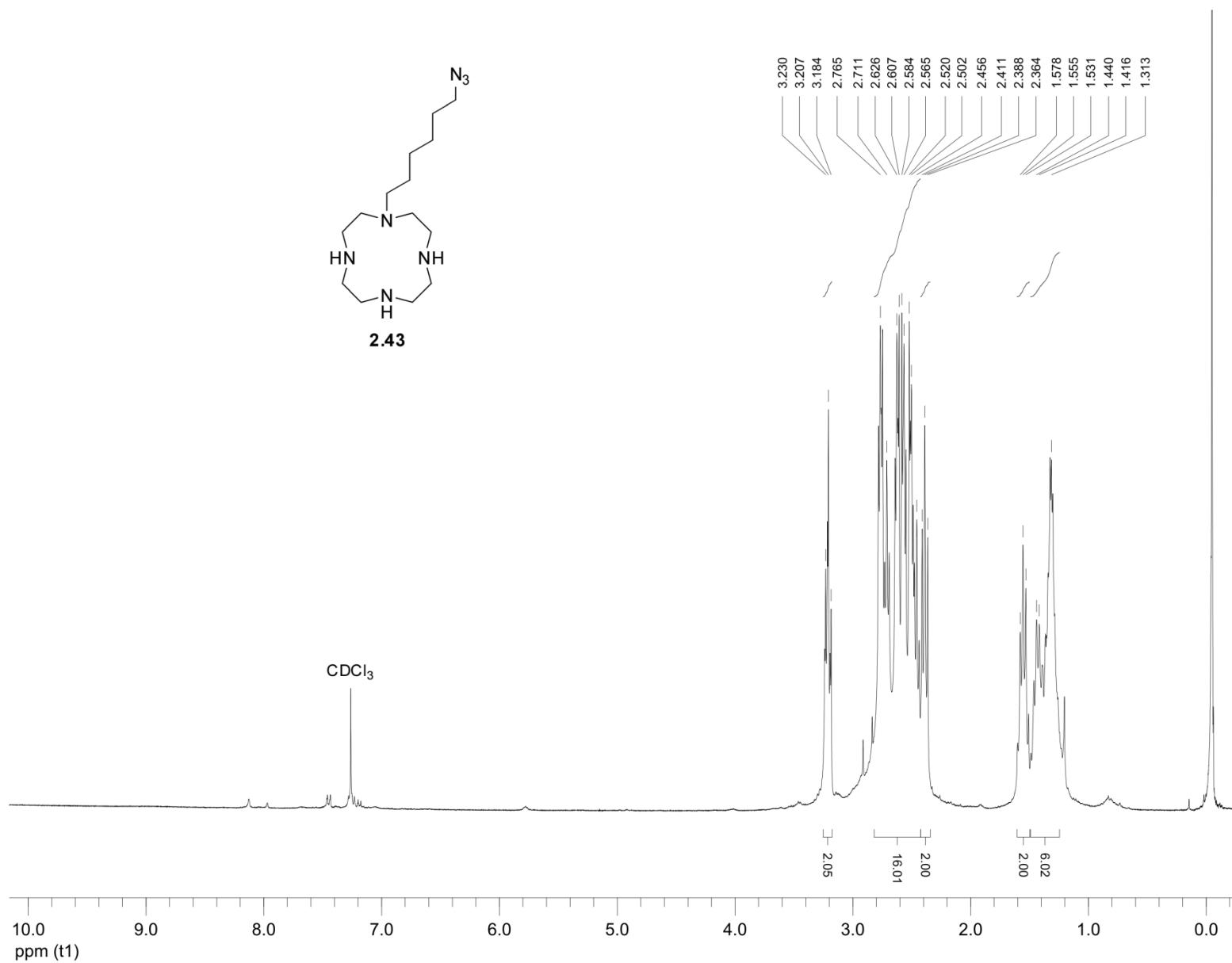
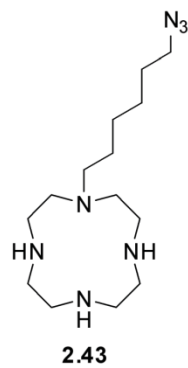


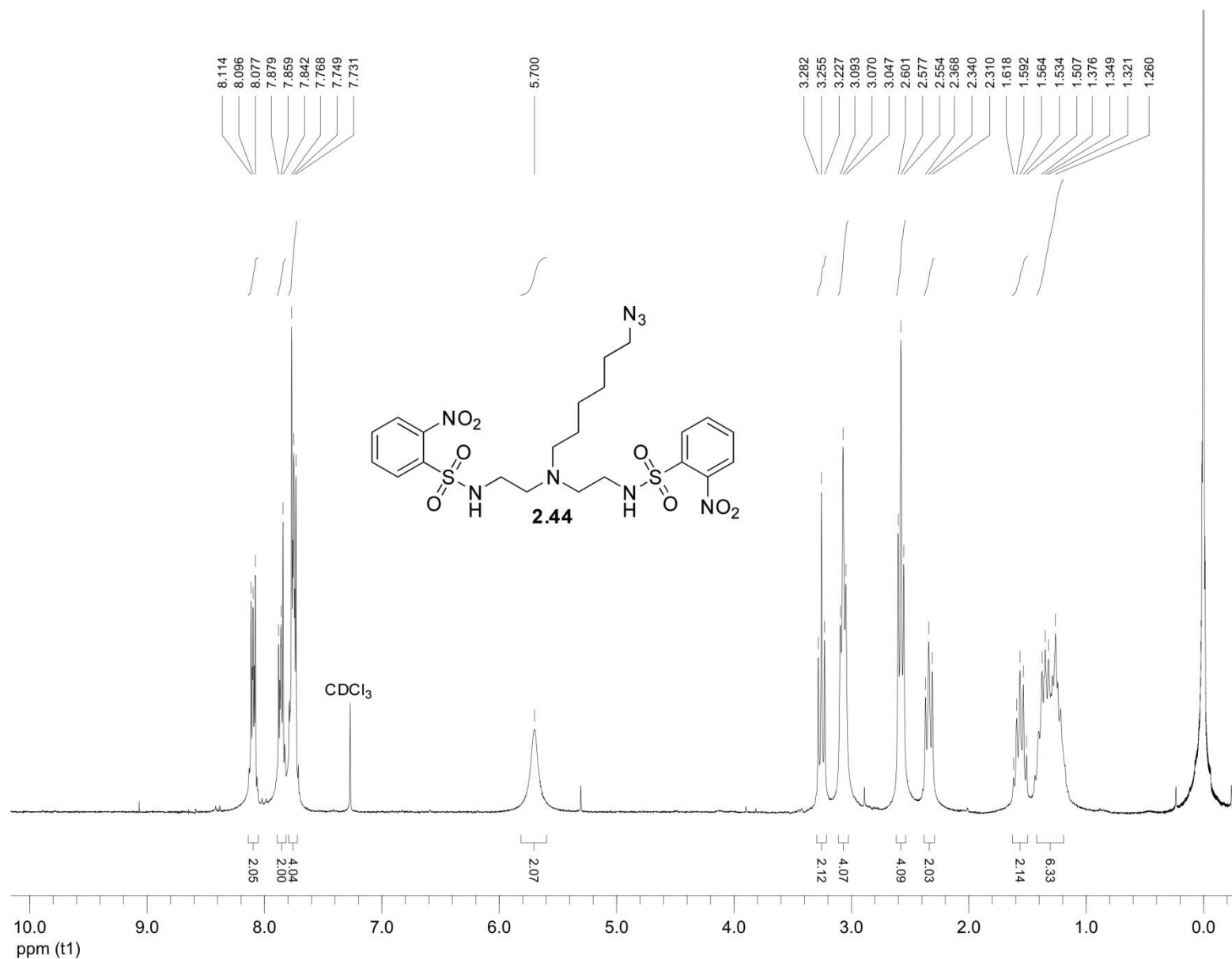


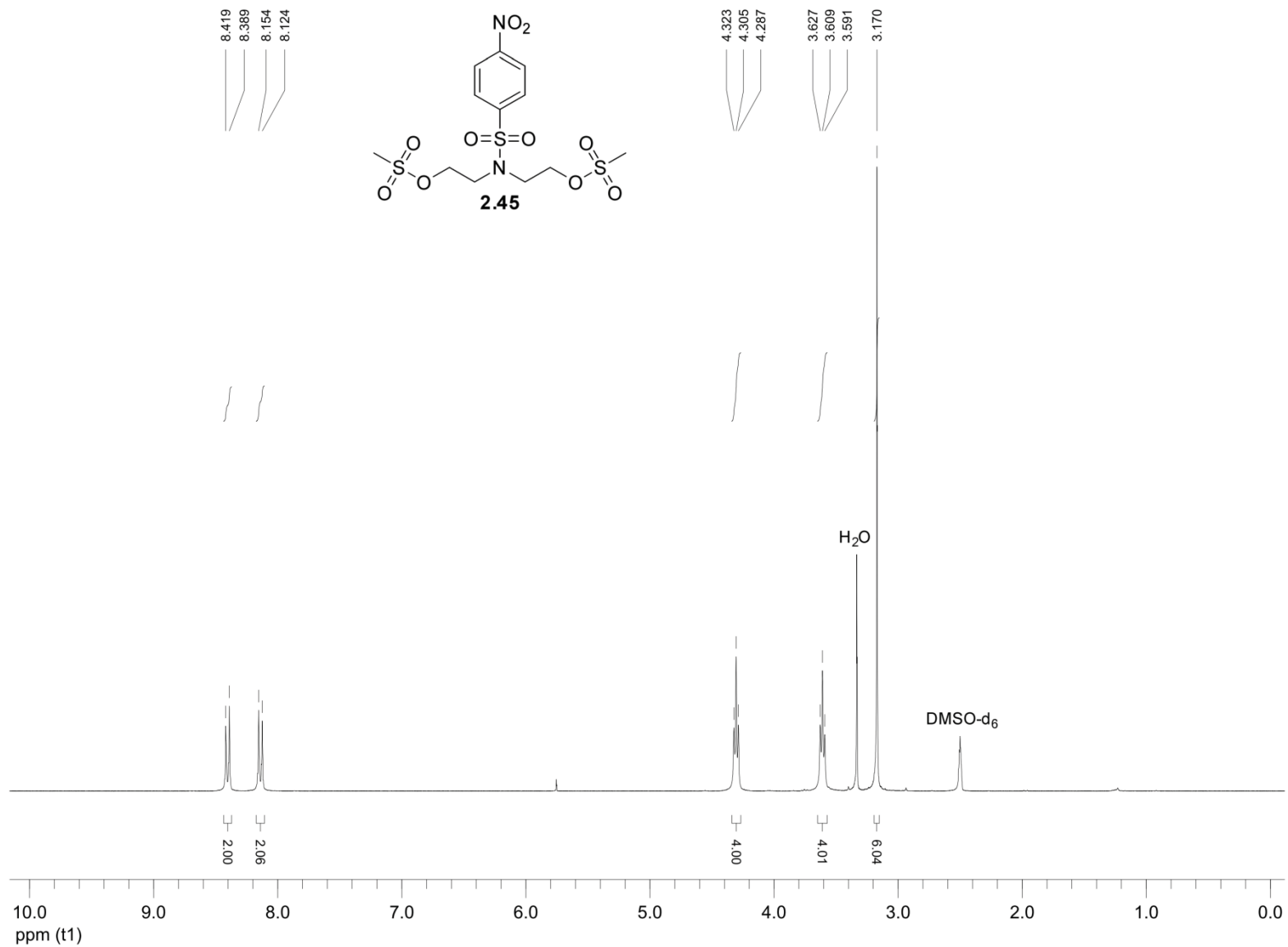


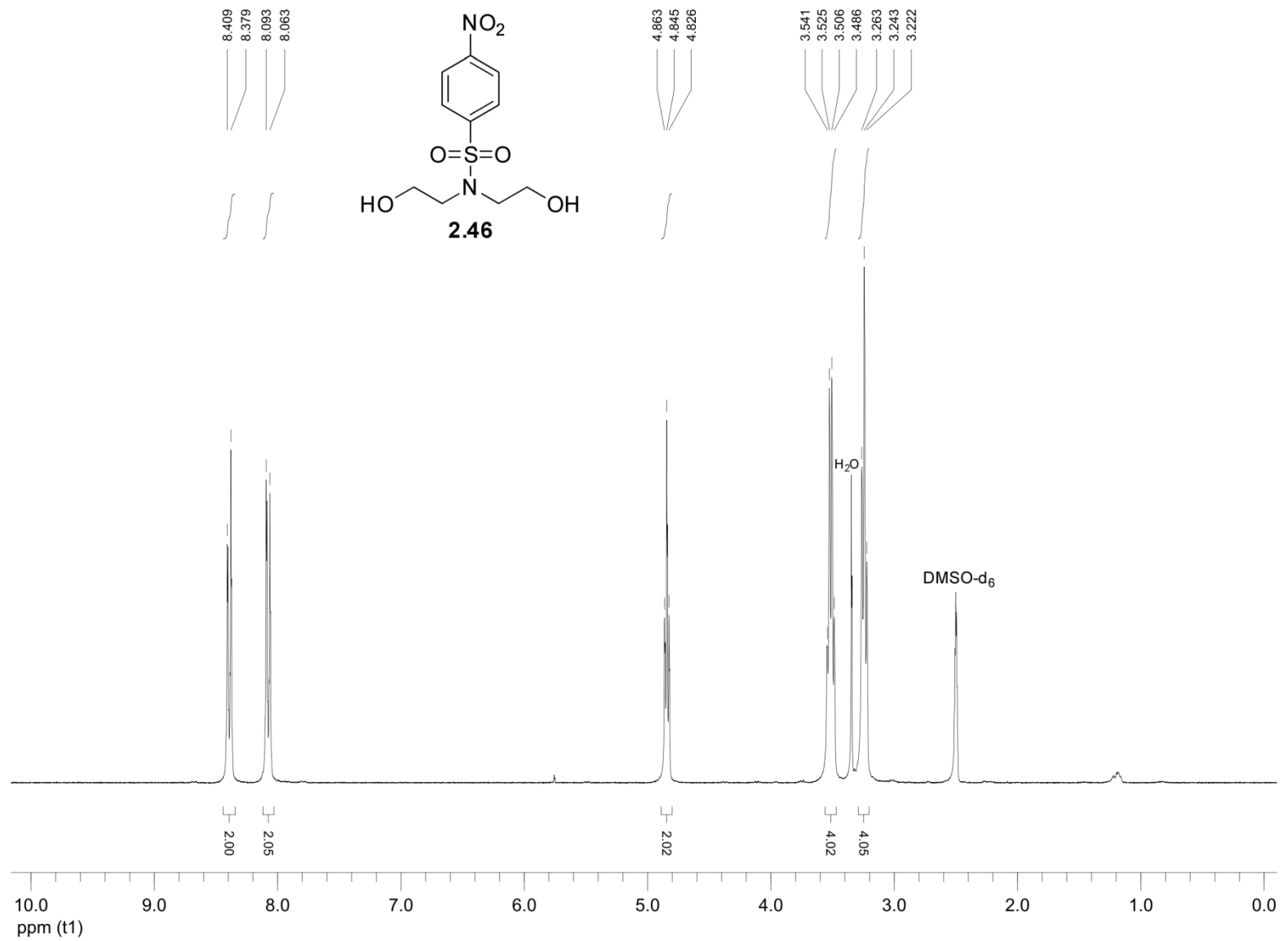


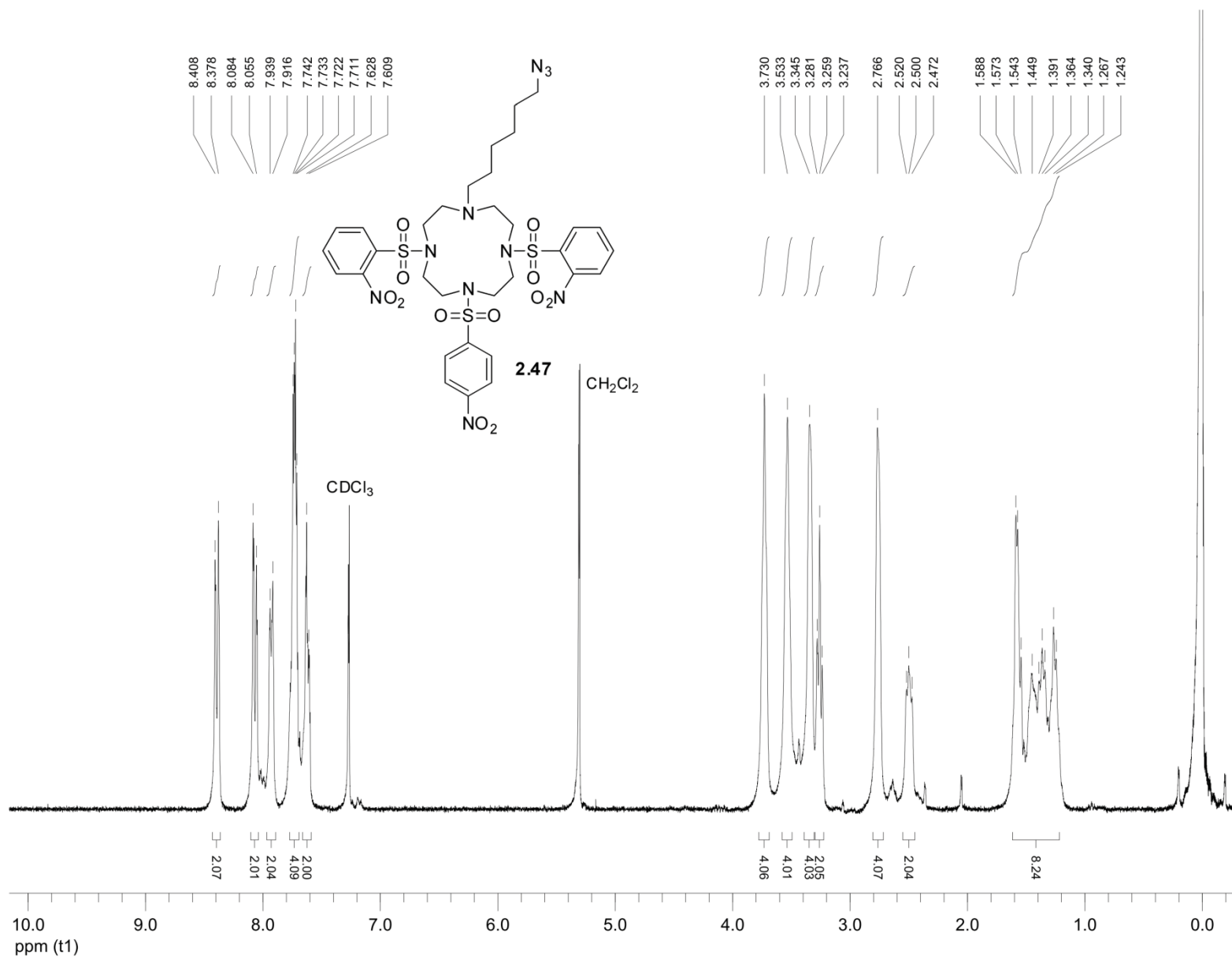












Chapter 3: Design and Synthesis of Boronic Acid-Based Carbohydrate Receptors

3.1 Introduction

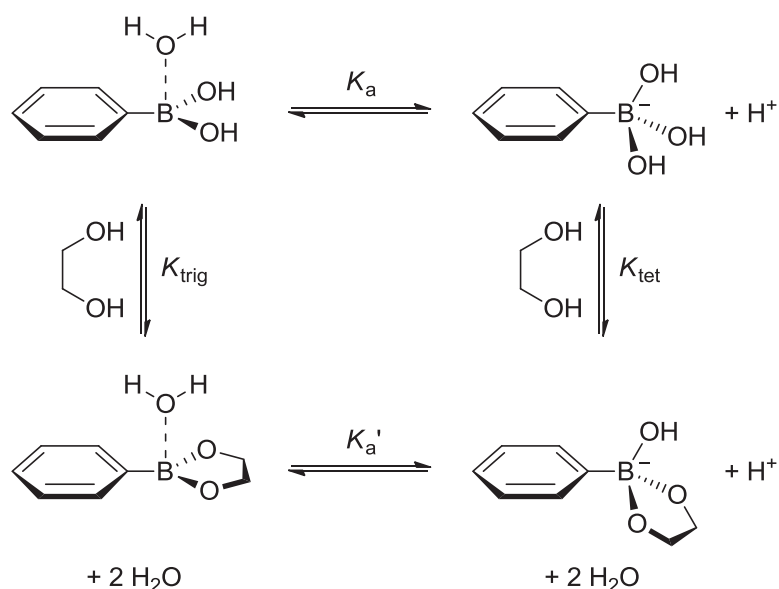
Carbohydrates, or saccharides, are the most abundant class of biomolecules in nature. In their most important roles, they provide structural support in the form of cellulose, and they store energy in the forms of starch and glycogen.¹⁰¹ Additionally, oligosaccharides, larger chains of sugars, are involved in protein targeting and folding, along with the regulation of cell recognition events for infection, inflammation, and immunity.¹⁰²

Since these biomolecules are present in the metabolic pathways of organisms, the detection of biologically important carbohydrates is crucial for numerous medical and industrial applications. For example, the monitoring of D-glucose is of particular importance because this sugar supplies the metabolic energy for most cells of higher organisms. In humans, the breakdown of D-glucose transport pathways has been linked to various diseases, including cancer,¹⁰³ cystic fibrosis,¹⁰⁴ renal glycosuria,¹⁰⁵ and diabetes.¹⁰⁶ Also, changes in glycosylation patterns often influence the function of a glycoprotein. The patterns of prostate-specific antigen from cancer cells in culture¹⁰⁷ and prostate cancer patients' tissue and sera¹⁰⁸ differ from those of the normal prostate. In industry, the applications of carbohydrate detection range from monitoring fermenting processes to determining the enantiomeric purity of synthesized drugs.

Saccharide recognition by boronic acids is unique in supramolecular chemistry. Single-point molecular recognition is possible, and the primary binding interaction consists of the reversible formation of a pair of covalent bonds as opposed to non-

covalent attractive forces. The first quantitative study of binding interactions between boronic acids and polyols was reported in 1959 by Lorand and Edwards.¹⁰⁹ The authors added a variety of polyols to solutions of phenylboronic acid in order to clarify the disputed structure of the phenylboronate anion. It was determined that the conjugate base of phenylboronic acid has a tetrahedral, not trigonal, structure. Additionally, the selectivity of phenylboronic acid towards saccharides was found to be D-fructose > D-galactose > D-glucose and seems to hold for all monoboronic acids.

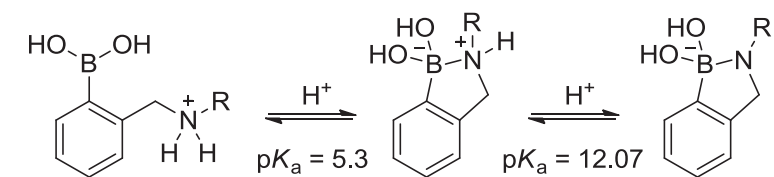
The equilibria involved in the binding of a diol by phenylboronate are usually summarized as a set of coupled equilibria (Scheme 3.1). While one explicitly associated water molecule is shown for clarity, water is in rapid exchange on the Lewis acidic boron in the same way that hydrated Lewis acidic metal ions exchange bound water. An analogy can be found with the ionization of Zn^{2+} in water to give a pK_a of 8.8 from the reaction $Zn-OH_2 \rightarrow Zn-OH + H^+$.¹¹⁰ As the phenylboronic acid reacts with water, a solvated proton is liberated, thus defining the acidity constant K_a ,¹¹¹ where pK_a



Scheme 3.1. Equilibria involved in phenylboronate binding of a diol.

= 8.70 in water at 25 °C.¹¹² The formation of a diol boronate anion complex is defined as K_{tet} , and the formation of a diol boronic acid complex is K_{trig} . It is observed that $K_{\text{tet}} > K_{\text{trig}}$, with differences commonly being up to five orders of magnitude. Also, it is known that the neutral boronic acid becomes more acidic upon binding. K_a' is defined as the acidity constant of the bound complex, and it is observed that $\text{p}K_a > \text{p}K_a'$, indicating that the boronic ester is more acidic than the boronic acid. The higher acidity of the ester is due to the reduction of bond angles upon formation of the cyclic boronate. Boronic acids have a bond angle of 120° which is shortened to 108° on binding, facilitating the change in hybridization from sp^2 to sp^3 .

For designing a useful boronic acid-based receptor, it is essential to achieve binding at neutral pH. The boronic acid–carbohydrate complex will only be present in significant amounts at neutral pH if the $\text{p}K_a$ of the boronic acid itself is ≤ 7 . Since the reported $\text{p}K_a$ value of phenylboronic acid is 8.8,¹¹³ it needs to be lowered for strong binding to occur at neutral pH. This can be accomplished by attaching electron-withdrawing groups to the aromatic structure. For example, the $\text{p}K_a$ of 4-carboxy-3-nitrophenylboronic acid was observed to be 7.0.^{113b} Another method, pioneered by Wulff, used a neighboring aminomethyl group (Scheme 3.2).¹¹⁴ The $\text{p}K_a$ for the second protonation in water of *ortho*-aminomethylphenylboronic acids was found to be 5.3.¹¹² The Anslyn group has shown via ¹¹B NMR studies that the monoprotonated species



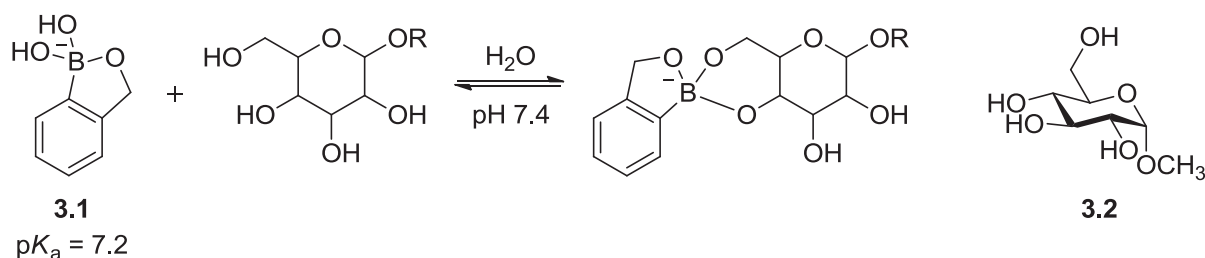
Scheme 3.2. Equilibria for *ortho*-aminomethylphenylboronic acids.

was tetrahedral at the boron atom.¹¹⁵

3.2 Boronic Acid-Based Receptors

It is well-known that boronic acids bind to diols on aromatic and five-membered rings much more tightly than diols on six-membered rings. Sensors consisting of bisboronic acids have been developed that can bind to six-membered ring diols with high affinities.¹¹⁶ For monoboronic acids, however, the interaction with a diol on a six-membered ring is so weak that measuring a binding constant under near physiological conditions is difficult. One exception is pinanediol,¹¹⁷ which is frequently used as a protecting group for boronic acids.

The general preference by boronic acids for diols on five-membered rings is particularly challenging for the recognition of carbohydrates released from or as part of a glycoprotein/peptide or glycolipid. These structures tend to contain only diols that are linear or on six-membered rings. Since there has been a high level of interest in receptors for many types of glycoproteins, including glycated hemoglobin¹¹⁸ and immunoglobulin G,¹¹⁹ it has been desirable to find boronic acids that have improved capabilities to bind diols on six-membered rings. The Hall lab developed *ortho*-hydroxymethylphenylboronic acid **3.1** (Scheme 3.3), also known as a benzoboroxole, that has been shown to recognize 1,3-diols on six-membered rings.¹²⁰ The design is similar to the previously mentioned neighboring amino group by Wulff. In neutral aqueous media, this sensor was able to bind hexopyranosides mainly using their 4,6-diol, which is presented on most cell-surface glycoconjugates. Binding constants with glycopyranosides were determined through an alizarin red-based UV assay at neutral



Scheme 3.3. Binding between boronic acid **3.1** and glycoconjugates, and glucopyranoside structure **3.2**.

pH in water.¹²¹ The K_a value with methyl α -D-glucopyranoside **3.2** was 22 M^{-1} , which was slightly lower than that with glucose. In comparison, the K_a of phenylboronic acid with glucose is approximately 5 M^{-1} at physiological pH.

Based on the same *ortho*-hydroxymethyl substituted system, Hindsgaul and co-workers designed a way to visually analyze the terminal glycosylation of glycoproteins.¹²² The boronic acid was incorporated in dye reagent **3.3** (Figure 3.1) containing tetramethylrhodamine. In this technique, an enzyme is used to release a saccharide such as galactose from a glycoprotein. The released sugar is then reacted with an amine that is immobilized on glass beads, followed by binding with **3.3** through the boronic acid functionality. This enables the labeling and visualization of the beads based on the presence of the sugar. The red color of the beads after binding to **3.3** can be seen by the human eye. The bound dye can also be released upon washing with a solution of glycerol, resulting in the boronate dye–glycerol complex and the beads turning back to white. The amount of released fluorescent complex was expected to be proportional to that of immobilized carbohydrate, allowing the sugar concentration to be determined. Various sugars including galactose, fucose, *N*-acetylglucosamine, and sialic acid were analyzed by this method.

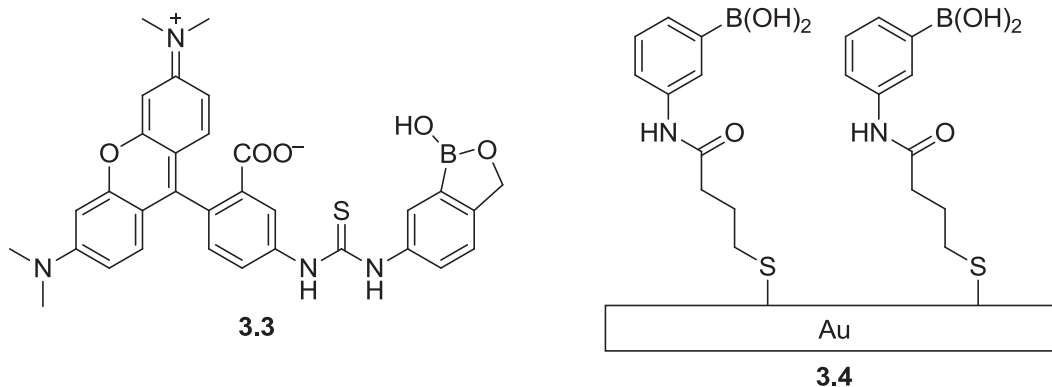


Figure 3.1. Tetramethylrhodamine-boronic acid **3.3** and polyphenylboronic acid monolayer **3.4**.

When binding with diols, the structure and charge of the boronic acid could change, resulting in potential energy changes in the system. Therefore, boronic acid-containing saccharide sensors based on electrochemical detection methods have been developed. Most current commercial D-glucose biosensors rely on electrochemical detection by enzymatic decomposition of saccharides.¹²³ One example of electrochemical sensing is polyphenylboronic acid-modified gold electrode **3.4** by the Anzai group.¹²⁴ The surface of the electrode was coated with a self-assembled monolayer film containing thiol-modified phenylboronic acids. In the presence of $[\text{Fe}(\text{CN})_6]^{3-}$ ion at neutral pH, the electrode displayed a concentration-dependent decrease in current with increasing sugar concentration. The detection range of the electrode was around the millimolar level for D-fructose, D-glucose, and D-mannose.

The examples above demonstrate a variety of ways of employing boronic acids in saccharide recognition. However, most boronic acid-based receptors so far were used to detect soluble sugar samples. Additional work is required in order to create effective sensors with high selectivity and sensitivity.

3.3 FRET-Based Detection

For the detection of glycosylated surfaces, a method is needed that offers high resolution in identifying regions with dense carbohydrate clusters on surfaces. This would be useful for lipid rafts, where cell membranes have separate domains that are enriched in specific components, such as sphingolipids, resulting in dense clusters of sugars.¹²⁵ These areas are “hot spots” of signaling activity in cells where proteins are recruited. Therefore, in order to characterize these important cell surface regions, it is essential to selectively detect areas of high carbohydrate density. To meet this goal, we set out to develop saccharide-binding receptors derivatized with FRET (Förster resonance energy transfer¹²⁶) pairs.

FRET involves the energy transfer between two chromophores. A donor chromophore in its excited state can transfer energy to an acceptor chromophore in proximity through non-radiative long-range dipole–dipole coupling, leading to the emission of the acceptor. As a result, for FRET to occur, the emission spectrum of the donor must overlap with the absorption spectrum of the acceptor, and the pair must be close in distance, typically within 10 nm.^{126b} If the molecules are too far apart, then no energy will be transferred, and only emission of the donor will be observed. The rate of energy transfer is inversely proportional to the sixth power of the distance between the chromophores, making FRET a very sensitive technique. It is possible to detect distances in the range of 20 to 80 Å, a convenient range for biomolecules.¹

In our strategy for the detection of carbohydrate clusters, saccharide surfaces will be treated with a mixture of carbohydrate-binding boronic acid receptors bearing either

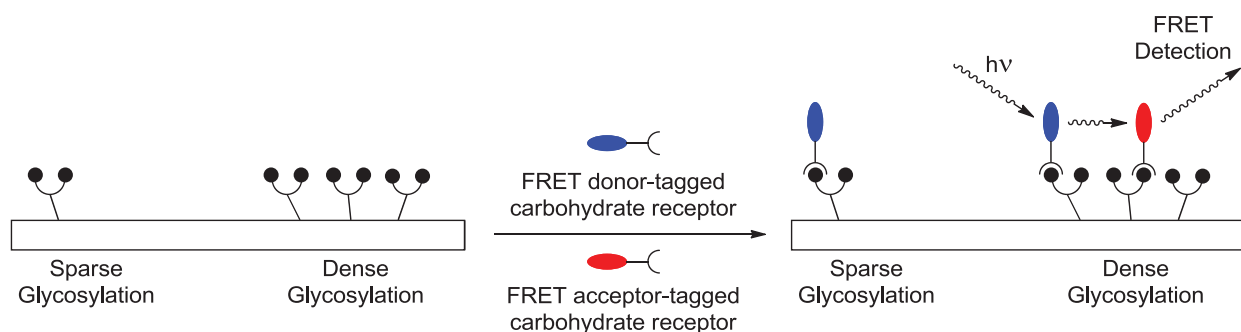


Figure 3.2. FRET-based assay for the detection of carbohydrate clustering on surfaces.

an attached donor or acceptor fluorophore (Figure 3.2). In areas of heavy glycosylation, the close distances between receptors with donor and acceptor fluorophores should result in FRET, leading to increases in acceptor emission. Regions of sparse glycosylation, on the other hand, should produce little background acceptor emission. Previously, a similar strategy was used to characterize FRET-tagged glycosylphosphatidylinositol (GPI)-anchored protein clusters in lipid rafts.¹²⁷ Therefore, in this manner, hot spots of high carbohydrate density are expected to be identified with high resolution.

Once the fluorophore-appended boronic acids have been synthesized, FRET activities can be tested by performing binding studies with divalent target analytes that contain diol functionalities coming from molecules such as catechol derivatives or mannose sugars. Upon binding to the boronic acid receptors, the divalent guests should bring the FRET donors and acceptors into proximity for FRET to occur.

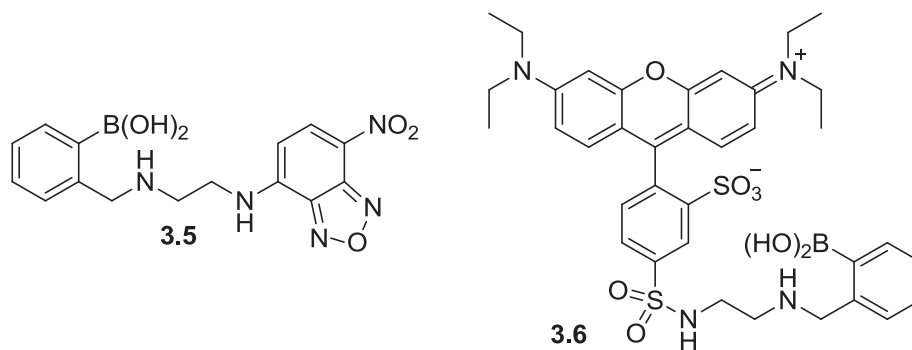
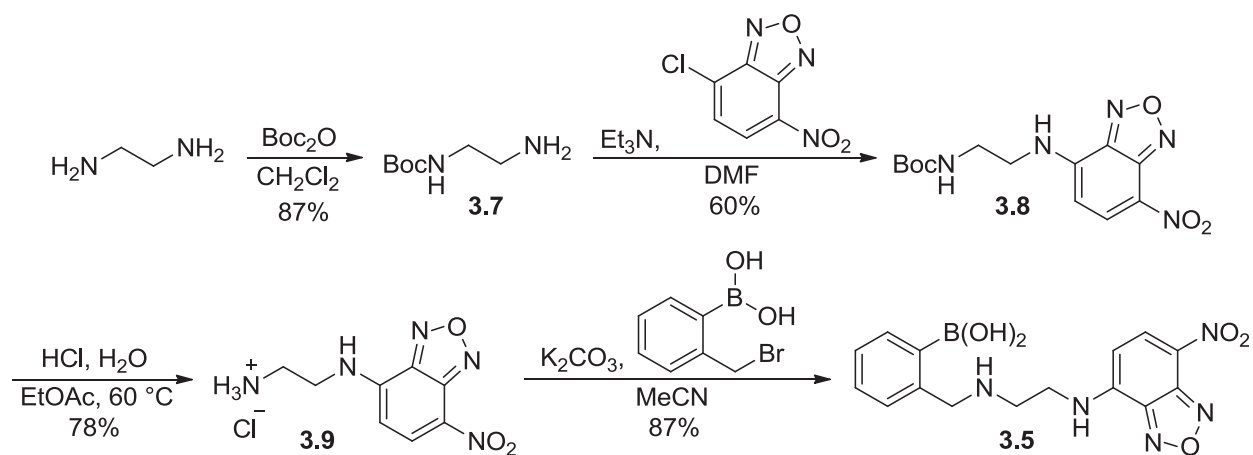


Figure 3.3. Phenylboronic acid-based receptors derivatized with FRET pairs.

3.4 Synthesis of Fluorophore-Tagged Boronic Acid Receptors

We planned on synthesizing fluorophore-tagged boronic acids **3.5** and **3.6**, which contain a phenylboronic acid receptor unit connected to the fluorophore via an ethylenediamine linker (Figure 3.3). The chosen fluorophores for FRET were 7-nitrobenzofurazan (NBD) as the donor in **3.5** and lissamine rhodamine B as the acceptor in **3.6**. We could either attach the boronic acid or the fluorophores to the linkers first. Since the polarity of the boronic acid could complicate purification steps, we decided to add it last. Therefore, the linkers were first derivatized with the fluorophores and then coupled with the boronic acid to create the receptors.

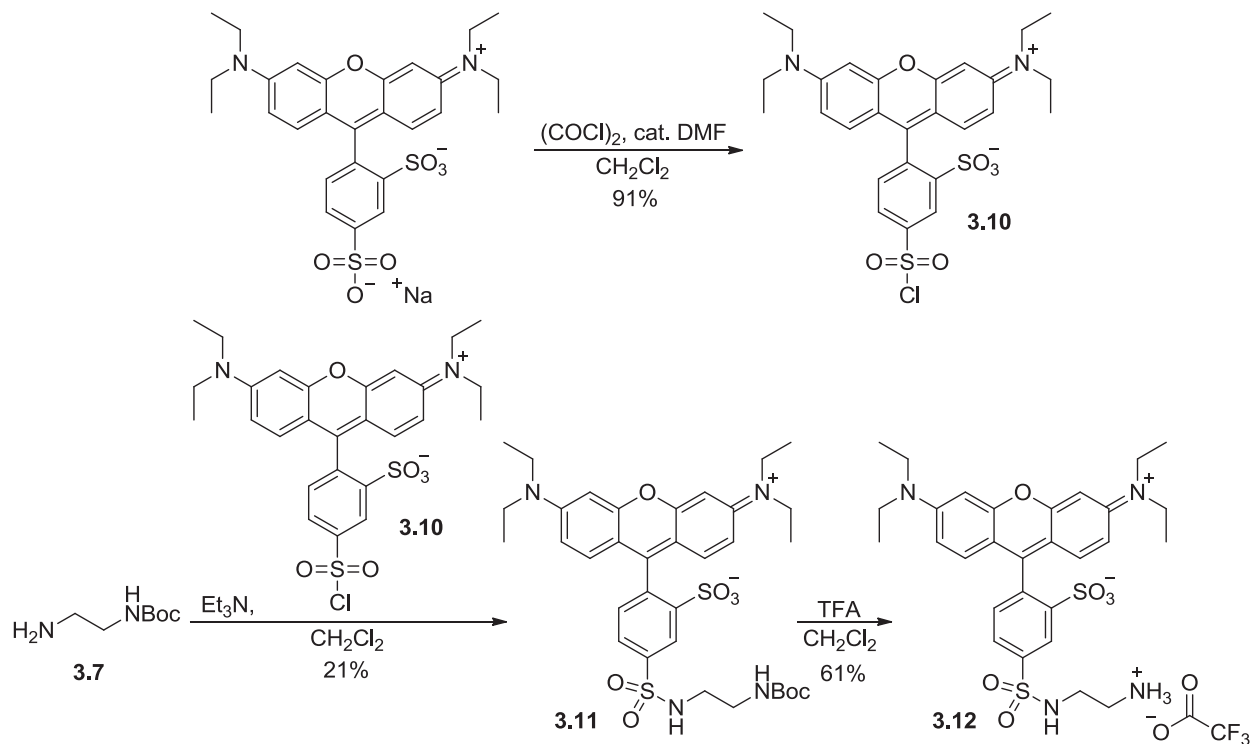
The synthesis of NBD-tagged **3.5** started with the mono-Boc protection of ethylenediamine to **3.7**, followed by attachment of the fluorophore via NBD chloride to form **3.8** (Scheme 3.4). Deprotection using hydrochloric acid, according to a known procedure,¹²⁸ gave amine **3.9**, which was then reacted with 2-bromomethyl phenylboronic acid in a nucleophilic substitution reaction to generate receptor **3.5**. Following similar procedures from the previous work of Manpreet Cheema in our lab, the boronic acid was successfully purified using reversed-phase column



Scheme 3.4. Synthesis of NBD-tagged boronic acid **3.5**.

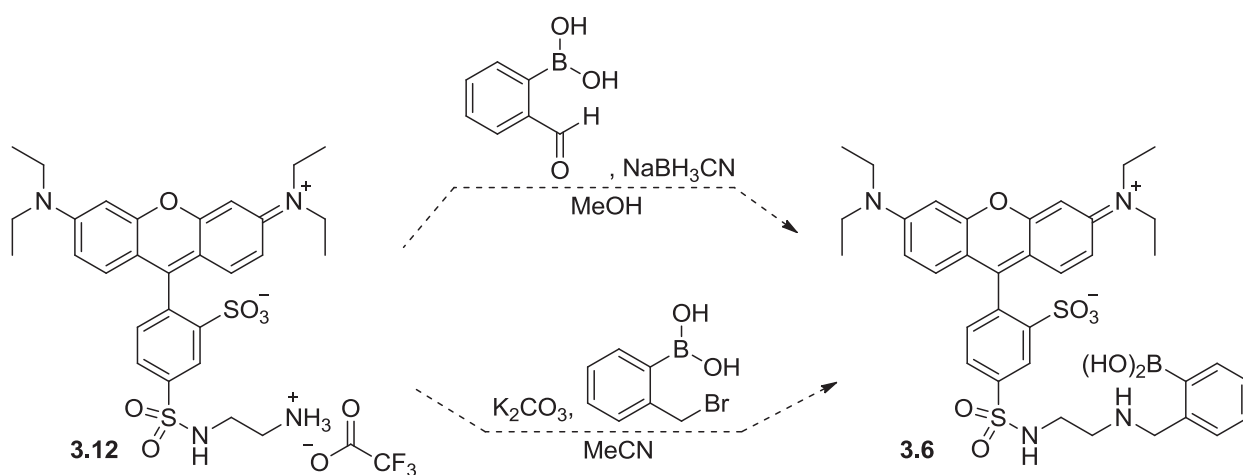
chromatography. With the FRET donor-tagged receptor in hand, we set out to synthesize rhodamine-appended boronic acid **3.6**.

The aforementioned mono-Boc protected amine **3.7** was coupled with lissamine rhodamine B sulfonyl chloride **3.10** to access fluorophore-tagged product **3.11** (Scheme



Scheme 3.5. Synthesis of rhodamine-tagged amine **3.12**.

3.5). This reaction resulted in two separable major products, which may be isomers due to the two sulfonyl groups on the rhodamine structure. Even though **3.10** is commercially available, we prepared it on a multigram scale from a significantly less expensive commercial precursor and oxalyl chloride in accordance with a literature report.¹²⁹ It should be noted that the major products in forming **3.11** were encountered when using both commercial and synthesized **3.10**. Boc deprotection of **3.11** with trifluoroacetic acid yielded amine **3.12**. Next, the attachment of the phenylboronic acid moiety to **3.12** was pursued. Two possible routes to make receptor **3.6** were attempted (Scheme 3.6). The first was a reductive amination using 2-formylphenylboronic acid and sodium cyanoborohydride, and the other was the same substitution reaction that was used to generate product **3.5**.



Scheme 3.6. Synthetic routes from amine **3.12** to rhodamine-tagged boronic acid **3.6**.

So far, initial attempts of both approaches have not yielded any clean products yet. Purification by reversed-phase column chromatography resulted in a possible mixture of product and unreacted rhodamine starting material, according to NMR spectra. The ^1H NMR spectrum showed all the peaks of **3.12** along with smaller

aromatic peaks corresponding to the phenylboronic acid, and the ^{11}B NMR spectrum displayed a single boron peak. This may indicate that the reaction did not reach completion, and some of product **3.6** was formed while some of the amine **3.12** was left unreacted. A clean separation was difficult to achieve here because both reactants, the amine **3.12** and the phenylboronic acid, contain highly polar groups.

3.5 SERS-Based Detection

One technique that can provide very high sensitivity in biomolecule detection is surface enhanced Raman spectroscopy (SERS). This surface-sensitive method enhances Raman scattering by adsorbed molecules on rough metal surfaces. In SERS, the target analyte is brought into close proximity to a nanostructured metal surface, such as silver, gold, or copper. When the incident light hits the surface, localized surface plasmons are excited, which enhances the electromagnetic energy near the target molecule. This, in turn, significantly amplifies the intensity of the inelastically scattered light.¹³⁰ The factor of total enhancement of the Raman signal can be as high as 10^{14} , allowing for the detection of single molecules.¹³¹

For sensing applications, an analyte with a receptor functionality is typically anchored to the metal surface through a thiolate group to form a self-assembled monolayer (SAM). An initial Raman signal can then be measured. Afterwards, a variety of guest molecules are added to interact with the analyte in the SAM. A new Raman signal is analyzed to determine which guest is bound to the receptor by providing information on individual functional groups on a molecule.

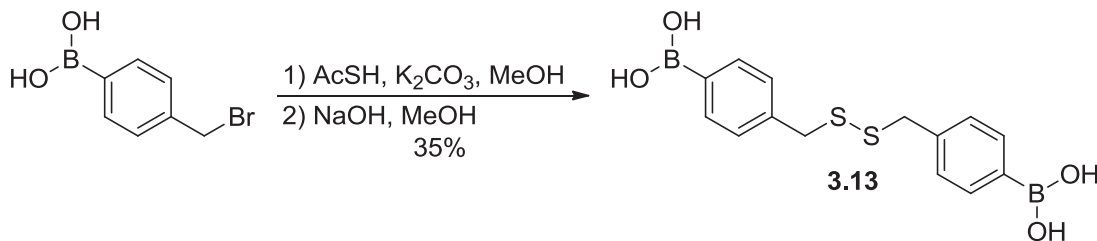
While SERS has been used to characterize SAMs containing phenylboronic acids,¹³² other analytical methods were employed to analyze the recognition of sugars in those reports. To date, the use of SERS to study interactions between boronic acid-based sensors and saccharides has not yet been demonstrated. This technique is particularly beneficial because it can distinguish between different functional groups. This is significant due to the low selectivity of boronic acids for various carbohydrates. It is difficult to develop a sensor for a particular type of sugar and identify glycosylation with specific carbohydrates. SERS would provide the ability to determine what exact type of sugar is bound to the boronic acid receptor.

Therefore, we planned to synthesize a boronic acid receptor with an appended thiol group to allow for attachment to metal surfaces. The sensor will be tested using SERS in collaboration with Dr. Jon Camden in our department. After attaching the boronic acid to the metal surface to form a SAM, carbohydrate guests will be introduced, and Raman signals should be able to characterize the saccharide that is bound to the receptor.

3.6 Synthesis of Thiol-Tagged Boronic Acid Receptor

Following the previous work of Paul Petersen in our group, a phenylboronic acid derivative with a short thiol tag was sought. This led to the synthesis of receptor **3.13** (Scheme 3.7) from 4-bromomethylphenylboronic acid. Initially, a literature protocol was followed that used thiolacetic acid and potassium carbonate in the conversion of benzylic bromides to benzylic thiols.¹³³ Using the reported reaction conditions, the

thioacetate intermediate was isolated as the product, indicating that the carbonate base was not sufficient in our case to hydrolyze the thioacetate into the desired thiol.



Scheme 3.7. Synthesis of phenylboronic acid disulfide **3.13**.

After increasing the amounts of potassium carbonate had no effect, sodium hydroxide was added to successfully transform the thioacetate. NMR spectra of the product suggested that the thiol dimerized to its disulfide form due to the basic conditions used in the reaction. The ¹H and ¹³C NMR chemical shifts were similar to the ones found for bis(benzyl) disulfide.¹³⁴ The disulfide can be used for studies without problems since the metal surface is expected to cleave the disulfide bond when forming a SAM.

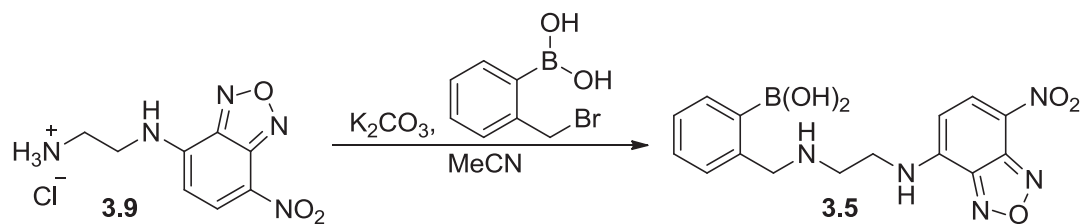
Following the synthesis of **3.13**, the same reaction conditions were applied to starting material isomers 2- and 3-bromomethylphenylboronic acid. Unfortunately, the ¹H NMR spectra of the observed products showed a peak corresponding to one methoxy group. This indicated that the methanol solvent participated in the substitution reaction by either displacing the bromide in the starting material or reacting with the boronic acid via addition of the methoxy group to the boron.

While the additional isomers did not yield the desired products to date, a phenylboronic acid receptor derivatized with a short tag containing a sulfur group was synthesized. This compound will be used to study carbohydrate interactions using

SERS, leading to the differentiation of individual sugars binding to the boronic acid group. This technique, along with future FRET-based detection of glycosylated surfaces, should allow for unprecedented and more sophisticated saccharide recognition studies with high sensitivity and selectivity.

3.7 Experimental

2-[2-(7-nitrobenzofurazan-4-yl)aminoethylaminomethyl]phenylboronic acid (**3.5**)



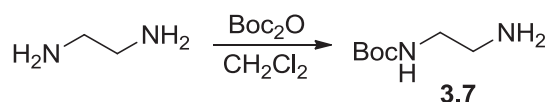
Potassium carbonate (0.32 g, 2.33 mmol) and 2-bromomethylphenylboronic acid (0.17 g, 2.33 mmol) were added to a solution of **3.9** (0.20 g, 0.78 mmol) in acetonitrile (15 mL). The reaction mixture was stirred in the dark at rt overnight, then filtered and concentrated. Purification on a reversed-phase column (10 g, C18) with gradient elution from 0 to 100% methanol/water gave the product as an orange solid (0.24 g, 87%).

1H NMR (300 MHz, CD_3OD) δ 8.47 (d, $J = 8.8$ Hz, 1H), 7.50–7.40 (m, 1H), 7.26–7.14 (m, 3H), 6.44 (d, $J = 8.8$ Hz, 1H), 4.11 (s, 2H), 4.00–3.88 (m, 2H), 3.32–3.25 (m, 2H).

^{13}C NMR (125 MHz, CD_3OD) δ 149.83, 142.82, 140.34, 136.70, 131.57, 128.67, 127.84, 123.98, 121.20, 112.13, 55.58, 47.30, 39.53. ^{11}B NMR (128 MHz, CD_3OD) δ 11.27.

DART–HRMS $[M-B(OH)_2+H]^+$ calcd: 314.1253, found: 314.1080.

tert-butyl (2-aminoethyl)carbamate (**3.7**)



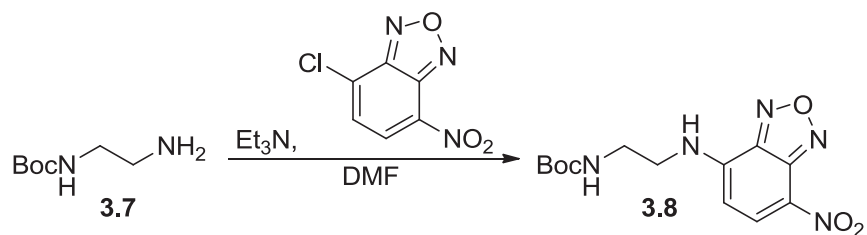
A solution of di-*tert*-butyldicarbonate (3.91 g, 17.93 mmol) in dichloromethane (40 mL) was added dropwise via addition funnel to a solution of ethylenediamine (12 mL, 179.30 mmol) in dichloromethane (20 mL). The reaction mixture was stirred at rt overnight and

then extracted with dichloromethane (2 × 50 mL) from saturated aqueous sodium carbonate (50 mL). The combined organic layers were dried over magnesium sulfate, filtered, and concentrated to give the product as a yellow oil (2.51 g, 87%).

Characterizations matched those reported in the literature.¹³⁵

¹H NMR (300 MHz, CDCl₃) δ 4.99 (bs, 1H), 3.18 (dd, *J* = 11.7, 5.8 Hz, 2H), 2.80 (t, *J* = 5.8 Hz, 2H), 1.45 (s, 9H), 1.37 (bs, 2H).

***N*-(*tert*-butoxycarbonyl)-*N'*-(7-nitrobenzofurazan-4-yl)ethylenediamine (3.8)**

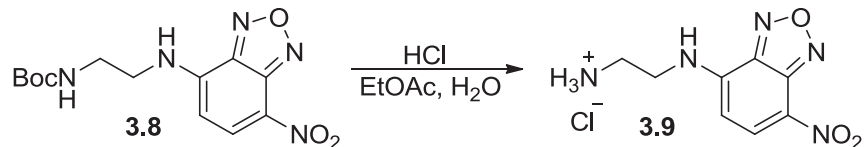


A solution of 4-chloro-7-nitrobenzofurazan (0.66 g, 3.23 mmol) in anhydrous *N,N*-dimethylformamide (6 mL) was added dropwise to a stirred solution of 3.7 (0.52 g, 3.23 mmol) and triethylamine (0.49 mL, 3.55 mmol) in anhydrous *N,N*-dimethylformamide (24 mL). The reaction mixture was stirred in the dark at rt overnight and then extracted with chloroform (2 × 40 mL) from water (40 mL). The combined organic layers were dried over magnesium sulfate, filtered, and concentrated. Column chromatography over silica gel with gradient elution from 50 to 75% ethyl acetate/hexanes yielded the product as a dark orange solid (0.62 g, 60%).

Characterizations matched those reported in the literature.¹²⁸

¹H NMR (300 MHz, CDCl₃) δ 8.47 (d, *J* = 8.7 Hz, 1H), 7.79 (bs, 1H), 6.18 (d, *J* = 8.7 Hz, 1H), 5.23 (bs, 1H), 3.69–3.56 (m, 4H), 1.46 (s, 9H).

***N*-(7-nitrobenzofurazan-4-yl)ethylenediamine hydrochloride (3.9)**

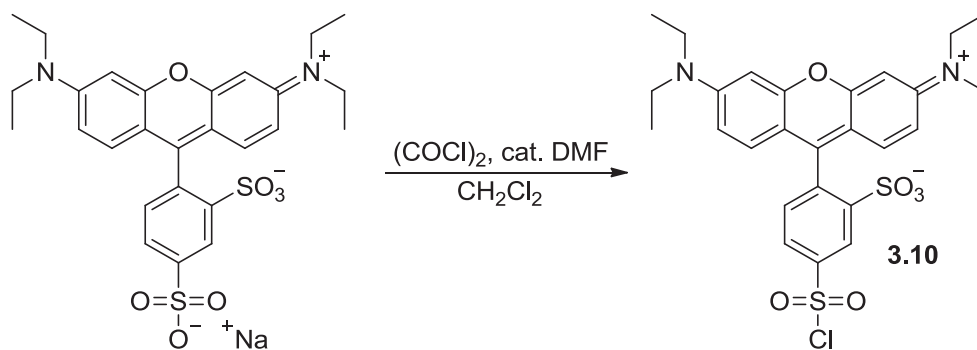


2 M hydrochloric acid (2.89 mL) was added to a solution of **3.8** (0.62 g, 1.93 mmol) in ethyl acetate (20 mL). After stirring in the dark at 60 °C for 2 h, the reaction mixture was concentrated by rotary evaporation, and the residue was washed with chloroform and filtered to give the product as an orange solid (0.39 g, 78%).

Characterizations matched those reported in the literature.¹²⁸

¹H NMR (300 MHz, DMSO-*d*₆) δ 9.41 (bs, 1H), 8.54 (d, *J* = 8.9 Hz, 1H), 8.29 (bs, 3H), 6.55 (d, *J* = 8.9 Hz, 1H), 3.91–3.67 (m, 2H), 3.20–3.05 (m, 2H).

Lissamine rhodamine B sulfonyl chloride (3.10)



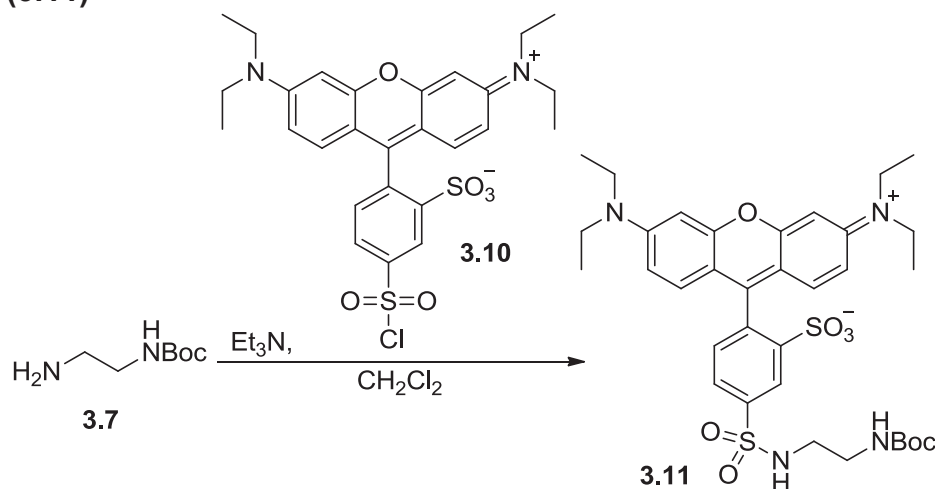
Oxalyl chloride (1.57 mL, 17.97 mmol) was added dropwise to a solution of Acid Red 52 sodium salt (2.09 g, 3.59 mmol) in dichloromethane (35 mL) at 0 °C. A catalytic amount of *N,N*-dimethylformamide (0.04 mL) was then added, and the reaction mixture was stirred in the dark at rt overnight, after which it was concentrated by rotary evaporation. Benzene (30 mL) was added, and the solvent was removed by rotary evaporation.

Diethyl ether (30 mL) was added to the residue, and the resulting precipitate was filtered and washed with ethyl acetate and dried under vacuum to yield the product as a shiny brown solid (1.88 g, 91%).

Characterizations matched those reported in the literature.¹²⁹

¹H NMR (300 MHz, DMSO-d₆) δ 8.26 (d, *J* = 1.6 Hz, 1H), 7.72 (dd, *J* = 7.8, 1.6 Hz, 1H), 7.16 (d, *J* = 7.8 Hz, 1H), 7.04–6.99 (m, 4H), 6.93–6.88 (m, 1H), 3.62 (q, *J* = 7.0 Hz, 8H), 1.19 (t, *J* = 7.0 Hz, 12H).

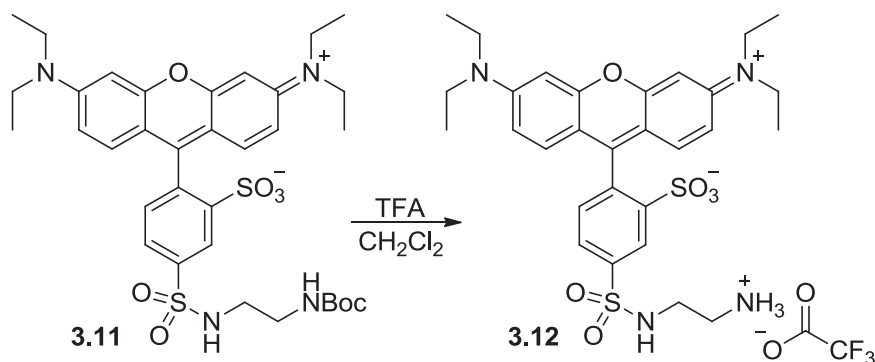
***N*-(*tert*-butoxycarbonyl)-*N'*-(lissamine rhodamine B sulfonyl)ethylenediamine (3.11)**



Lissamine rhodamine B sulfonyl chloride **3.10** (0.23 g, 0.40 mmol) was added in small portions to a stirred solution of **3.7** (0.064 g, 0.40 mmol) and triethylamine (0.061 mL, 0.44 mmol) in dichloromethane (10 mL) at 0 °C. The reaction mixture was stirred in the dark at rt overnight and then concentrated by rotary evaporation. Column chromatography over silica gel with gradient elution from 3 to 15% methanol/dichloromethane gave the product as a purple solid (0.059 g, 21%).

^1H NMR (300 MHz, CD_3OD) δ 8.58 (s, 1H), 8.21 (d, $J = 7.9$ Hz, 1H), 7.51 (d, $J = 7.9$ Hz, 1H), 7.14–7.02 (m, 4H), 6.99–6.94 (m, 2H), 3.68 (q, $J = 7.0$ Hz, 8H), 2.98 (t, $J = 5.7$ Hz, 2H), 2.85 (t, $J = 6.3$ Hz, 2H), 1.36 (s, 9H), 1.31 (t, $J = 7.0$ Hz, 12H). ^{13}C NMR (125 MHz, CD_3OD) δ 159.41, 157.36, 156.39, 149.38, 142.42, 133.91, 133.16, 132.96, 130.89, 127.74, 115.61, 97.34, 80.27, 47.05, 43.74, 41.56, 28.86, 13.04. MALDI–HRMS $[\text{M}+\text{Na}]^+$ calcd: 723.2498, found: 723.2506.

***N*-(lissamine rhodamine B sulfonyl)ethylenediamine (3.12)**

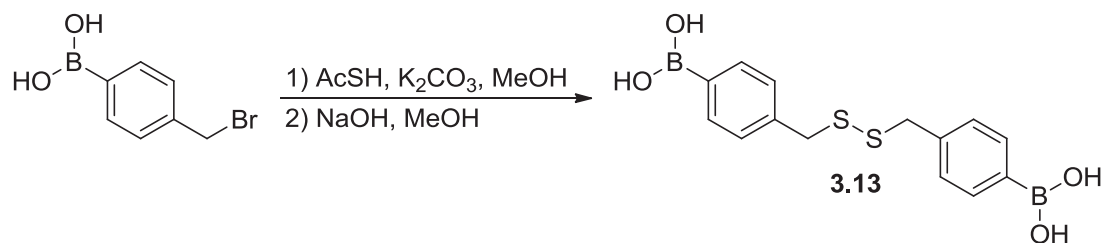


Trifluoroacetic acid (5 mL) was added dropwise to a solution of **3.11** (0.051 g, 0.073 mmol) in dichloromethane (5 mL). The reaction mixture was stirred in the dark at rt for 2 h and then concentrated and dried under vacuum to obtain a purple solid of trifluoroacetate salts (0.032 g, 61%).

^1H NMR (300 MHz, CD_3OD) δ 8.59 (s, 1H), 8.22 (d, $J = 7.9$ Hz, 1H), 7.54 (d, $J = 7.9$ Hz, 1H), 7.14–7.01 (m, 4H), 7.01–6.91 (m, 2H), 3.68 (q, $J = 7.2$ Hz, 8H), 3.13 (t, $J = 6.0$ Hz, 2H), 2.97 (t, $J = 6.0$ Hz, 2H), 1.30 (t, $J = 7.2$ Hz, 12H). ^{13}C NMR (75 MHz, CD_3OD) δ 159.39, 157.35, 155.72, 149.30, 141.40, 134.15, 133.36, 133.03, 131.26, 127.73,

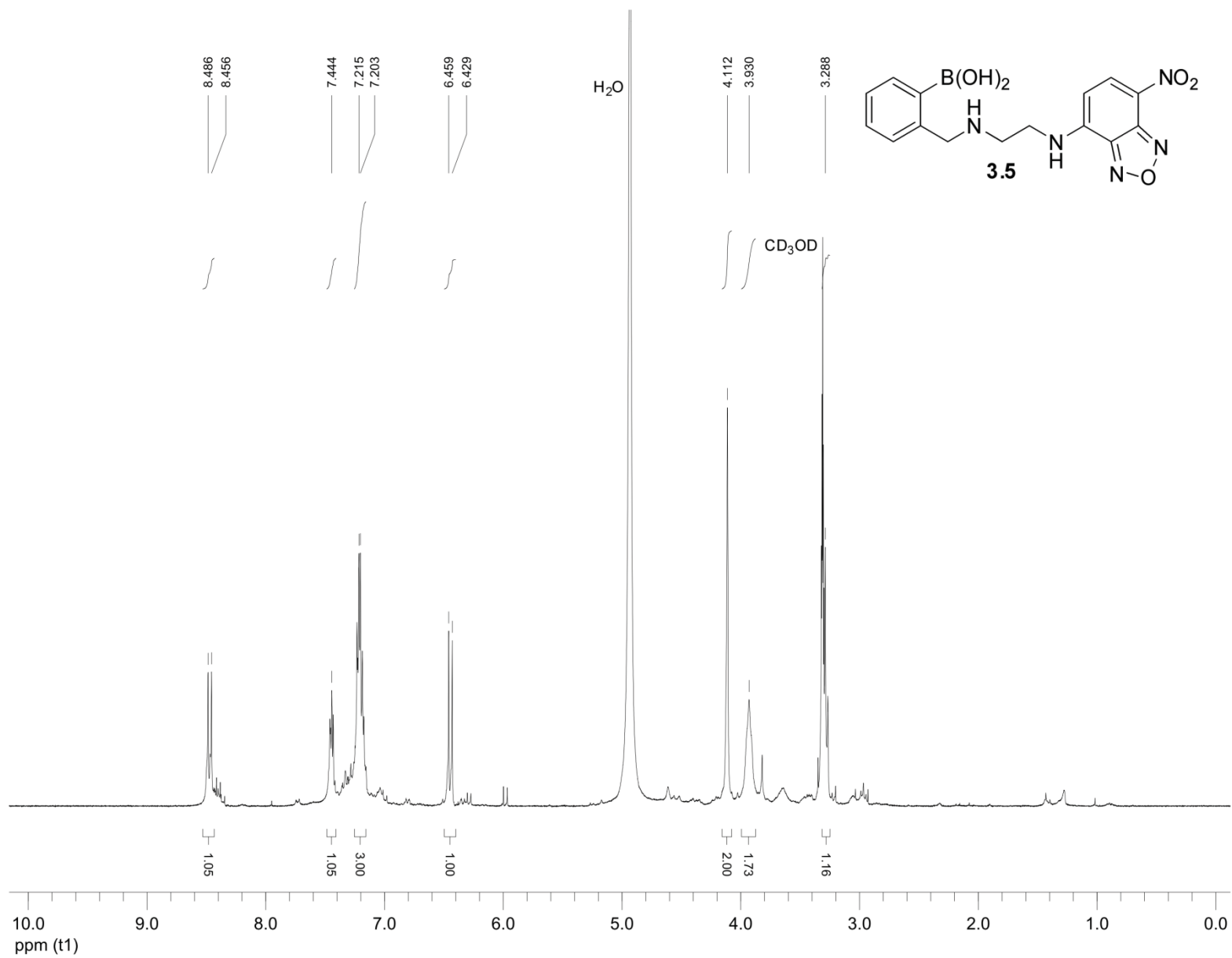
115.64, 115.31, 97.36, 47.02, 41.42, 40.69, 12.98. MALDI–HRMS $[M+Na]^+$ calcd: 623.1974, found: 623.1981.

{[disulfanediy]bis(methylene)]bis(4,1-phenylene)}diboronic acid (3.13)

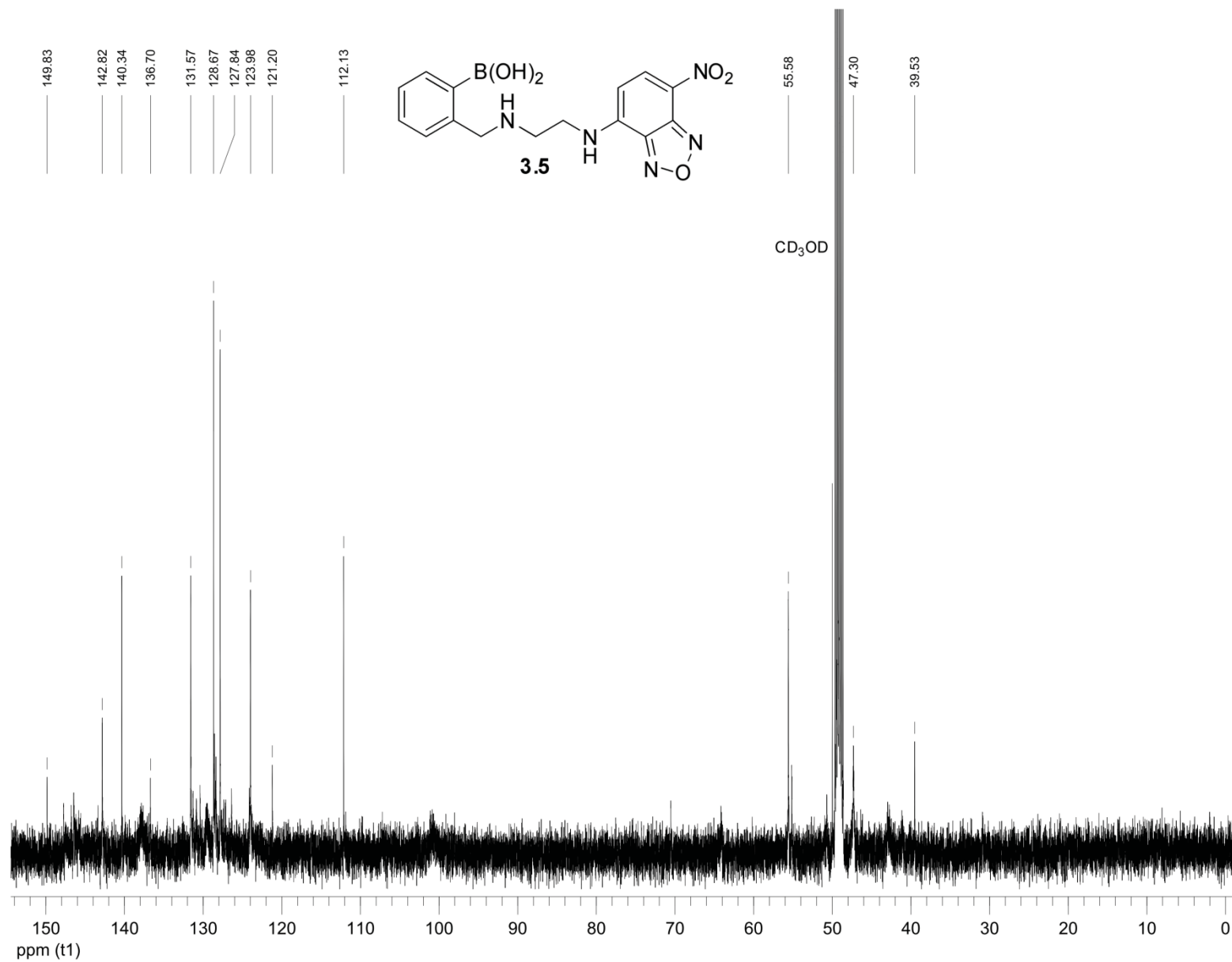


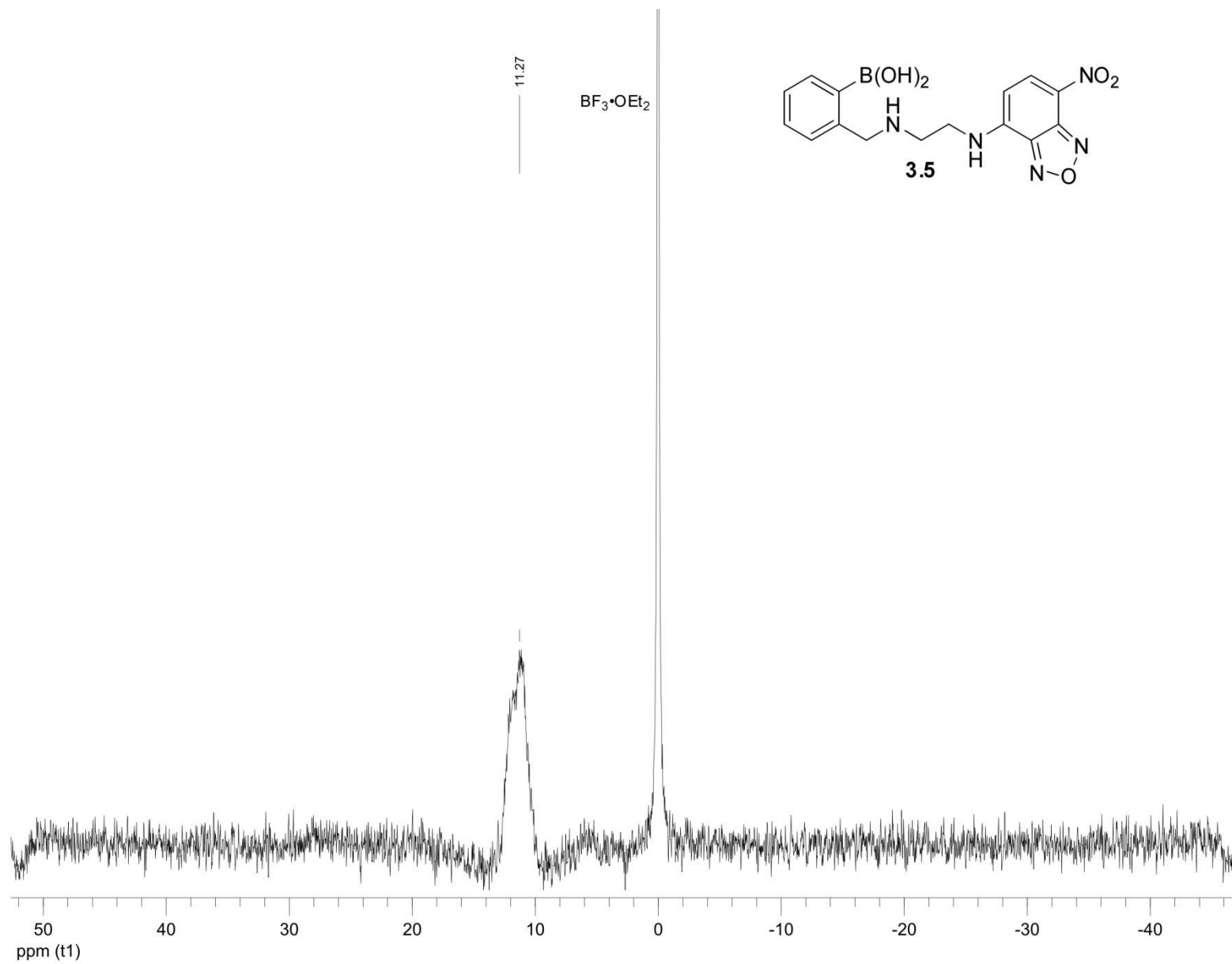
Potassium carbonate (0.076 g, 0.55 mmol) was added to a solution of 4-bromomethylphenylboronic acid (0.10 g, 0.46 mmol) in methanol (10 mL). Thiolacetic acid (0.040 mL, 0.55 mmol) was added dropwise, and the reaction mixture was stirred at rt for 1 h. Then, 2 M aqueous sodium hydroxide (0.69 mL) was added, and stirring continued at rt overnight, followed by extraction with dichloromethane (2 × 20 mL) from 0.5 M hydrochloric acid (20 mL). The combined organic layers were dried over magnesium sulfate, filtered, and concentrated. Column chromatography over silica gel with gradient elution from ethyl acetate to 10% methanol/dichloromethane yielded the disulfide product as a colorless liquid (0.0271 g, 35%).

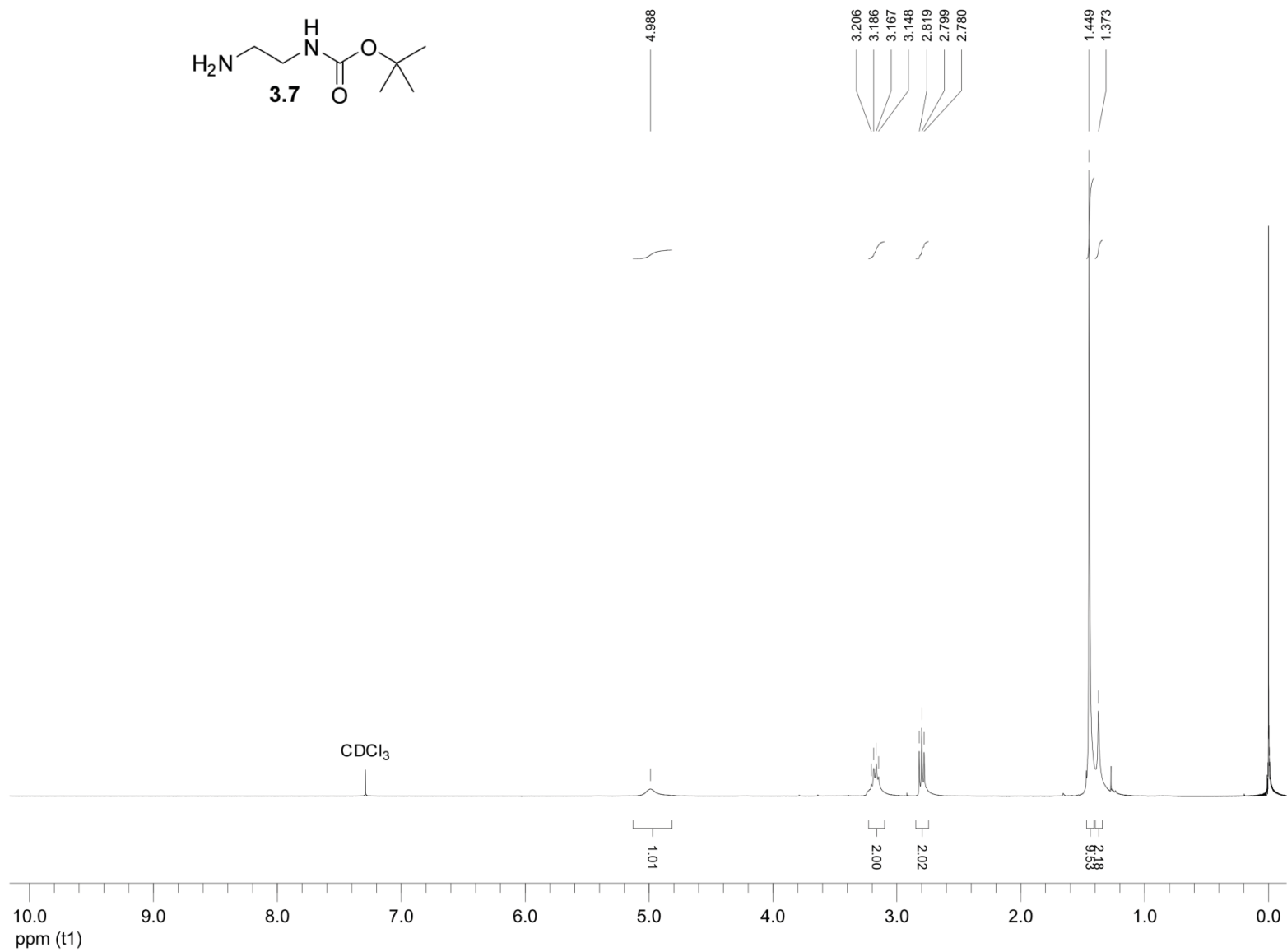
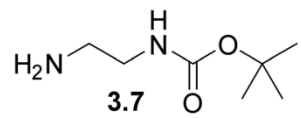
¹H NMR (300 MHz, CD₃OD) δ 7.70 (d, *J* = 7.6 Hz, 2H), 7.57 (d, *J* = 7.6 Hz, 2H), 7.27–7.17 (m, 4H), 3.60 (s, 4H). ¹³C NMR (75 MHz, CD₃OD) δ 141.07, 140.58, 135.19, 134.86, 129.95, 129.84, 43.96. ¹¹B NMR (128 MHz, CD₃OD) δ 30.04.



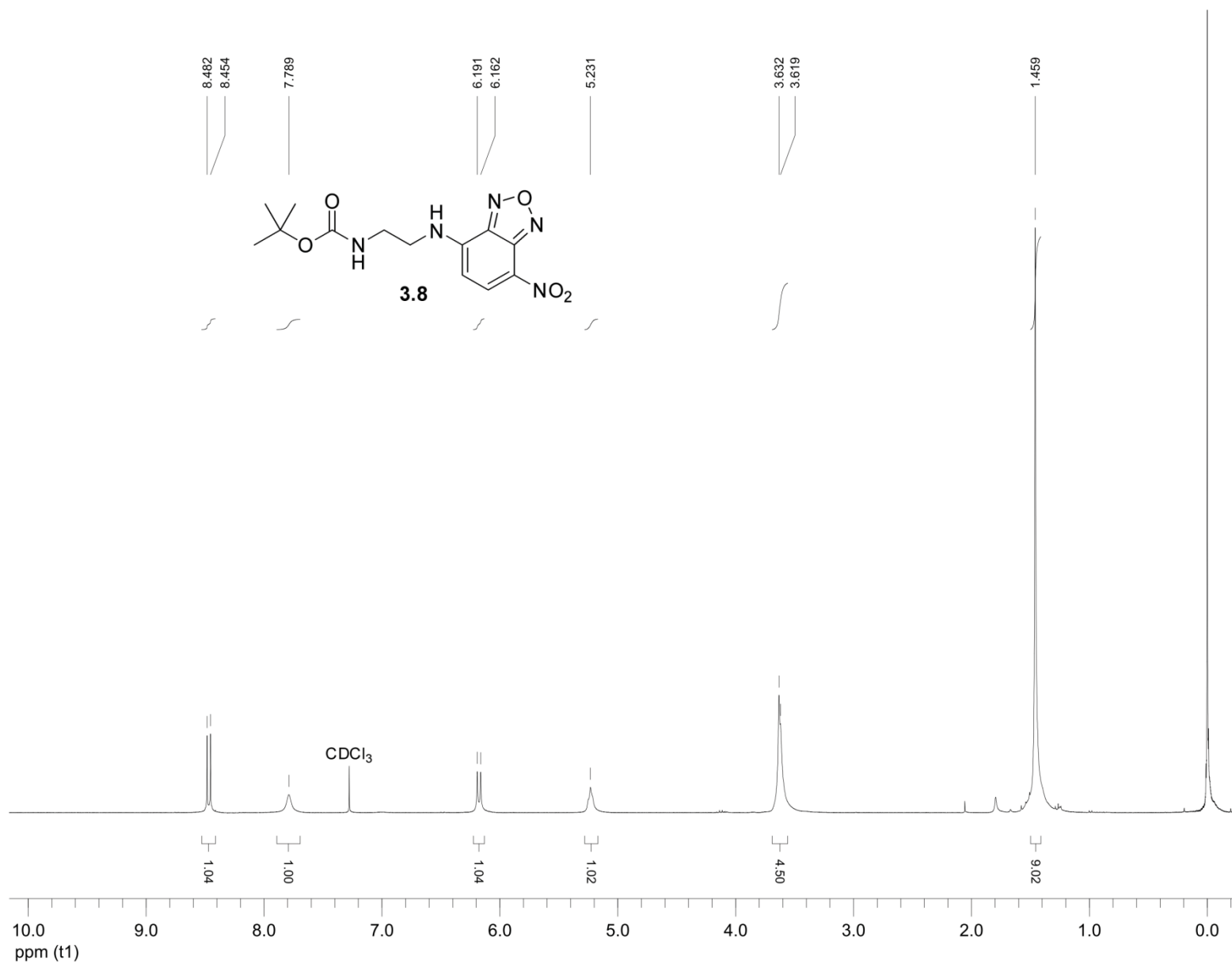
138

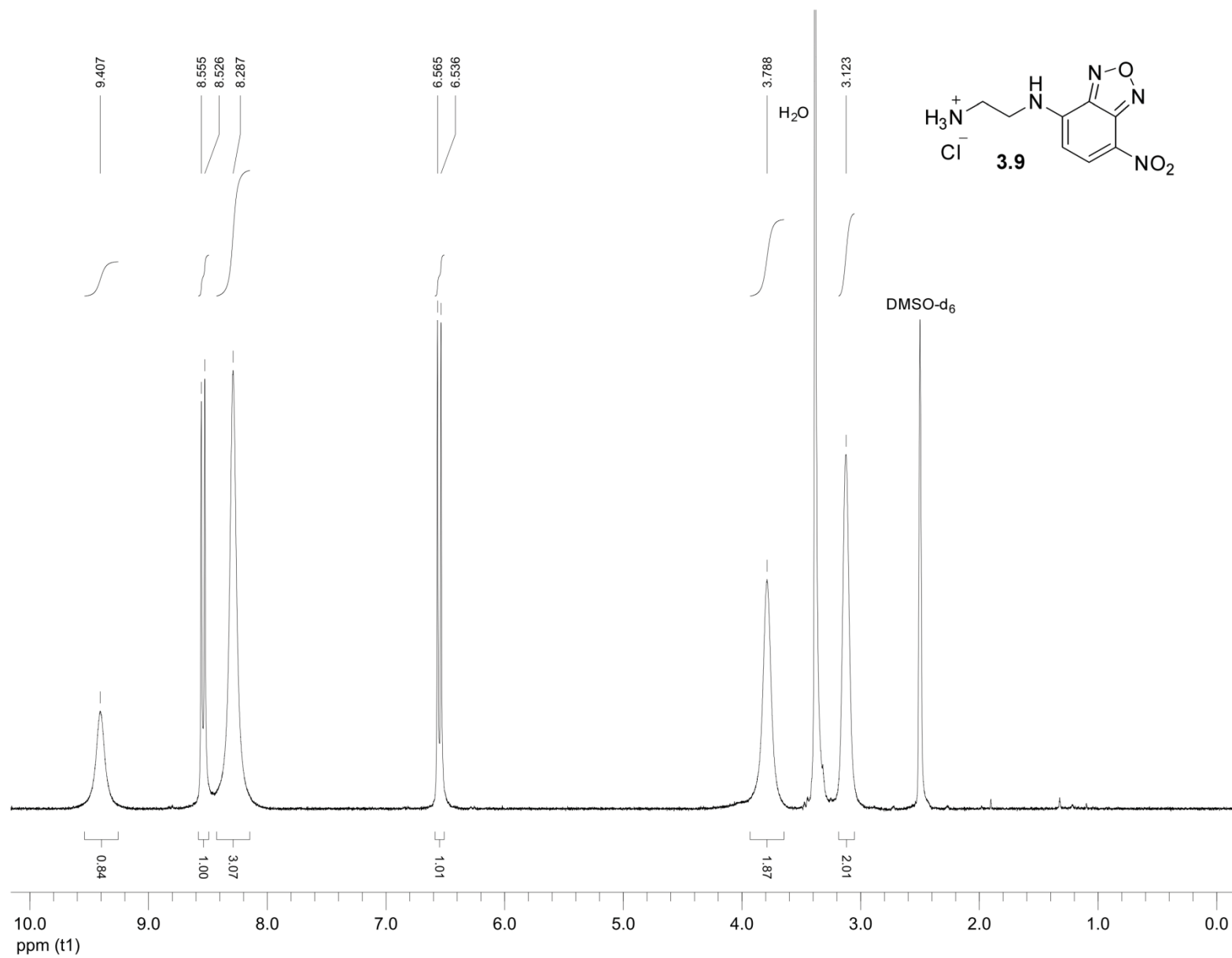


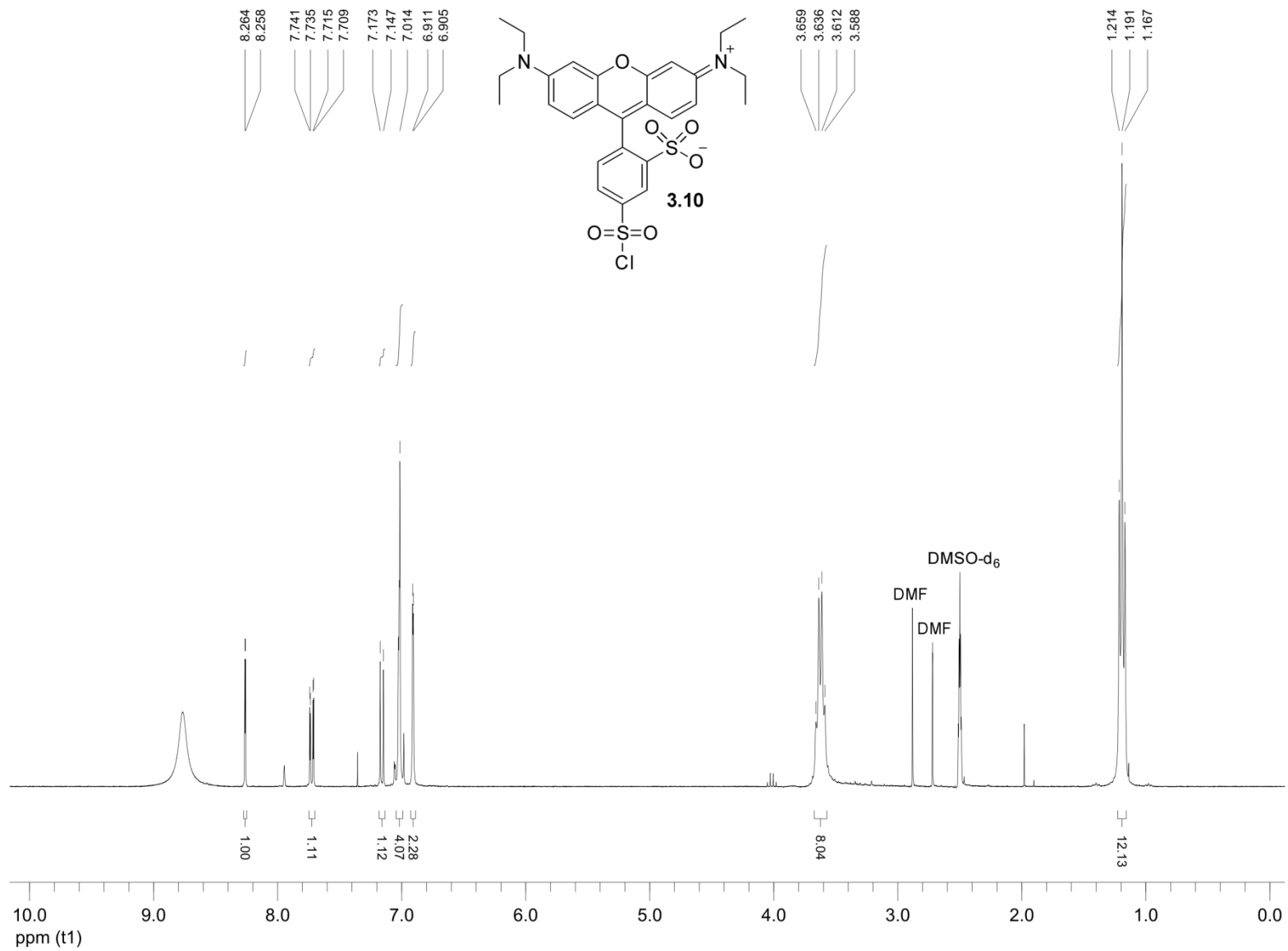


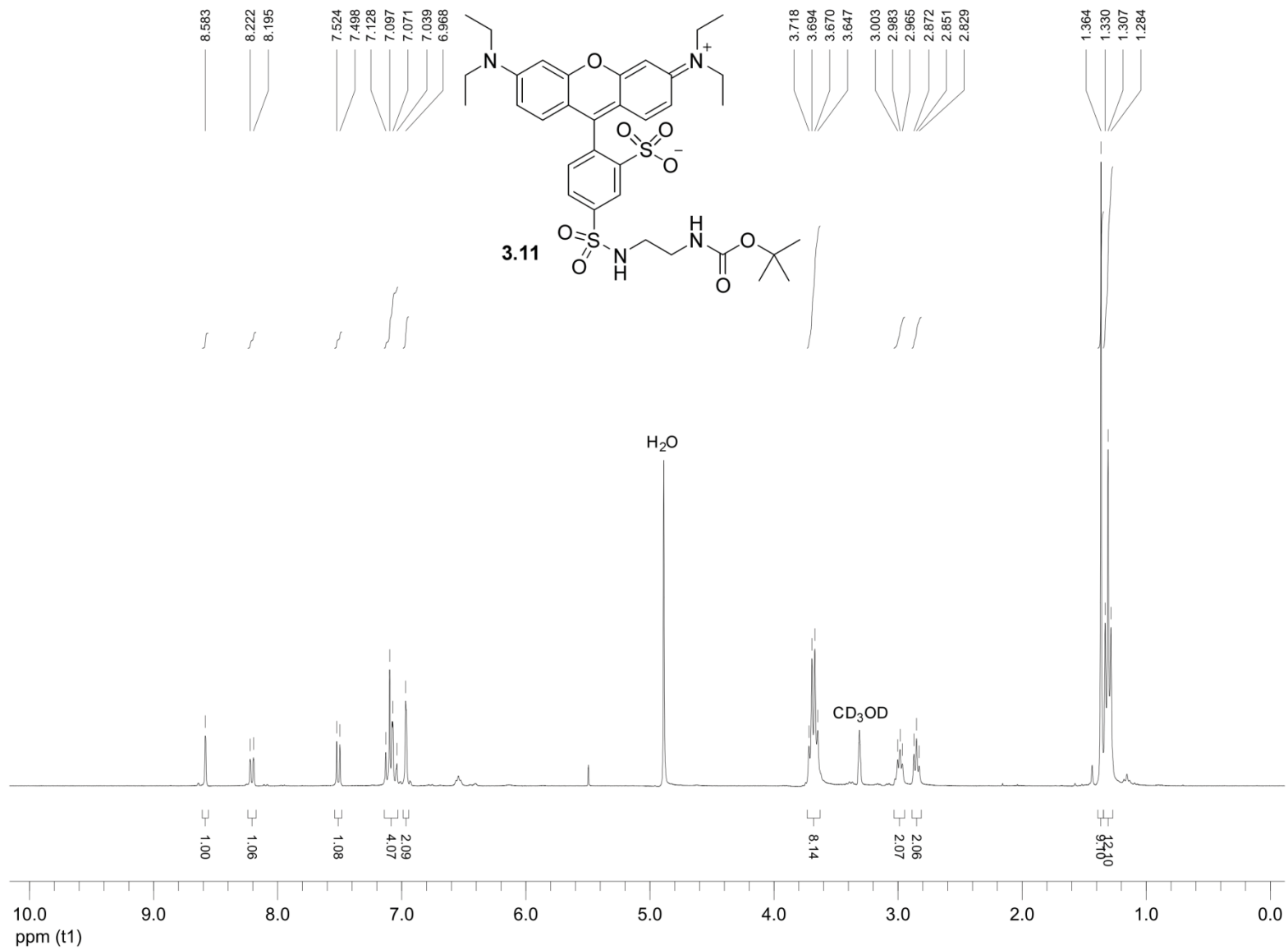


141

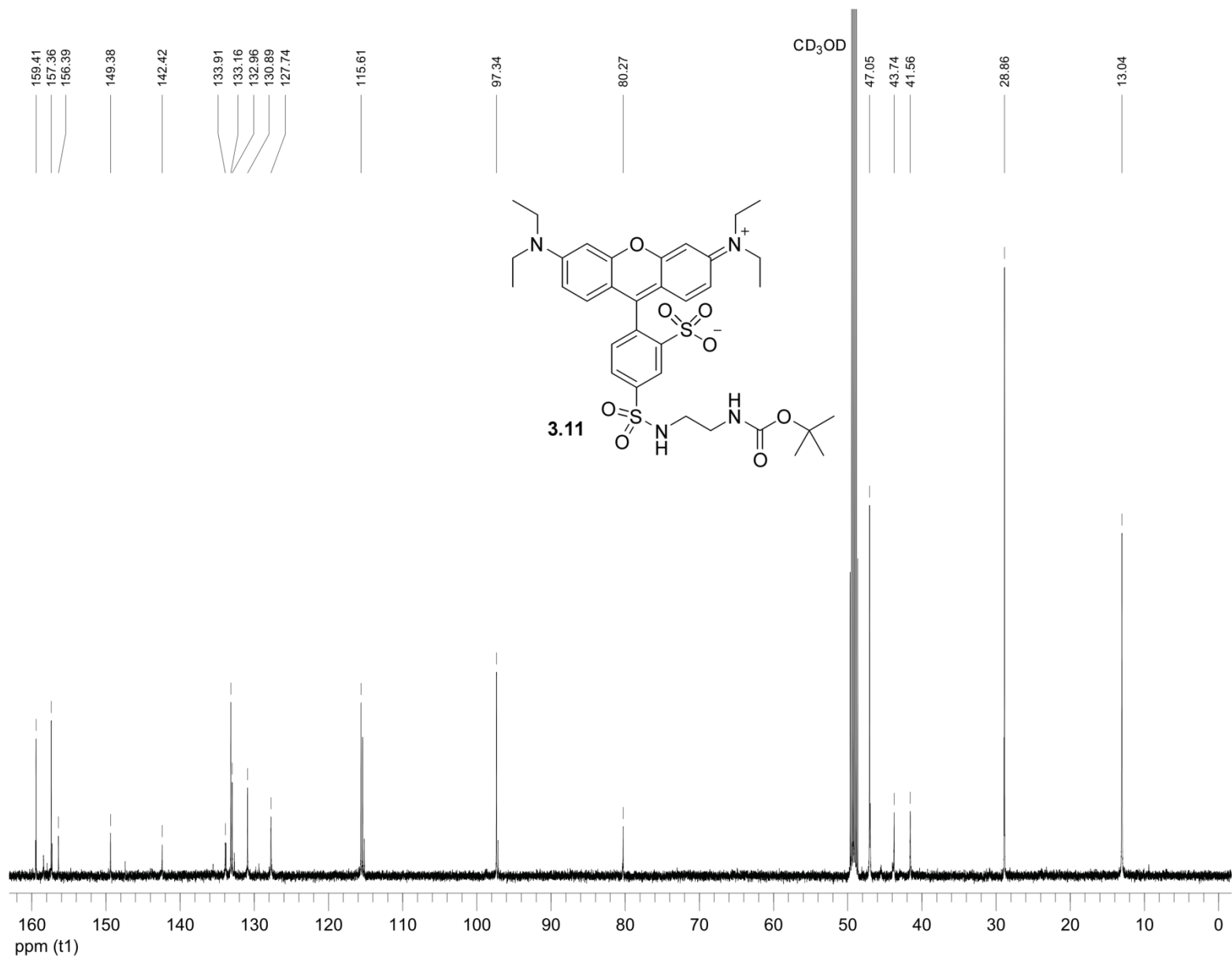




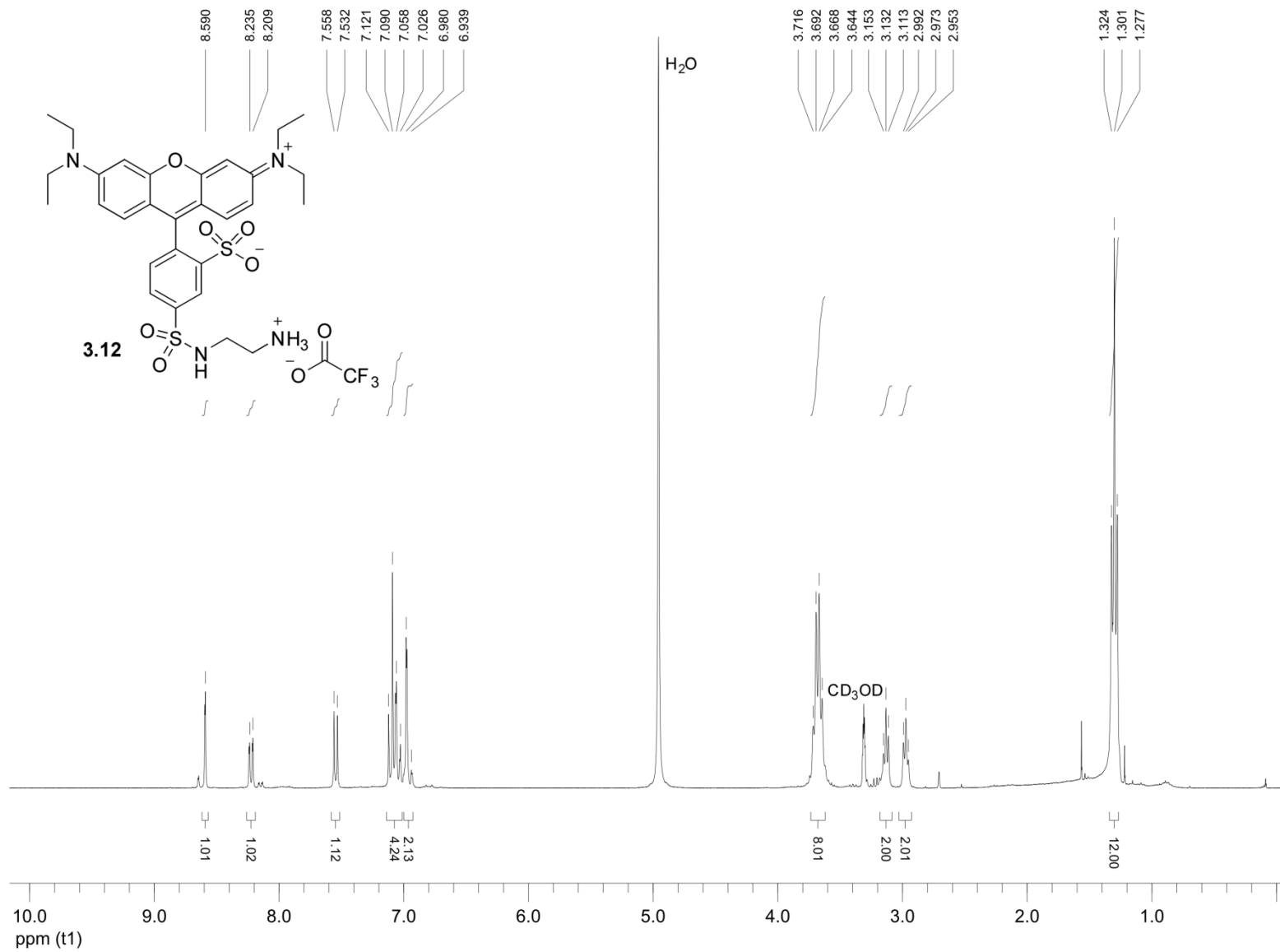


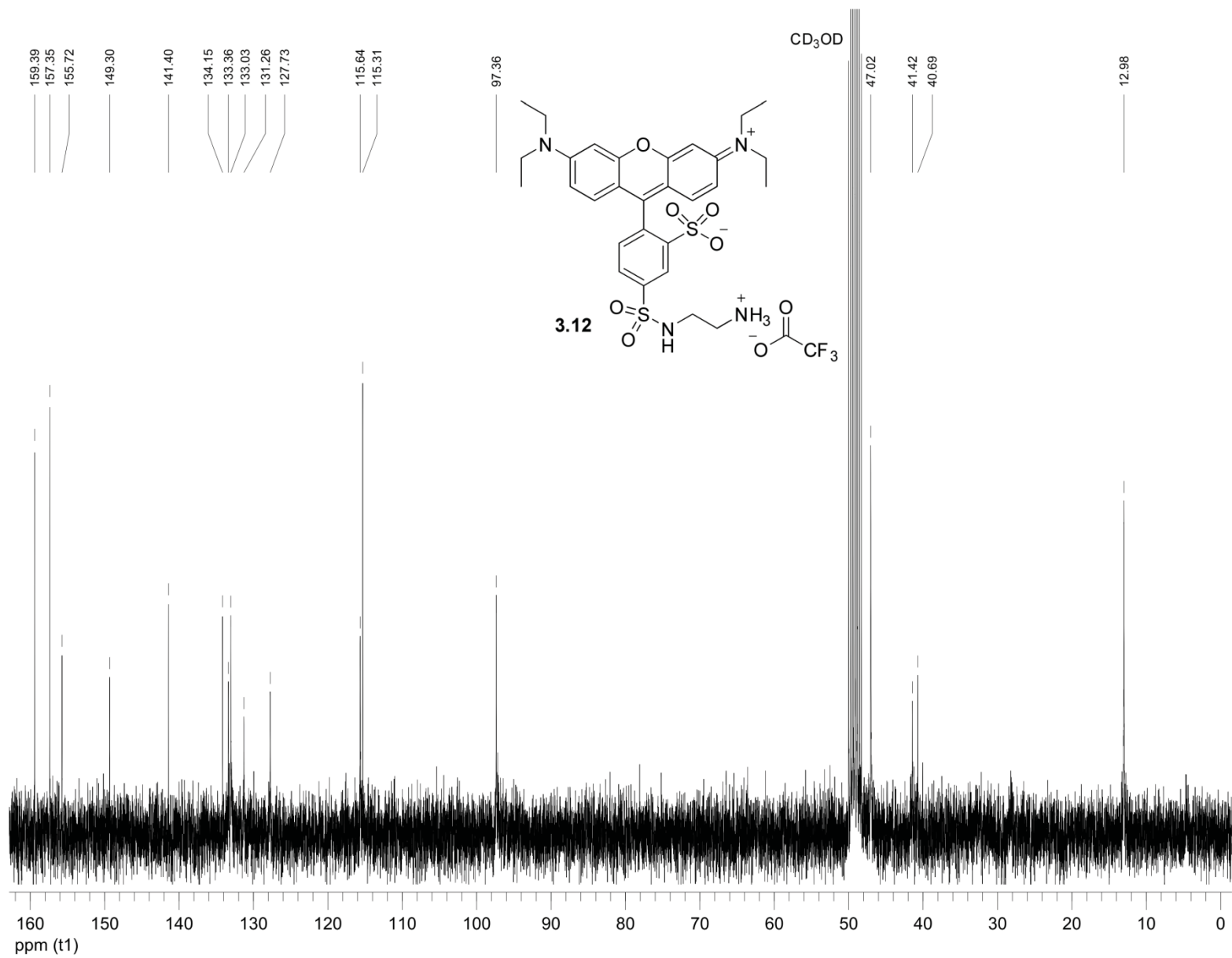


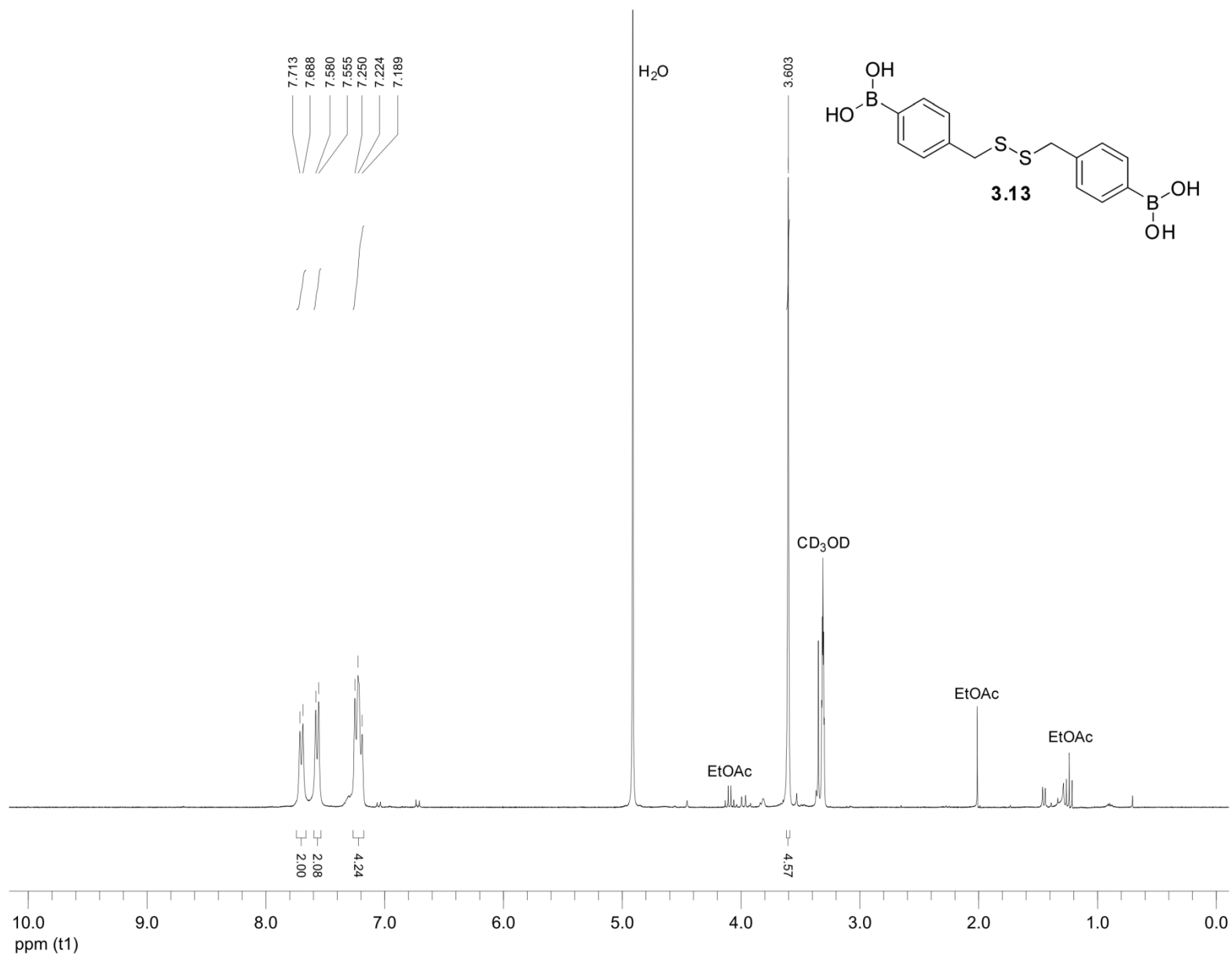
145



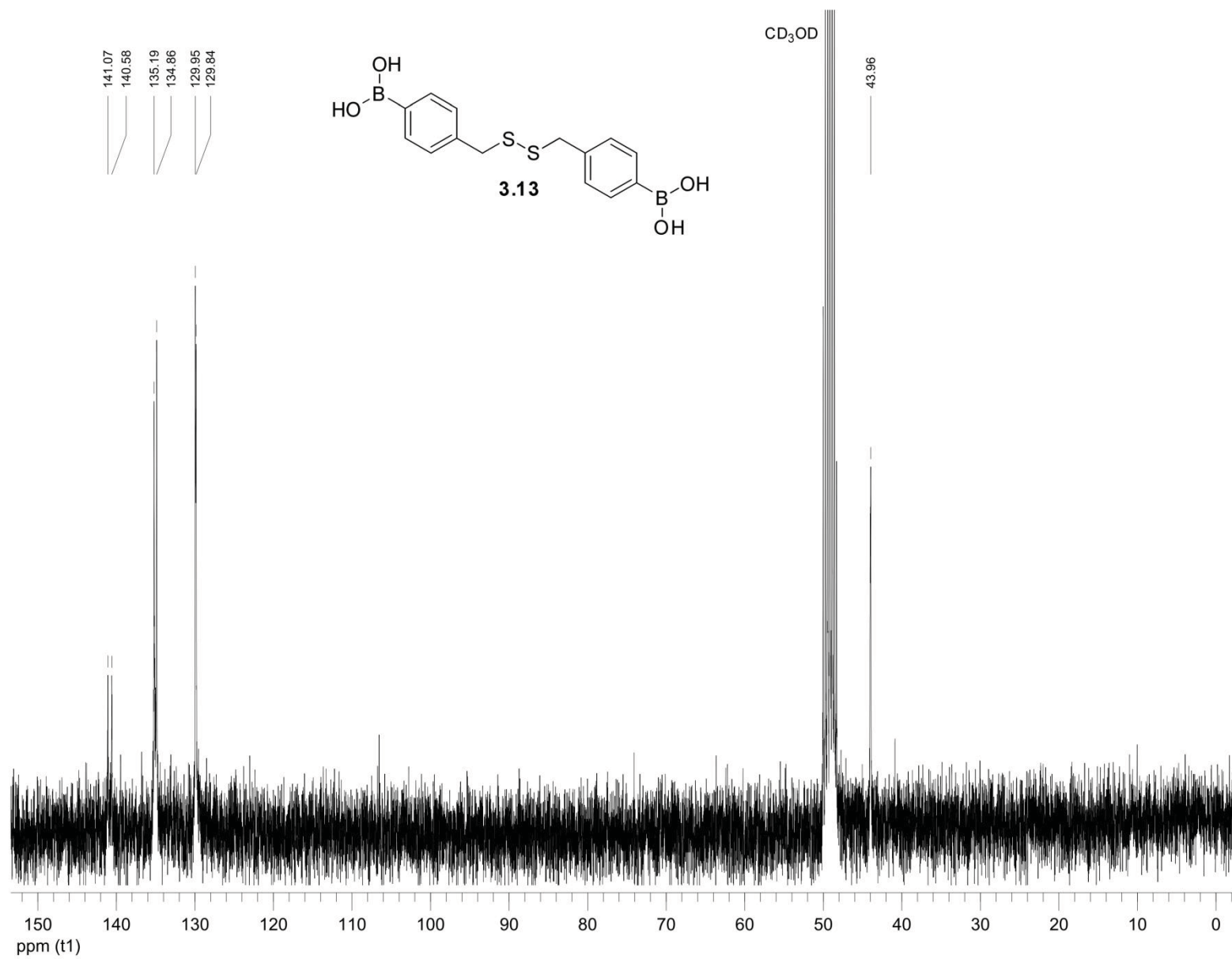
146

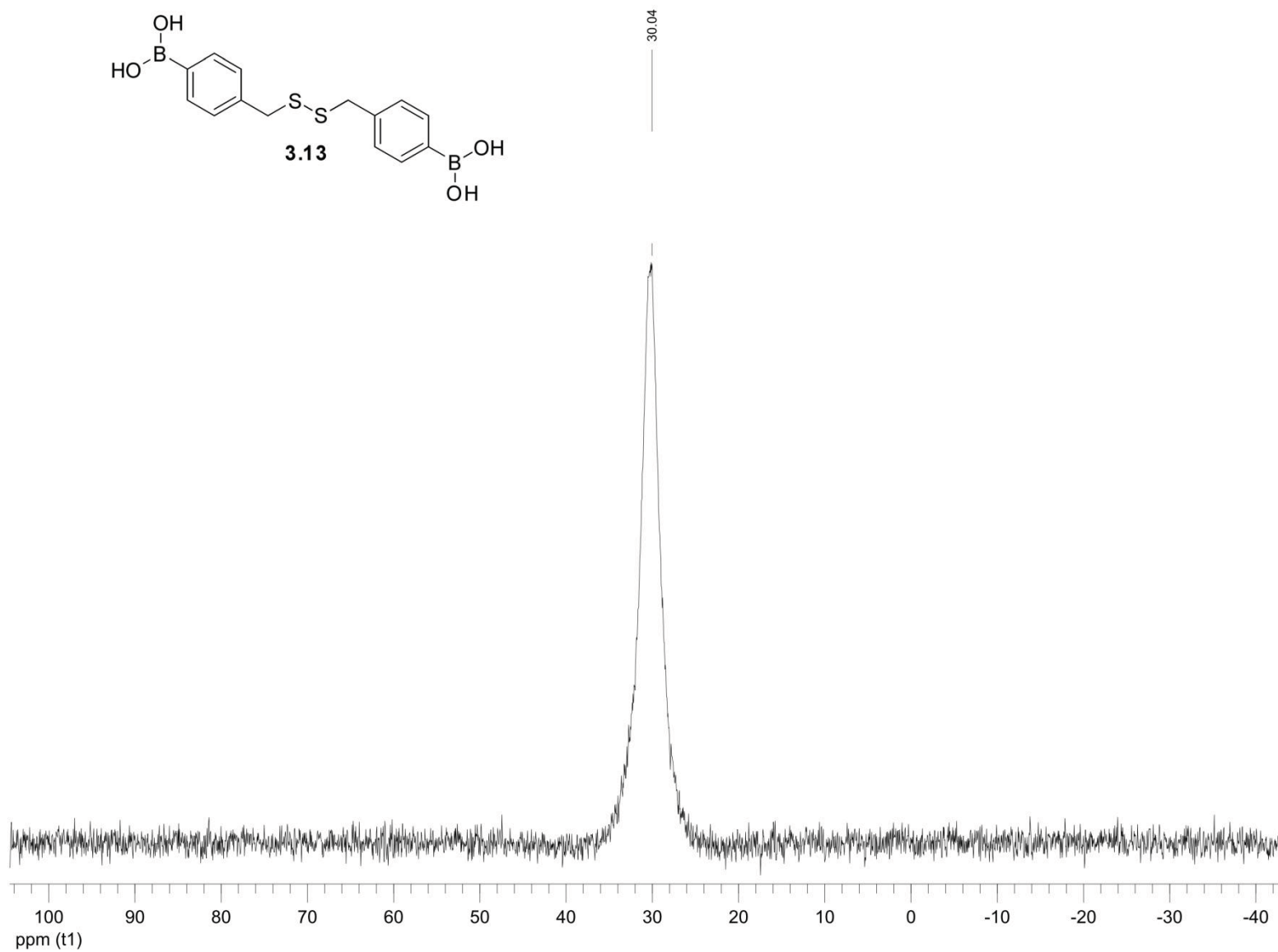
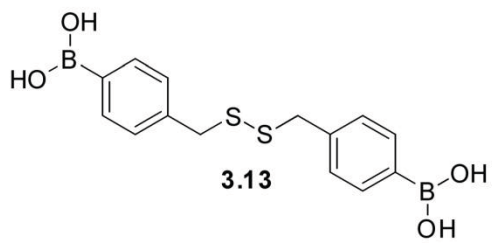






149





151

Chapter 4: Evaluation of Novel Auxin Herbicides through the Synthesis and Screening of a Small Molecule Library

4.1 Introduction

Auxins are an important class of plant growth substances called phytohormones. They play essential roles in many growth and behavioral processes in a plant's life cycle. There are four natural auxins (Figure 4.1) that are synthesized by plants: indole-3-acetic acid (IAA), which is considered the most important member of the class, indole-3-butyric acid (IBA), 4-chloroindole-3-acetic acid (4-Cl-IAA), and phenylacetic acid (PAA).¹³⁶ Since IAA influences almost every part of plant growth and development, it is believed to act as a “master hormone” in the network of interactions with other phytohormones.¹³⁷ In general, auxins regulate cell division, elongation, and developmental processes, which include vascular tissue and floral meristem differentiation, leaf initiation, phyllotaxy, senescence, apical dominance, and root formation.¹³⁸

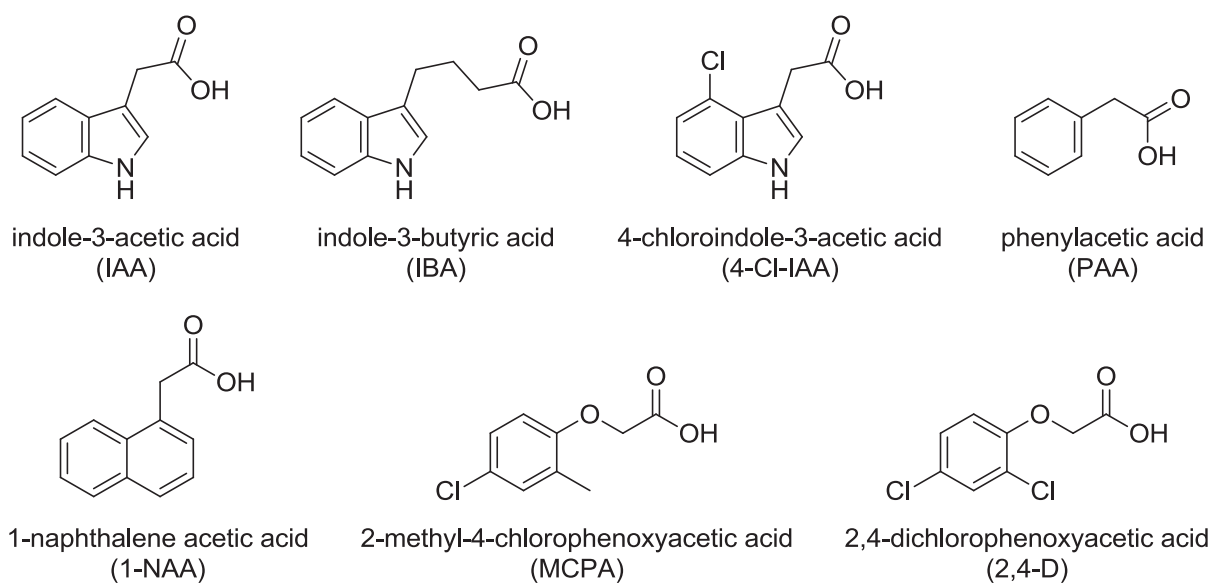


Figure 4.1. Structures of natural and synthetic auxins.

The stability and concentration of natural auxins is regulated by the plant through synthesis, conjugation, and degradation via multiple pathways.¹³⁹ At low auxin concentration, growth and developmental activities are stimulated, while at high concentration, growth is interrupted, and the plant is lethally damaged. As a result, there has been considerable interest in the chemical manipulation of the auxin system via synthetic analogs in order to study auxin function.¹⁴⁰ In the 1940s, a variety of derivatives of IAA were synthesized that were some of the most auxin-active molecules at the time. These included 1-naphthalene acetic acid (1-NAA, Figure 4.1), 2-methyl-4-chlorophenoxyacetic acid (MCPA), and 2,4-dichlorophenoxyacetic acid (2,4-D).¹⁴¹ They produce the same plant responses as IAA but are more durable and effective because they are not rendered inactive by the plant as rapidly as the endogenous auxins.¹⁴²

Synthetic auxins have found practical use not only as growth regulators for improving yields in agriculture and horticulture,¹⁴³ and as media components in tissue culture and plant micropropagation,¹⁴⁴ but also as herbicides to control weeds.¹⁴¹ MCPA and 2,4-D launched a new era of weed control in modern agriculture after being introduced to the worldwide market after World War II. Since then, several chemical types of auxin herbicides have been commercially produced. These include benzoic acids, phenoxy-carboxylic acids, pyridine-carboxylic acids, quinoline-carboxylic acids, and aromatic carboxymethyl derivatives. To possess auxin activity, it seems to be crucial for a chemical structure to have a strong negative charge on the carboxylic acid group that is separated by a distinct distance from a weaker positive charge on an aromatic ring.¹⁴⁵ When used as herbicides, synthesized auxins mimic the growth-inhibiting effects as

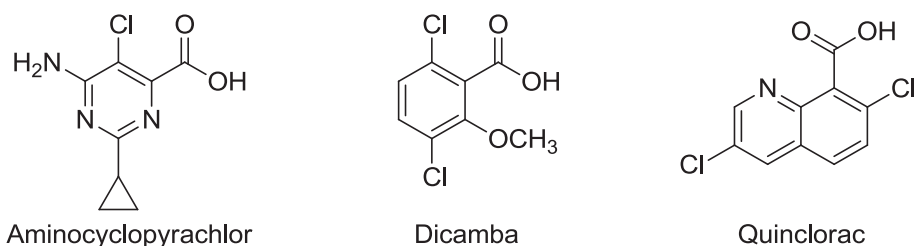


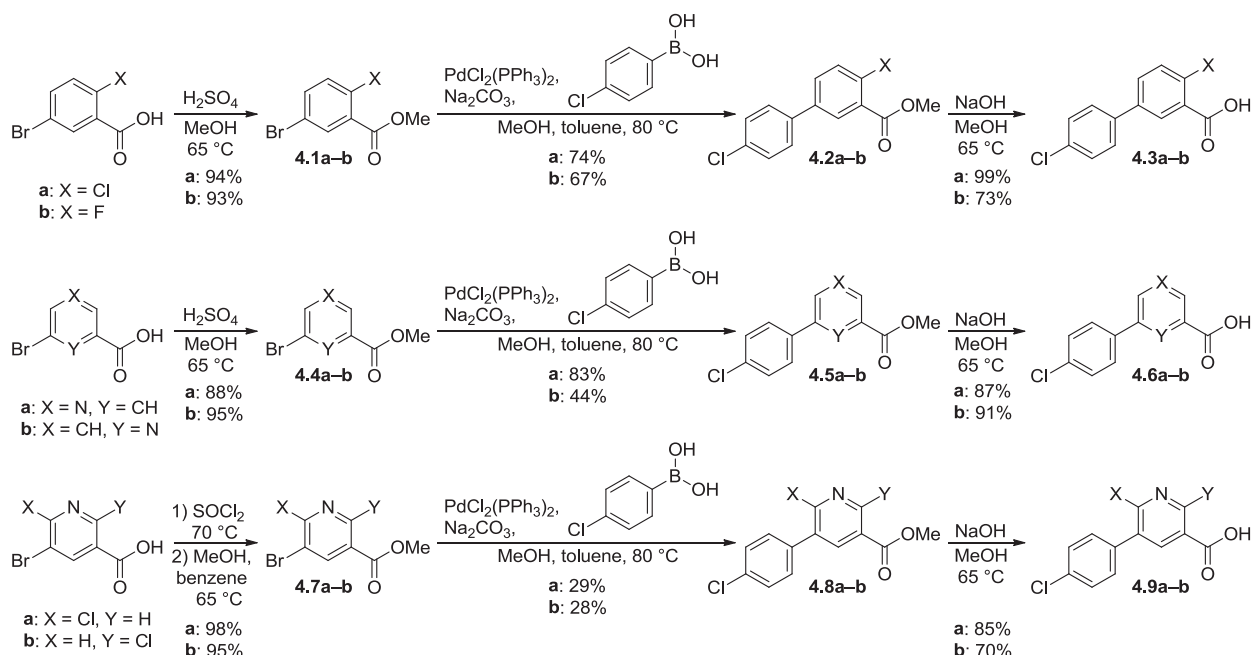
Figure 4.2. Commercial herbicides used as controls in testing auxin activities.

those caused by IAA applied at high concentrations, which is also observed in transgenic, IAA-overproducing plants.¹⁴⁶ This occurrence has been described as an “auxin overdose,” which is an effect of greater-than-optimal endogenous auxin concentrations, causing an imbalance in auxin homeostasis and interactions with other hormones in the tissue.¹⁴²

The goal of the research presented in this chapter was to synthesize a library of small molecules via a short series of steps and then test their activities as herbicides on a variety of plants alongside the three commercial herbicides Aminocyclopyrachlor,¹⁴⁷ Dicamba,¹⁴⁸ and Quinclorac¹⁴⁹ (Figure 4.2). This was done in collaboration with Dr. Gregory Armel from the Department of Plant Sciences who performed the plant testing and identified the target structures to be synthesized. Compounds were designed with aspects of previous effective herbicide structures, such as halogenated benzoic acids, chlorophenyl groups, and nitrogen-containing heterocycles. After testing, new structures will be explored based on the results and through Dr. Armel’s knowledge of patent literature.

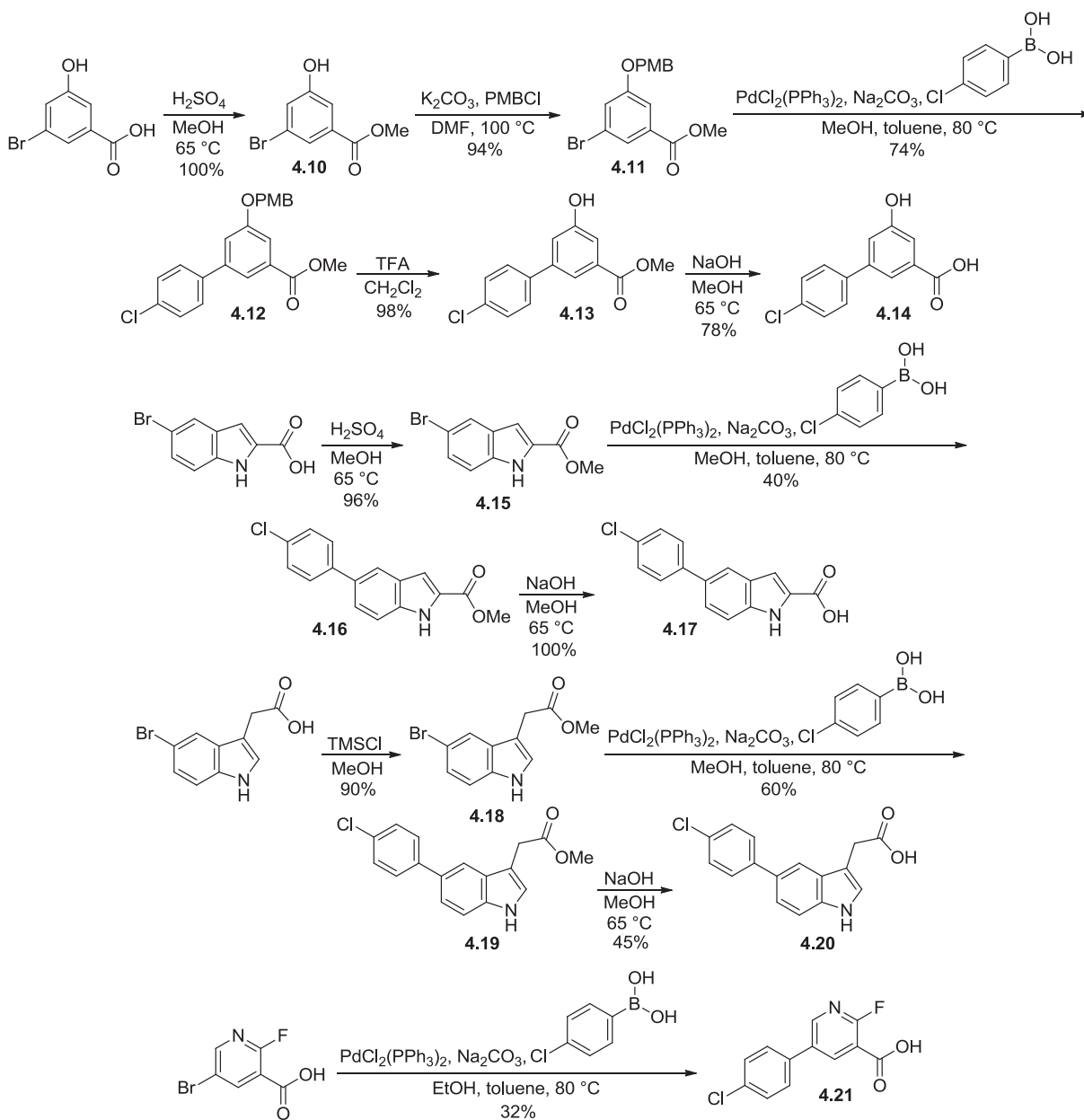
4.2 Synthesis of Aromatic Compounds

Generally, most of the synthesized targets consisted of aromatic carboxylic acids connected to a chlorophenyl group. In most cases, a commercially available carboxylic acid was converted to the methyl ester, followed by reaction with 4-chlorophenylboronic acid via Suzuki coupling to attach the chlorophenyl group, and then ester hydrolysis in base to restore the carboxylic acid functionality (Scheme 4.1). The esterification steps were done to facilitate the purification of intermediates.



Scheme 4.1. General synthetic route to aromatic acid targets.

One notable exception was the synthesis of fluoronicotinic acid target **4.21** (Scheme 4.2). Here, the carboxylic acid starting material was used directly in the Suzuki reaction because all esterification attempts either had no effect or resulted in the fluorine atom being substituted by the alcohol group. Additionally, some reactive functional groups had to be protected, as seen in the synthetic route to **4.14**. The

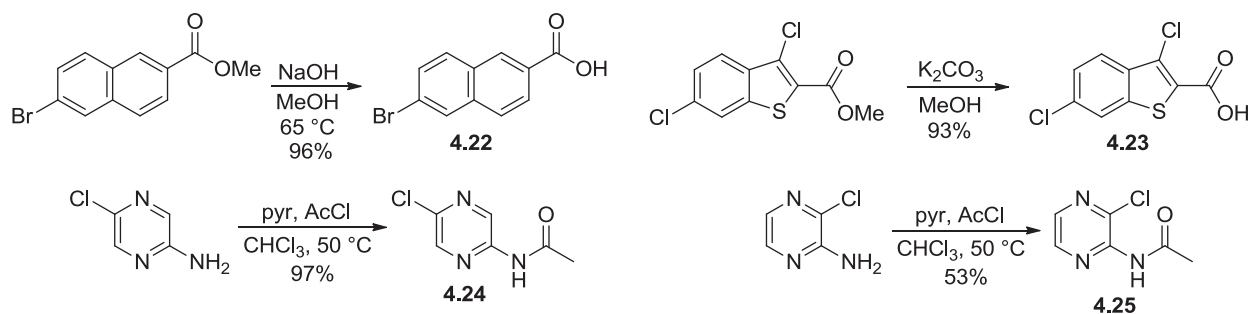


Scheme 4.2. Synthesis of various aromatic acid targets.

phenol moiety was protecting using the *para*-methoxybenzyl group, which was later removed with trifluoroacetic acid following the Suzuki coupling step.

Additional compounds were also made from commercially available methyl esters by hydrolysis in one step (Scheme 4.3). Naphthoic acid **4.22** and benzothiophene **4.23** were generated under conventional basic conditions. And finally,

N-acetyl derivatives **4.24** and **4.25** of pyrazinamines were formed in one-step procedures. Initial attempts using acetic anhydride and triethylamine as the base failed to convert the starting materials, but after switching to the more reactive acetyl chloride and pyridine as the base, the products were successfully formed.



Scheme 4.3. Additional aromatic acid and *N*-acetyl compounds.

4.3 Growth Control Testing

Following the synthesis of the desired compounds, their herbicidal activities were evaluated by Dr. Armel at the Department of Plant Sciences. The compounds in the form of a spraying solution were applied to a variety of common weeds in row crops and vegetable crops, in addition to sweet corn. An ideal auxin herbicide would be highly active against all the weeds but show little to no activity against crops such as corn. As controls, the commercial herbicides Aminocyclopyrachlor, Dicamba, and Quinclorac (Figure 4.2) were tested alongside the newly synthesized compounds.

To date, 11 of the synthesized molecules have been tested against six different weeds and sweet corn (Figure 4.3). As expected, the commercial herbicides showed high percentages of growth control activity for most of the weeds, with only Aminocyclopyrachlor showing little effect on the corn. Out of the synthetic compounds, chlorobenzoic acid **4.3a** had the highest activity, with about 75% growth control of

Herbicides Growth Control Data

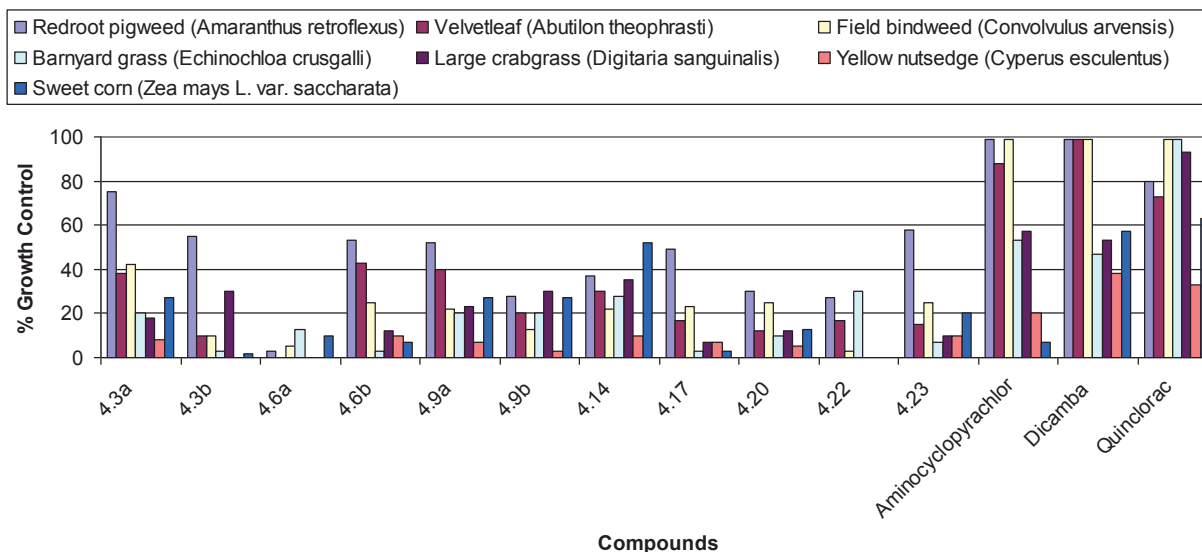


Figure 4.3. Growth control data for synthetic compounds and commercial herbicides.

pigweed, but also close to 30% control of the corn. The fluorinated analog **4.3b** exhibited 55% control of pigweed while having little to no effect on the corn. The only other two chemicals with close to 50% control of a weed and less than 10% for sweet corn were picolinic acid **4.6b** and indole derivative **4.17**.

Overall, the test results so far showed that even though most of the observed activities were far below commercial levels, three compounds had decent growth control of one weed while still being safe for sweet corn. It should be noted that certain other compounds that showed good activities were omitted from this dissertation due to pending information protection. Further testing and synthesis would need to be done in order to narrow down the search for a novel synthetic auxin with activity levels that are comparable to those of commercial herbicides.

4.4 Experimental

General Procedure A: Esterification of Aromatic Carboxylic Acids

Concentrated sulfuric acid (1 mL) was added to a solution of the carboxylic acid (10 mmol) in methanol (20 mL). The reaction mixture was stirred at 65 °C overnight, after which a saturated aqueous sodium bicarbonate solution was added to adjust the pH to about 8. The mixture was then extracted twice with dichloromethane, and the combined organic layers were dried with magnesium sulfate, filtered, and concentrated to give the product.

General Procedure B: Palladium-Catalyzed Coupling of Aryl Bromides with 4-Chlorophenylboronic Acid

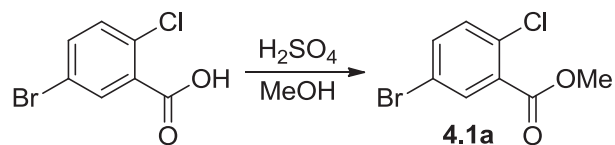
The procedure described by Miyaura, Yanagi, and Suzuki¹⁵⁰ was modified in the following manner. To a suspension of the aryl bromide (10 mmol), bis(triphenylphosphine)palladium(II) chloride (0.5 mmol), and 4-chlorophenylboronic acid (15 mmol) in methanol (30 mL) and toluene (30 mL) was added a 2 M aqueous sodium carbonate solution (20 mmol). The reaction mixture was stirred at 80 °C overnight and then filtered through Celite. The filtrate was extracted twice with diethyl ether from water, and the combined organic layers were dried over magnesium sulfate, filtered, and concentrated. Column chromatography over silica gel afforded the pure product.

General Procedure C: Ester Hydrolysis

A 2 M aqueous sodium hydroxide solution (15 mmol) was added to a suspension of the ester (5 mmol) in methanol (50 mL). The reaction mixture was stirred at 65 °C for 3 h and then extracted twice with dichloromethane from 1 M hydrochloric acid. The

combined organic layers were dried over magnesium sulfate, filtered, and concentrated. When necessary, column chromatography over silica gel afforded the pure product.

methyl 5-bromo-2-chlorobenzoate (4.1a)

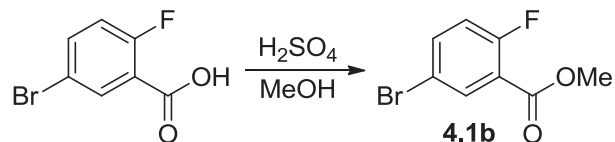


This compound was prepared, following General Procedure A, from 5-bromo-2-chlorobenzoic acid (2.09 g, 8.89 mmol) as a white solid (2.08 g, 94%).

Characterizations matched those reported in the literature.¹⁵¹

¹H NMR (300 MHz, CDCl₃) δ 7.96 (d, *J* = 2.5 Hz, 1H), 7.53 (dd, *J* = 8.5, 2.5 Hz, 1H), 7.32 (d, *J* = 8.5 Hz, 1H), 3.94 (s, 3H).

methyl 5-bromo-2-fluorobenzoate (4.1b)

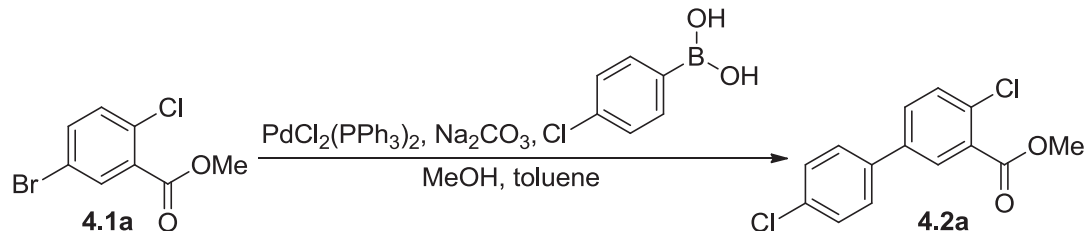


This compound was prepared, following General Procedure A, from 5-bromo-2-fluorobenzoic acid (2.00 g, 9.14 mmol) as a colorless liquid (1.98 g, 93%).

Characterizations matched those reported in the literature.¹⁵²

¹H NMR (300 MHz, CDCl₃) δ 8.06 (dd, *J* = 6.3, 2.6 Hz, 1H), 7.62 (ddd, *J* = 8.8, 4.2, 2.6 Hz, 1H), 7.05 (dd, *J* = 10.1, 8.8 Hz, 1H), 3.94 (s, 3H).

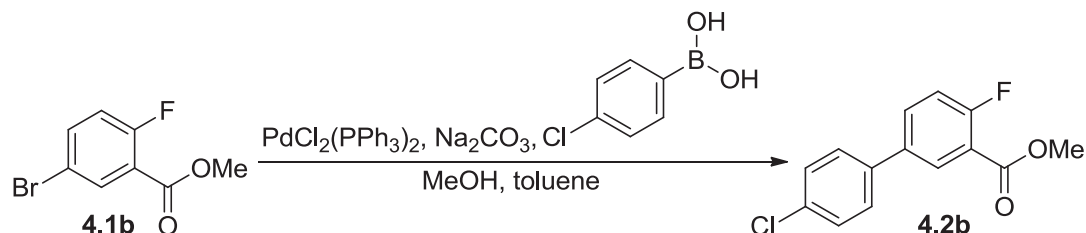
methyl 2-chloro-5-(4-chlorophenyl)benzoate (**4.2a**)



This compound was prepared, following General Procedure B, from **4.1a** (1.99 g, 7.96 mmol). Column chromatography over silica gel with gradient elution from 5 to 15% ethyl acetate/hexanes gave the product as a white solid (1.66 g, 74%).

^1H NMR (250 MHz, CDCl_3) δ 8.00 (d, $J = 2.2$ Hz, 1H), 7.63–7.36 (m, 6H), 3.96 (s, 3H).

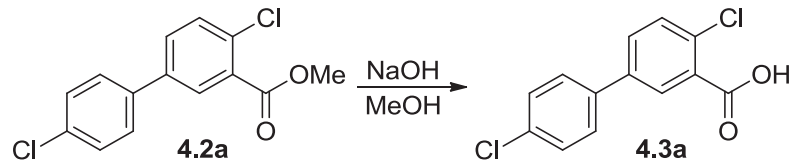
methyl 5-(4-chlorophenyl)-2-fluorobenzoate (**4.2b**)



This compound was prepared, following General Procedure B, from **4.1b** (1.95 g, 8.37 mmol). Column chromatography over silica gel with gradient elution from 5 to 15% ethyl acetate/hexanes gave the product as a white solid (1.48 g, 67%).

^1H NMR (300 MHz, CDCl_3) δ 8.12 (dd, $J = 6.8, 2.5$ Hz, 1H), 7.69 (ddd, $J = 8.6, 4.5, 2.5$ Hz, 1H), 7.50 (d, $J = 8.8$ Hz, 2H), 7.42 (d, $J = 8.8$ Hz, 2H), 7.22 (dd, $J = 10.3, 8.6$ Hz, 1H), 3.97 (s, 3H).

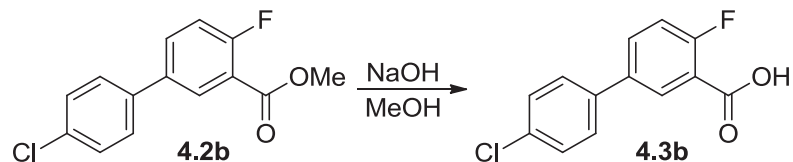
2-chloro-5-(4-chlorophenyl)benzoic acid (4.3a)



This compound was prepared, following General Procedure C, from **4.2a** (1.34 g, 4.75 mmol). Column chromatography over silica gel with gradient elution from 5 to 30% methanol/dichloromethane gave the product as a pale yellow solid (1.25 g, 99%).

^1H NMR (300 MHz, CD_3OD) δ 8.05 (d, $J = 2.4$ Hz, 1H), 7.72 (dd, $J = 8.4, 2.4$ Hz, 1H), 7.62 (d, $J = 8.8$ Hz, 2H), 7.56 (d, $J = 8.4$ Hz, 1H), 7.46 (d, $J = 8.8$ Hz, 2H).

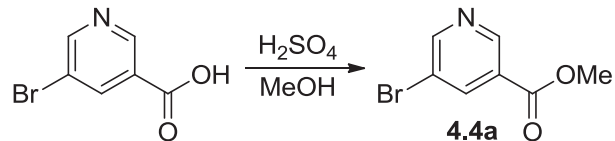
5-(4-chlorophenyl)-2-fluorobenzoic acid (4.3b)



This compound was prepared, following General Procedure C, from **4.2b** (1.47 g, 5.54 mmol). Column chromatography over silica gel with gradient elution from 5 to 30% methanol/dichloromethane gave the product as a white solid (1.01 g, 73%).

^1H NMR (300 MHz, CD_3OD) δ 8.12 (dd, $J = 6.9, 2.5$ Hz, 1H), 7.80 (ddd, $J = 8.6, 4.5, 2.5$ Hz, 1H), 7.59 (d, $J = 8.8$ Hz, 2H), 7.44 (d, $J = 8.8$ Hz, 2H), 7.27 (dd, $J = 10.5, 8.6$ Hz, 1H).

methyl 5-bromonicotinate (4.4a)

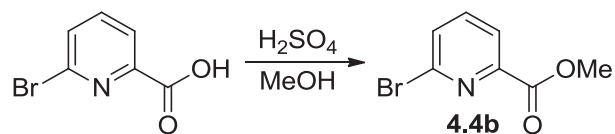


This compound was prepared, following General Procedure A, from 5-bromonicotinic acid (2.03 g, 10.04 mmol) as a white solid (1.91 g, 88%).

Characterizations matched those reported in the literature.¹⁵³

¹H NMR (300 MHz, CDCl₃) δ 9.13 (d, *J* = 1.8 Hz, 1H), 8.84 (d, *J* = 2.3 Hz, 1H), 8.44 (t, *J* = 2.1 Hz, 1H), 3.97 (s, 3H).

methyl 6-bromopicolinate (4.4b)

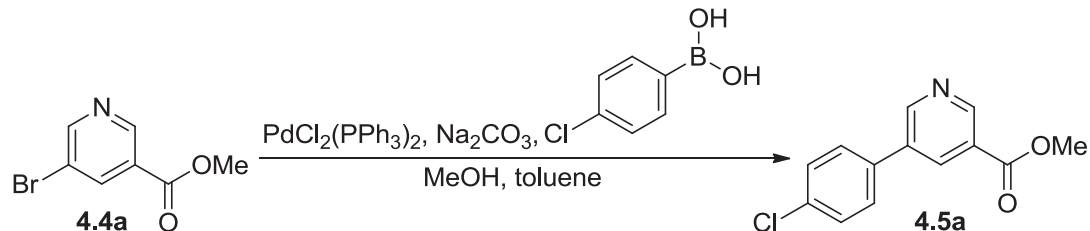


This compound was prepared, following General Procedure A, from 6-bromopicolinic acid (0.33 g, 1.58 mmol) as a white solid (0.33 g, 95%).

Characterizations matched those reported in the literature.¹⁵⁴

¹H NMR (300 MHz, CDCl₃) δ 8.11 (dd, *J* = 7.3, 0.8 Hz, 1H), 7.81–7.68 (m, 2H), 4.01 (s, 3H).

methyl 5-(4-chlorophenyl)nicotinate (4.5a)

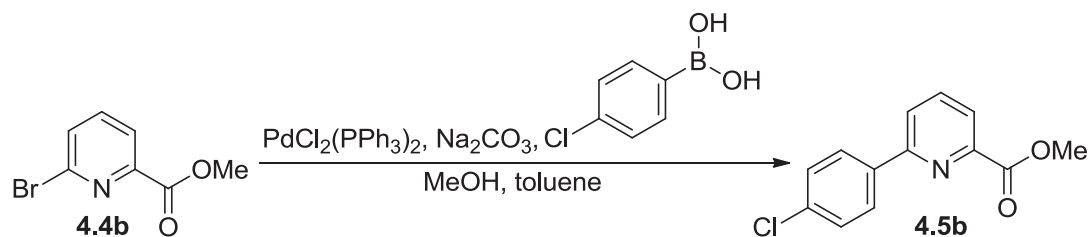


This compound was prepared, following General Procedure B, from **4.4a** (1.75 g, 8.11 mmol). Column chromatography over silica gel with gradient elution from 10 to 50% ethyl acetate/hexanes gave the product as a light yellow solid (1.67 g, 83%).

Characterizations matched those reported in the literature.¹⁵⁵

^1H NMR (250 MHz, CDCl_3) δ 9.20 (d, $J = 1.7$ Hz, 1H), 8.98 (d, $J = 2.2$ Hz, 1H), 8.46 (t, $J = 2.2$ Hz, 1H), 7.56 (d, $J = 8.8$ Hz, 2H), 7.48 (d, $J = 8.8$ Hz, 2H), 3.99 (s, 3H).

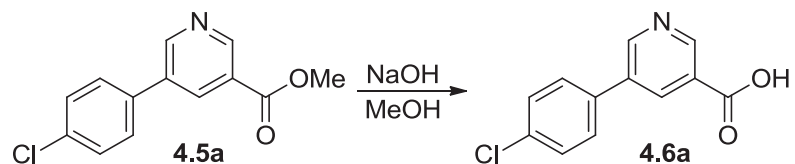
methyl 6-(4-chlorophenyl)picolinate (4.5b)



This compound was prepared, following General Procedure B, from **4.4b** (0.17 g, 0.78 mmol). Column chromatography over silica gel with gradient elution from 5 to 20% ethyl acetate/hexanes gave the product as a white solid (0.084 g, 44%).

^1H NMR (300 MHz, CDCl_3) δ 8.06 (d, $J = 7.0$ Hz, 1H), 8.00 (d, $J = 8.7$ Hz, 2H), 7.93–7.83 (m, 2H), 7.45 (d, $J = 8.7$ Hz, 2H), 4.02 (s, 3H).

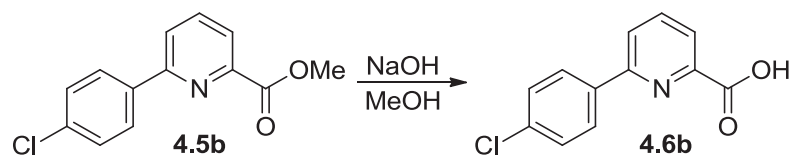
5-(4-chlorophenyl)nicotinic acid (**4.6a**)



This compound was prepared, following General Procedure C, from **4.5a** (1.63 g, 6.59 mmol). Column chromatography over silica gel with gradient elution from 10 to 50% methanol/dichloromethane gave the product as a white solid (1.34 g, 87%).

^1H NMR (300 MHz, CD_3OD) δ 9.10 (s, 1H), 8.97 (s, 1H), 8.58 (t, $J = 2.1$ Hz, 1H), 7.71 (d, $J = 8.8$ Hz, 2H), 7.53 (d, $J = 8.8$ Hz, 2H).

6-(4-chlorophenyl)picolinic acid (**4.6b**)

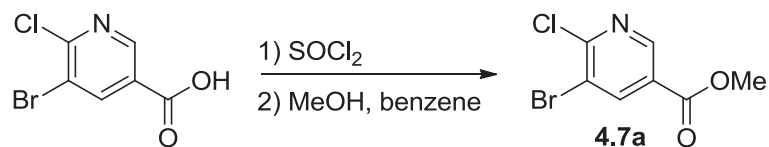


This compound was prepared, following General Procedure C, from **4.5a** (0.084 g, 0.34 mmol). Column chromatography over silica gel with gradient elution from 5 to 20% methanol/dichloromethane gave the product as a white solid (0.072 g, 91%).

Characterizations matched those reported in the literature.¹⁵⁶

^1H NMR (300 MHz, CD_3OD) δ 8.16–7.91 (m, 5H), 7.45 (d, $J = 7.9$ Hz, 2H).

methyl 5-bromo-6-chloronicotinate (4.7a)

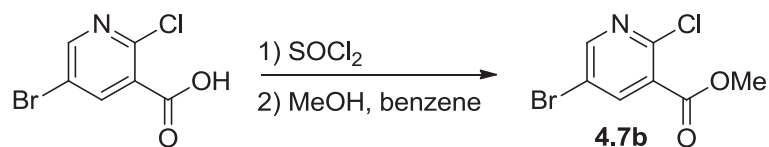


This compound was prepared according to a literature procedure.¹⁵⁷ A solution of 5-bromo-6-chloronicotinic acid (0.16 g, 0.67 mmol) in thionyl chloride (5 mL) was stirred at 70 °C for 1 h and then concentrated by rotary evaporation. Benzene (10 mL) and anhydrous methanol (5 mL) were added to the residue, followed by stirring at 65 °C for 1 h. The reaction mixture was then concentrated and extracted with dichloromethane (2 × 20 mL) from saturated aqueous sodium bicarbonate (20 mL). The combined organic layers were dried over magnesium sulfate, filtered, and concentrated to give the product as a light yellow solid (0.16 g, 98%).

Characterizations matched those reported in the literature.¹⁵⁷

¹H NMR (300 MHz, CDCl₃) δ 8.92 (d, *J* = 2.0 Hz, 1H), 8.52 (d, *J* = 2.0 Hz, 1H), 3.98 (s, 3H).

methyl 5-bromo-2-chloronicotinate (4.7b)

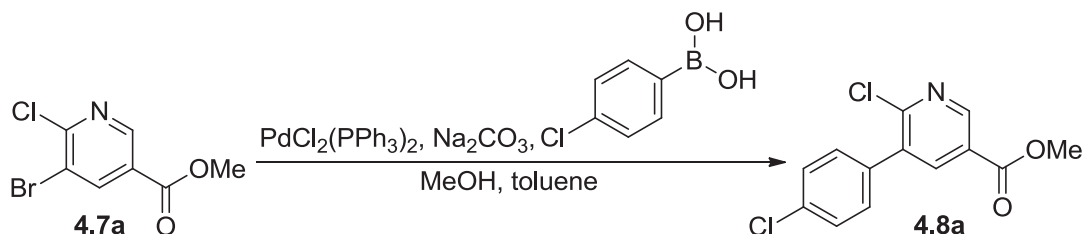


This compound was prepared, in the same manner as **4.7a** described above, from 5-bromo-2-chloronicotinic acid (0.20 g, 0.84 mmol) as a light yellow solid (0.20 g, 95%).

Characterizations matched those reported in the literature.¹⁵⁷

^1H NMR (300 MHz, CDCl_3) δ 8.58 (d, $J = 2.5$ Hz, 1H), 8.30 (d, $J = 2.5$ Hz, 1H), 3.98 (s, 3H).

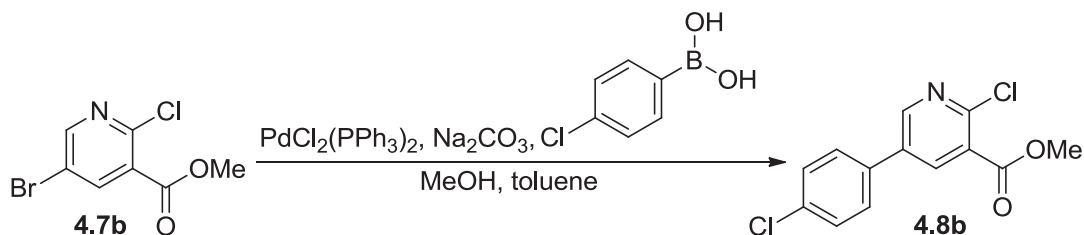
methyl 6-chloro-5-(4-chlorophenyl)nicotinate (**4.8a**)



This compound was prepared, following General Procedure B, from **4.7a** (0.083 g, 0.32 mmol). Column chromatography over silica gel with gradient elution from 10 to 30% ethyl acetate/hexanes gave the product as a white solid (0.027 g, 29%).

^1H NMR (300 MHz, CDCl_3) δ 8.99 (d, $J = 2.3$ Hz, 1H), 8.25 (d, $J = 2.3$ Hz, 1H), 7.47 (d, $J = 8.8$ Hz, 2H), 7.41 (d, $J = 8.8$ Hz, 2H), 3.98 (s, 3H).

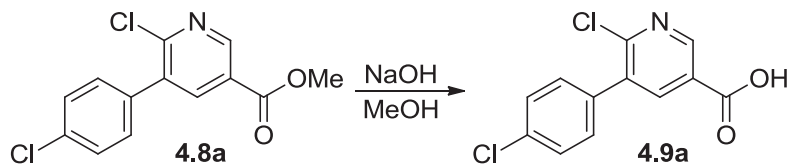
methyl 2-chloro-5-(4-chlorophenyl)nicotinate (**4.8b**)



This compound was prepared, following General Procedure B, from **4.7b** (0.097 g, 0.39 mmol). Column chromatography over silica gel with gradient elution from 10 to 30% ethyl acetate/hexanes gave the product as a white solid (0.031 g, 28%).

^1H NMR (300 MHz, CDCl_3) δ 8.69 (d, $J = 2.6$ Hz, 1H), 8.32 (d, $J = 2.6$ Hz, 1H), 7.53 (d, $J = 8.9$ Hz, 2H), 7.48 (d, $J = 8.9$ Hz, 2H), 4.00 (s, 3H).

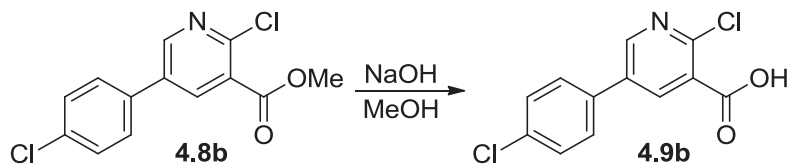
6-chloro-5-(4-chlorophenyl)nicotinic acid (**4.9a**)



This compound was prepared, following General Procedure C, from **4.8a** (0.061 g, 0.22 mmol). Column chromatography over silica gel with gradient elution from 3 to 20% methanol/dichloromethane gave the product as a white solid (0.049 g, 85%).

^1H NMR (300 MHz, CD_3OD) δ 8.88 (s, 1H), 8.28 (s, 1H), 7.49–7.39 (m, 4H).

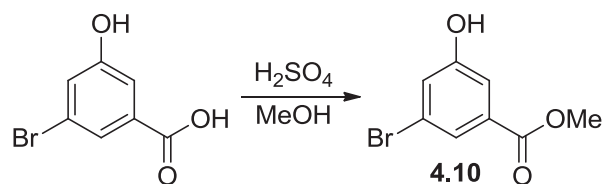
2-chloro-5-(4-chlorophenyl)nicotinic acid (**4.9b**)



This compound was prepared, following General Procedure C, from **4.8b** (0.11 g, 0.39 mmol). Column chromatography over silica gel with gradient elution from 5 to 15% methanol/dichloromethane gave the product as a white solid (0.074 g, 70%).

^1H NMR (300 MHz, CD_3OD) δ 8.63 (s, 1H), 8.31 (s, 1H), 7.65 (d, $J = 8.2$ Hz, 2H), 7.48 (d, $J = 8.2$ Hz, 2H).

methyl 3-bromo-5-hydroxybenzoate (**4.10**)

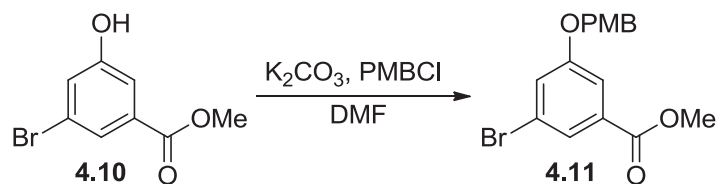


This compound was prepared, following General Procedure A, from 3-bromo-5-hydroxybenzoic acid (0.10 g, 0.45 mmol) as a light yellow solid (0.10 g, 100%).

Characterizations matched those reported in the literature.¹⁵⁸

¹H NMR (300 MHz, CDCl₃) δ 7.74 (t, *J* = 1.5 Hz, 1H), 7.54 (dd, *J* = 2.4, 1.5 Hz, 1H), 7.25 (dd, *J* = 2.4, 1.8 Hz, 1H), 6.07 (bs, 1H), 3.93 (s, 3H).

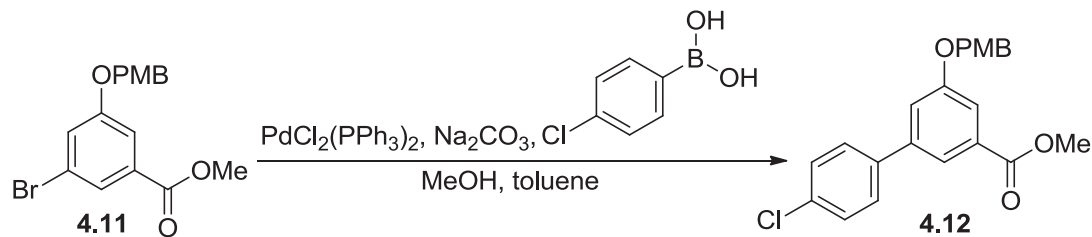
methyl 3-bromo-5-(4-methoxybenzyloxy)benzoate (**4.11**)



To a solution of **4.10** (0.10 g, 0.44 mmol) and potassium carbonate (0.090 g, 0.65 mmol) in *N,N*-dimethylformamide (10 mL) was added 4-methoxybenzyl chloride (0.092 mL, 0.65 mmol) dropwise. The reaction mixture was stirred at 100 °C overnight and then extracted with ethyl acetate (2 × 30 mL) from water (30 mL). The combined organic layers were dried over magnesium sulfate, filtered, and concentrated. Column chromatography over silica gel with gradient elution from 3 to 15% ethyl acetate/hexanes gave the product as a colorless oil (0.14 g, 94%).

^1H NMR (300 MHz, CDCl_3) δ 7.77–7.73 (m, 1H), 7.56 (dd, $J = 2.4, 1.3$ Hz, 1H), 7.33 (d, $J = 8.7$ Hz, 2H), 7.29 (dd, $J = 2.4, 1.8$ Hz, 1H), 6.91 (d, $J = 8.7$ Hz, 2H), 4.98 (s, 2H), 3.89 (s, 3H), 3.80 (s, 3H).

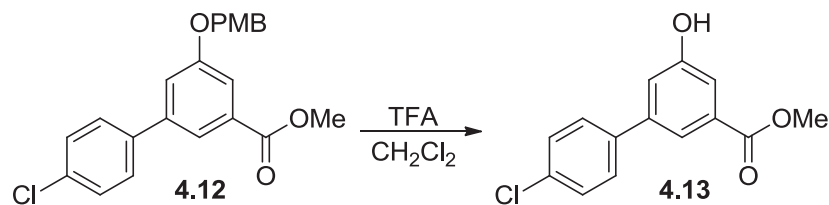
methyl 3-(4-chlorophenyl)-5-(4-methoxybenzyloxy)benzoate (4.12)



This compound was prepared, following General Procedure B, from **4.11** (2.71 g, 7.72 mmol). Column chromatography over silica gel with gradient elution from 5 to 25% ethyl acetate/hexanes gave the product as a dark yellow solid (2.17 g, 74%).

^1H NMR (300 MHz, CDCl_3) δ 7.83 (t, $J = 1.5$ Hz, 1H), 7.62 (dd, $J = 2.5, 1.5$ Hz, 1H), 7.49 (d, $J = 8.7$ Hz, 2H), 7.41–7.34 (m, 4H), 7.32 (dd, $J = 2.5, 1.7$ Hz, 1H), 6.92 (d, $J = 8.7$ Hz, 2H), 5.04 (s, 2H), 3.93 (s, 3H), 3.80 (s, 3H).

methyl 3-(4-chlorophenyl)-5-hydroxybenzoate (4.13)

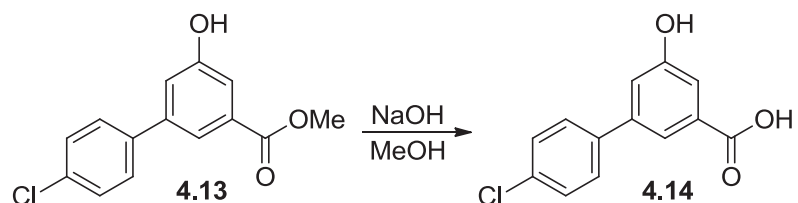


Trifluoroacetic acid (5 mL) was added dropwise to a solution of **4.12** (0.12 g, 0.30 mmol) in dichloromethane (5 mL) at rt. The reaction mixture was stirred at rt for 3 h, followed

by extraction with dichloromethane (2 × 20 mL) from water (20 mL). The combined organic layers were dried over magnesium sulfate, filtered, and concentrated. Column chromatography over silica gel with gradient elution from 20 to 40% ethyl acetate/hexanes yielded the product as a white solid (0.078 g, 98%).

^1H NMR (300 MHz, 1:1 CDCl_3 : CD_3OD) δ 7.72 (t, J = 1.6 Hz, 1H), 7.54 (d, J = 8.7 Hz, 2H), 7.45 (dd, J = 2.4, 1.4 Hz, 1H), 7.41 (d, J = 8.7 Hz, 2H), 7.24 (dd, J = 2.4, 1.7 Hz, 1H), 3.93 (s, 3H).

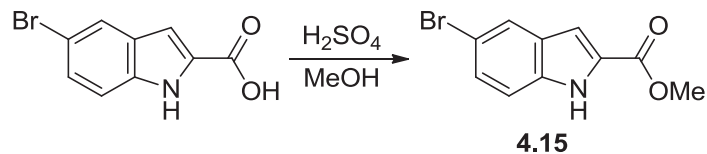
3-(4-chlorophenyl)-5-hydroxybenzoic acid (4.14)



This compound was prepared, following General Procedure C, from **4.13** (1.12 g, 4.28 mmol). Column chromatography over silica gel with gradient elution from 3 to 25% methanol/dichloromethane gave the product as a white solid (0.83 g, 78%).

^1H NMR (300 MHz, CD_3OD) δ 7.72 (t, J = 1.5 Hz, 1H), 7.55 (d, J = 8.7 Hz, 2H), 7.44 (dd, J = 2.4, 1.4 Hz, 1H), 7.40 (d, J = 8.7 Hz, 2H), 7.21 (dd, J = 2.4, 1.7 Hz, 1H).

methyl 5-bromoindole-2-carboxylate (4.15)

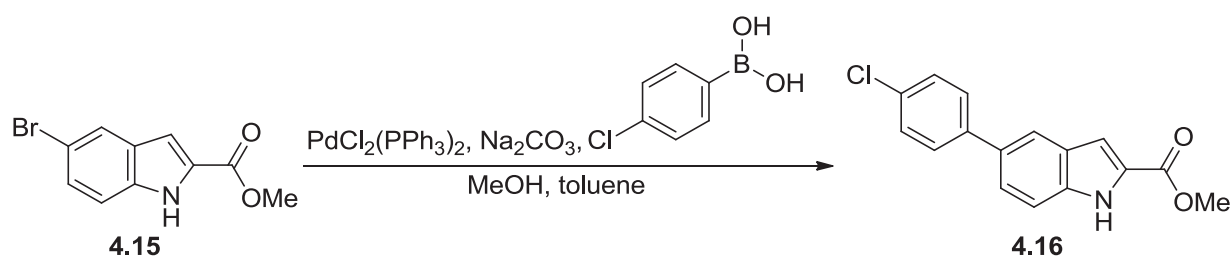


This compound was prepared, following General Procedure A, from 5-bromoindole-2-carboxylic acid (0.32 g, 1.35 mmol) as a light yellow solid (0.33 g, 96%).

Characterizations matched those reported in the literature.¹⁵⁹

¹H NMR (300 MHz, CDCl₃) δ 8.99 (bs, 1H), 7.85–7.82 (m, 1H), 7.41 (dd, *J* = 8.8, 1.9 Hz, 1H), 7.31 (d, *J* = 8.8 Hz, 1H), 7.16–7.13 (m, 1H), 3.96 (s, 3H).

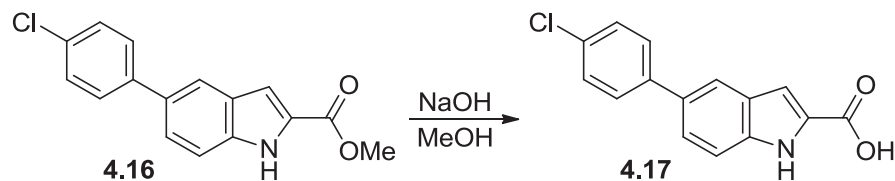
methyl 5-(4-chlorophenyl)indole-2-carboxylate (4.16)



This compound was prepared, following General Procedure B, from **4.15** (0.33 g, 1.29 mmol). Column chromatography over silica gel with gradient elution from 5 to 25% ethyl acetate/hexanes gave the product as a white solid (0.15 g, 40%).

¹H NMR (300 MHz, CDCl₃) δ 8.99 (bs, 1H), 7.85 (s, 1H), 7.59–7.46 (m, 4H), 7.41 (d, *J* = 8.6 Hz, 2H), 7.27–7.26 (m, 1H), 3.97 (s, 3H).

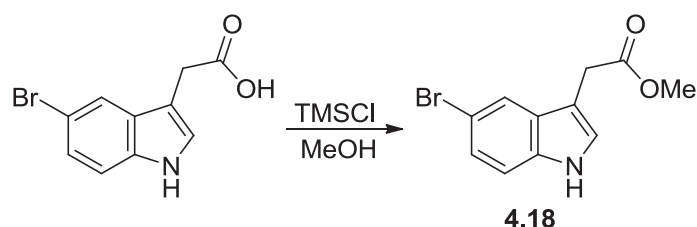
5-(4-chlorophenyl)indole-2-carboxylic acid (4.17)



This compound was prepared, following General Procedure C, from **4.16** (0.065 g, 0.23 mmol). Column chromatography over silica gel with gradient elution from 3 to 30% methanol/dichloromethane gave the product as a light yellow solid (0.062 g, 100%).

^1H NMR (300 MHz, CD_3OD) δ 7.83 (s, 1H), 7.59 (d, J = 8.4 Hz, 2H), 7.50 (s, 2H), 7.39 (d, J = 8.4 Hz, 2H), 7.18 (s, 1H).

methyl 2-(5-bromoindol-3-yl)acetate (**4.18**)

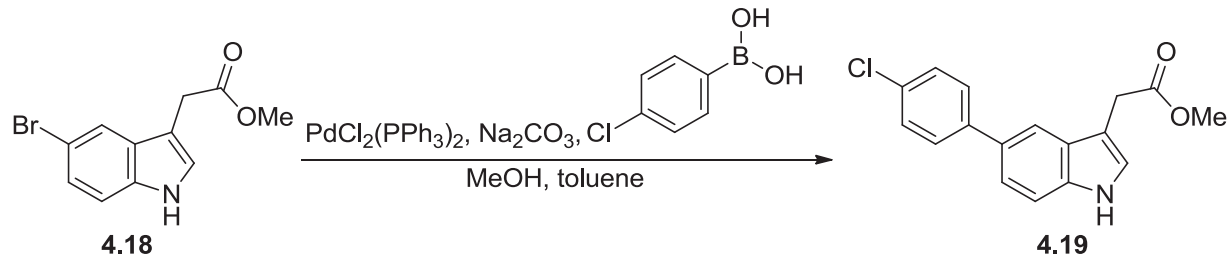


This compound was prepared according to a known procedure.¹⁶⁰ A solution of chlorotrimethylsilane (1 mL) in anhydrous methanol (10 mL) was cooled to -20 °C and then added to a solution of 5-bromoindole-3-acetic acid (0.31 g, 1.20 mmol) in anhydrous methanol (10 mL). The reaction mixture was stirred at rt overnight and then concentrated by rotary evaporation. The residue was dissolved with dichloromethane, filtered through a pad of silica gel, and washed with 50% ethyl acetate/hexanes (50 mL). The filtrate was then concentrated to provide the product as a light brown solid (0.29 g, 90%).

Characterizations matched those reported in the literature.¹⁶⁰⁻¹⁶¹

^1H NMR (300 MHz, CDCl_3) δ 8.30 (bs, 1H), 7.70 (d, J = 1.9 Hz, 1H), 7.23 (dd, J = 8.6, 1.9 Hz, 1H), 7.11 (d, J = 8.6 Hz, 1H), 7.02 (d, J = 2.4 Hz, 1H), 3.72–3.71 (m, 5H).

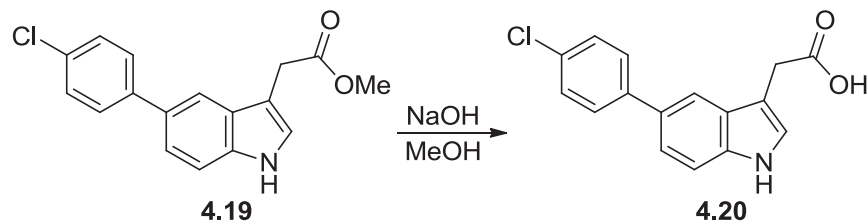
methyl 2-[5-(4-chlorophenyl)indol-3-yl]acetate (4.19)



This compound was prepared, following General Procedure B, from **4.18** (0.25 g, 0.93 mmol). Column chromatography over silica gel with gradient elution from 20 to 40% ethyl acetate/hexanes gave the product as a light yellow oil (0.17 g, 60%).

^1H NMR (300 MHz, CDCl_3) δ 8.19 (bs, 1H), 7.76 (s, 1H), 7.56 (d, $J = 8.6$ Hz, 2H), 7.43–7.35 (m, 4H), 7.17 (d, $J = 2.4$ Hz, 1H), 3.81 (s, 2H), 3.71 (s, 3H).

2-[5-(4-chlorophenyl)indol-3-yl]acetic acid (4.20)

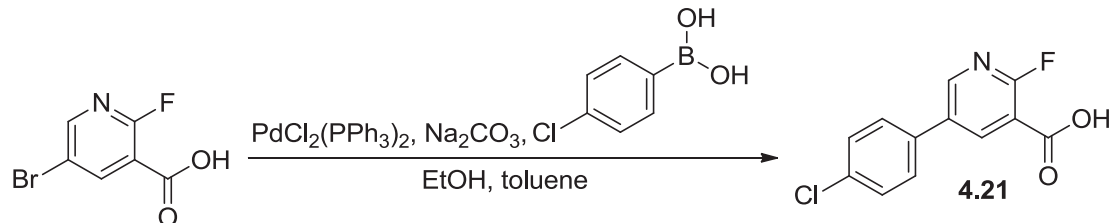


This compound was prepared, following General Procedure C, from **4.19** (0.17 g, 0.57 mmol). Column chromatography over silica gel with gradient elution from 5 to 20% methanol/dichloromethane gave the product as a white solid (0.072 g, 45%).

Characterizations matched those reported in the literature.¹⁶²

^1H NMR (300 MHz, CD_3OD) δ 10.42 (bs, 1H), 7.77–7.74 (m, 1H), 7.57 (d, $J = 8.3$ Hz, 2H), 7.42–7.31 (m, 4H), 7.19 (s, 1H), 3.76 (s, 2H).

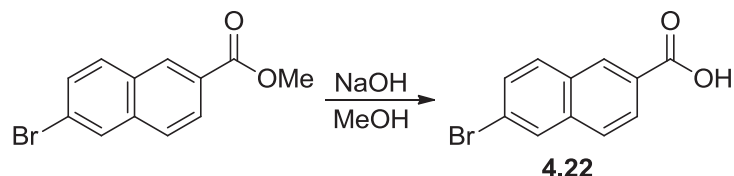
5-(4-chlorophenyl)-2-fluoronicotinic acid (4.21)



This compound was similarly prepared, following General Procedure B, from 5-bromo-2-fluoronicotinic acid (0.051 g, 0.23 mmol) in ethanol (5 mL) and toluene (5 mL). The reaction mixture was filtered through Celite, and the filtrate was extracted with diethyl ether (2 × 20 mL) from 1 M hydrochloric acid (20 mL). The combined organic layers were dried over magnesium sulfate, filtered, and concentrated. Column chromatography over silica gel with gradient elution from 5 to 20% methanol/dichloromethane provided the product as a white solid (0.019 g, 32%).

^1H NMR (300 MHz, CD_3OD) δ 8.60–8.51 (m, 2H), 7.65 (d, J = 8.7 Hz, 2H), 7.50 (d, J = 8.7 Hz, 2H).

6-bromo-2-naphthoic acid (4.22)

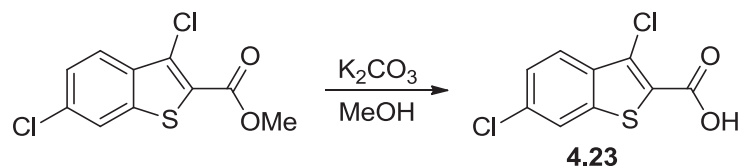


This compound was prepared, following General Procedure C, from methyl 6-bromo-2-naphthoate (0.54 g, 1.98 mmol). Column chromatography over silica gel with gradient elution from 3 to 25% methanol/dichloromethane gave the product as a white solid (0.48 g, 96%).

Characterizations matched those reported in the literature.¹⁶³

¹H NMR (300 MHz, DMSO-d₆) δ 8.62 (s, 1H), 8.30 (d, *J* = 1.8 Hz, 1H), 8.09 (d, *J* = 8.8 Hz, 1H), 8.05–7.96 (m, 2H), 7.72 (dd, *J* = 8.8, 2.0 Hz, 1H).

3,6-dichlorobenzo[*b*]thiophene-2-carboxylic acid (4.23)

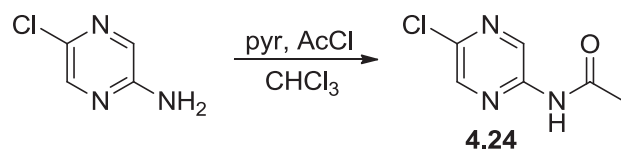


A 0.80 M aqueous potassium carbonate solution (4.20 mL) was added to a suspension of methyl 3,6-dichlorobenzo[*b*]thiophene-2-carboxylate (0.30 g, 1.12 mmol) in methanol (20 mL). The reaction mixture was stirred at rt overnight and then extracted with dichloromethane (2 × 30 mL) from 1 M hydrochloric acid (30 mL). The combined organic layers were dried over magnesium sulfate, filtered, and concentrated. Column chromatography over silica gel with gradient elution from 5 to 15% methanol/dichloromethane gave the product as a white solid (0.26 g, 93%).

Characterizations matched those reported in the literature.¹⁶⁴

¹H NMR (300 MHz, CD₃OD) δ 7.99 (d, *J* = 1.4 Hz, 1H), 7.90 (d, *J* = 8.7 Hz, 1H), 7.51 (dd, *J* = 8.7, 1.9 Hz, 1H).

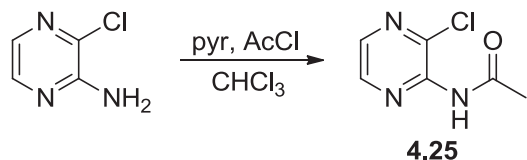
N-(5-chloropyrazin-2-yl)acetamide (4.24)



Acetyl chloride (0.19 mL, 2.69 mmol) was added dropwise to a solution of 5-chloropyrazin-2-amine (0.058 g, 0.43 mmol) in chloroform (10 mL) and pyridine (5 mL) at 0 °C. After stirring at 50 °C overnight, the reaction mixture was concentrated via rotary evaporation. Column chromatography over silica gel with gradient elution from 10 to 40% ethyl acetate/hexanes then provided the product as a white solid (0.071 g, 97%).

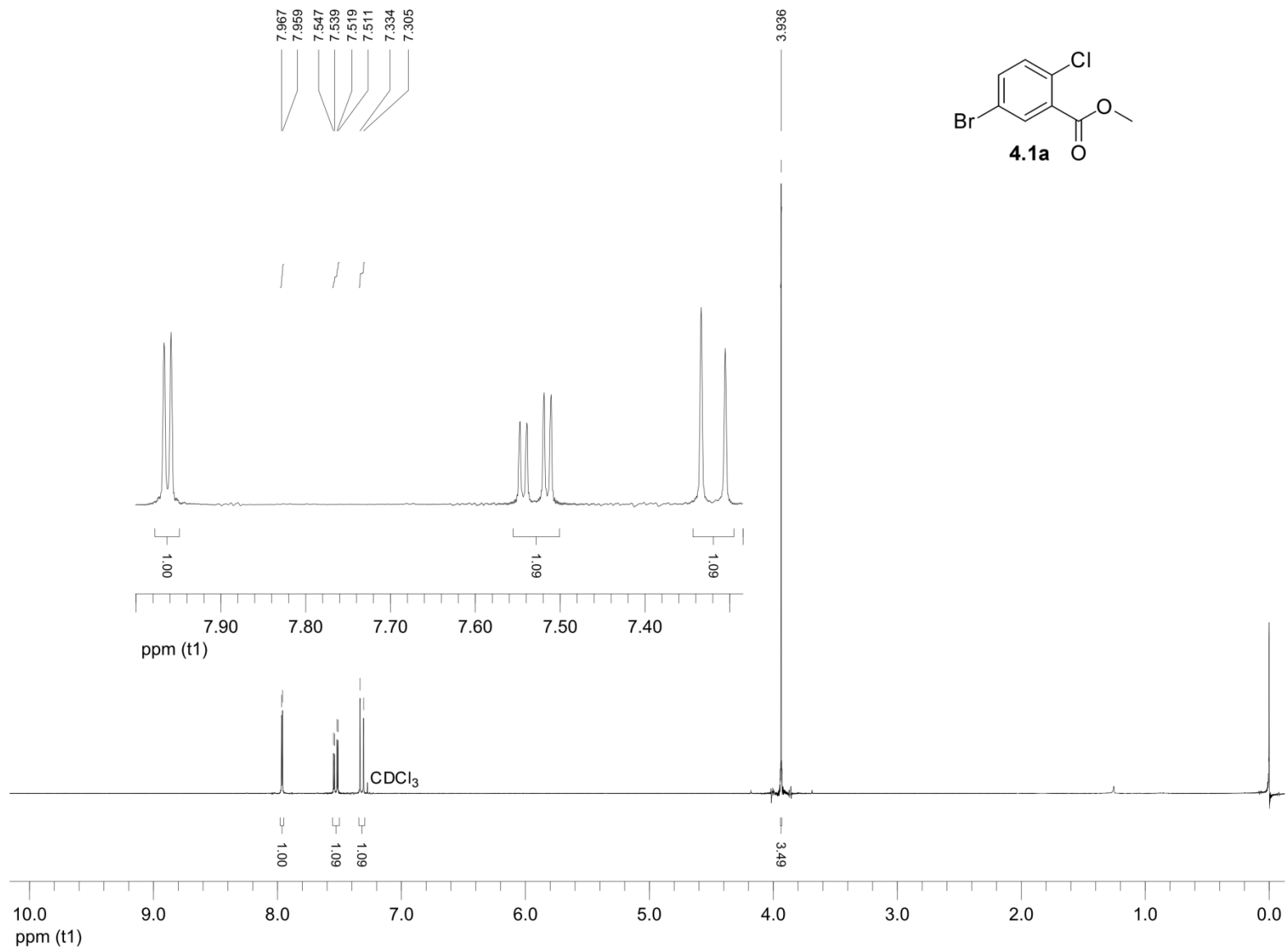
^1H NMR (300 MHz, CDCl_3) δ 9.32 (s, 1H), 8.24 (d, $J = 1.4$ Hz, 1H), 7.87 (bs, 1H), 2.26 (s, 3H).

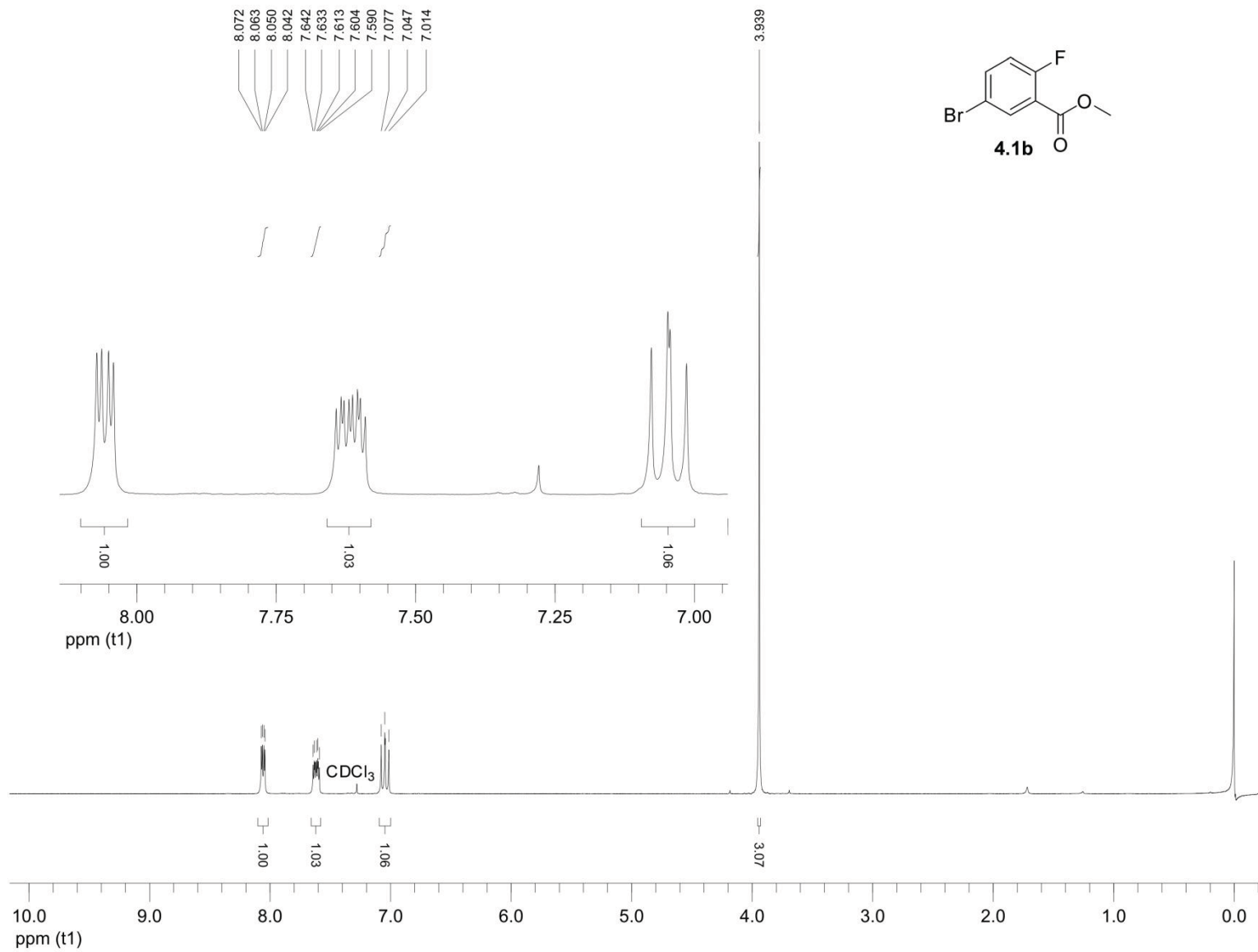
***N*-(3-chloropyrazin-2-yl)acetamide (4.25)**

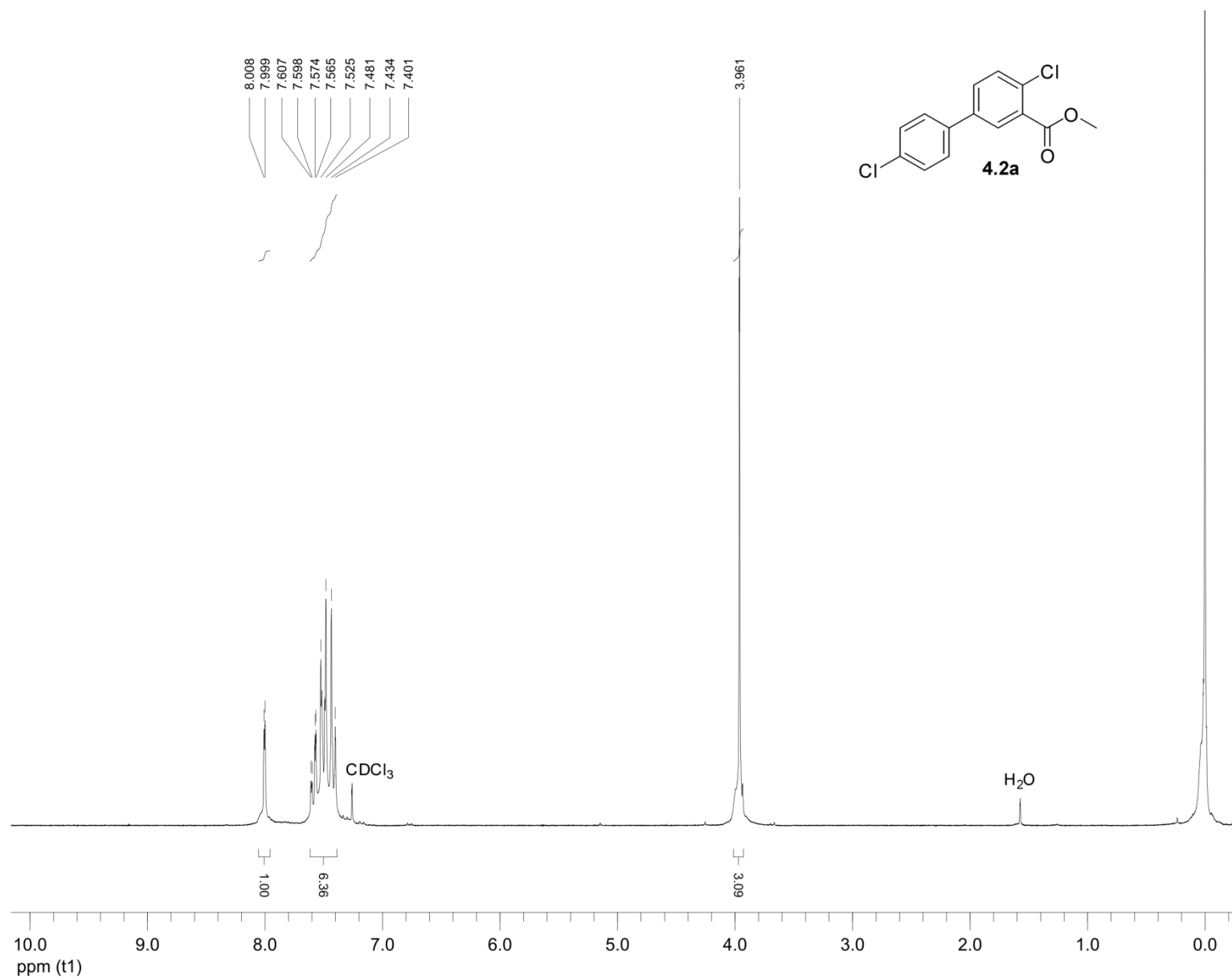


Acetyl chloride (0.11 mL, 1.53 mmol) was added dropwise to a solution of 3-chloropyrazin-2-amine (0.10 g, 0.76 mmol) and pyridine (0.12 mL, 1.53 mmol) in chloroform (10 mL) at 0 °C. After stirring at 50 °C overnight, the reaction mixture was concentrated via rotary evaporation. Column chromatography over silica gel with gradient elution from 20 to 50% ethyl acetate/hexanes then provided the product as a white solid (0.070 g, 53%).

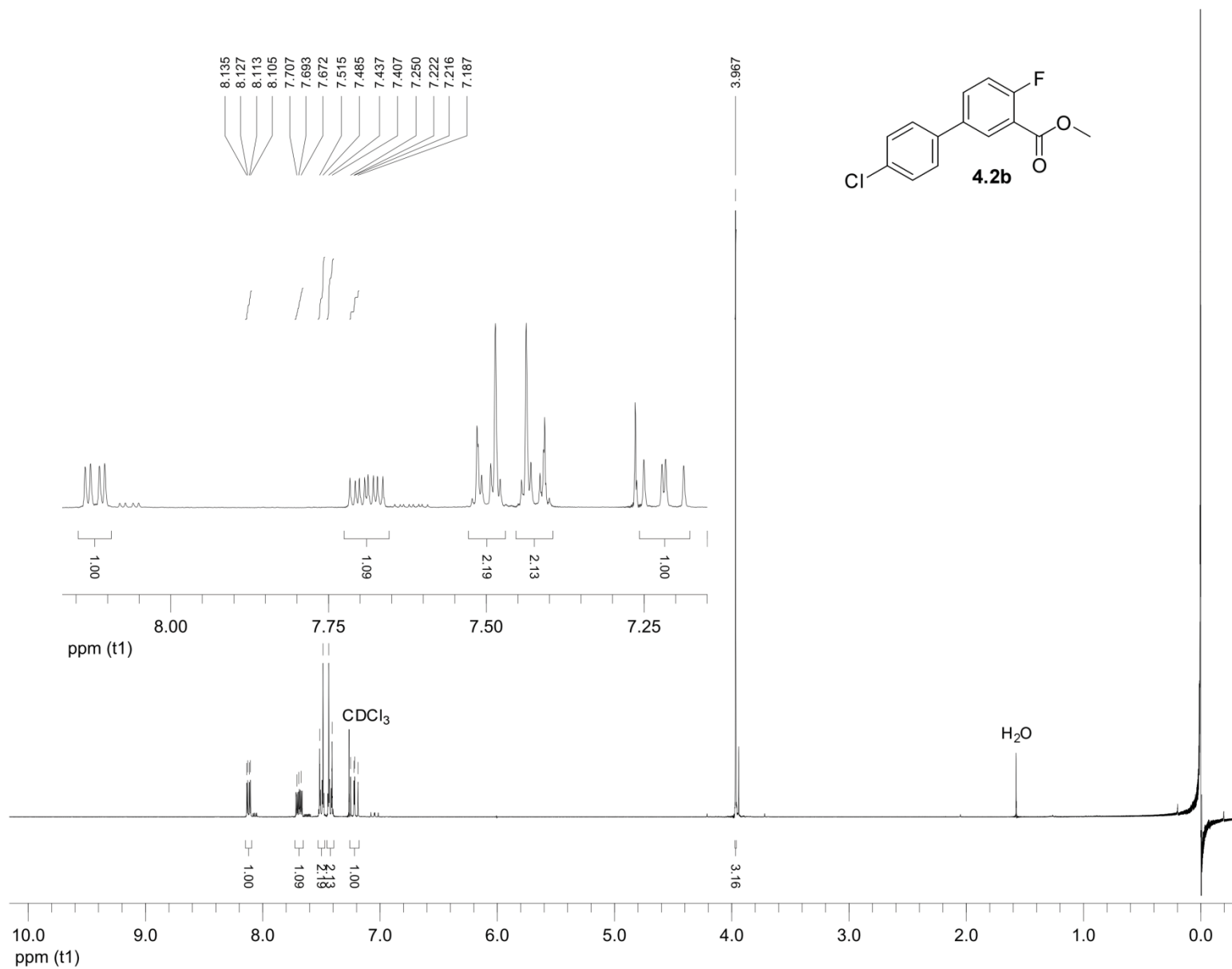
^1H NMR (300 MHz, CDCl_3) δ 8.30 (d, $J = 2.5$ Hz, 1H), 8.20 (bs, 1H), 8.12 (d, $J = 2.5$ Hz, 1H), 2.47 (s, 3H).

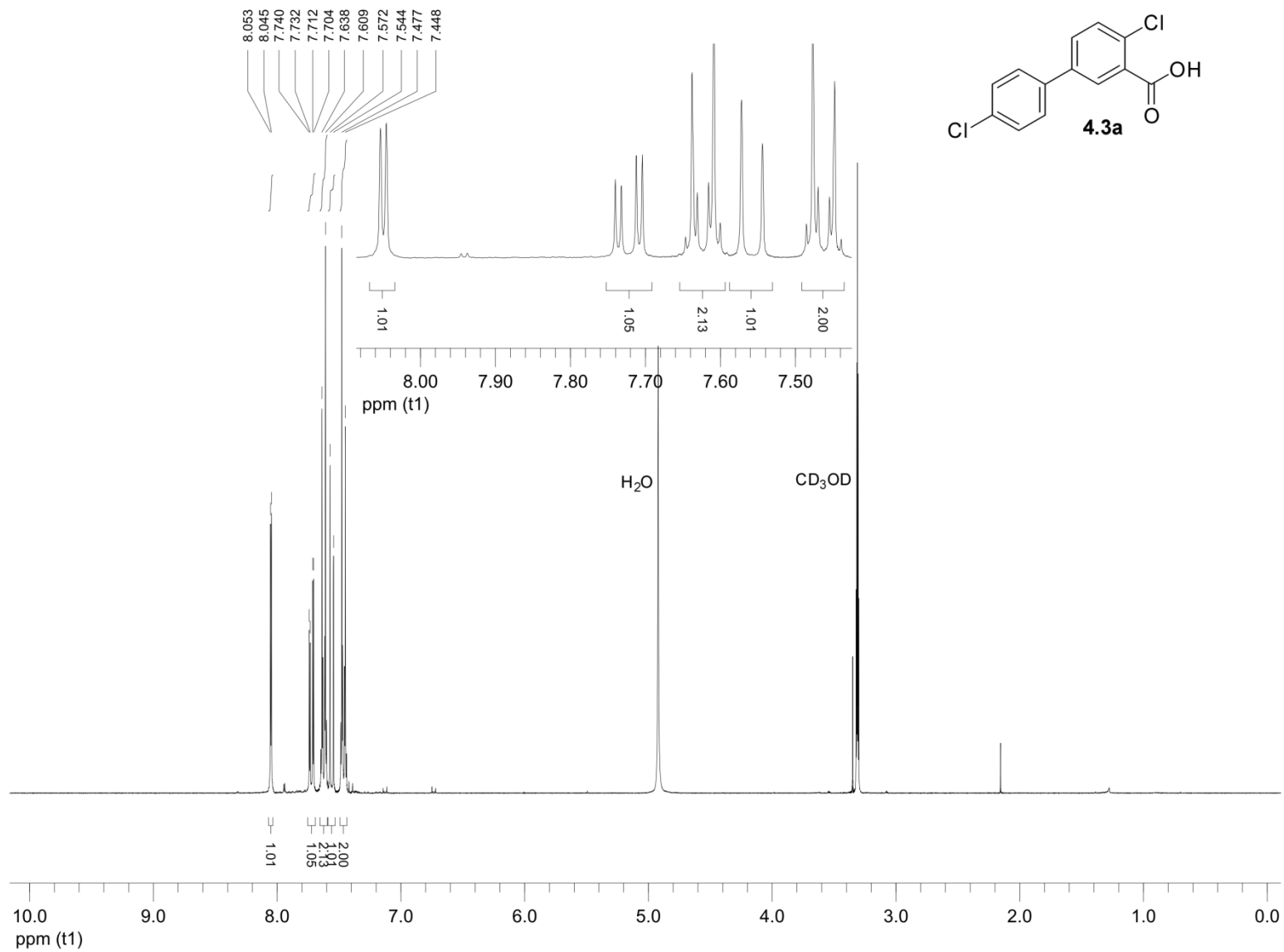


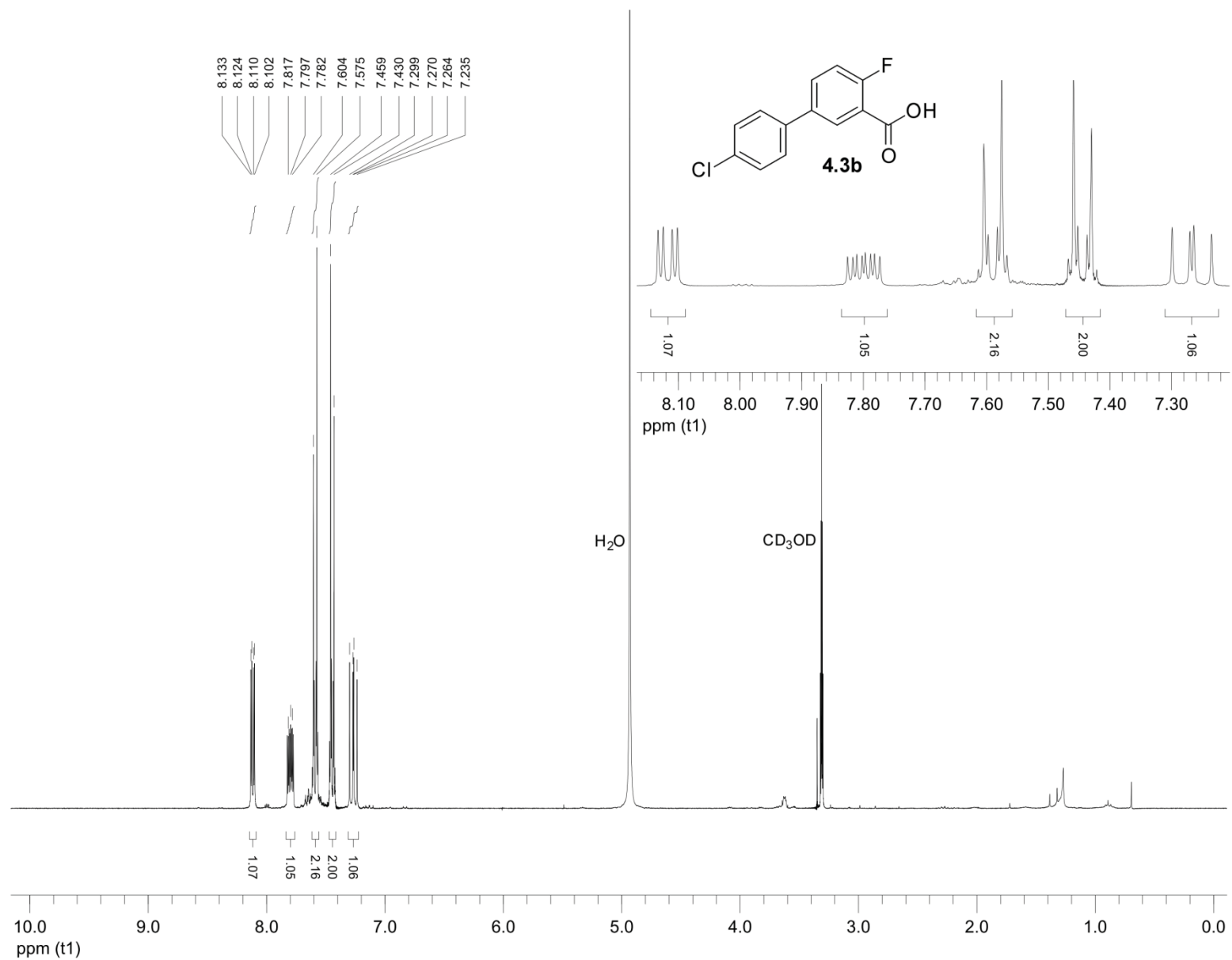


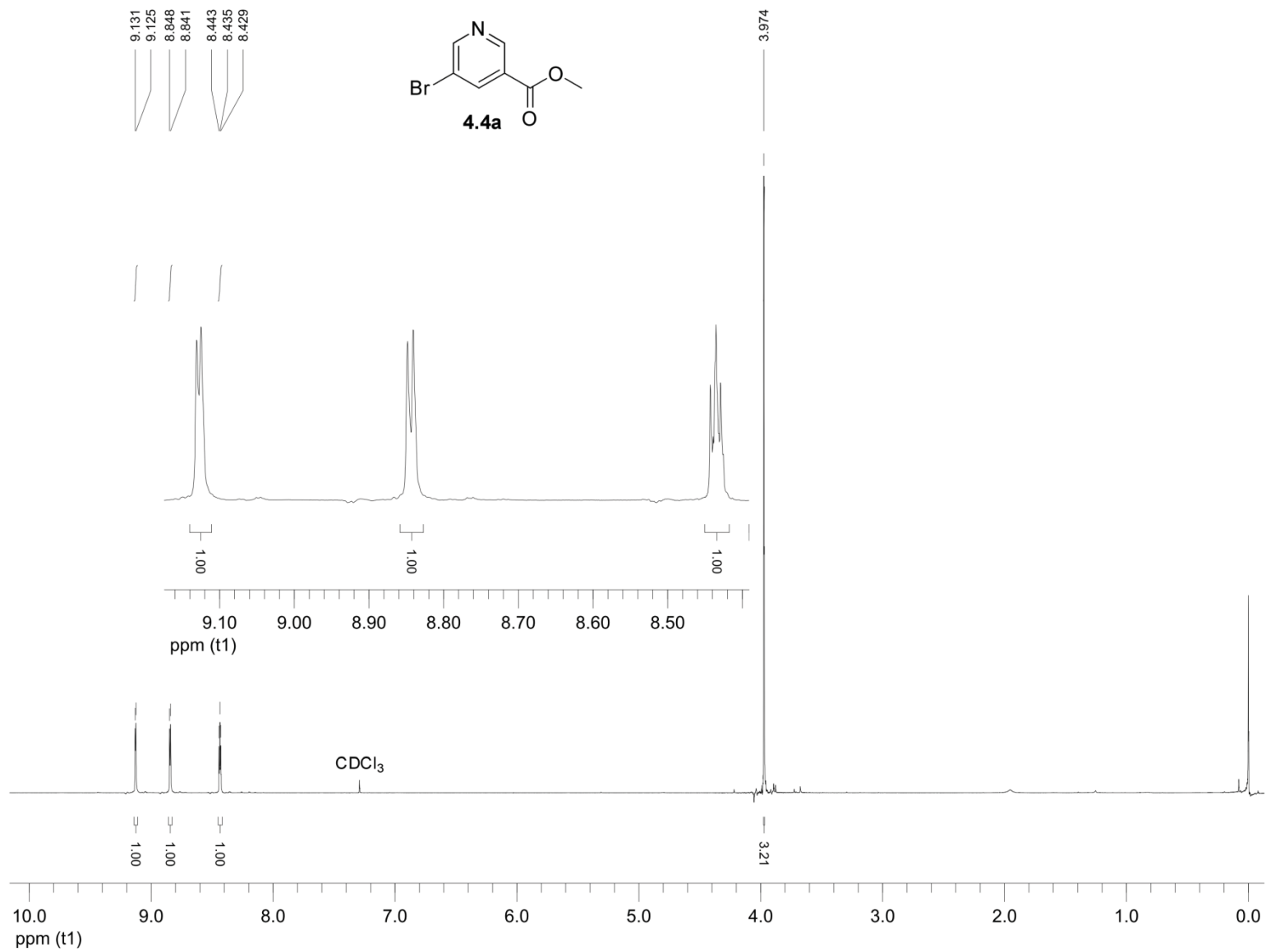


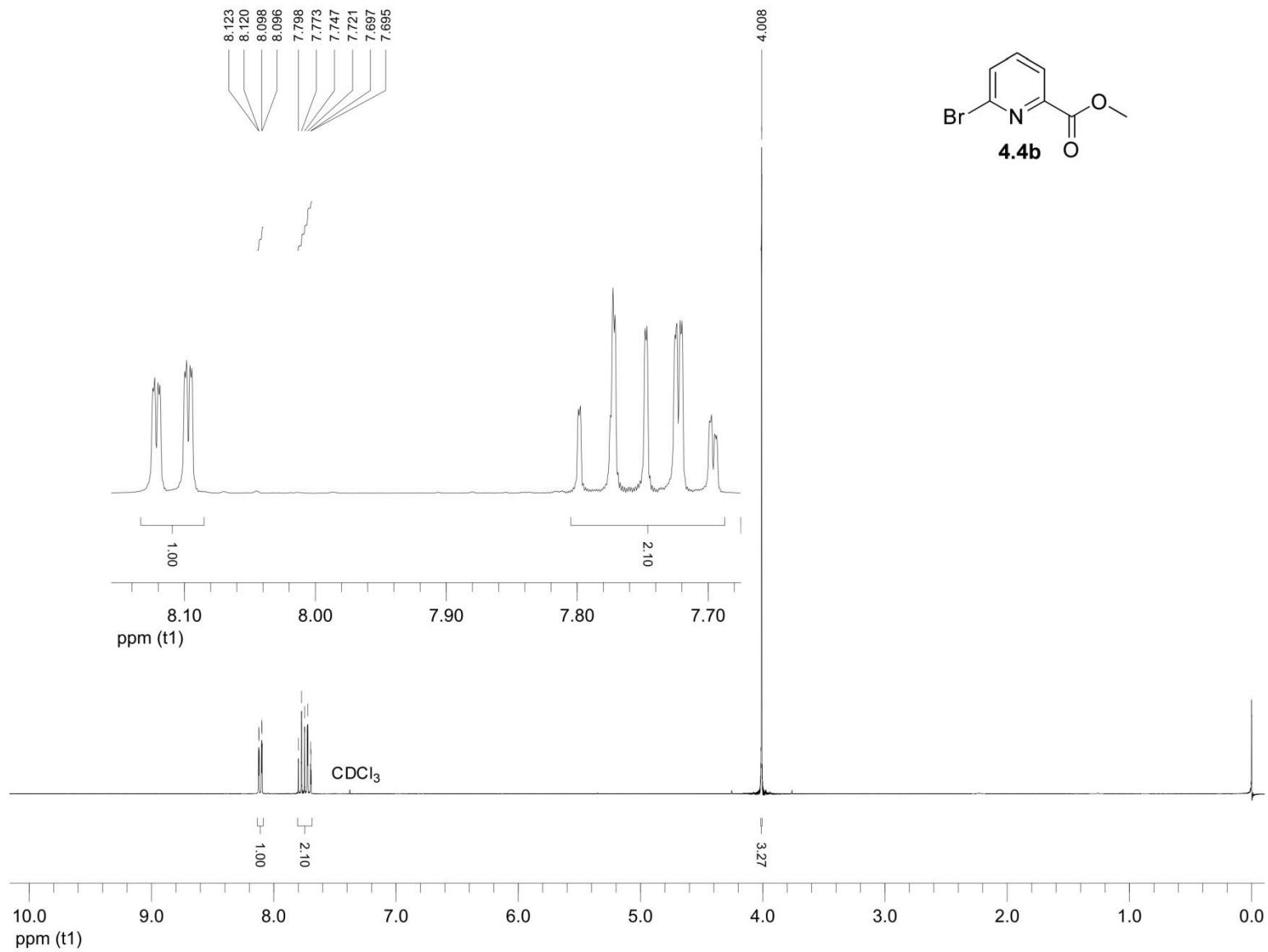
180

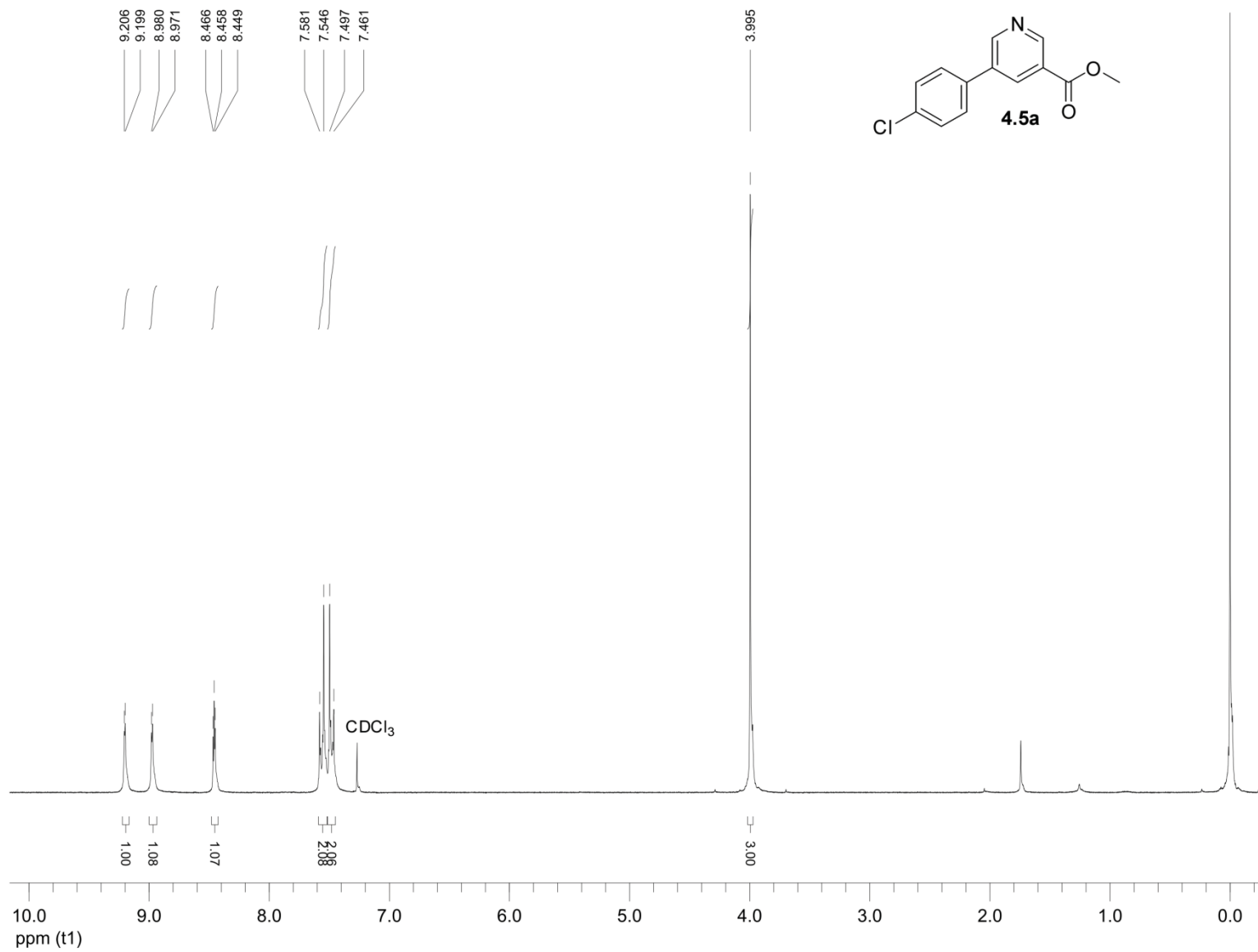


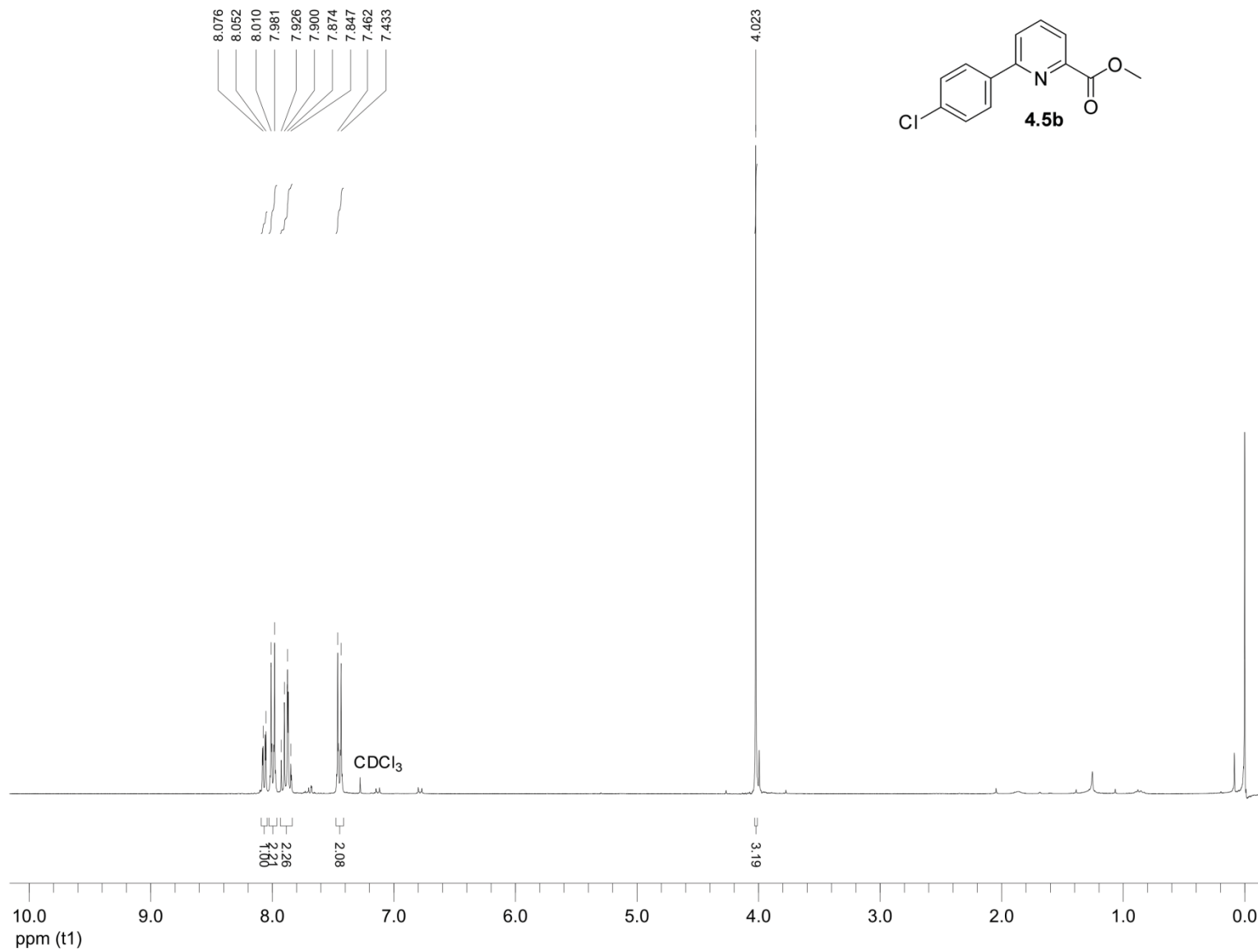


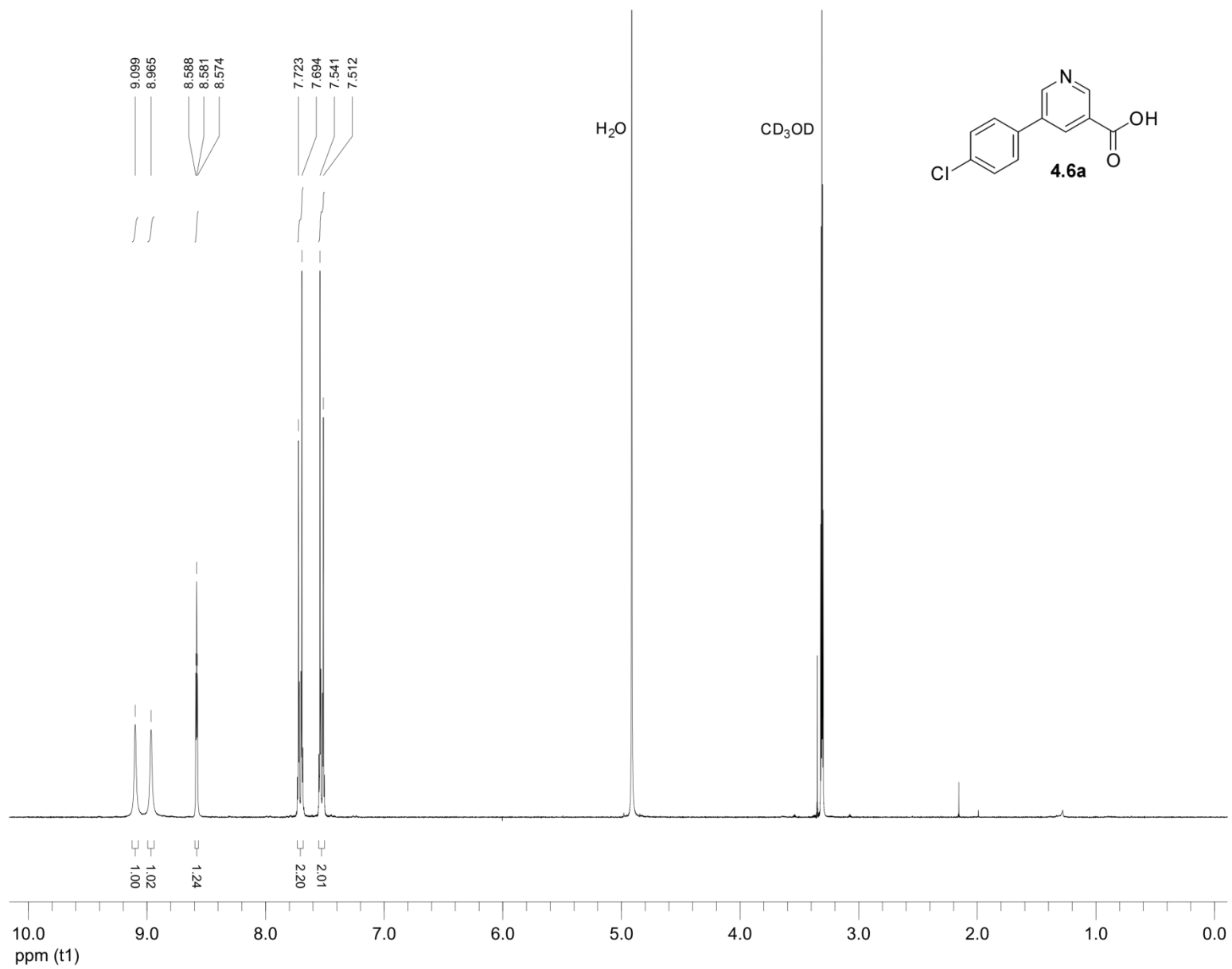




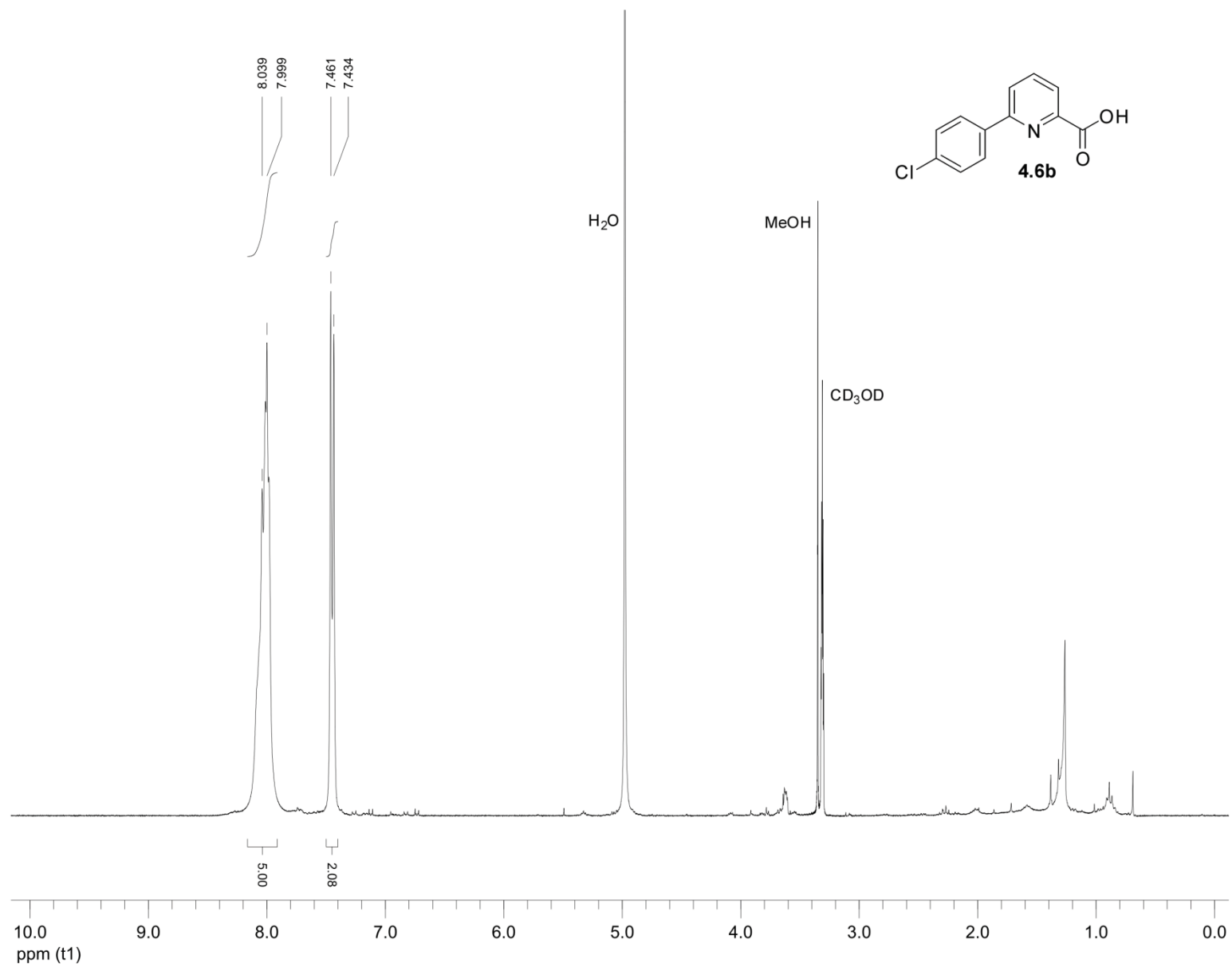


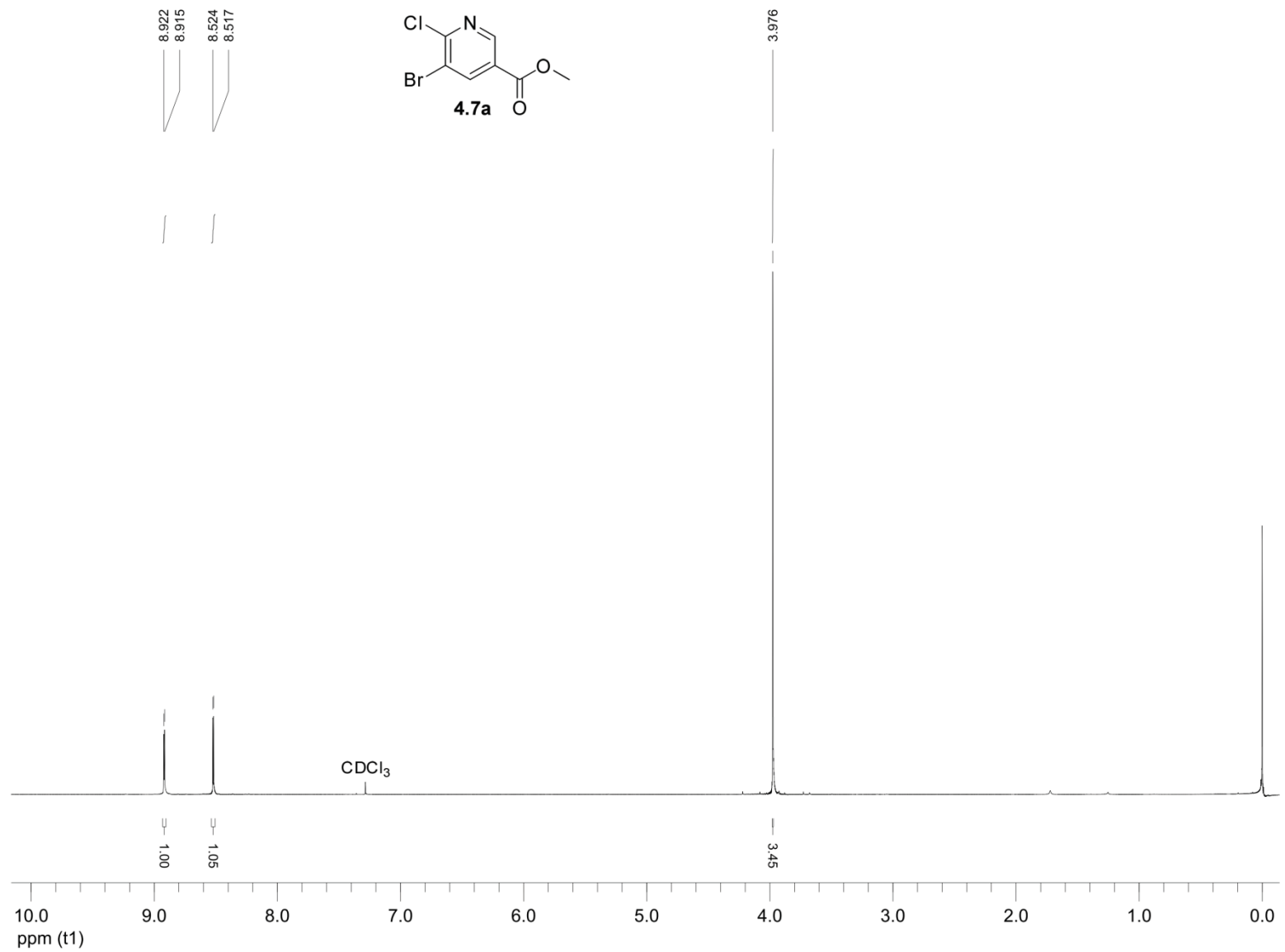


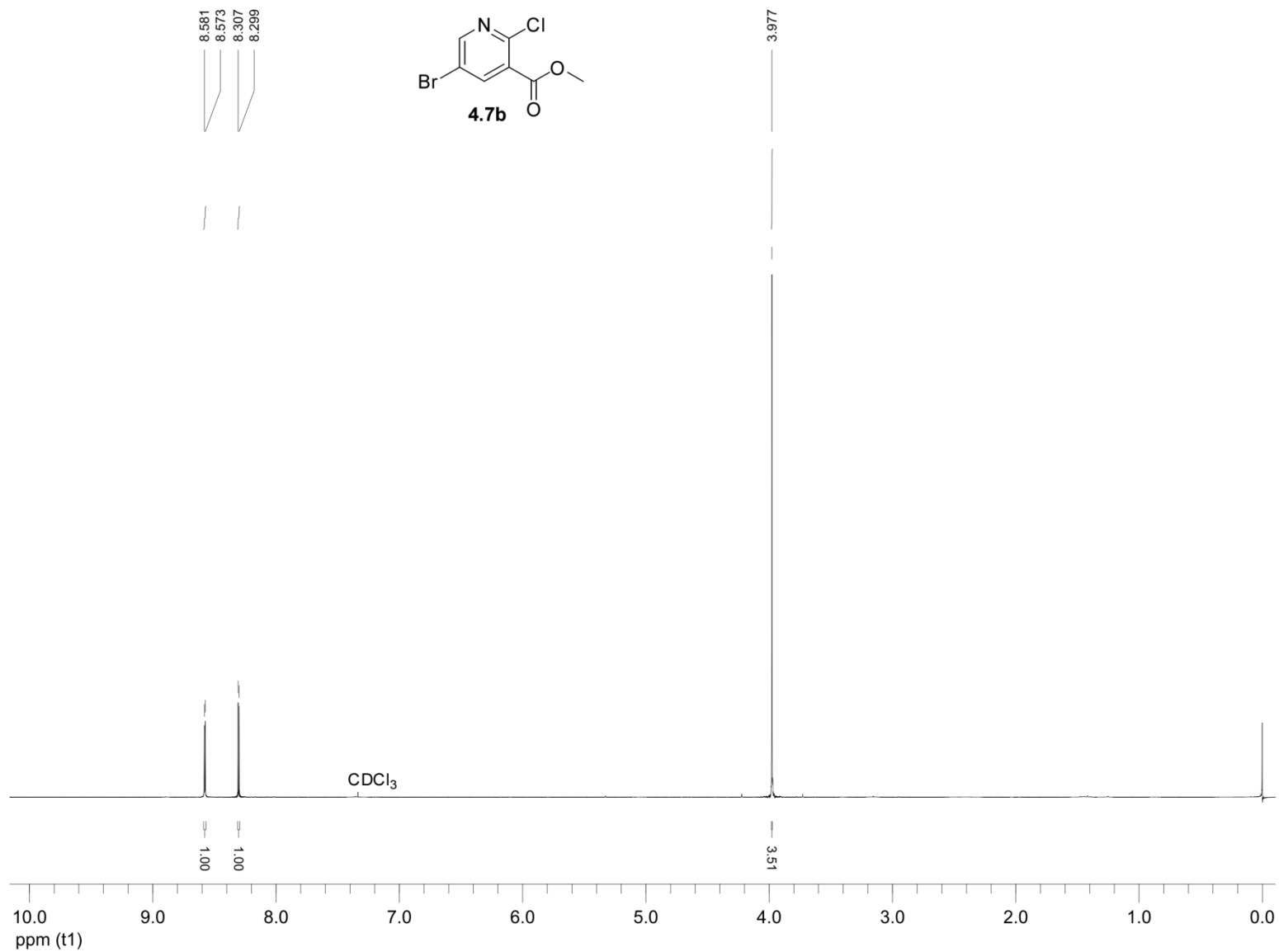




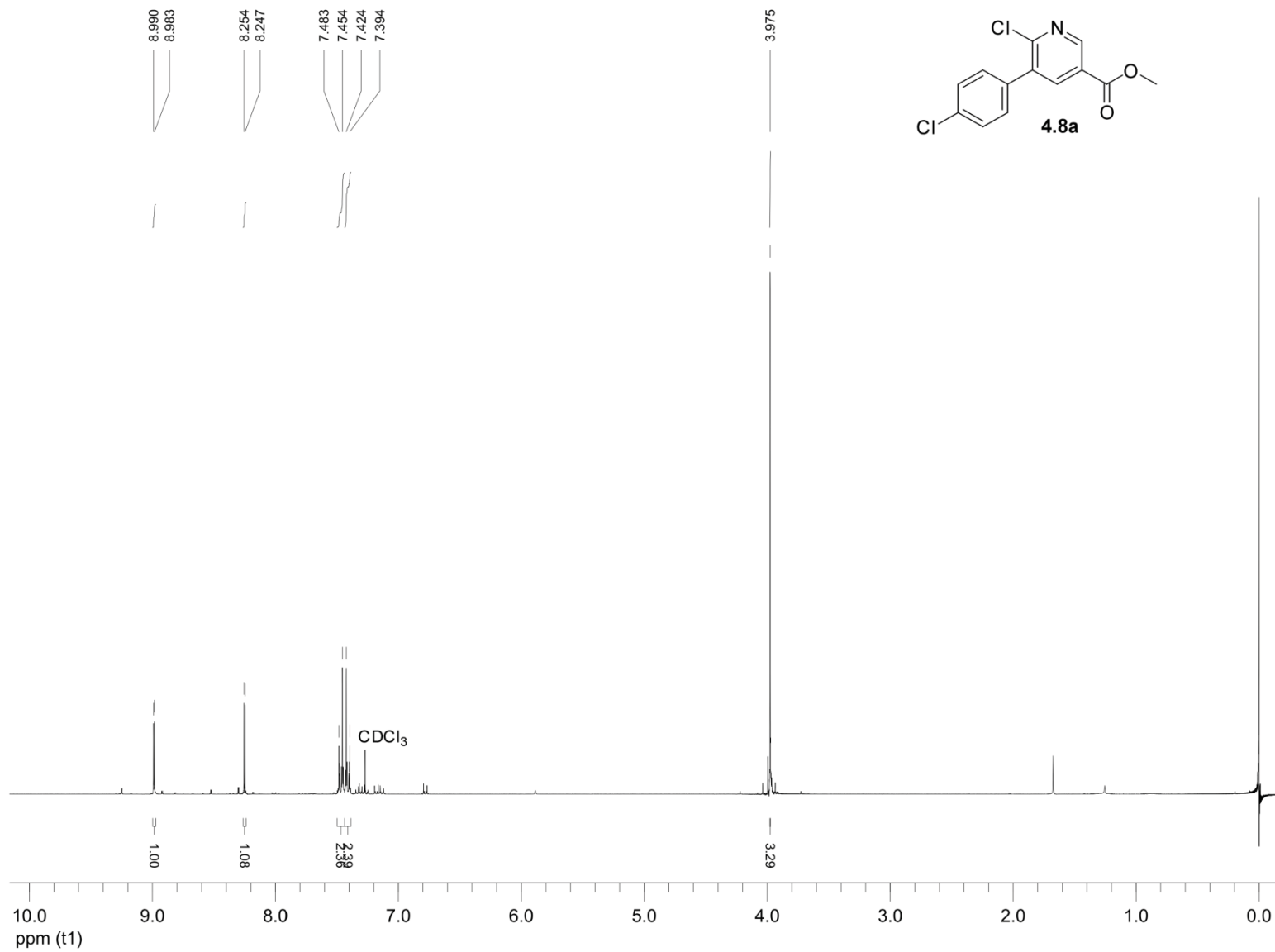
188

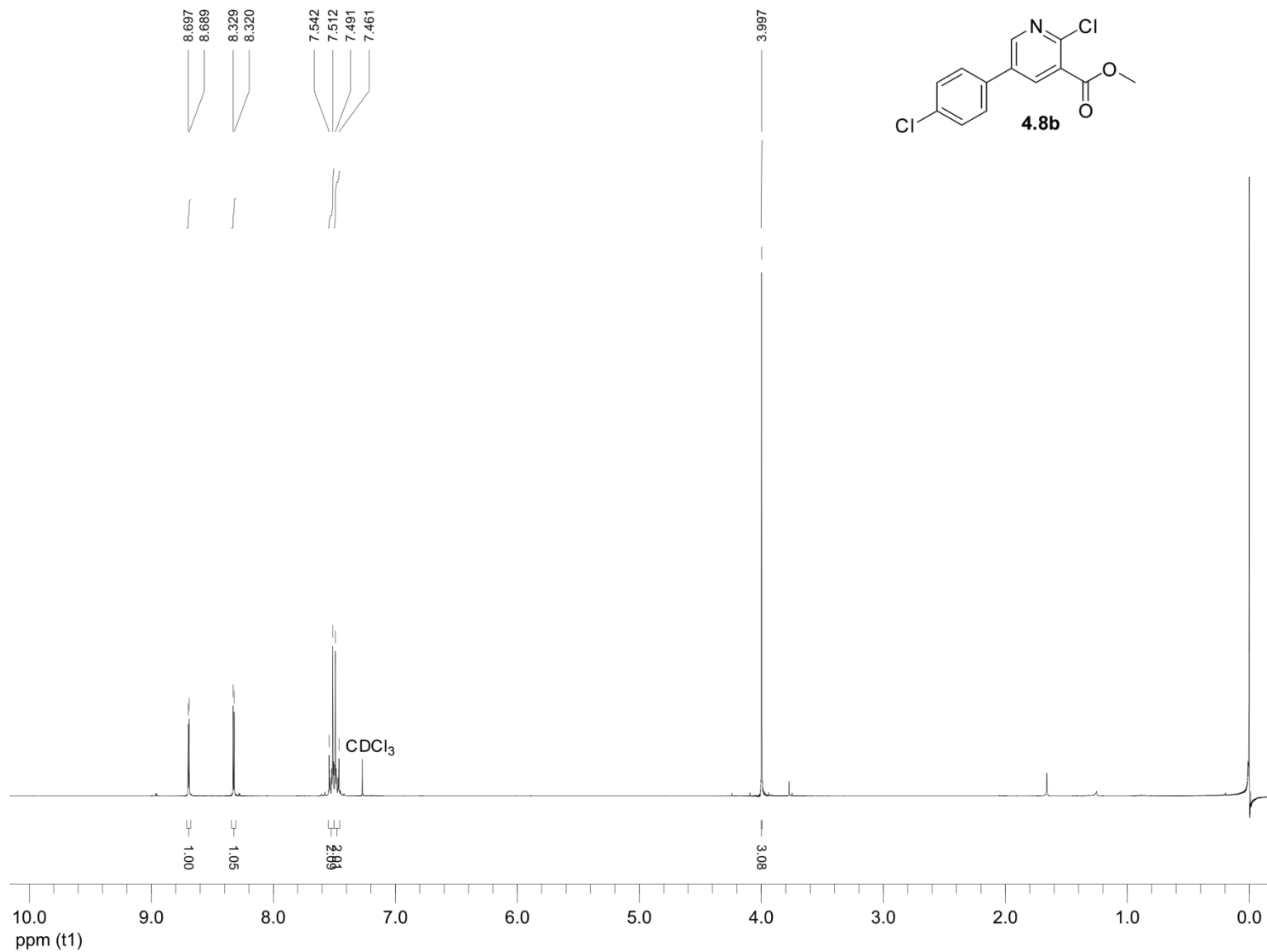


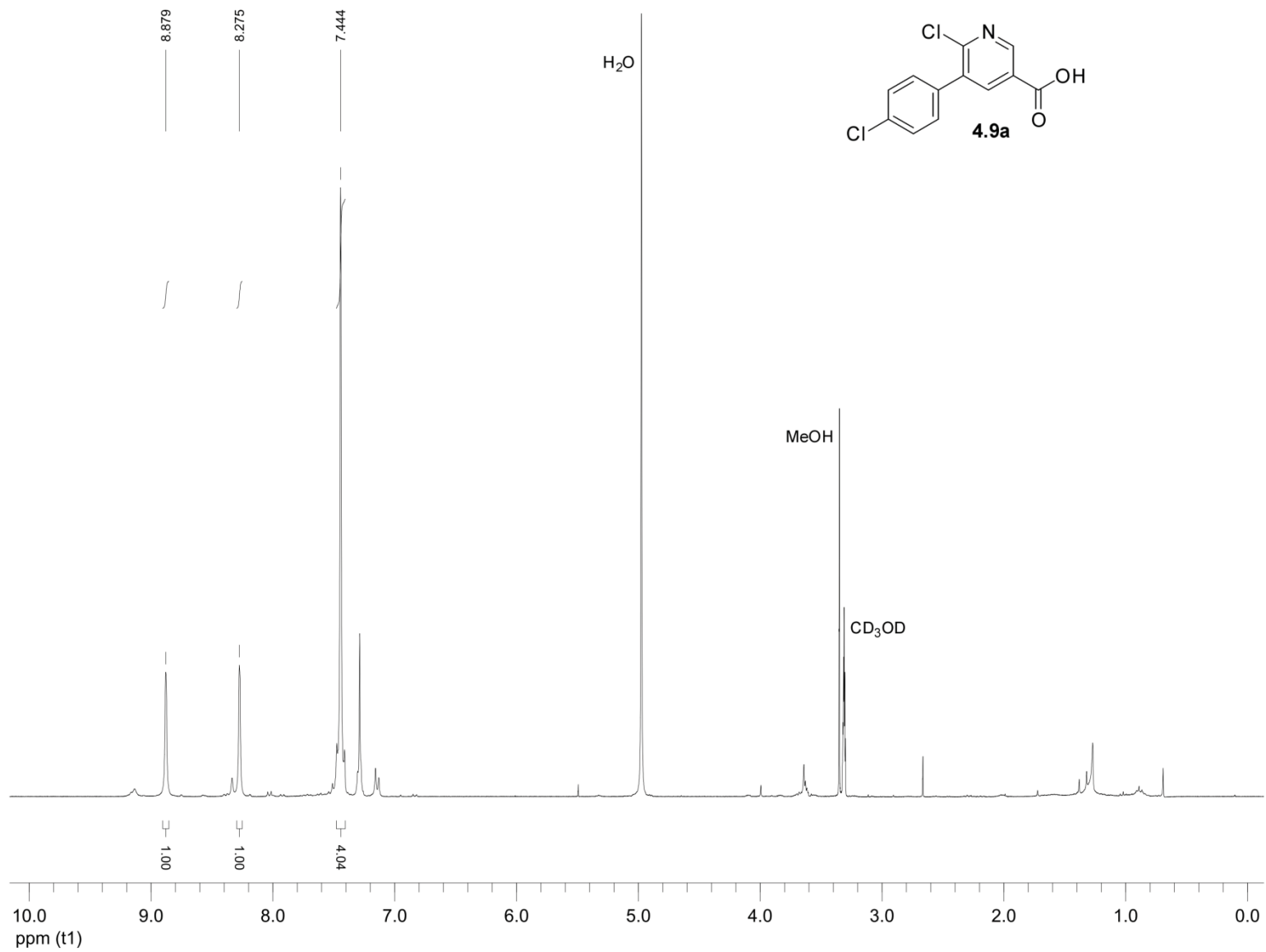




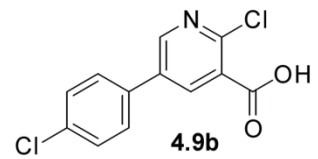
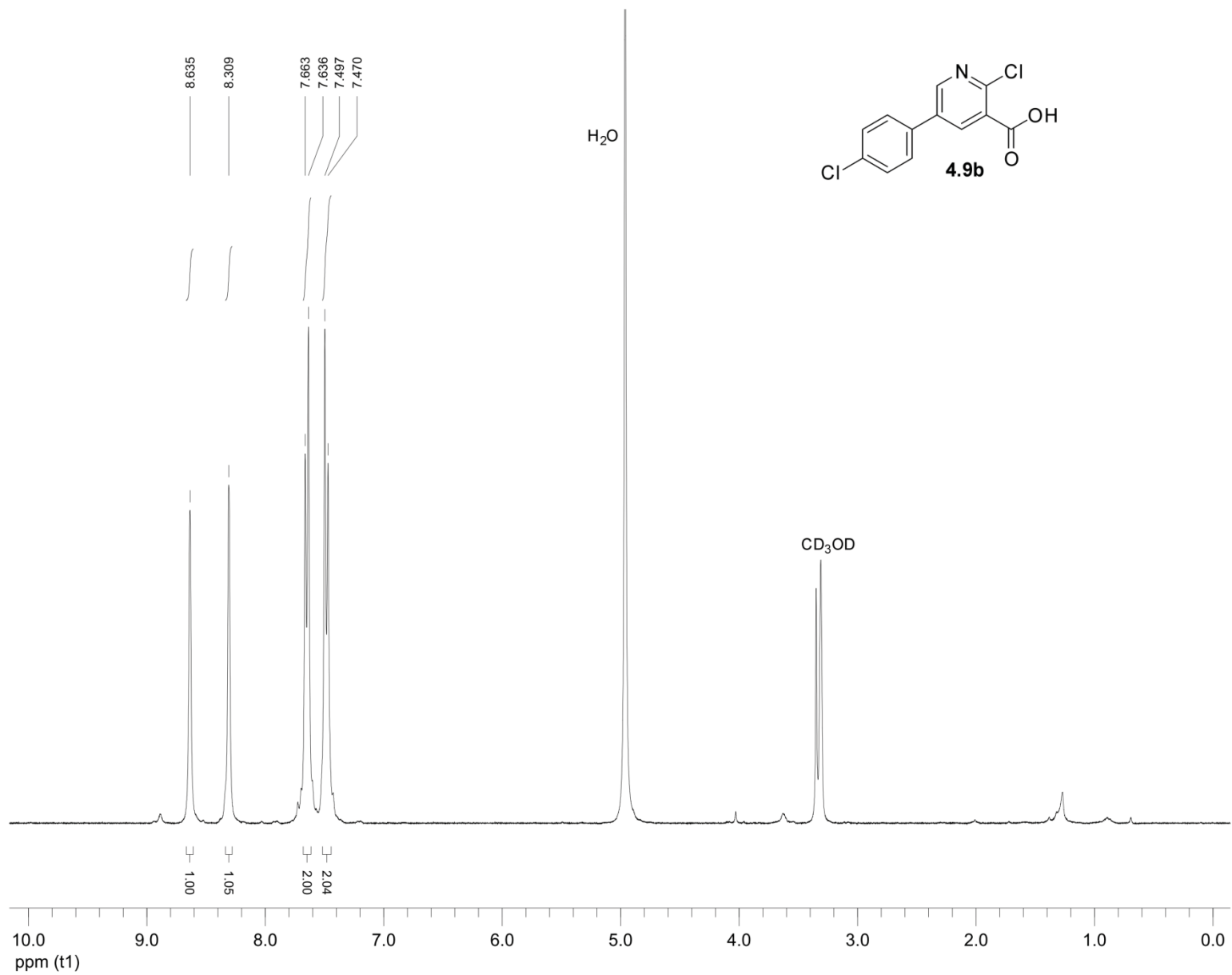
191

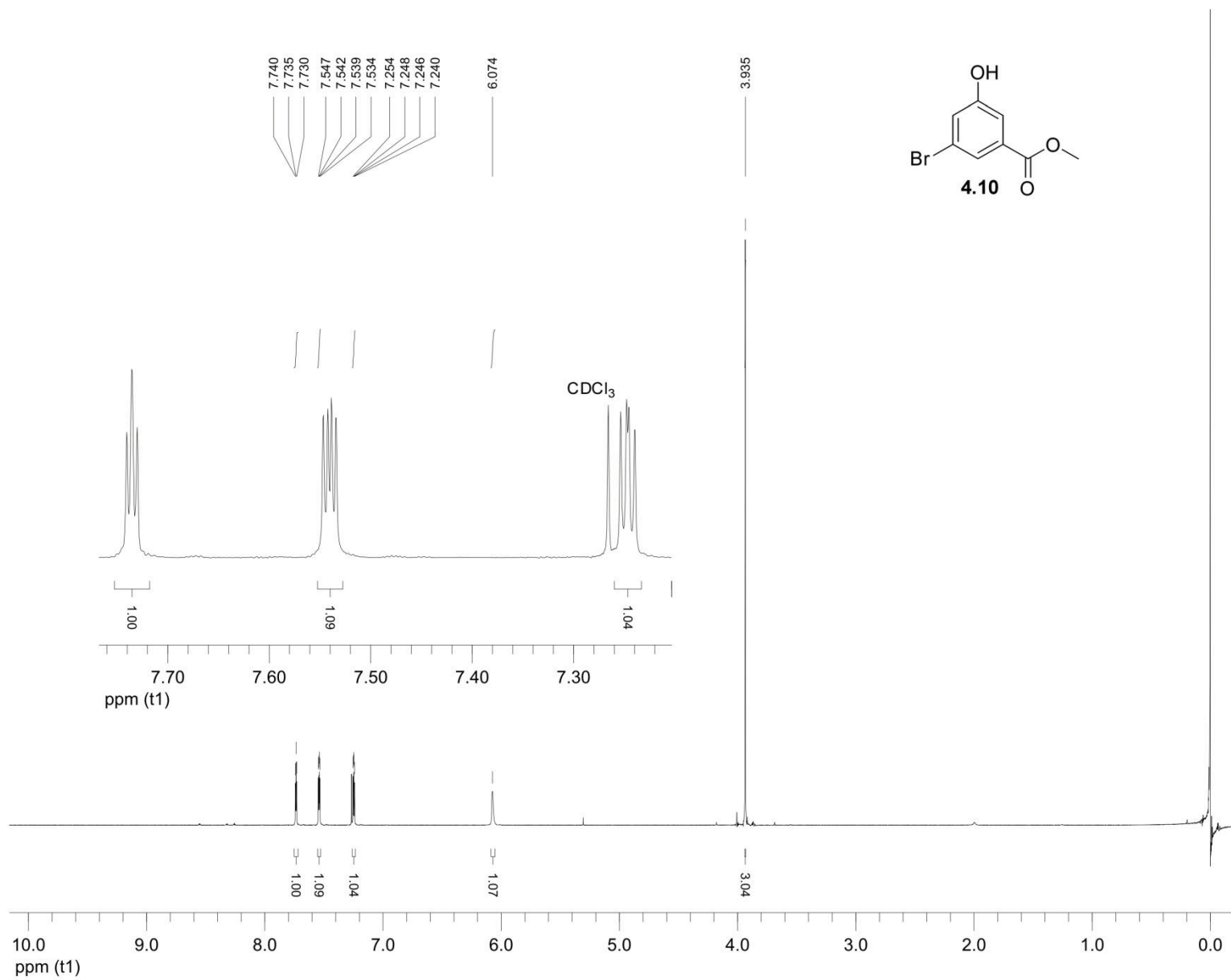


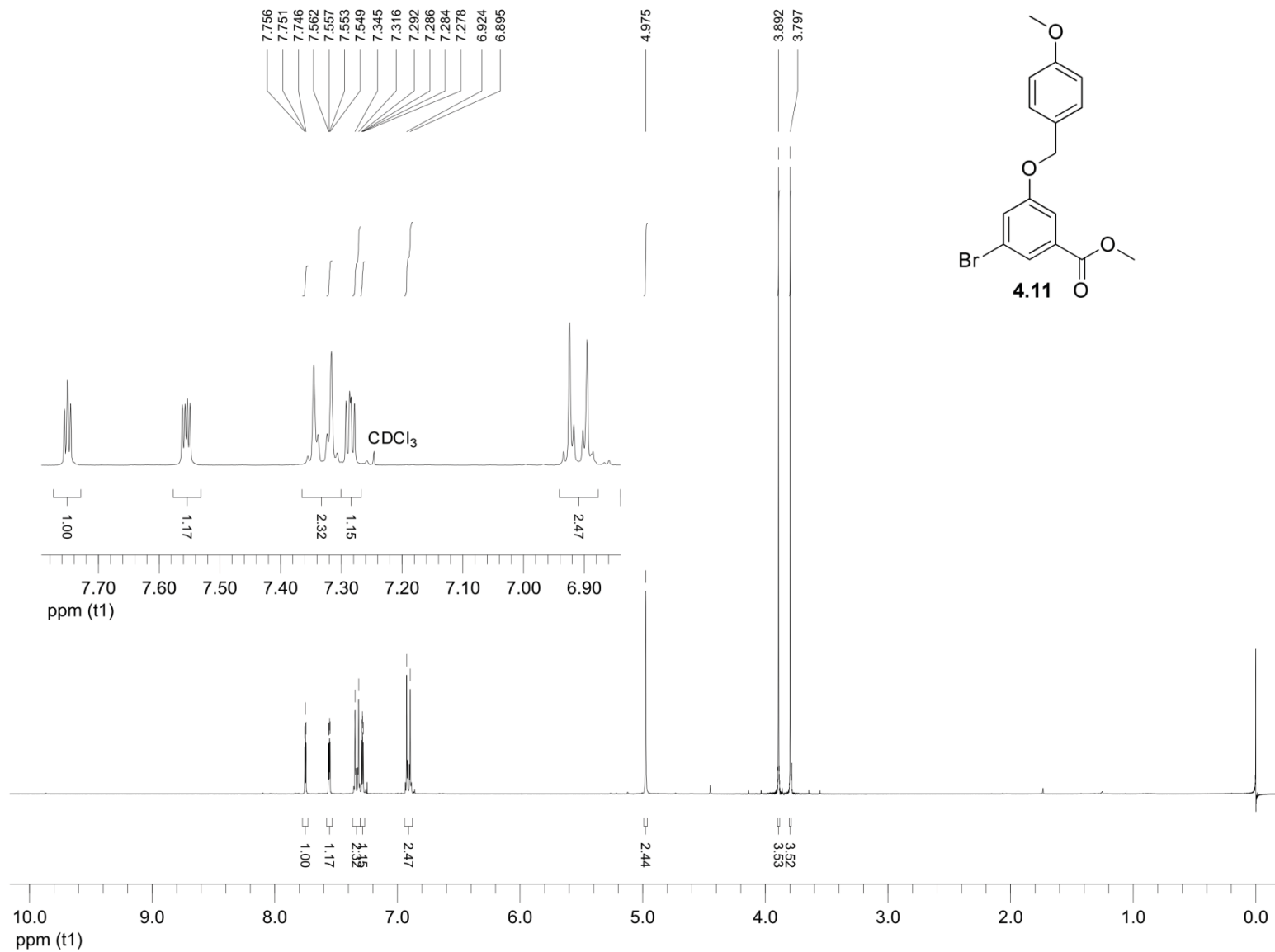


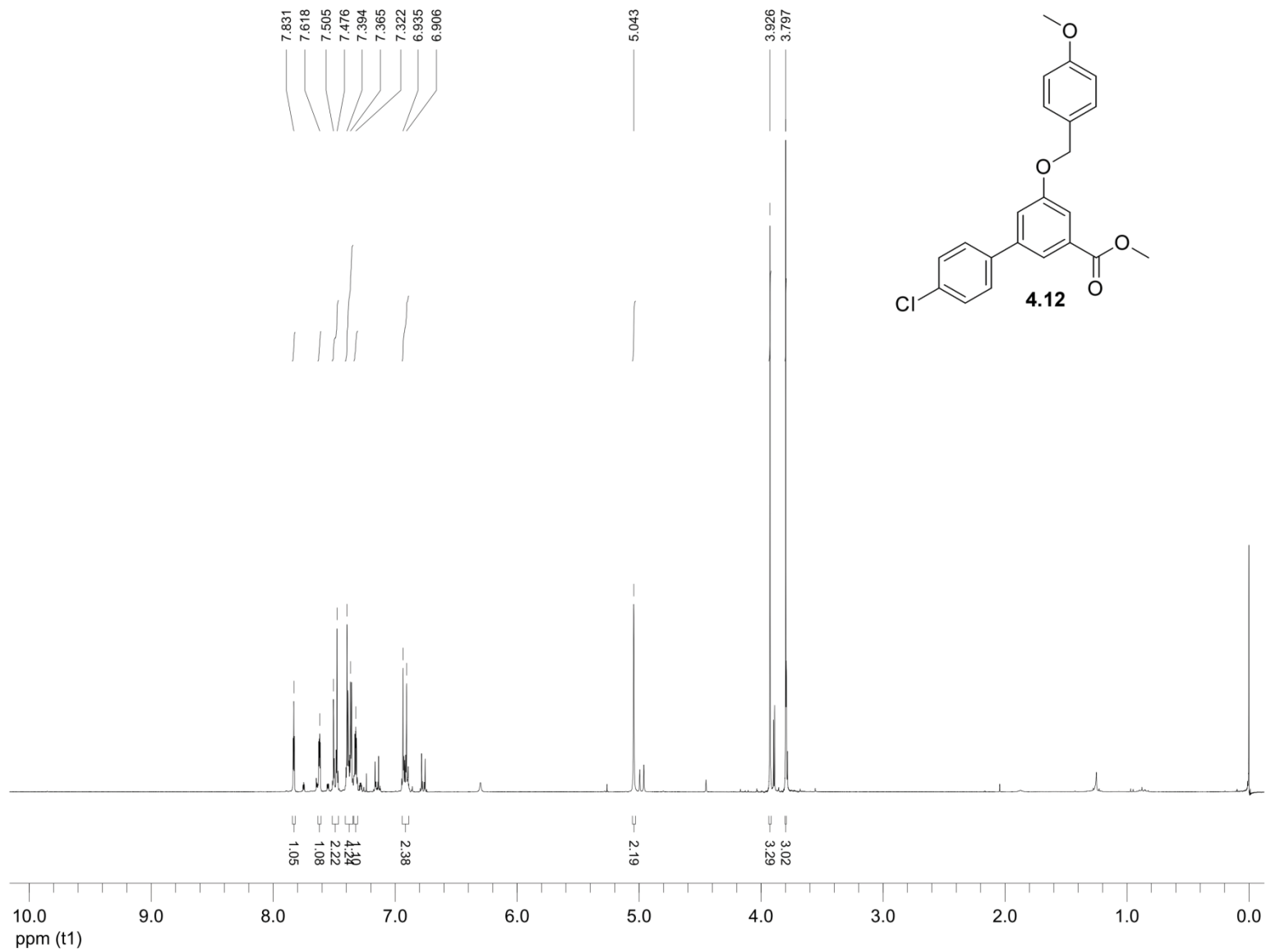


194

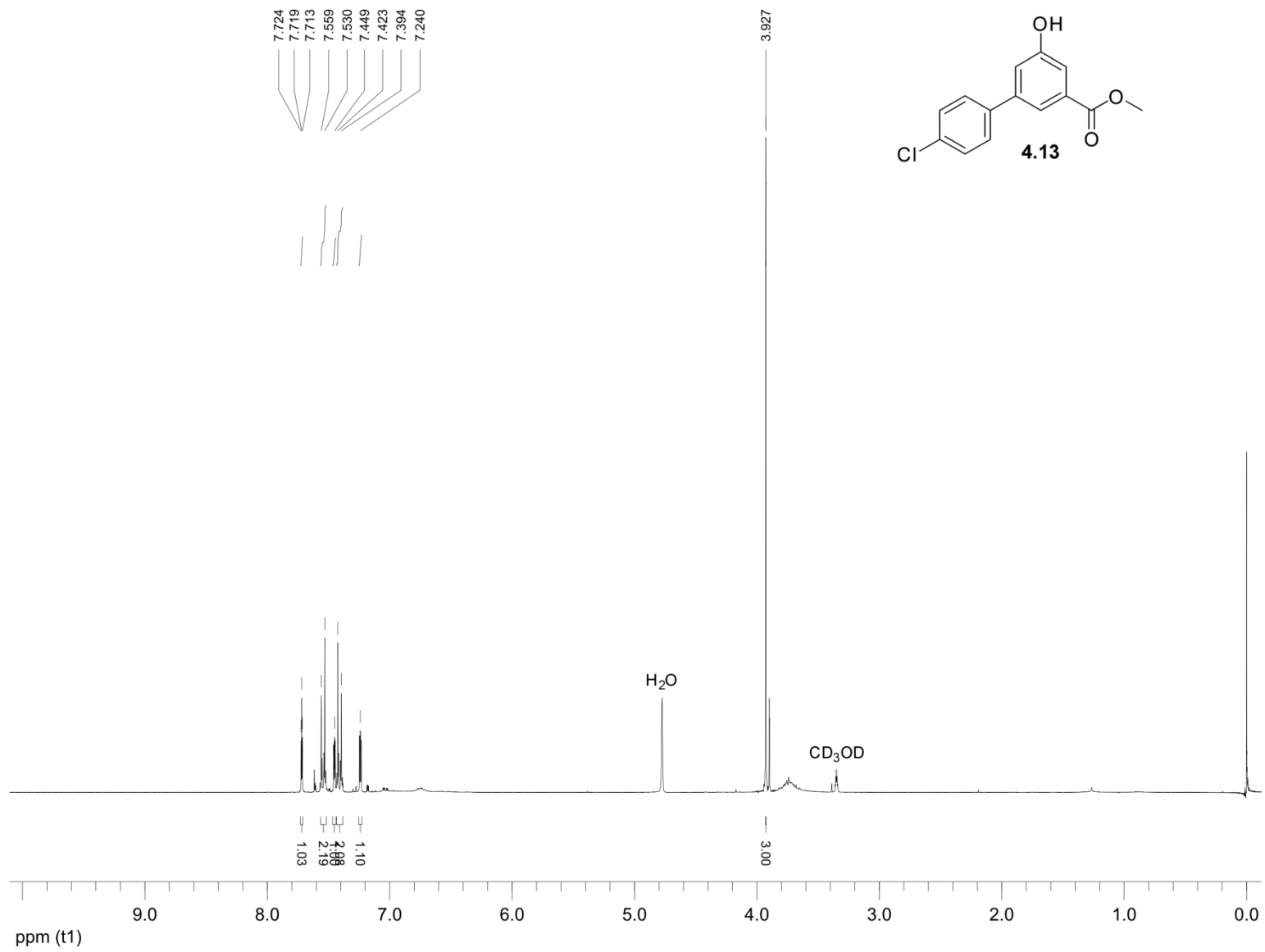




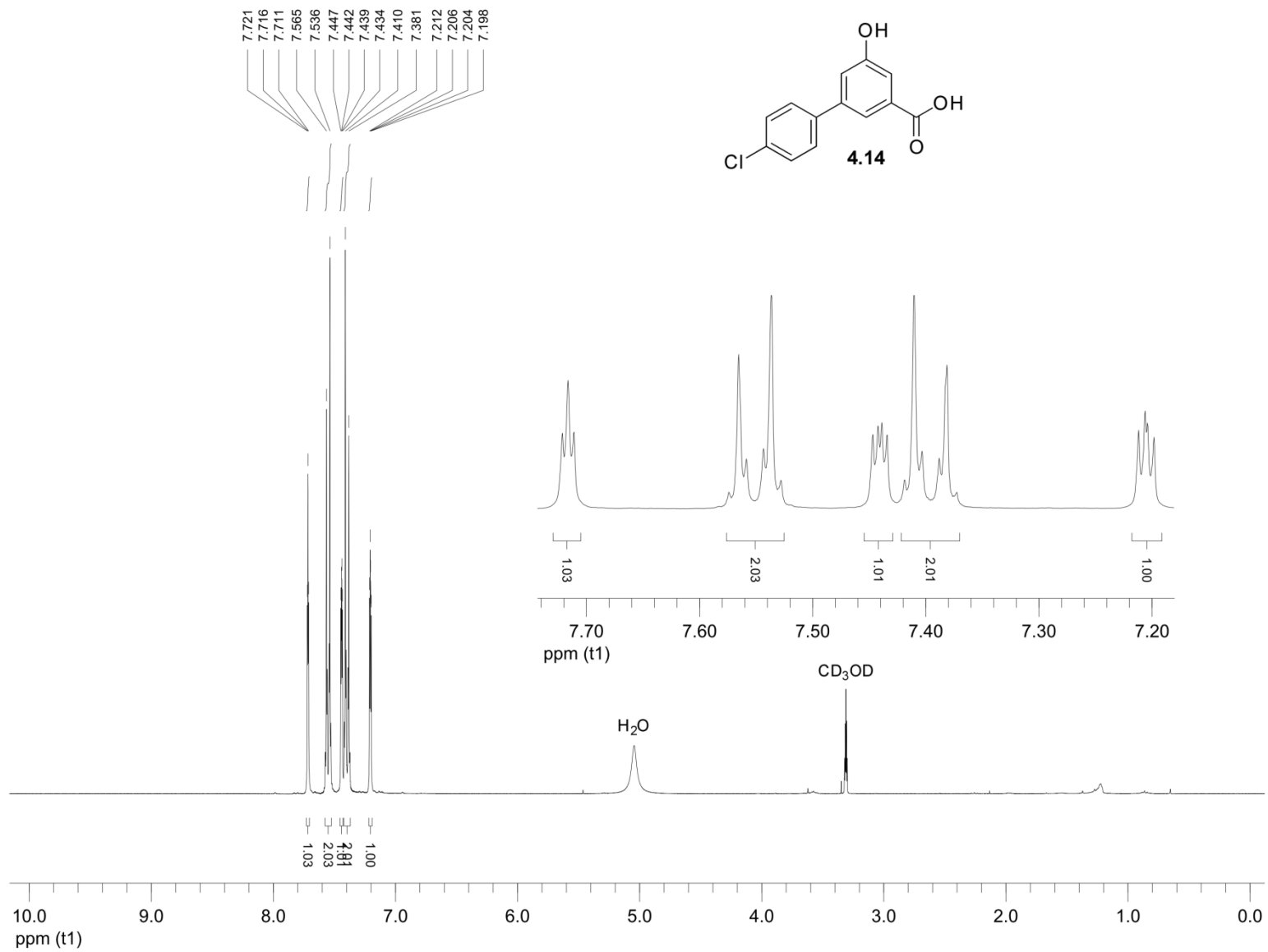




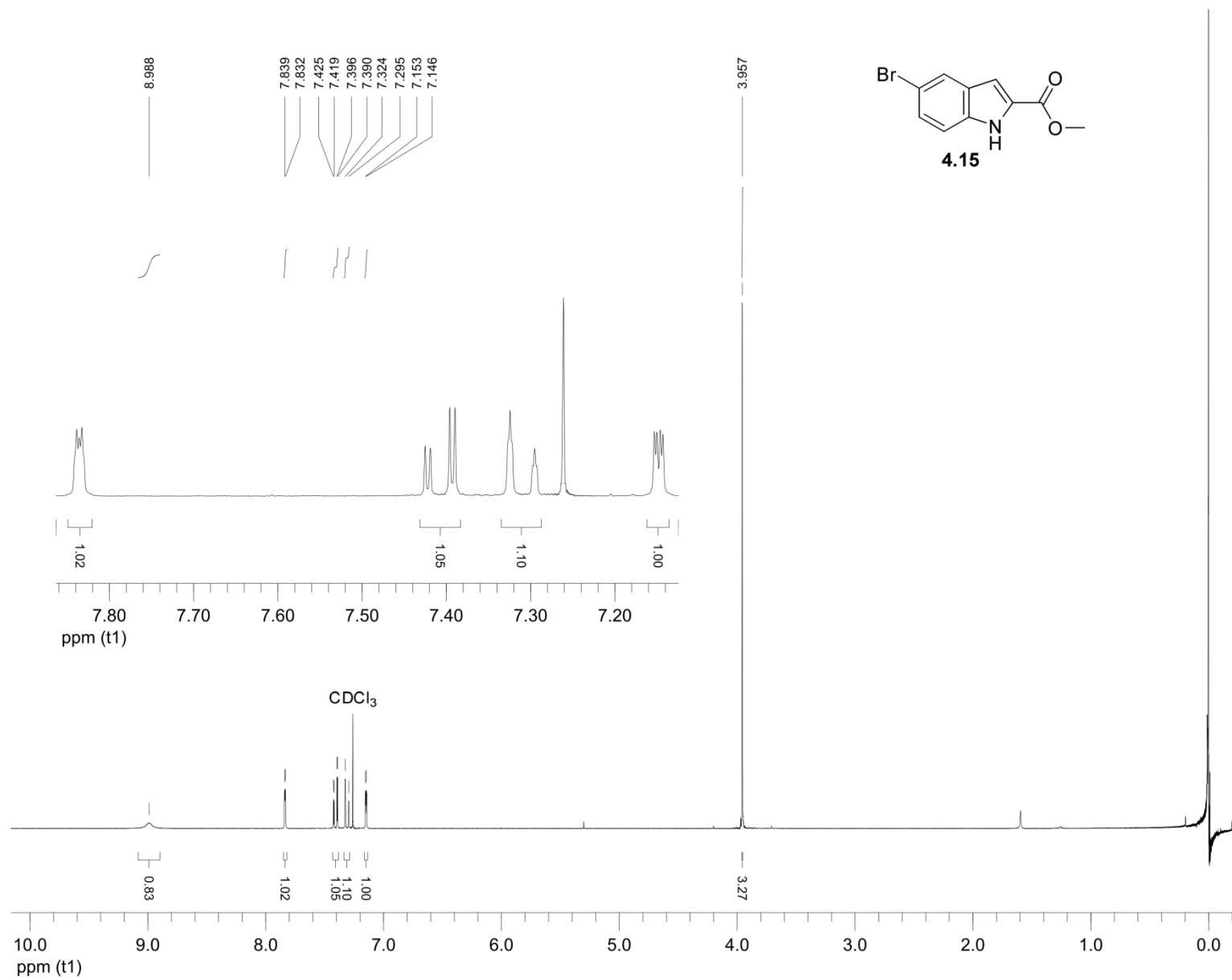
198

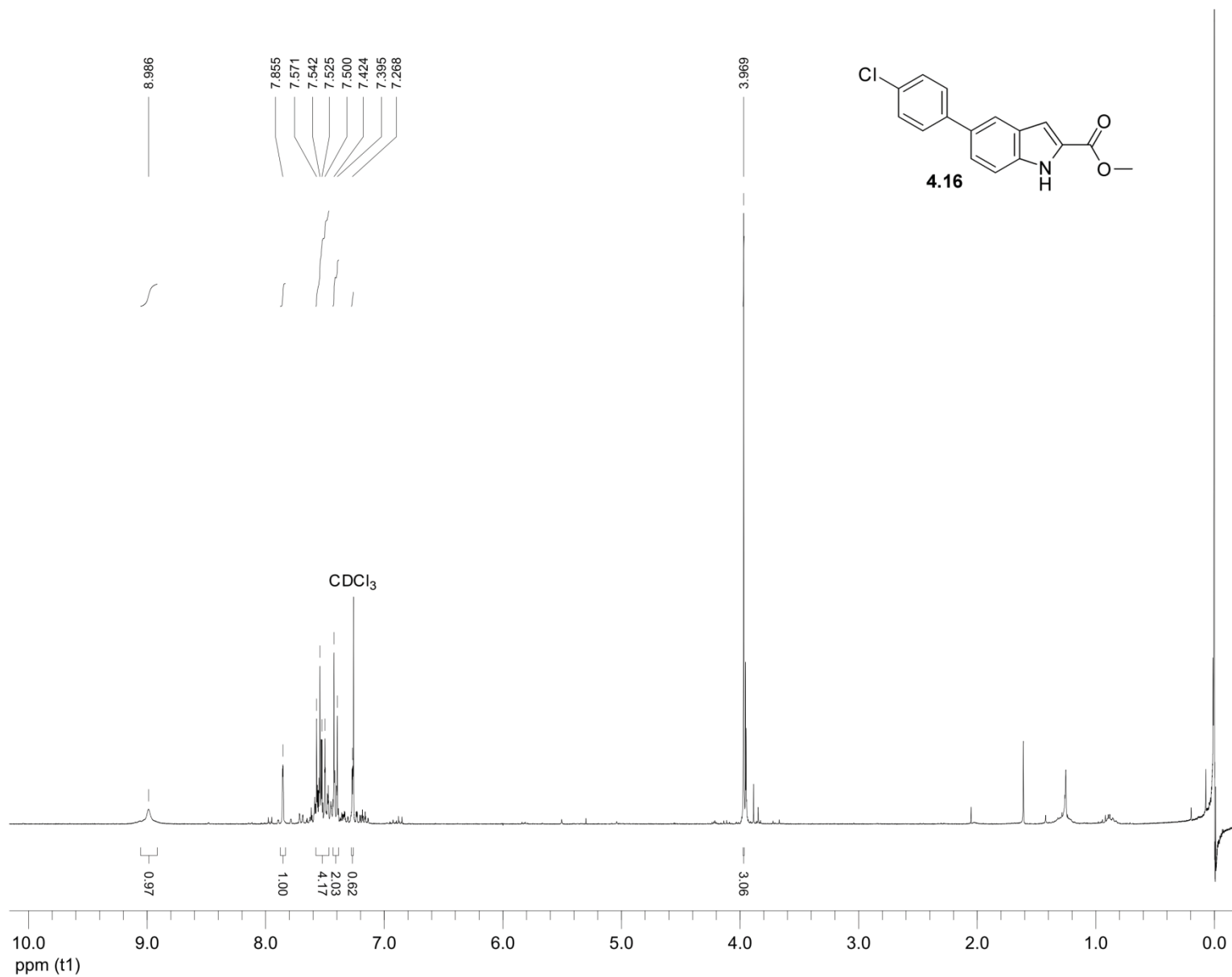


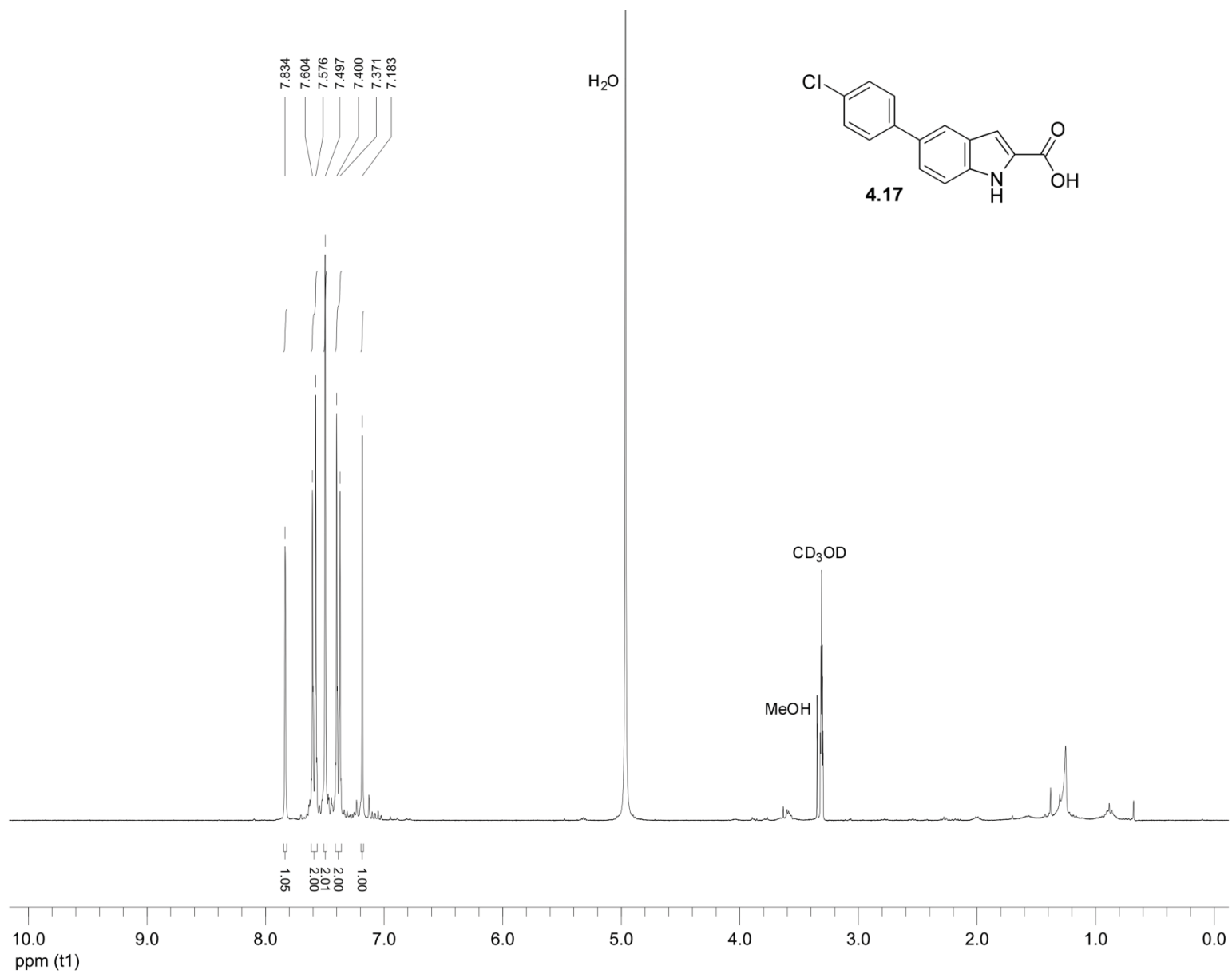
199



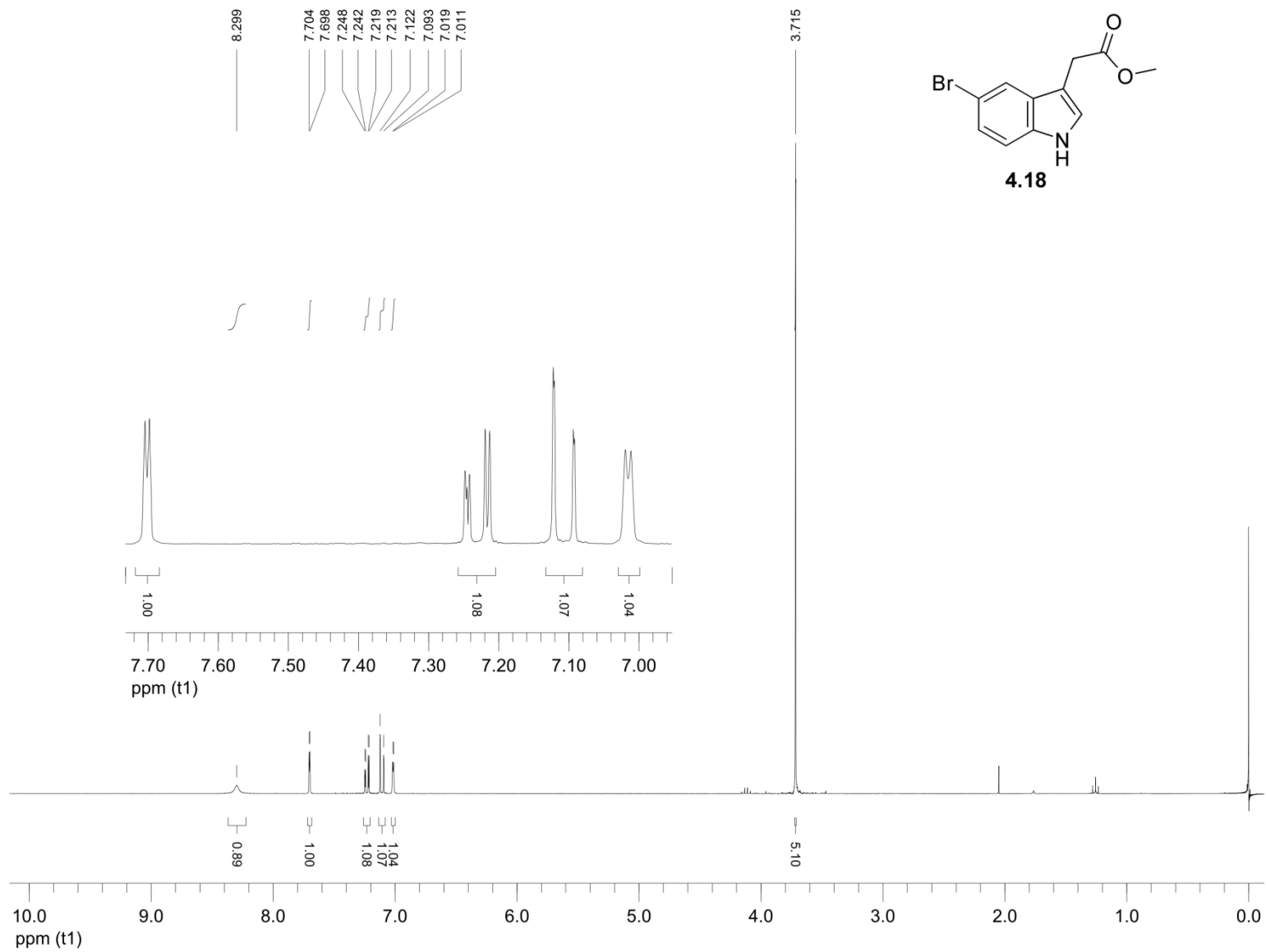
200

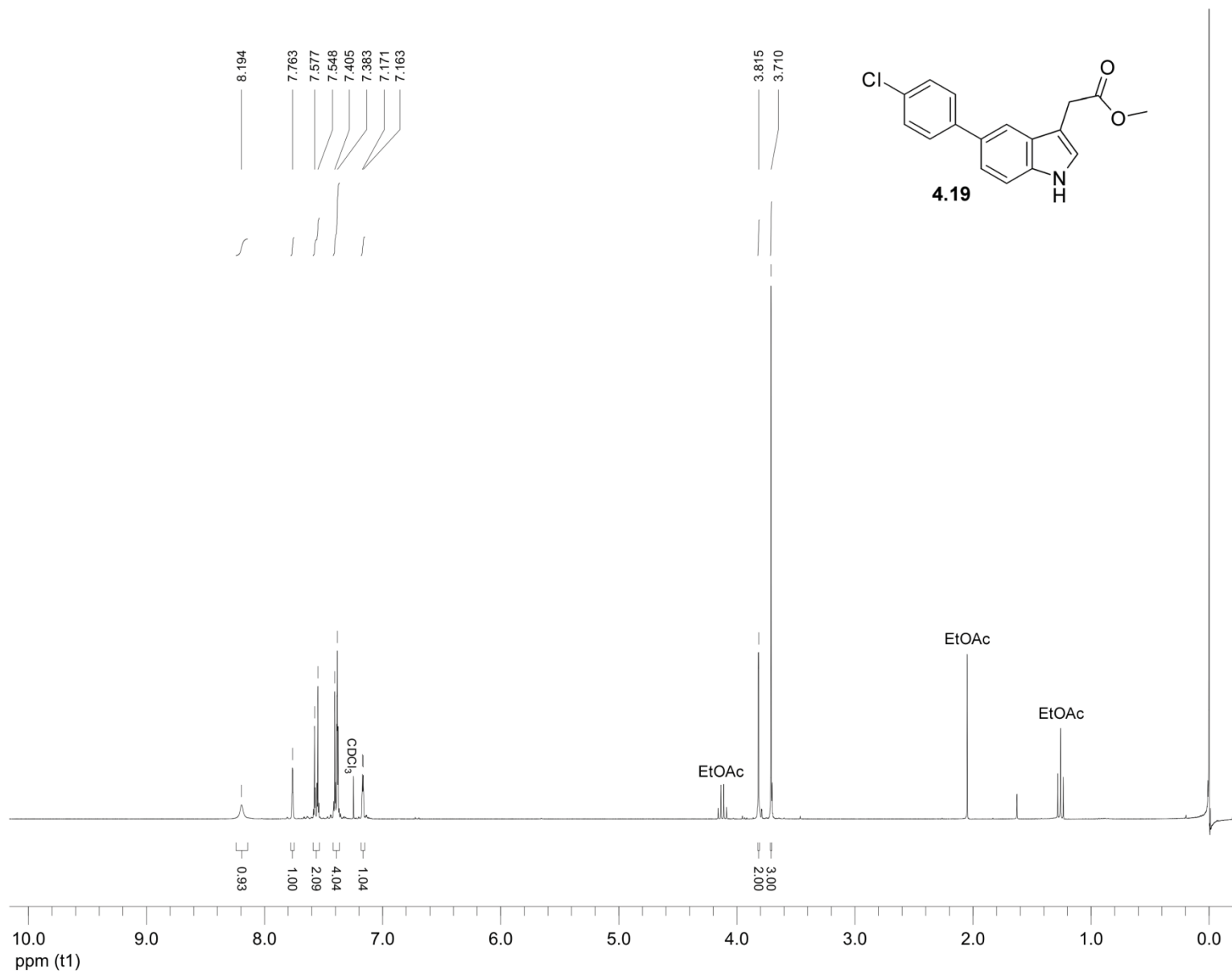


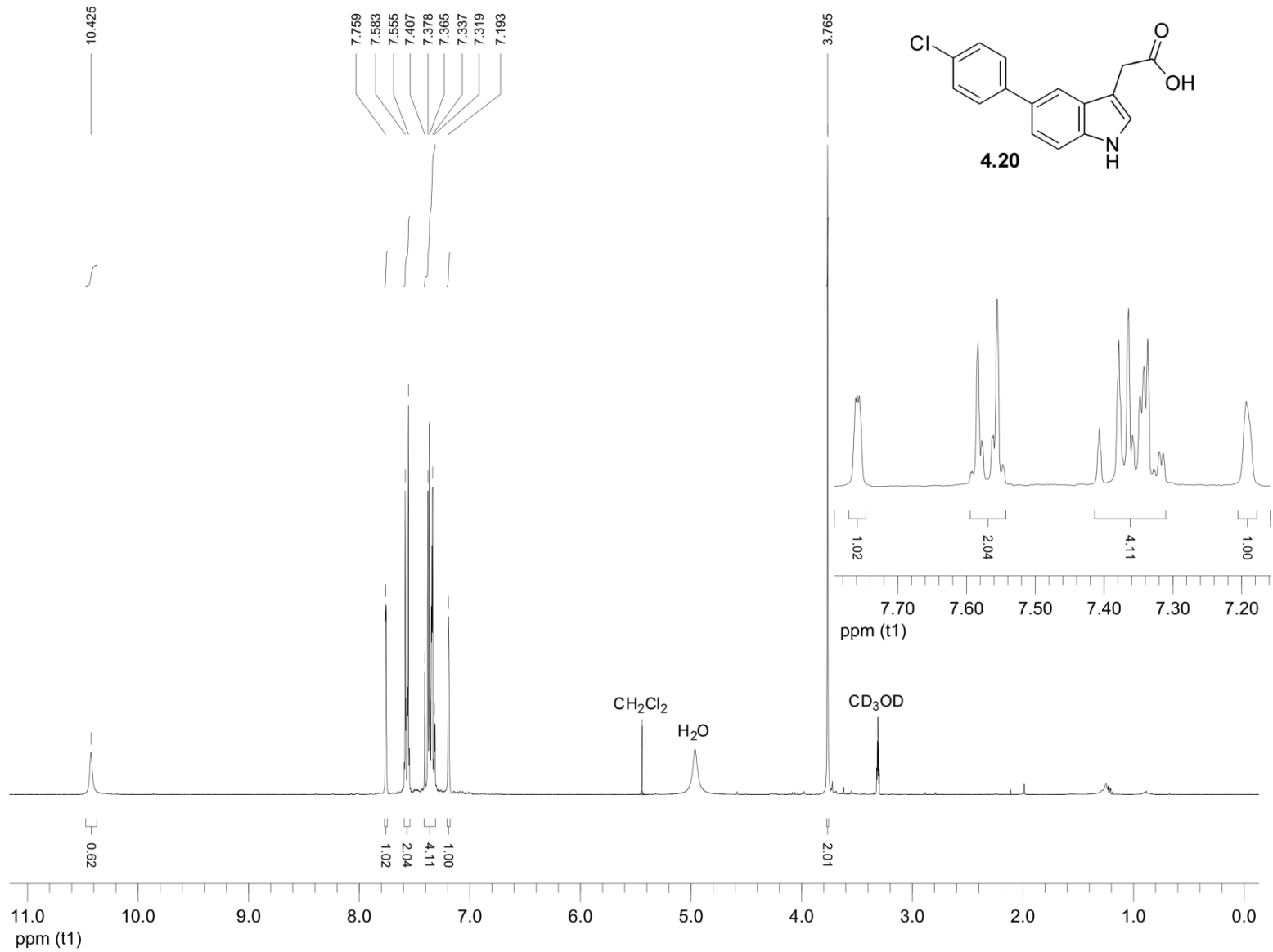


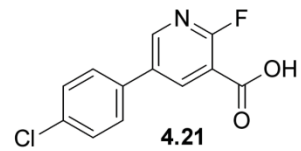
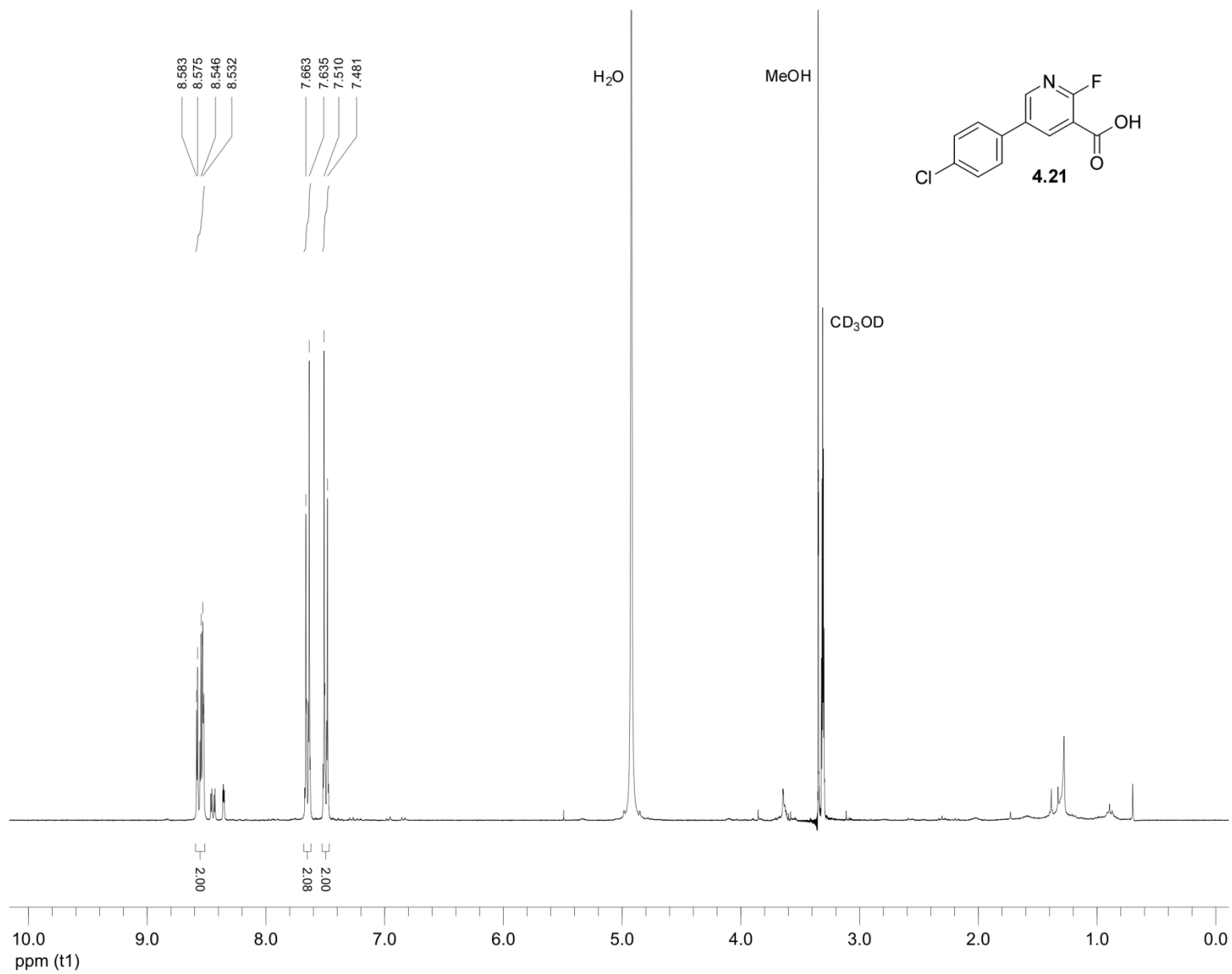


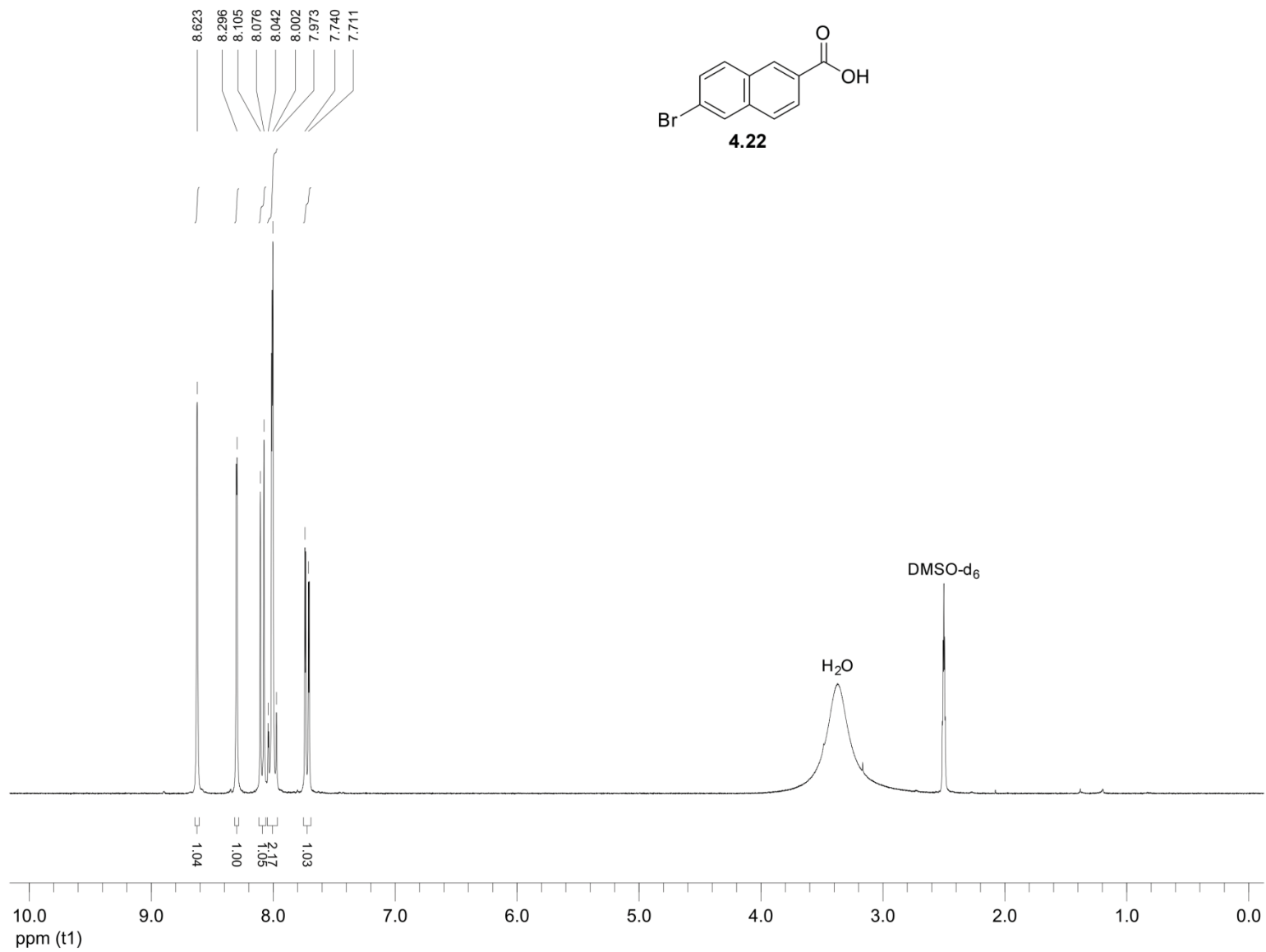
203

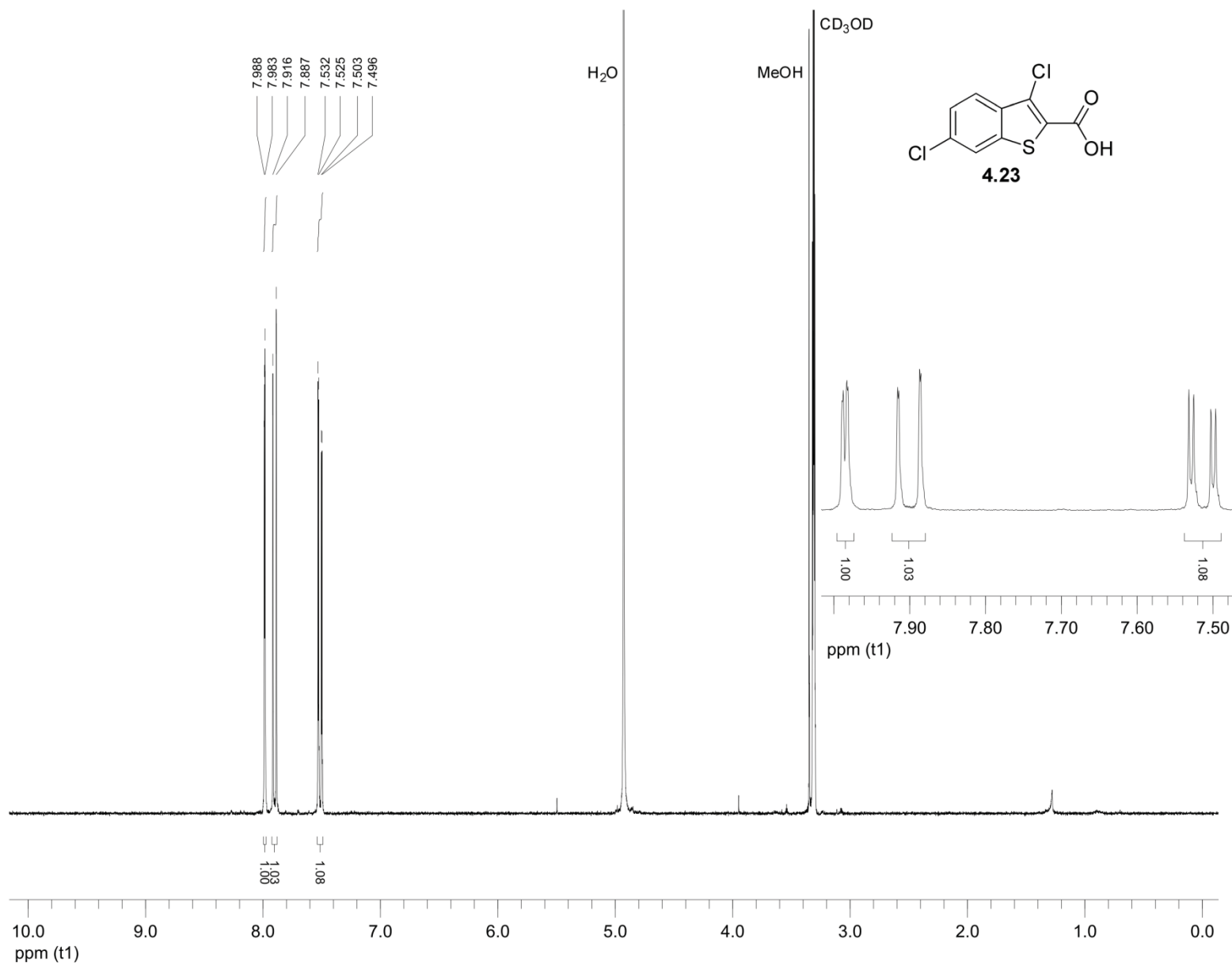


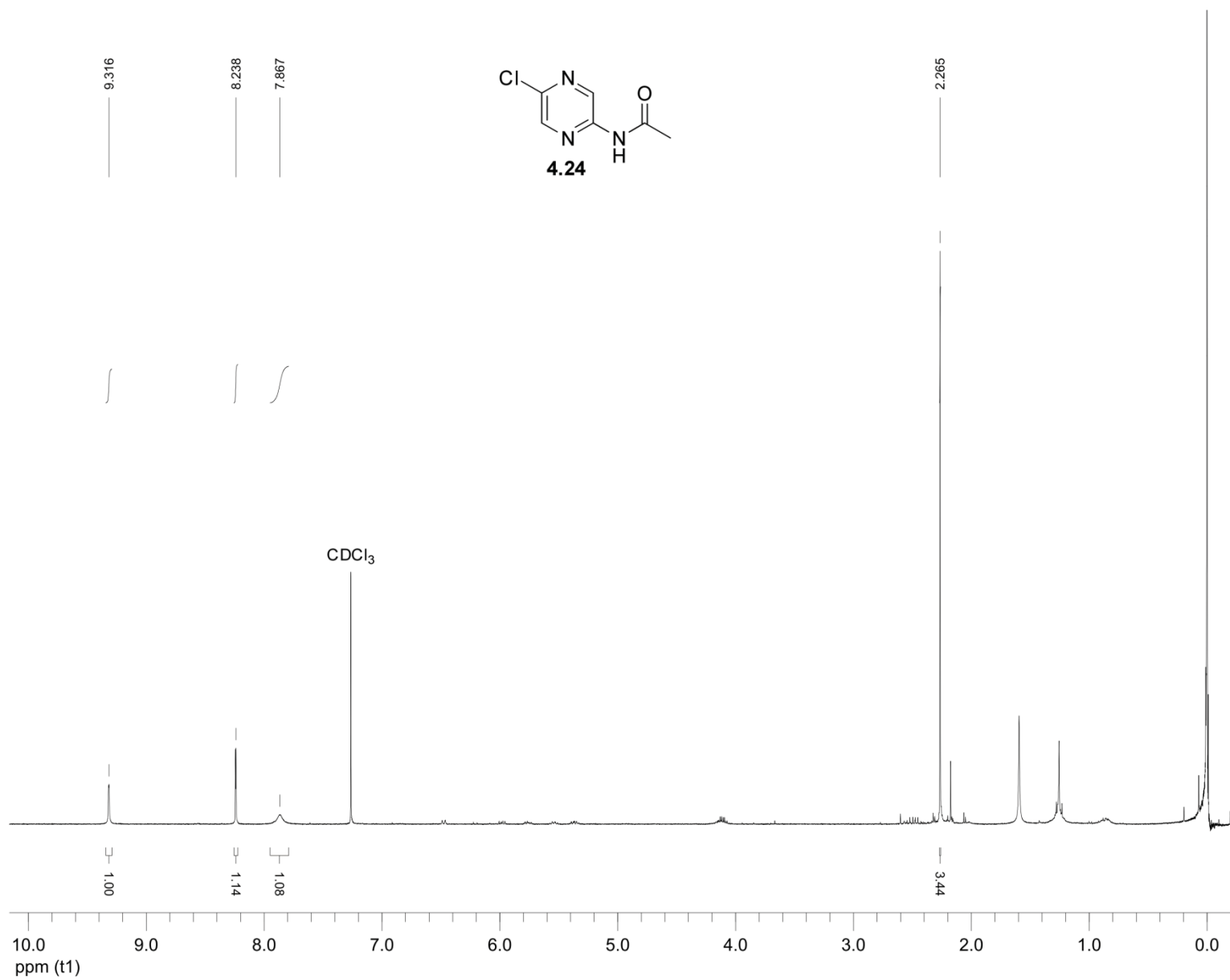




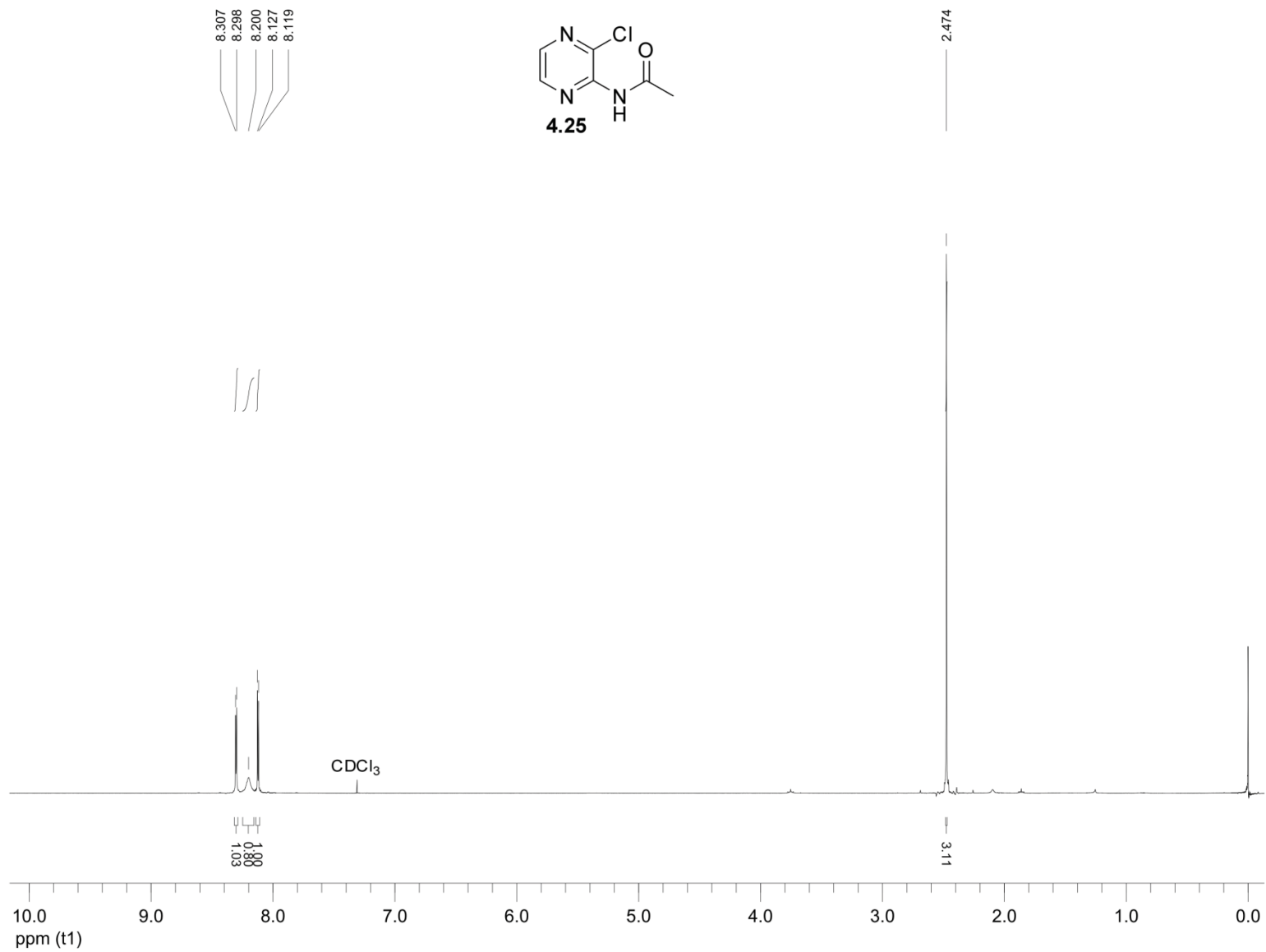








210



Chapter 5: Synthesis and Assembly of Geometrically Defined Building Blocks for Dynamic Covalent Synthesis of Robust Higher Order Organic Frameworks

5.1 Introduction

The development of novel materials with beneficial properties depends on the ability to accurately predict and control structure at the molecular level. The self-assembly of single molecules into larger, more complex structures has been accomplished via supramolecular strategies, such as the formation of non-covalent interactions¹⁶⁵ and metal-organic frameworks (MOFs).¹⁶⁶ However, the resulting structures generally have fragile properties. An advantageous method for the controlled assembly of robust architectures is that of dynamic combinatorial chemistry (DCC).

DCC, the combinatorial chemistry under thermodynamic control, is a tool for the efficient synthesis of libraries of complex structures whose individual properties may be explored through the library's response to the stabilizing influence of external stimuli.¹⁶⁷ A dynamic combinatorial library (DCL) is created by combining building blocks with complementary functionalities that allow them to react with each other either through reversible covalent reactions or specific non-covalent interactions. This initially results in a mixture of interconverting library members, and as the exchange of building blocks between the members continues, the product distribution moves towards equilibrium, which is the thermodynamic minimum of the system.

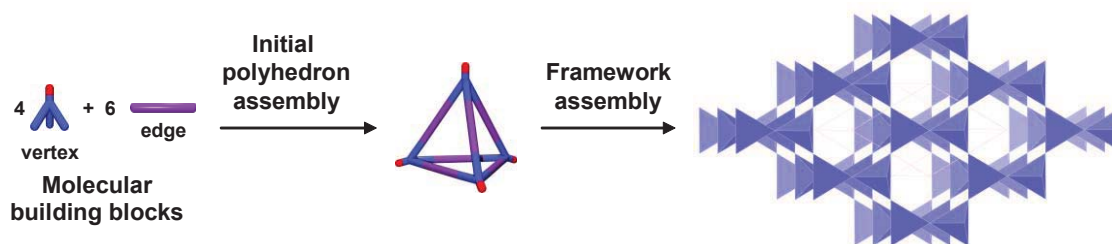
However, the composition of the DCL is not fixed, and the introduction of an external stimulus, such as a change in the surrounding medium or a specific molecular recognition event, can alter the product distribution.¹⁶⁸ For example, if a target molecule

is added to an equilibrium mixture, then the system will re-equilibrate. The stabilization of a particular library member through interactions with the target will shift the equilibrium and result in the increased formation of the stabilized member at the expense of the others in the mixture.

5.2 Assembly Strategy

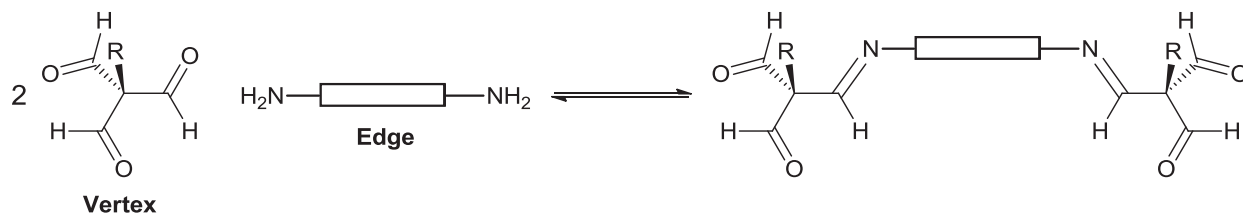
The goal of this project was to exploit DCC to complete the self-assembly of building blocks with defined geometric presentation of functionality into covalently-bonded ordered crystalline structures made of only organic atoms (carbon, hydrogen, nitrogen, and oxygen). Novel advanced materials would be produced for applications such as catalysis and the storage and conversion of energy. This work was done in collaboration with Dr. Benjamin Hay and Dr. Radu Custelcean from the Chemical Separations Group in the Chemical Sciences Division at Oak Ridge National Laboratory.

In our assembly approach, the building blocks, represented as vertex and edge structures (Scheme 5.1), would be linked using DCC, leading to their assembly into polyhedral shapes. Afterwards, the remaining reactive groups at the vertices of the resulting polyhedra would be coupled via DCC again to assemble into defined higher order frameworks with predictable structures. Initial building blocks that self-assemble



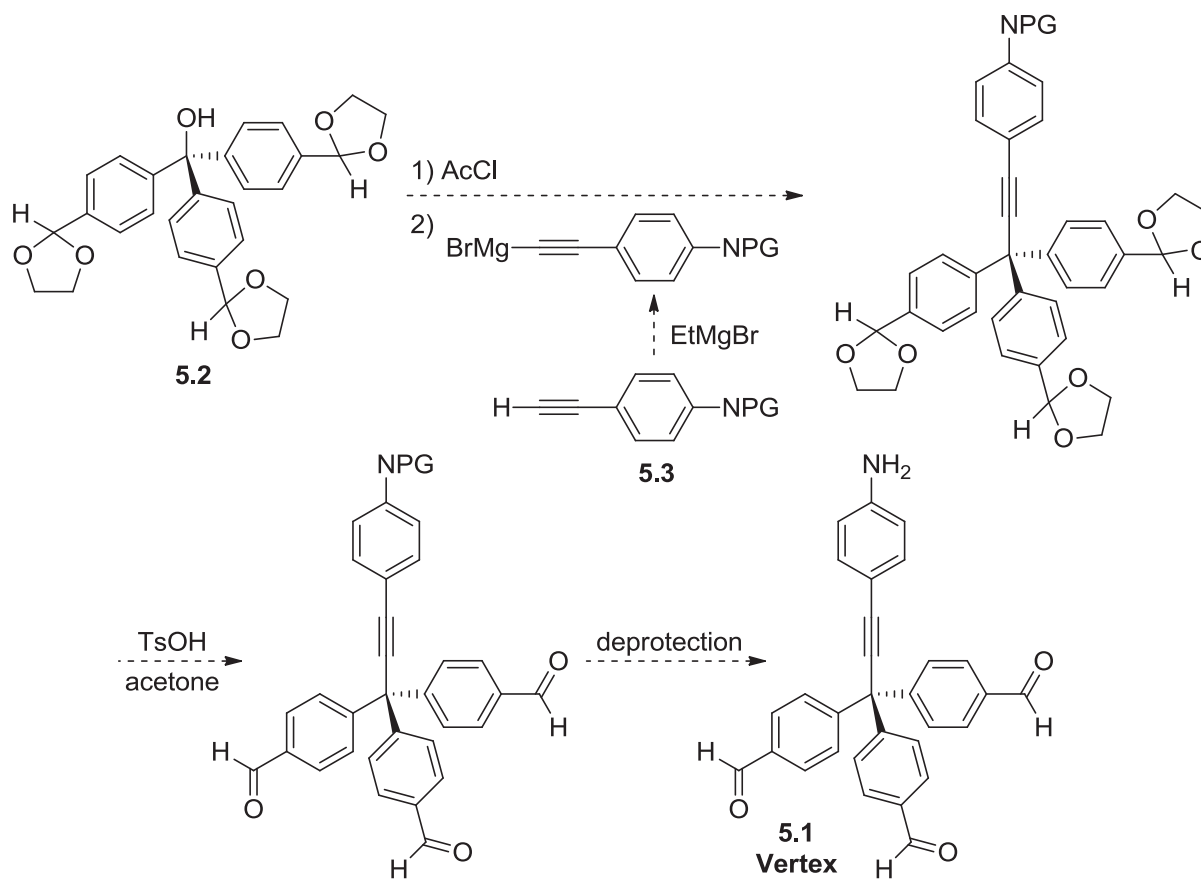
Scheme 5.1. Strategy for the assembly of ordered crystalline organic frameworks using DCC.

into predictable shapes were identified using computational methods developed by Dr. Hay. Our approach involved vertex pieces with three aldehyde groups and edges made of diamines (Scheme 5.2). Reversible imine formation¹⁶⁹ would link the vertex and edge pieces by means of DCC. The linkage of four tetrahedral vertices and six linear edges should form pyramidal assemblies (Scheme 5.1).



Scheme 5.2. Example of reversible imine formation between vertex and edge pieces.

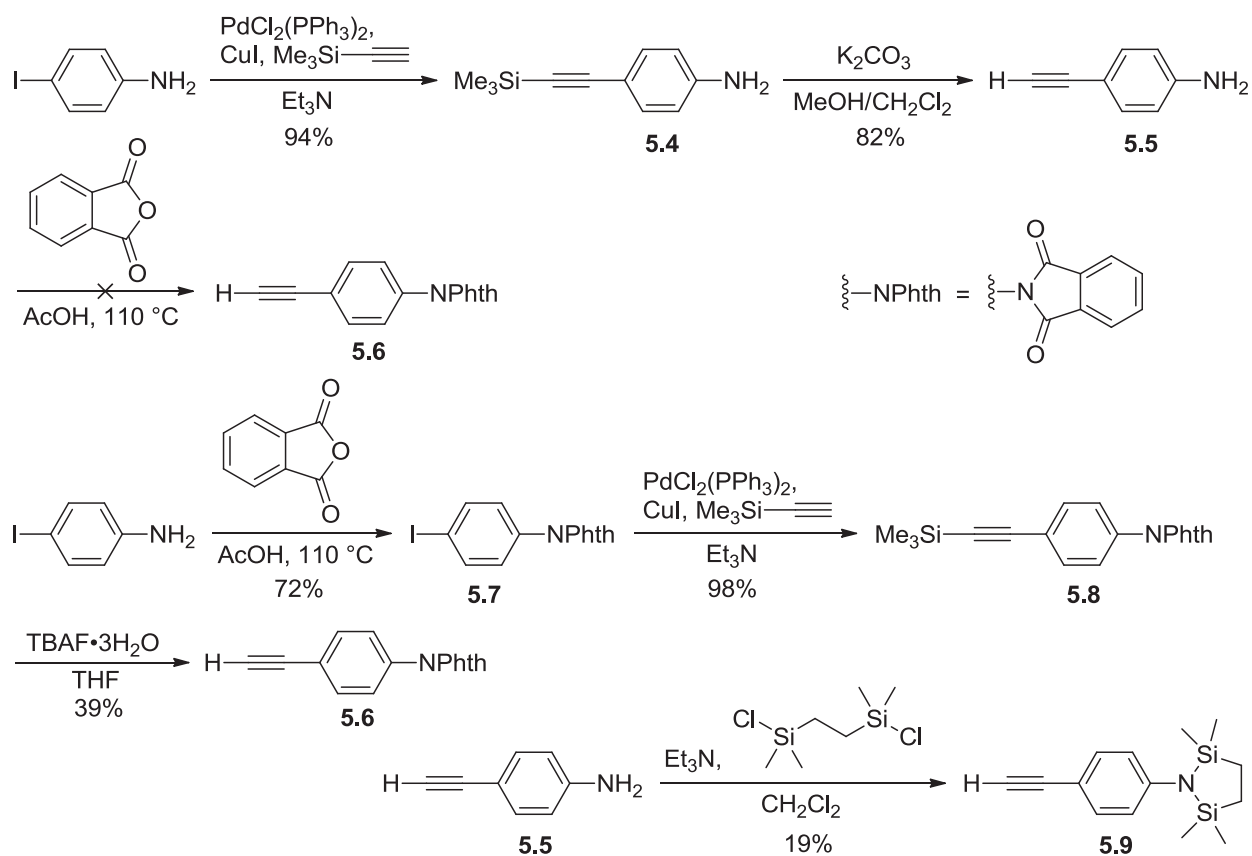
5.3 Synthesis of Building Blocks



Scheme 5.3. General synthetic route to vertex structure 5.1.

For the assembly, tris(benzaldehyde) structure **5.1** was chosen as the vertex (Scheme 5.3). The key building blocks for it are tertiary alcohol **5.2** and ethynylaniline **5.3** with a protecting group (PG) on nitrogen. Chlorination of **5.2**, followed by substitution by the Grignard reagent made from **5.3** and subsequent deprotections of the dioxolanes and amine protecting group would yield vertex **5.1**. The need for this 3-fold symmetry in **5.1** limits the use to certain structures, according to the computational modeling done by Dr. Hay. For example, attaching another benzene group directly to the central carbon in **5.1** would distort from the desired 3-fold symmetry.

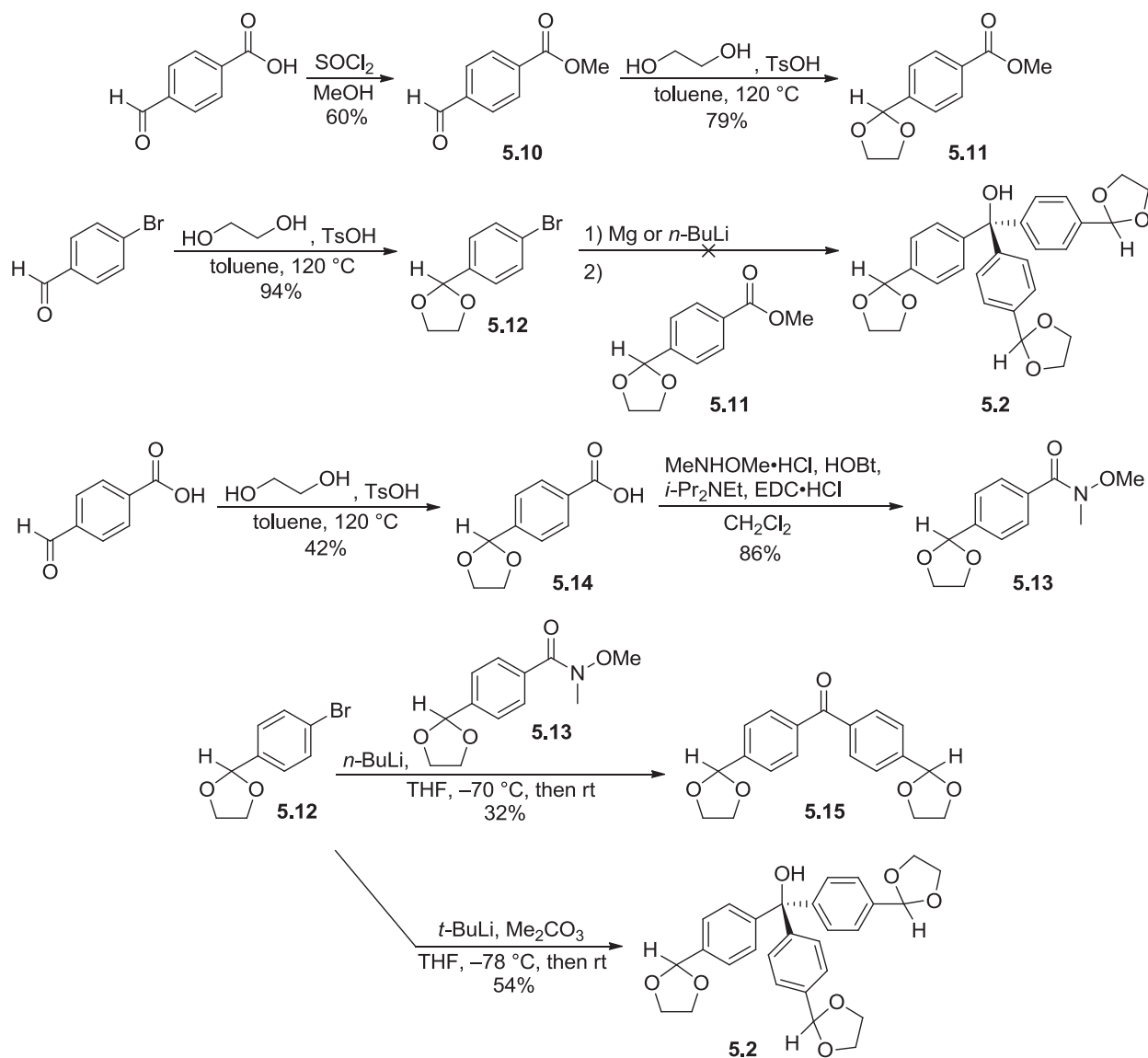
The synthesis of the ethynylaniline component started with a series of known procedures.¹⁷⁰ A Sonogashira reaction between 4-iodoaniline and trimethylsilylacetylene formed adduct **5.4**, which was then deprotected to ethynylaniline **5.5** (Scheme 5.4). Since the ensuing protection of the amine with phthalic anhydride failed to give desired building block **5.6**, the order of reactions in the sequence was changed by performing the amino group protection first. Accordingly, phthalimide **5.7** was generated, followed by Sonogashira coupling to **5.8** and deprotection to successfully obtain **5.6**. However, one concern with the *N*-phthaloyl (NPhth) protecting group was that it is known to be only marginally stable under Grignard reaction conditions.¹⁷¹ Consequently, we explored the 1,1,4,4-tetramethyldisilylazacyclopentane (STABASE) group,¹⁷² which protects primary amines and is stable under basic conditions. *N*-protected ethynylaniline **5.9** was made from **5.5**, although the yield was low (Scheme 5.4).



Scheme 5.4. Synthesis of *N*-protected ethynylanilines **5.6** and **5.9**.

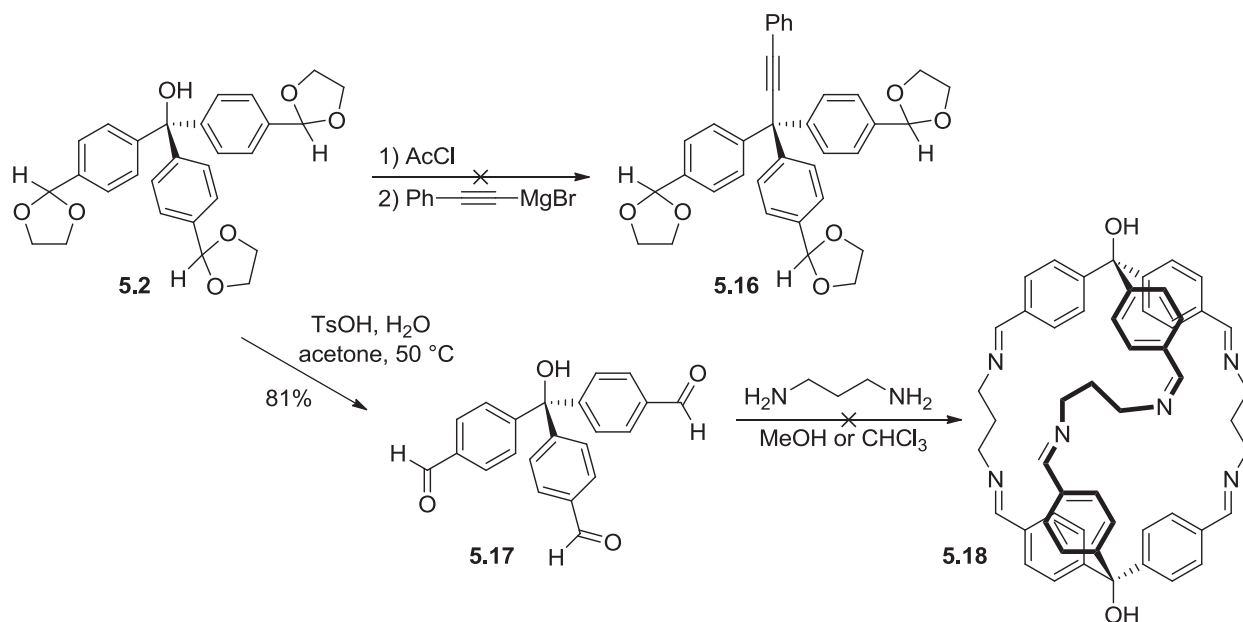
Next, we focused our attention on synthesizing alcohol building block **5.2**. 4-carboxybenzaldehyde was esterified to give **5.10**, followed by aldehyde protection with ethylene glycol to produce dioxolane **5.11** (Scheme 5.5). This was set to react with the Grignard or organolithium reagent from bromide **5.12** to form target **5.2**, but all reaction attempts proved to be ineffective. While the Grignard reagent was never successfully formed, the reaction with *n*-butyllithium always formed an unknown, possibly highly symmetrical product that displayed a large aromatic singlet in the ^1H NMR spectrum. As an alternative, Weinreb amide¹⁷³ **5.13** was prepared from 4-carboxybenzaldehyde via dioxolane intermediate **5.14**. The reaction between **5.13** and the organolithium reagent from **5.12** resulted in ketone **5.15**. This was set to react with a separate

equivalent of the organolithium reagent from **5.12** to lead to **5.2**. At the same time, a further alternative approach from the literature was followed that reacted **5.12** with *n*-butyllithium and dimethyl carbonate to arrive at **5.2**.¹⁷⁴ Using the reported conditions, only a small amount of desired product was isolated, with the major product coming from the nucleophilic addition of the *n*-butyl group from the base. As a consequence, the less nucleophilic *tert*-butyllithium was used instead to finally access alcohol building block **5.2** in > 50% yield. Since a successful route to **5.2** was established, any further reactions with ketone **5.15** were abandoned.



Scheme 5.5. Synthetic approaches to tertiary alcohol building block **5.2**.

Alcohol **5.2** was then tested with the Grignard reagent from phenylacetylene to form vertex structure **5.16**, but no anticipated product was observed (Scheme 5.6). Instead, the observed ^1H NMR spectrum contained aldehyde hydrogen peaks, indicating that the dioxolane groups were deprotected during the reaction. At this point, the deprotection of these groups would not be an issue since they would have to be removed for the imine formation step. However, the spectrum also displayed not



Scheme 5.6. Attempts of vertex and imine bond formations.

enough aromatic hydrogens and a peak corresponding to an acetyl group. This suggested that the alcohol was acylated, and substitution by the phenylacetylene did not take place.

Additionally, **5.2** was deprotected with *para*-toluenesulfonic acid (TsOH) to restore the aldehyde groups. Tris(aldehyde) **5.17** was reacted with 1,3-diaminopropanol in a 2:3 molar ratio in order to form assembled structure **5.18** via reversible imine bond formation. In all attempts, only a highly insoluble precipitate was generated, which indicated the presence of a polymer. The reaction conditions from a series of reports were followed that used imine bond formations between diamines and tetraformylcavitands to assemble various covalent container molecules.¹⁷⁵ These reports described several factors that can influence the assembled product structure. For example, different solvents and different lengths of the diamines have been shown to lead to different assembly products. In order to further examine the possible

formation of **5.18**, all combinations of various solvents and diamines would have to be attempted.

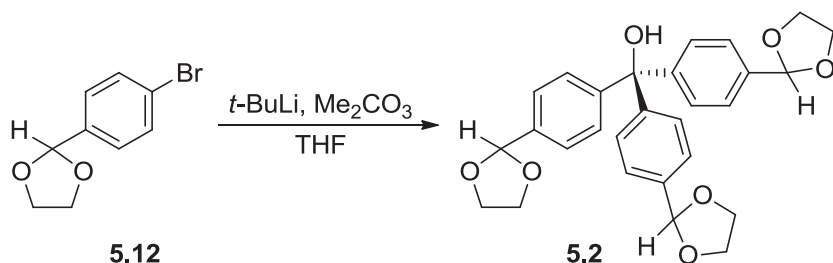
Overall, while the intended assembly via imine formation did not succeed so far, a variety of building blocks for the vertex structure has been synthesized. Most of these building blocks could be modified further if needed. Some additional structural adjustments may be required to form a vertex with the ideal geometry to generate pyramidal assemblies under the right conditions.

5.4 Experimental

Titration of *tert*-butyllithium with *N*-benzylbenzamide

Under argon, anhydrous tetrahydrofuran (5 mL) was added to *N*-benzylbenzamide (0.11 g, 0.50 mmol) via syringe. The solution was allowed to stir and cooled to $-40\text{ }^{\circ}\text{C}$. A solution of *tert*-butyllithium in pentane was added via syringe dropwise until the mixture became consistently dark blue. The volume of *tert*-butyllithium solution added (0.45 mL) and the number of moles of titrating reagent were used to calculate the *tert*-butyllithium solution concentration.

tris[4-(1,3-dioxolan-2-yl)phenyl]methanol (**5.2**)



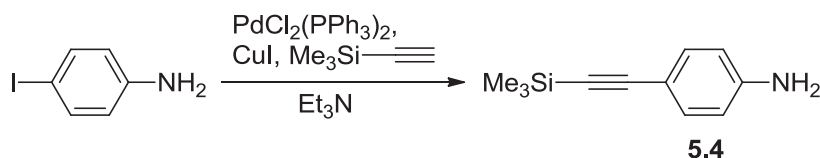
Under argon, anhydrous tetrahydrofuran (25 mL) was added to **5.12** via syringe. The solution was cooled to $-78\text{ }^{\circ}\text{C}$, and a solution of *tert*-butyllithium in pentane (3.97 mL, 4.37 mmol, 1.10 M) was added via syringe. The mixture was stirred and allowed to warm up to $0\text{ }^{\circ}\text{C}$ for 1 h, followed by cooling to $-78\text{ }^{\circ}\text{C}$ again. Dimethyl carbonate (0.11 mL, 1.25 mmol) in anhydrous tetrahydrofuran (5 mL) was added via syringe, and the reaction mixture was stirred at rt overnight, followed by extraction with ethyl acetate ($2 \times 30\text{ mL}$) from saturated aqueous ammonium chloride (30 mL). The combined organic layers were dried over magnesium sulfate, filtered, and concentrated. Column

chromatography over silica gel with gradient elution from 25 to 100% ethyl acetate/hexanes gave the product as a white solid (0.32 g, 54%).

Characterizations matched those reported in the literature.¹⁷⁴

¹H NMR (300 MHz, CDCl₃) δ 7.39 (d, *J* = 8.0 Hz, 6H), 7.27 (d, *J* = 8.0 Hz, 6H), 5.78 (s, 3H), 4.16–3.97 (m, 12H), 2.93 (s, 1H). ¹³C NMR (75 MHz, CDCl₃) δ 147.56, 136.87, 127.98, 126.09, 103.45, 81.60, 65.32.

4-trimethylsilylethynylaniline (5.4)

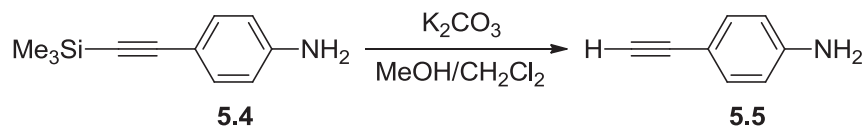


Under argon, triethylamine (7 mL) was added via syringe to a flask containing 4-iodoaniline (0.20 g, 0.90 mmol), bis(triphenylphosphine)palladium(II) chloride (0.013 g, 0.018 mmol), and copper iodide (0.010 g, 0.054 mmol). Trimethylsilylacetylene (0.20 mL, 1.35 mmol) was then added via syringe, and the reaction mixture was stirred at rt overnight. After rotary evaporation, column chromatography over silica gel with gradient elution from 10 to 40% ethyl acetate/hexanes gave the product as a light brown solid (0.16 g, 94%).

Characterizations matched those reported in the literature.^{170,176}

¹H NMR (300 MHz, CDCl₃) δ 7.28 (d, *J* = 8.6 Hz, 2H), 6.57 (d, *J* = 8.6 Hz, 2H), 3.79 (bs, 2H), 0.24 (s, 9H).

4-ethynylaniline (5.5)

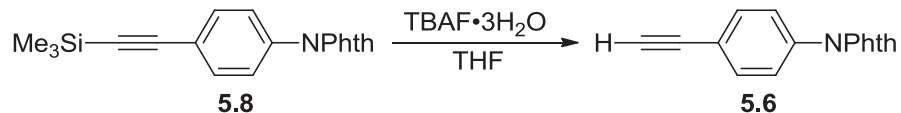


Potassium carbonate (1.49 g, 10.80 mmol) and methanol (40 mL) were added to a solution of **5.4** (1.02 g, 5.40 mmol) in dichloromethane (20 mL), and the reaction mixture was stirred at rt overnight. The crude product was then filtered and washed with dichloromethane, and the filtrate was concentrated. A 30% ethyl acetate/hexanes solution (50 mL) was added to the residue, and the mixture was filtered through a pad of silica gel and washed with 30% ethyl acetate/hexanes. The filtrate was concentrated to obtain the product as a yellow solid (0.52 g, 82%).

Characterizations matched those reported in the literature.^{170b,176h,177}

1H NMR (300 MHz, $CDCl_3$) δ 7.30 (d, $J = 8.6$ Hz, 2H), 6.59 (d, $J = 8.6$ Hz, 2H), 3.81 (bs, 2H), 2.96 (s, 1H).

N-(4-ethynylphenyl)phthalimide (5.6)

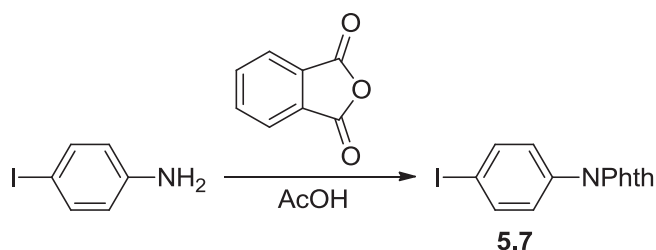


A solution of tetrabutylammonium fluoride trihydrate (0.18 g, 0.57 mmol) in tetrahydrofuran (3 mL) was added to a solution of **5.8** in tetrahydrofuran (7 mL). After stirring at rt for 3 h, the reaction mixture was extracted with dichloromethane (2×20 mL) from water (20 mL). The combined organic layers were dried over magnesium sulfate, filtered, and concentrated. Column chromatography over silica gel with gradient

elution from 10 to 40% ethyl acetate/hexanes provided the product as a white solid (0.045 g, 39%).

^1H NMR (300 MHz, CDCl_3) δ 7.95 (dd, $J = 5.5, 3.0$ Hz, 2H), 7.80 (dd, $J = 5.5, 3.0$ Hz, 2H), 7.62 (d, $J = 8.7$ Hz, 2H), 7.45 (d, $J = 8.7$ Hz, 2H), 3.13 (s, 1H).

***N*-[4-iodophenyl]phthalimide (5.7)**

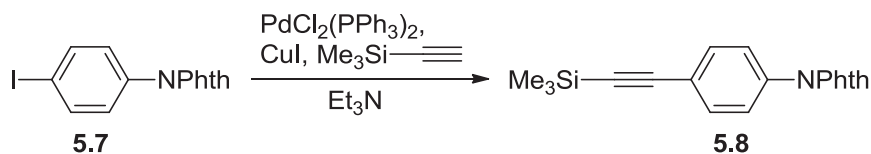


Phthalic anhydride (0.41 g, 2.78 mmol) was added to a solution of 4-iodoaniline (0.62 g, 2.78 mmol) in glacial acetic acid (30 mL), and the reaction mixture was stirred at 110 °C for 6 h. Afterwards, water (50 mL) was added, and the resulting precipitate was filtered, washed with water, and collected as a light purple solid (0.70 g, 72%).

Characterizations matched those reported in the literature.¹⁷⁸

^1H NMR (300 MHz, CDCl_3) δ 7.96 (dd, $J = 5.4, 3.1$ Hz, 2H), 7.86–7.78 (m, 4H), 7.23 (d, $J = 8.7$ Hz, 2H).

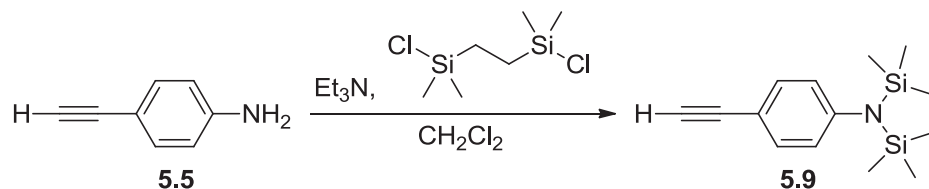
***N*-[4-(trimethylsilylethynyl)phenyl]phthalimide (5.8)**



This compound was prepared in a similar manner to **5.4** from **5.7** (0.70 g, 2.00 mmol), bis(triphenylphosphine)palladium(II) chloride (0.028 g, 0.040 mmol), copper iodide (0.023 g, 0.12 mmol), trimethylsilylacetylene (0.44 mL, 3.01 mmol), and triethylamine (15 mL). Column chromatography over silica gel with gradient elution from 10 to 40% ethyl acetate/hexanes gave the product as a cream-colored solid (0.63 g, 98%).

^1H NMR (300 MHz, CDCl_3) δ 7.95 (dd, $J = 5.6, 3.0$ Hz, 2H), 7.80 (dd, $J = 5.5, 3.0$ Hz, 2H), 7.59 (d, $J = 8.8$ Hz, 2H), 7.43 (d, $J = 8.8$ Hz, 2H), 0.26 (s, 9H). ^{13}C NMR (75 MHz, CDCl_3) δ 166.81, 134.44, 132.47, 131.51, 125.92, 123.70, 122.70, 104.16, 95.27, -0.13 .

1-(4-ethynylphenyl)-2,2,5,5-tetramethyl-1,2,5-azadisilolidine (**5.9**)

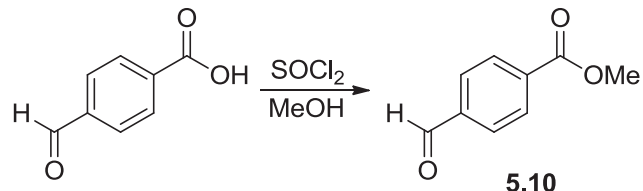


A solution of 1,2-bis(chlorodimethylsilyl)ethane (0.21 g, 0.94 mmol) in dichloromethane (3 mL) was added dropwise to a solution of **5.5** (0.11 g, 0.94 mmol) and triethylamine (0.26 mL, 1.87 mmol) in dichloromethane (7 mL). After stirring at rt for 3 h, the reaction mixture was filtered and washed with hexanes, and the filtrate was concentrated. Column chromatography over basic alumina with gradient elution from 0 to 20% dichloromethane/hexanes gave the product (0.046 g, 19%).

Characterizations matched those reported in the literature.¹⁷⁹

^1H NMR (300 MHz, CDCl_3) δ 7.33 (d, $J = 8.7$ Hz, 2H), 6.82 (d, $J = 8.7$ Hz, 2H), 3.00 (s, 1H), 0.86 (s, 4H), 0.25 (s, 12H).

methyl 4-formylbenzoate (**5.10**)

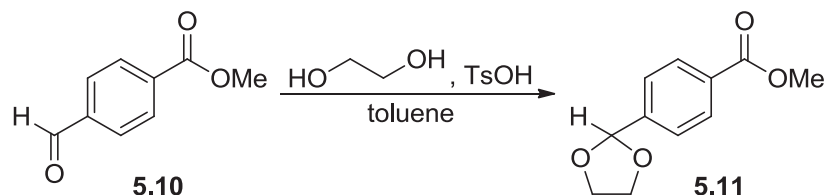


Thionyl chloride (1.07 mL, 14.70 mmol) was added dropwise to a solution of 4-carboxybenzaldehyde (2.05 g, 13.37 mmol) in methanol (50 mL) at 0 °C. The reaction mixture was stirred at rt overnight and then concentrated. The residue was extracted with dichloromethane (2 × 40 mL) from water (40 mL). The combined organic layers were dried over magnesium sulfate, filtered, and concentrated to give the product as a light yellow solid (1.32 g, 60%).

Characterizations matched those reported in the literature.¹⁸⁰

¹H NMR (300 MHz, CDCl₃) δ 10.11 (s, 1H), 8.20 (d, *J* = 8.1 Hz, 2H), 7.96 (d, *J* = 8.1 Hz, 2H), 3.97 (s, 3H).

methyl 4-(1,3-dioxolan-2-yl)benzoate (**5.11**)



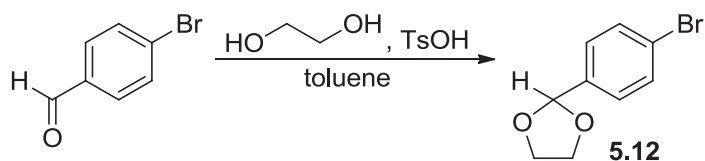
Ethylene glycol (2.12 mL, 38.04 mmol) and a catalytic amount of *para*-toluenesulfonic acid monohydrate (0.0058 g, 0.030 mmol) were added to a solution of **5.10** (1.40 g, 7.61 mmol) in toluene (50 mL). The reaction mixture was stirred at 120 °C under a Dean–Stark apparatus for 2 days, after which it was extracted with dichloromethane (2 × 40

mL) from water (40 mL). The combined organic layers were dried over magnesium sulfate, filtered, and concentrated. Column chromatography over silica gel with gradient elution from 10 to 25% ethyl acetate/hexanes provided the product as a white solid (1.25 g, 79%).

Characterizations matched those reported in the literature.¹⁸¹

¹H NMR (300 MHz, CDCl₃) δ 8.06 (d, *J* = 8.1 Hz, 2H), 7.55 (d, *J* = 8.1 Hz, 2H), 5.86 (s, 1H), 4.16–4.02 (m, 4H), 3.92 (s, 3H).

2-(4-bromophenyl)-1,3-dioxolane (5.12)

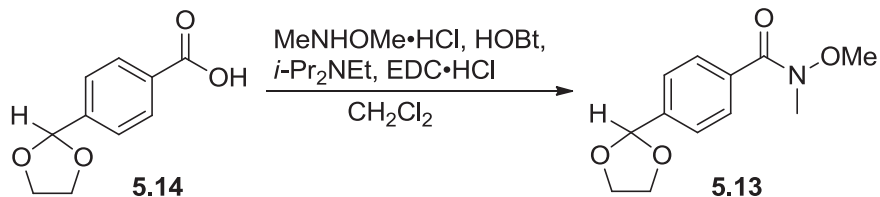


This compound was prepared in a similar manner as **5.11** from 4-bromobenzaldehyde (6.07 g, 32.16 mmol). Column chromatography over silica gel with gradient elution from 3 to 20% ethyl acetate/hexanes gave the product as a colorless liquid (6.95 g, 94%).

Characterizations matched those reported in the literature.¹⁸²

¹H NMR (300 MHz, CDCl₃) δ 7.51 (d, *J* = 8.4 Hz, 2H), 7.35 (d, *J* = 8.4 Hz, 2H), 5.77 (s, 1H), 4.15–4.00 (m, 4H).

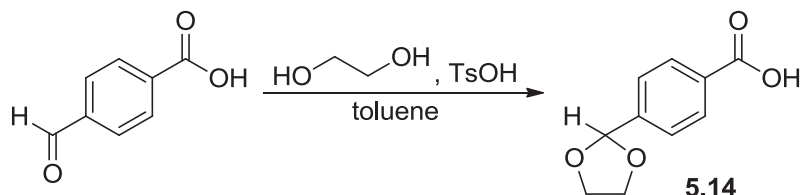
4-(1,3-dioxolan-2-yl)-*N*-methoxy-*N*-methylbenzamide (5.13)



N,*O*-dimethylhydroxylamine hydrochloride (0.44 g, 4.38 mmol), 1-hydroxybenzotriazole (0.46 g, 3.37 mmol), and *N,N*-diisopropylethylamine (0.61 mL, 3.71 mmol) were added to a solution of **5.14** (0.65 g, 3.37 mmol) in dichloromethane (35 mL). The mixture was cooled to 0 °C, and 1-(3-dimethylaminopropyl)-3-ethylcarbodiimide hydrochloride (0.65 g, 3.37 mmol) was added. The reaction mixture was stirred at rt overnight and then extracted with dichloromethane (2 × 30 mL) from water (30 mL). The combined organic layers were dried over magnesium sulfate, filtered, and concentrated. Column chromatography over silica gel with gradient elution from 25 to 75% ethyl acetate/hexanes yielded the Weinreb amide as a colorless liquid (0.68 g, 86%).

¹H NMR (300 MHz, CDCl₃) δ 7.70 (d, *J* = 8.2 Hz, 2H), 7.52 (d, *J* = 8.2 Hz, 2H), 5.83 (s, 1H), 4.18–3.97 (m, 4H), 3.53 (s, 1H), 3.35 (s, 1H). ¹³C NMR (75 MHz, CDCl₃) δ 169.41, 167.25, 140.25, 134.79, 128.25, 126.10, 103.11, 65.33, 61.08, 33.65.

4-(1,3-dioxolan-2-yl)benzoic acid (5.14)



This compound was prepared in a similar manner as **5.11** from 4-carboxybenzaldehyde (0.23 g, 1.47 mmol). Column chromatography over silica gel with gradient elution from 25 to 75% ethyl acetate/hexanes gave the product as a white solid (0.12 g, 42%).

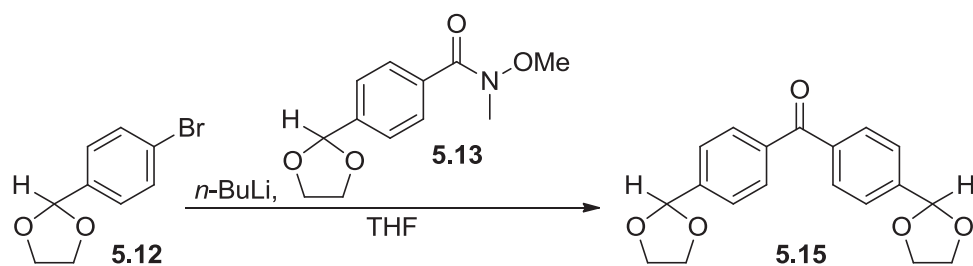
Characterizations matched those reported in the literature.¹⁸³

¹H NMR (300 MHz, CDCl₃) δ 8.14 (d, *J* = 8.4 Hz, 2H), 7.60 (d, *J* = 8.4 Hz, 2H), 5.89 (s, 1H), 4.17–4.03 (m, 4H).

Titration of *n*-butyllithium with 1,3-diphenylacetone *p*-tosylhydrazone

Under argon, anhydrous tetrahydrofuran (10 mL) was added to 1,3-diphenylacetone *p*-tosylhydrazone (0.18 g, 0.47 mmol) via syringe. The solution was allowed to stir and cooled to 0 °C. A solution of *n*-butyllithium in hexanes was added via syringe dropwise until the mixture became consistently dark yellow. The volume of *n*-butyllithium solution added (0.50 mL) and the number of moles of titrating reagent were used to calculate the *n*-butyllithium solution concentration.

bis[4-(1,3-dioxolan-2-yl)phenyl]methanone (**5.15**)

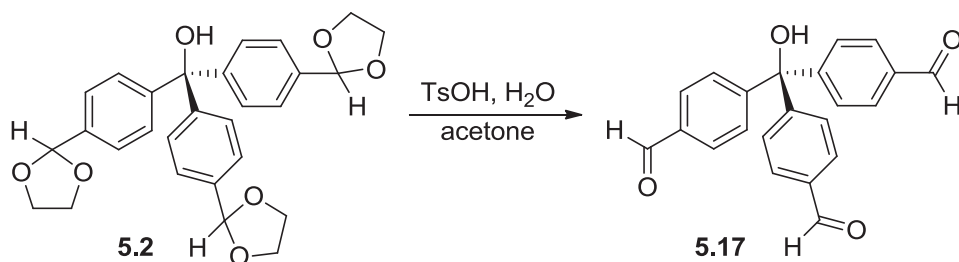


Under argon, anhydrous tetrahydrofuran (8 mL) was added to **5.12** via syringe. The solution was cooled to -70 °C, and a solution of *n*-butyllithium in hexanes (0.39 mL,

0.37 mmol, 0.93 M) was added via syringe. The mixture was stirred for 30 min before a solution of Weinreb amide **5.13** (0.058 g, 0.24 mmol) in anhydrous tetrahydrofuran (2 mL) was added via syringe. The reaction mixture was then stirred at rt overnight, followed by extraction with ethyl acetate (2 × 20 mL) from saturated aqueous ammonium chloride (20 mL). The combined organic layers were dried over magnesium sulfate, filtered, and concentrated. Column chromatography over silica gel with gradient elution from 10 to 40% ethyl acetate/hexanes gave the product as a yellow liquid (0.025 g, 42%).

^1H NMR (300 MHz, CDCl_3) δ 7.81 (d, J = 8.3 Hz, 4H), 7.60 (d, J = 8.3 Hz, 4H), 5.89 (s, 2H), 4.25–3.97 (m, 8H). ^{13}C NMR (75 MHz, CDCl_3) δ 195.98, 142.30, 138.13, 130.13, 126.39, 103.00, 65.42.

4,4',4''-triformyltrityl alcohol (**5.17**)

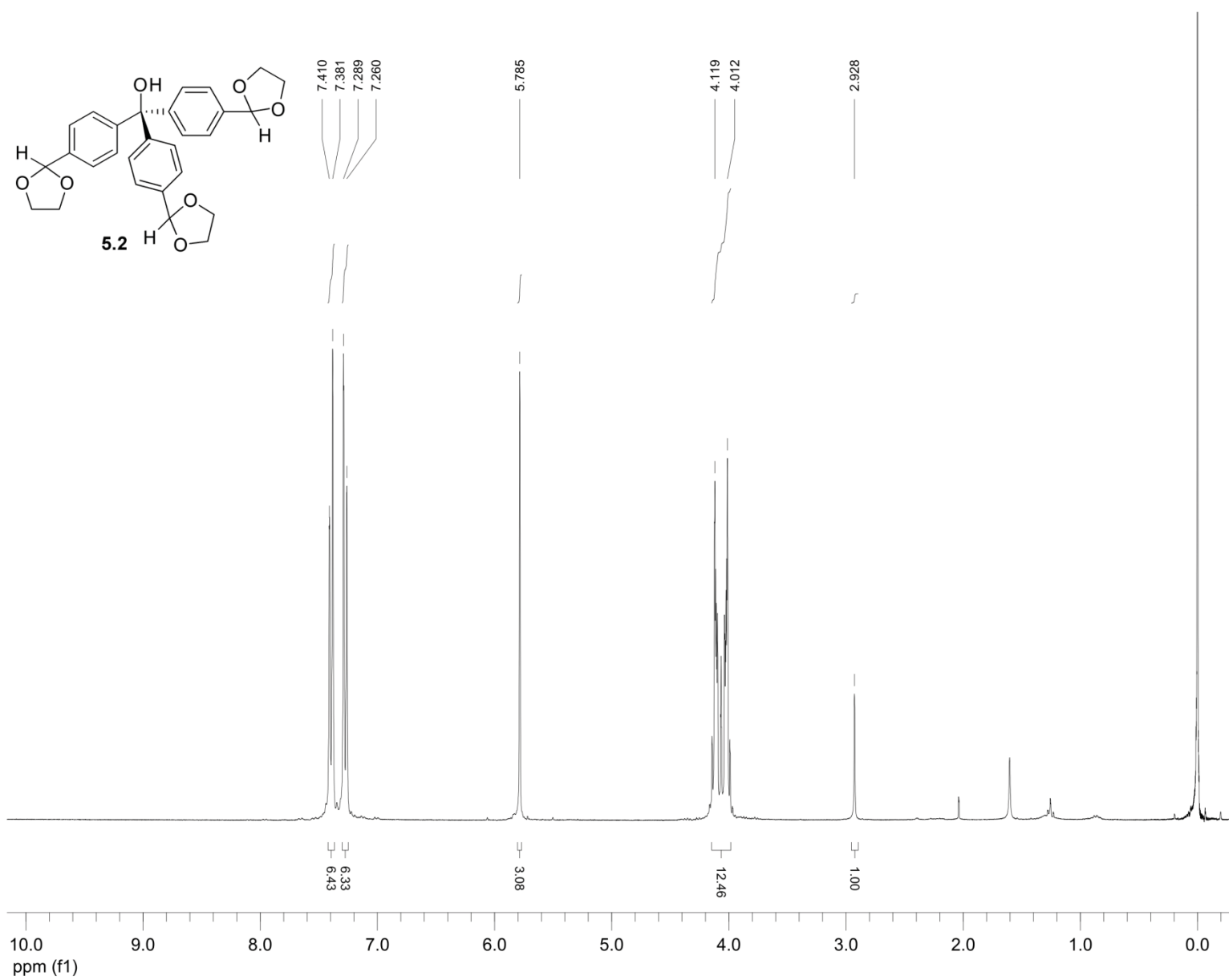


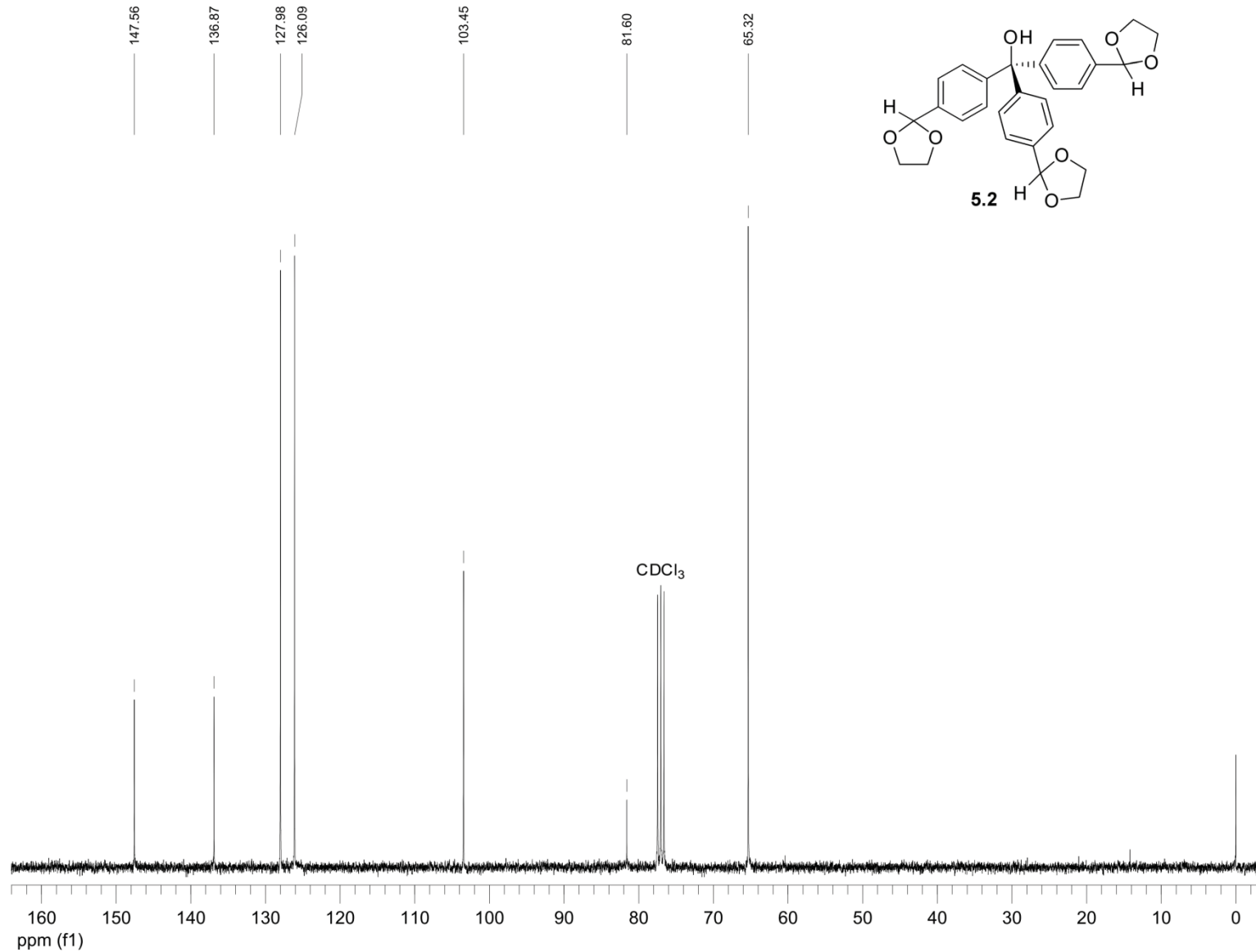
Water (1.5 mL) and *para*-toluenesulfonic acid monohydrate (0.15 g, 0.78 mmol) were added to a solution of **5.2** (0.37 g, 0.78 mmol) in acetone (30 mL). The reaction was stirred at 50 °C overnight and then concentrated. The residue was extracted with chloroform (2 × 30 mL) from water (30 mL), and the combined organic layers were dried over magnesium sulfate, filtered, and concentrated. Column chromatography over silica

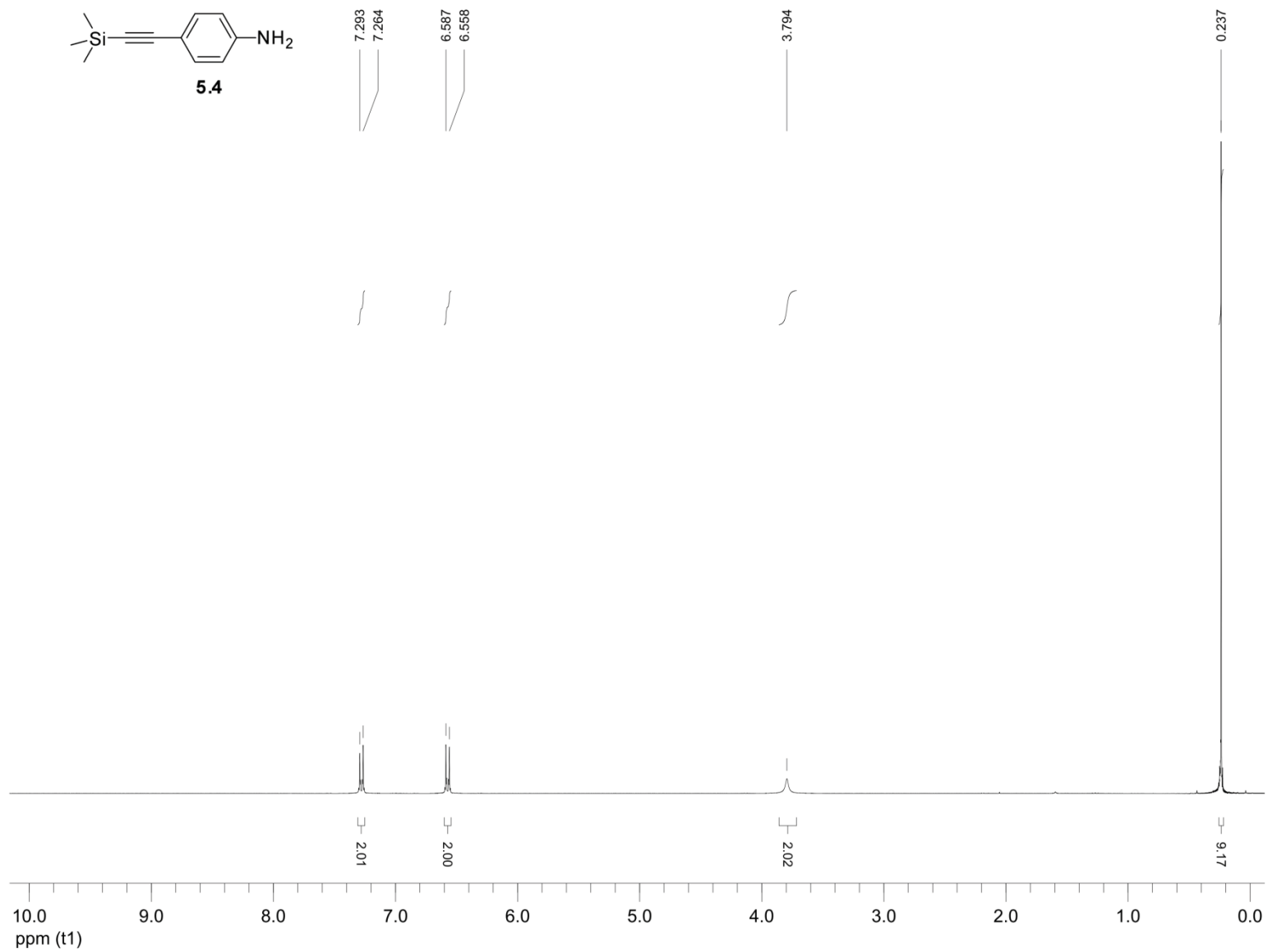
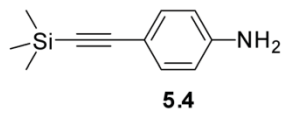
gel with gradient elution from 25 to 55% ethyl acetate/hexanes gave the product as a colorless liquid (0.22 g, 81%).

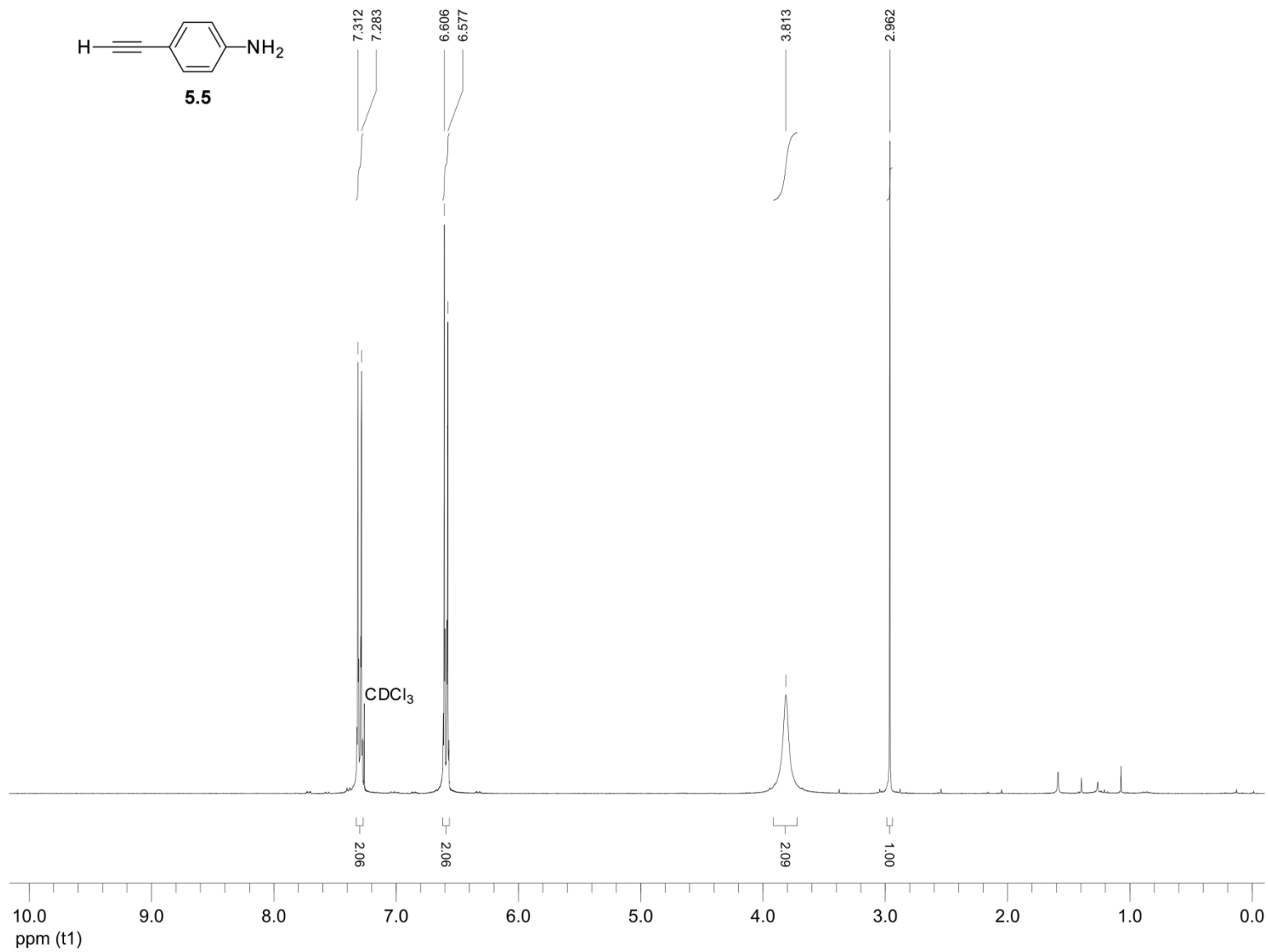
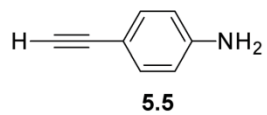
Characterizations matched those reported in the literature.¹⁸⁴

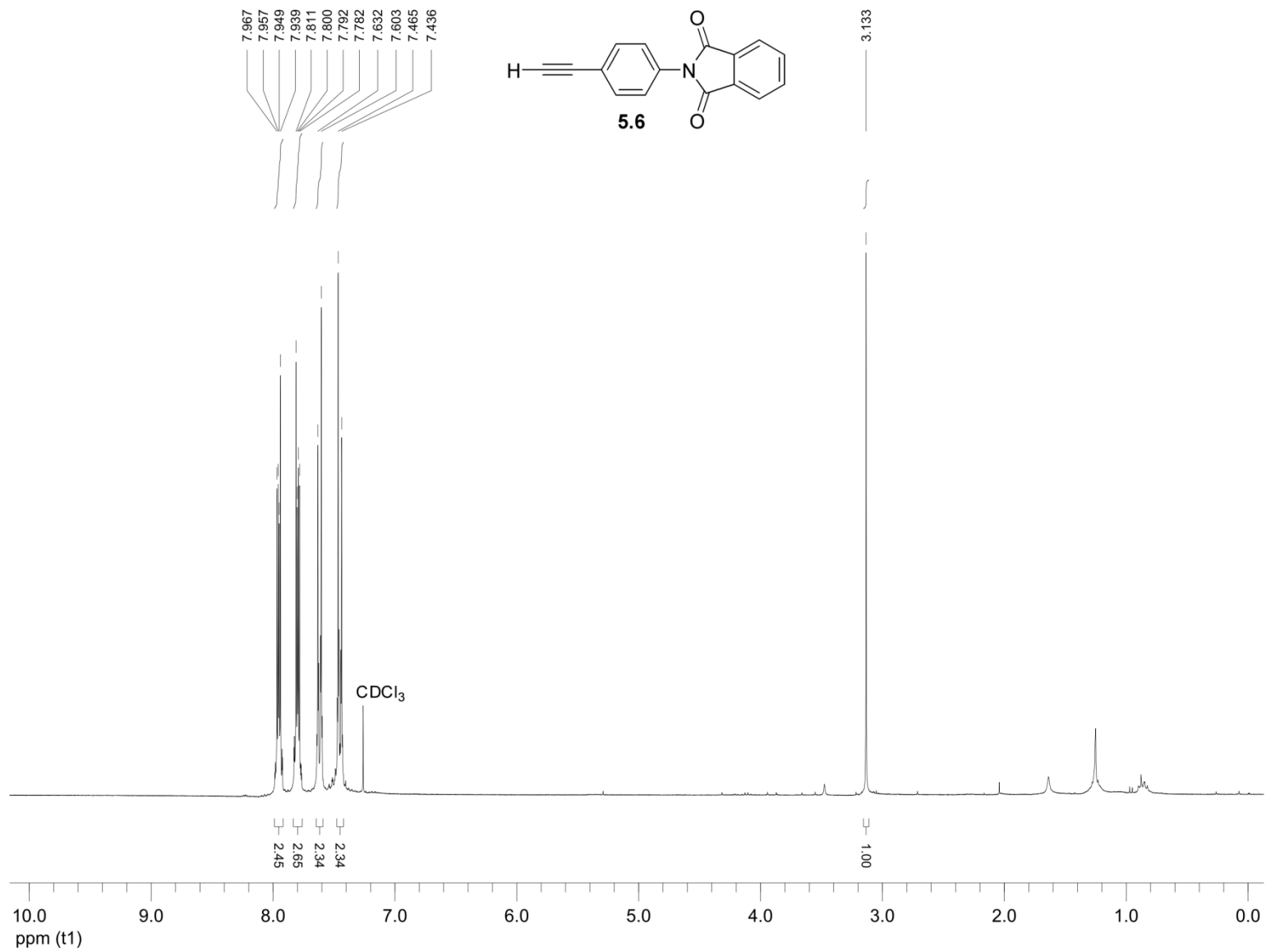
¹H NMR (300 MHz, CDCl₃) δ 9.99 (s, 3H), 7.85 (d, *J* = 8.5 Hz, 6H), 7.50 (d, *J* = 8.5 Hz, 6H), 3.72 (s, 1H). ¹³C NMR (75 MHz, CDCl₃) δ 191.98, 151.87, 135.43, 129.67, 128.44, 81.53.

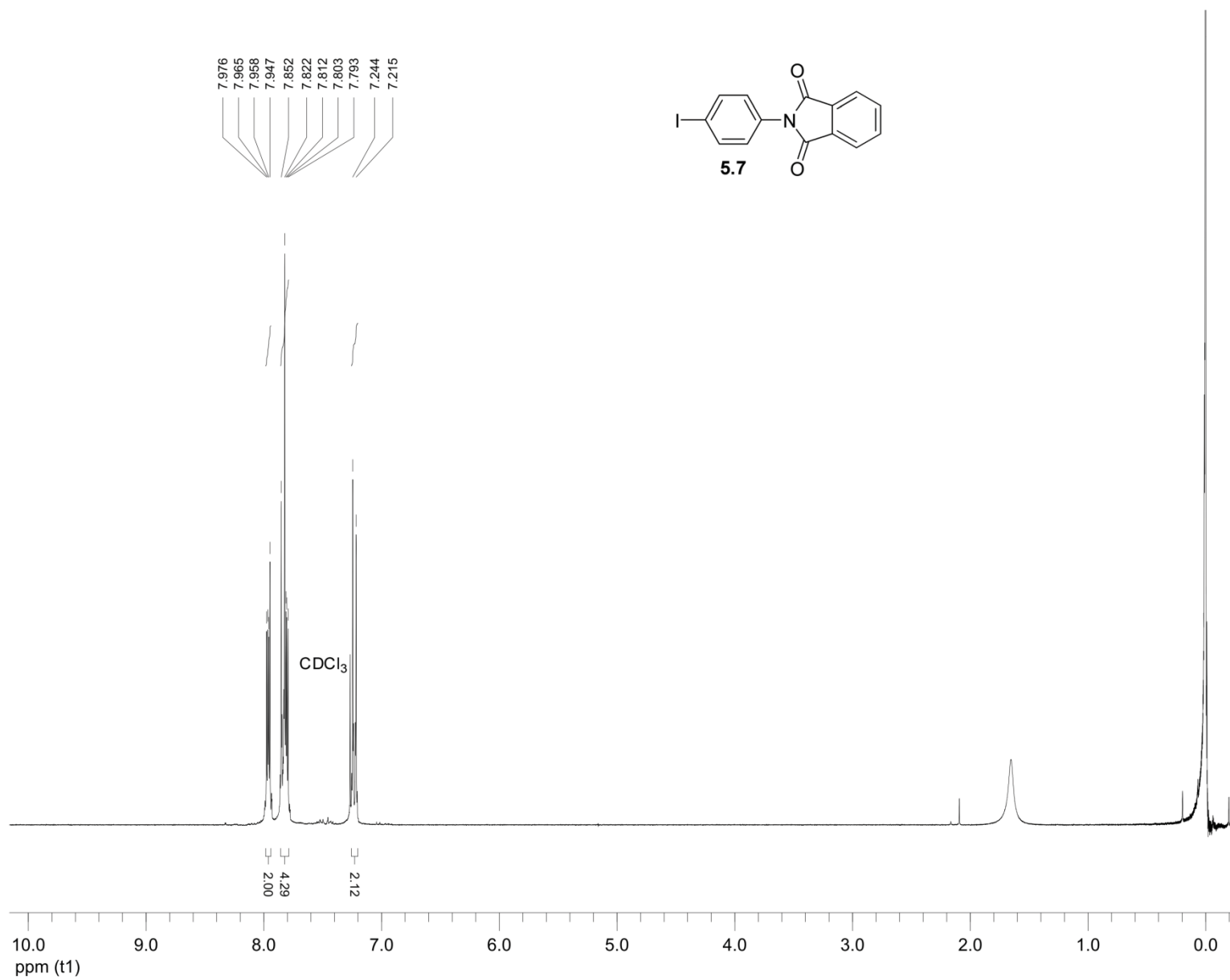


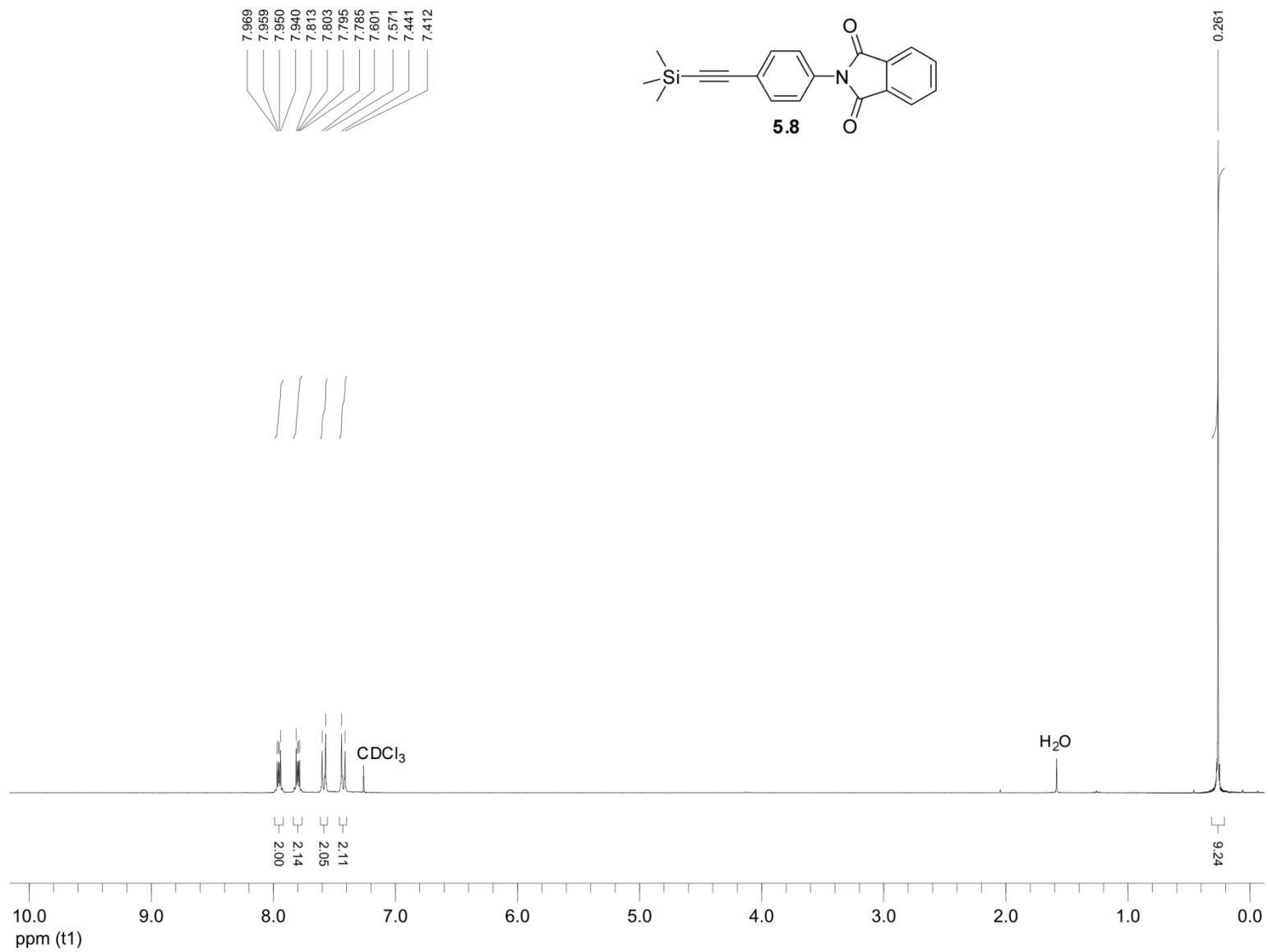




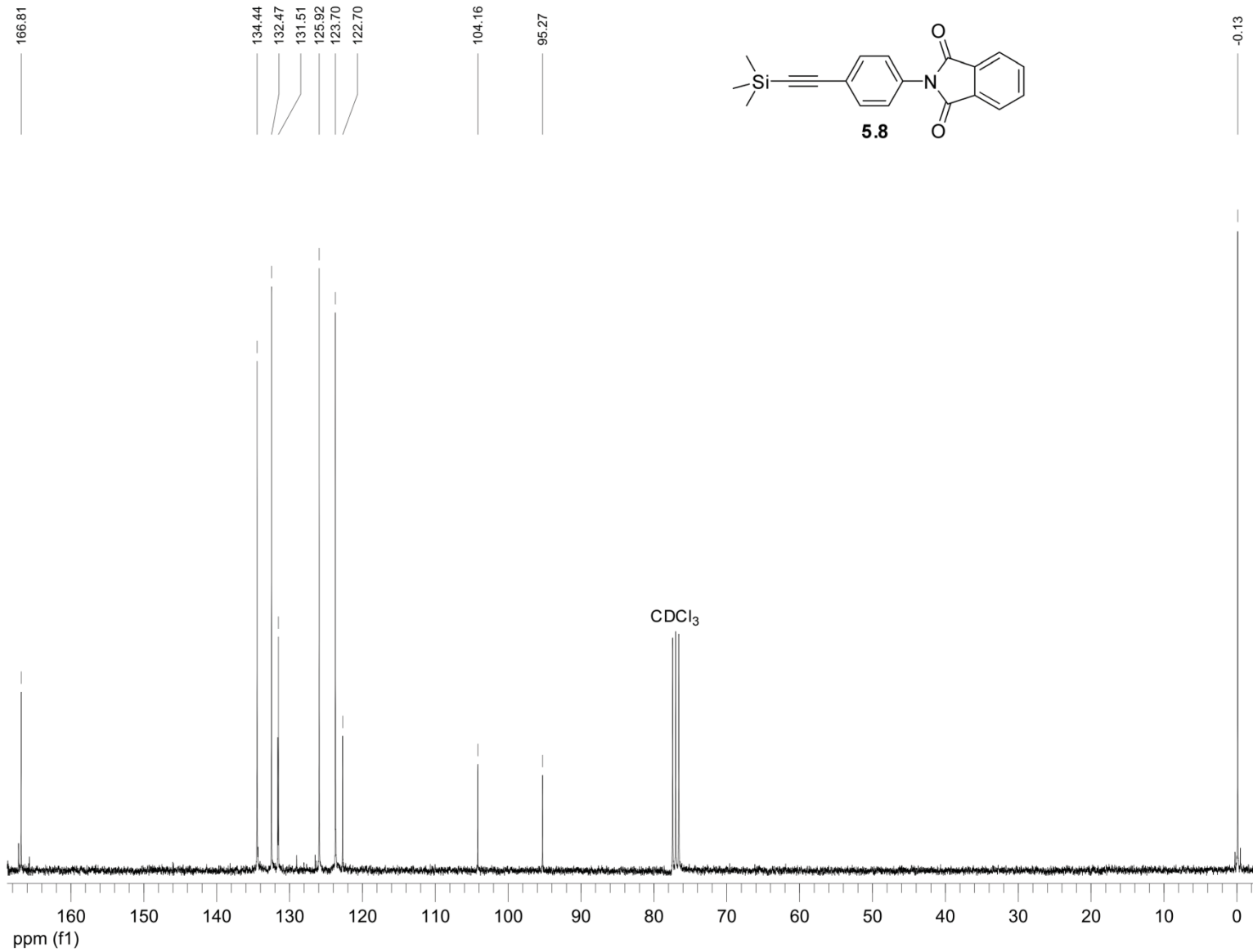


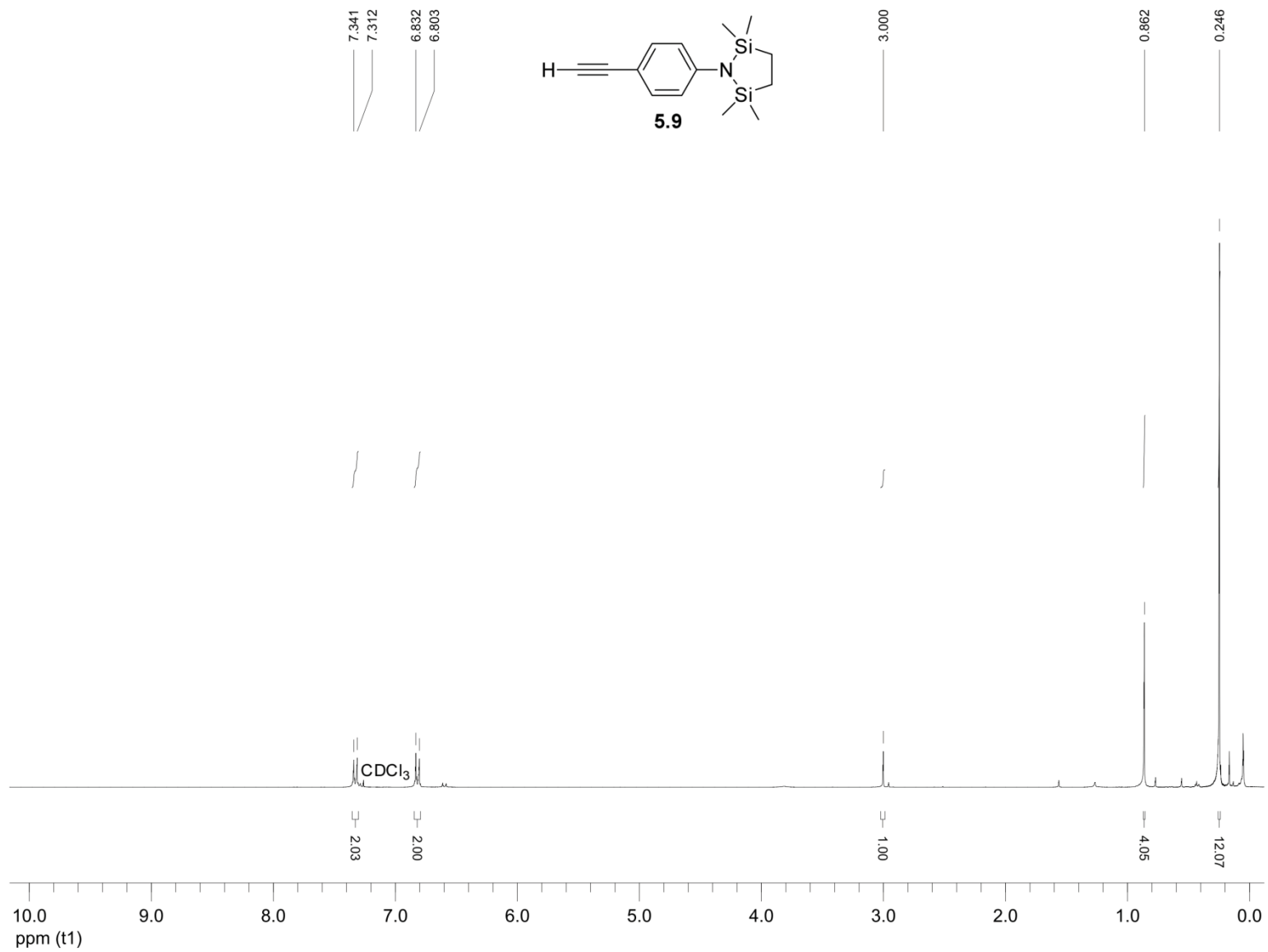




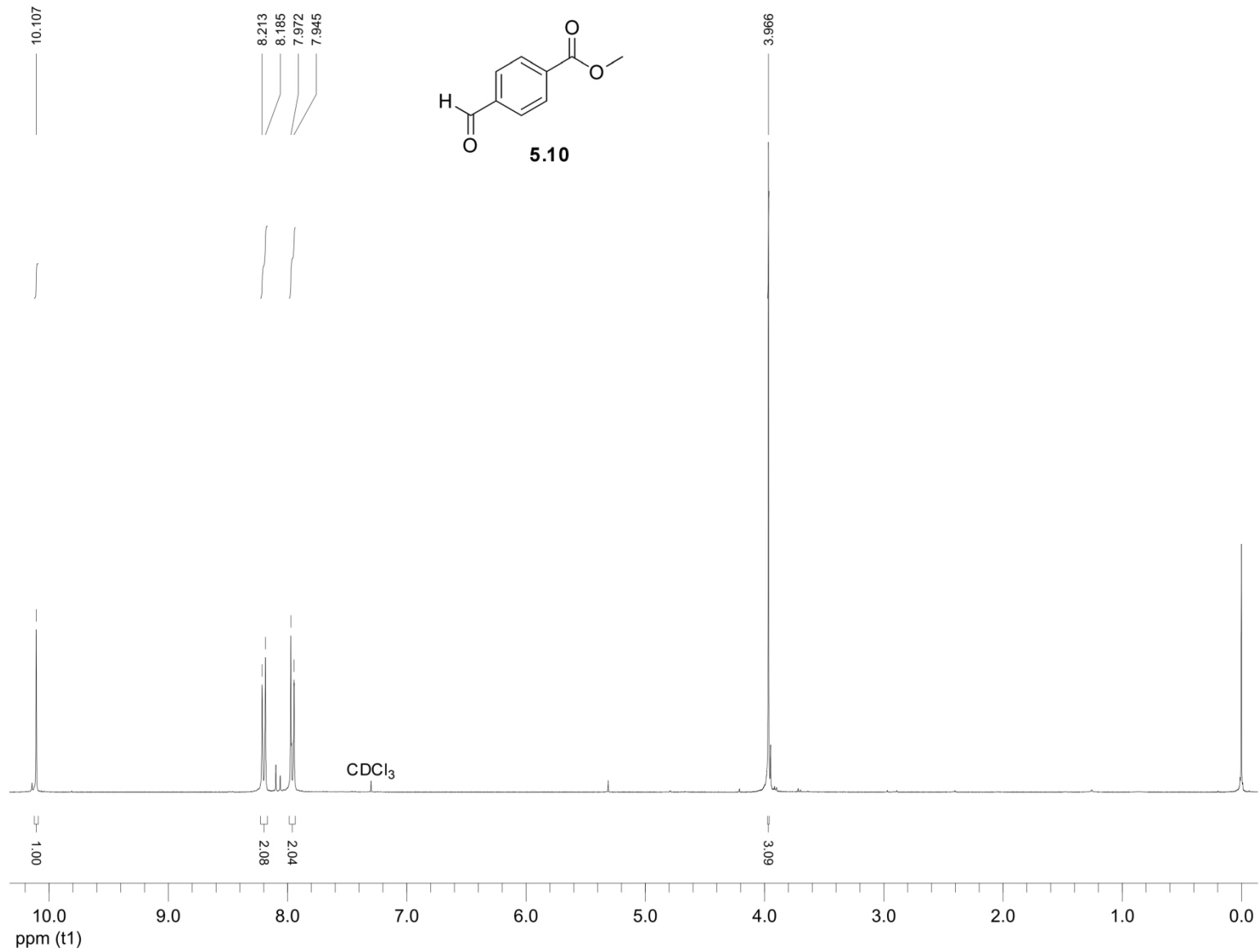


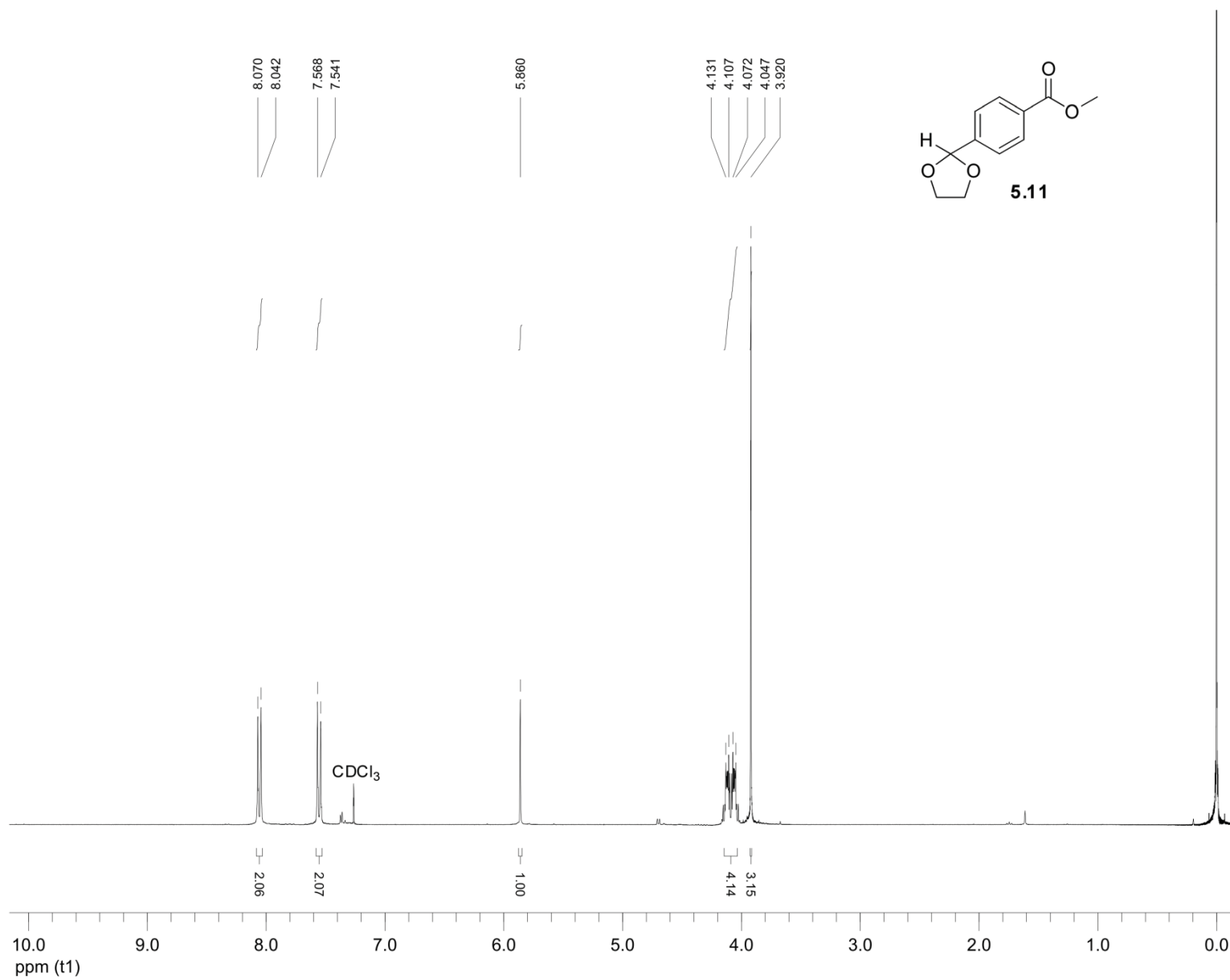
238

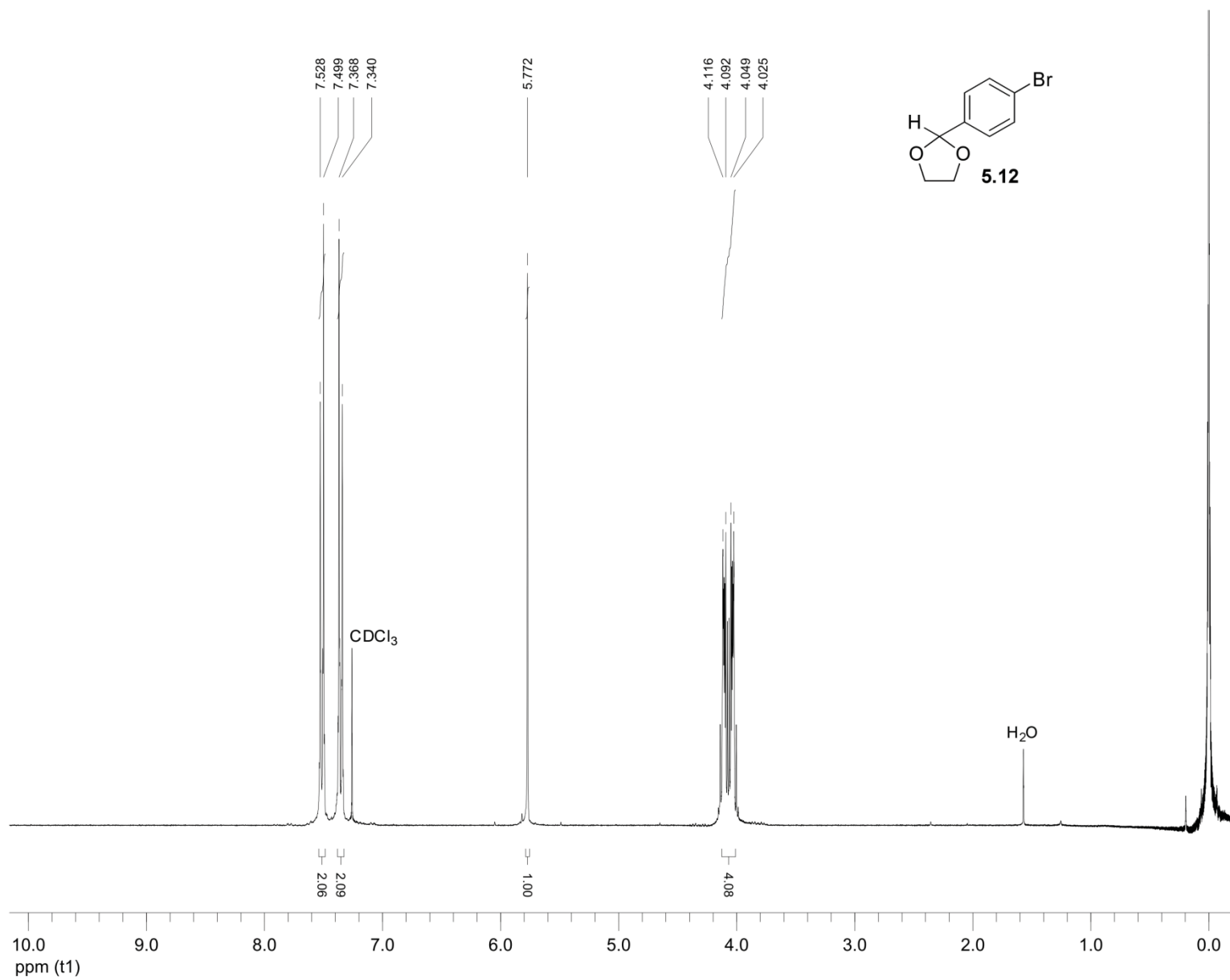




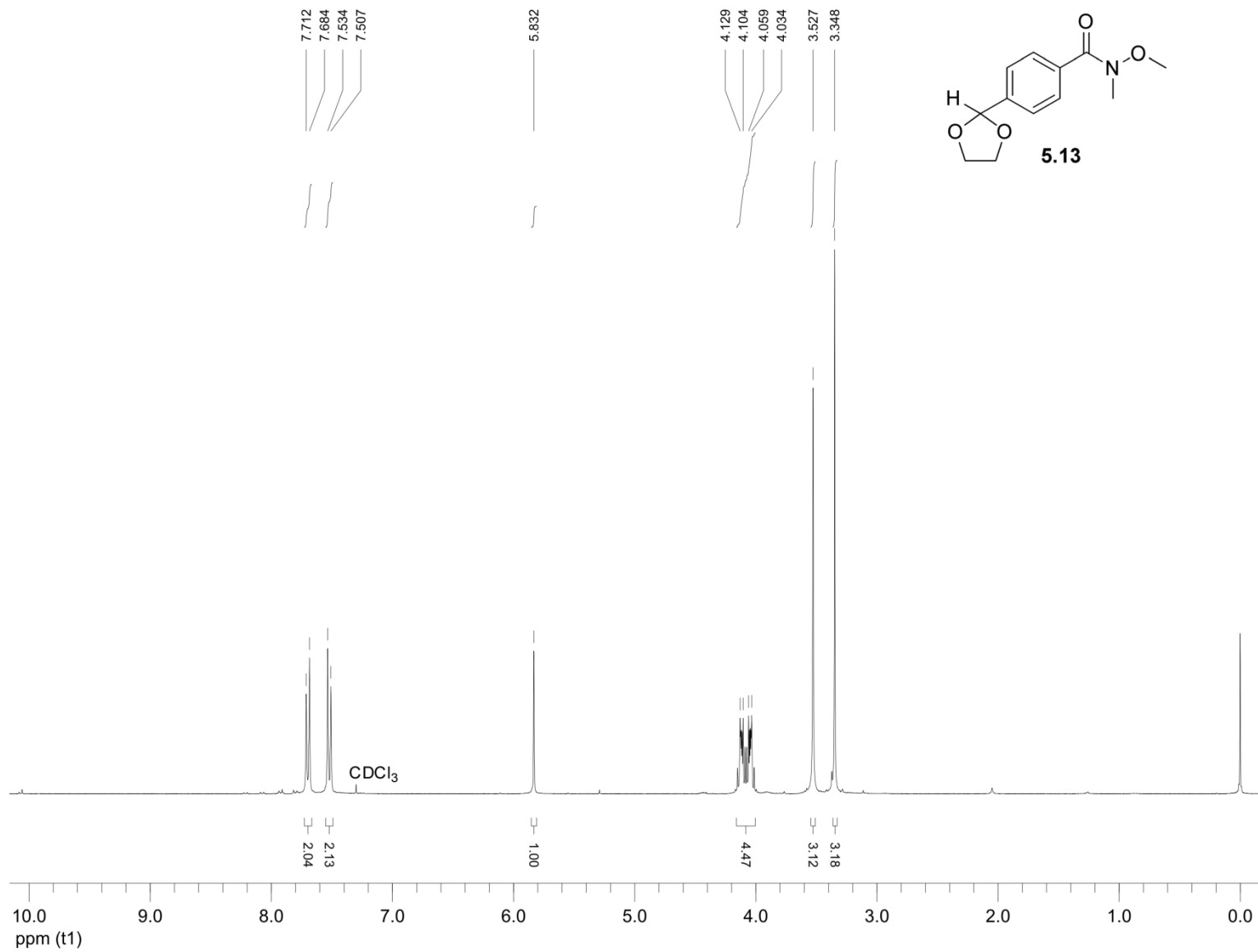
240

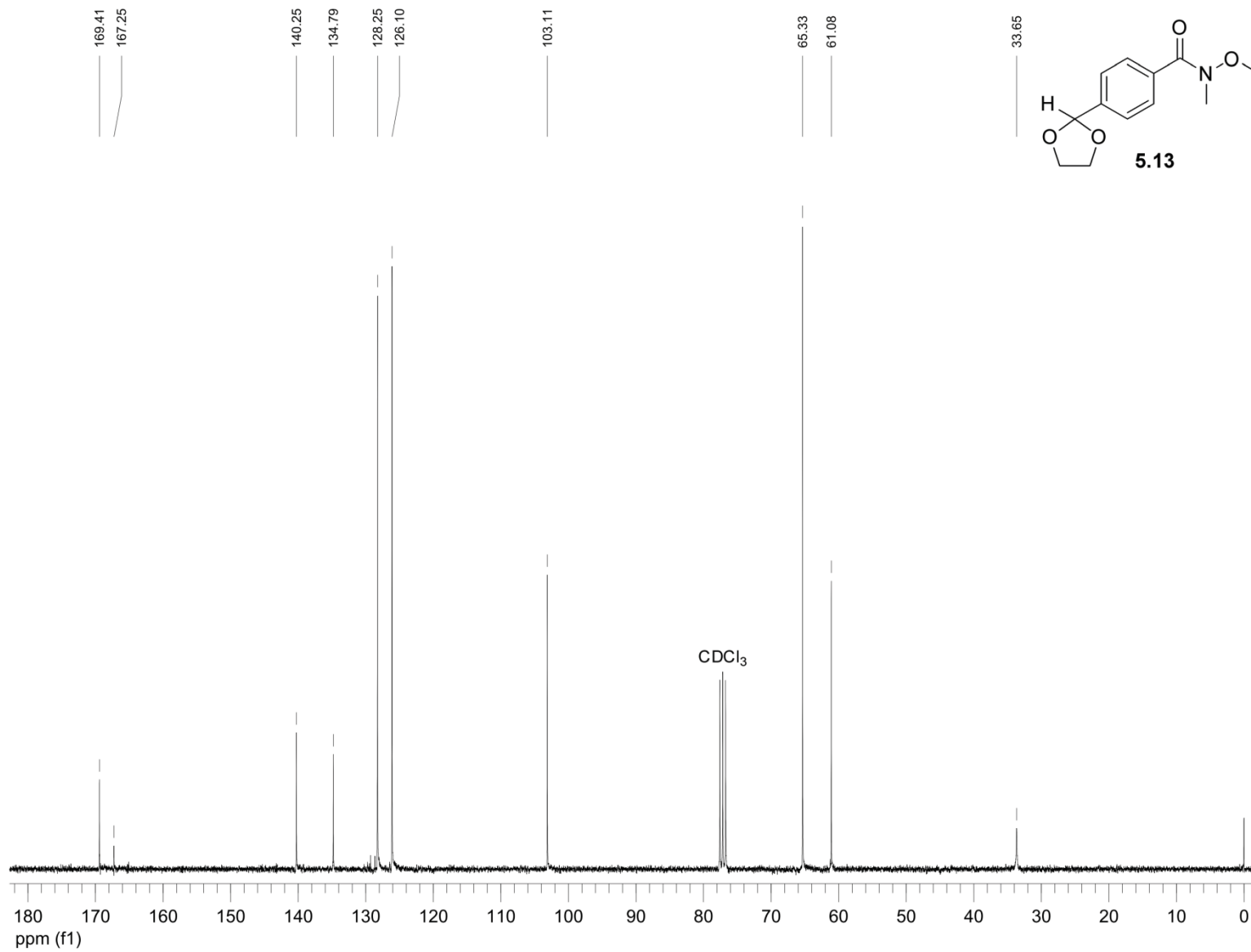




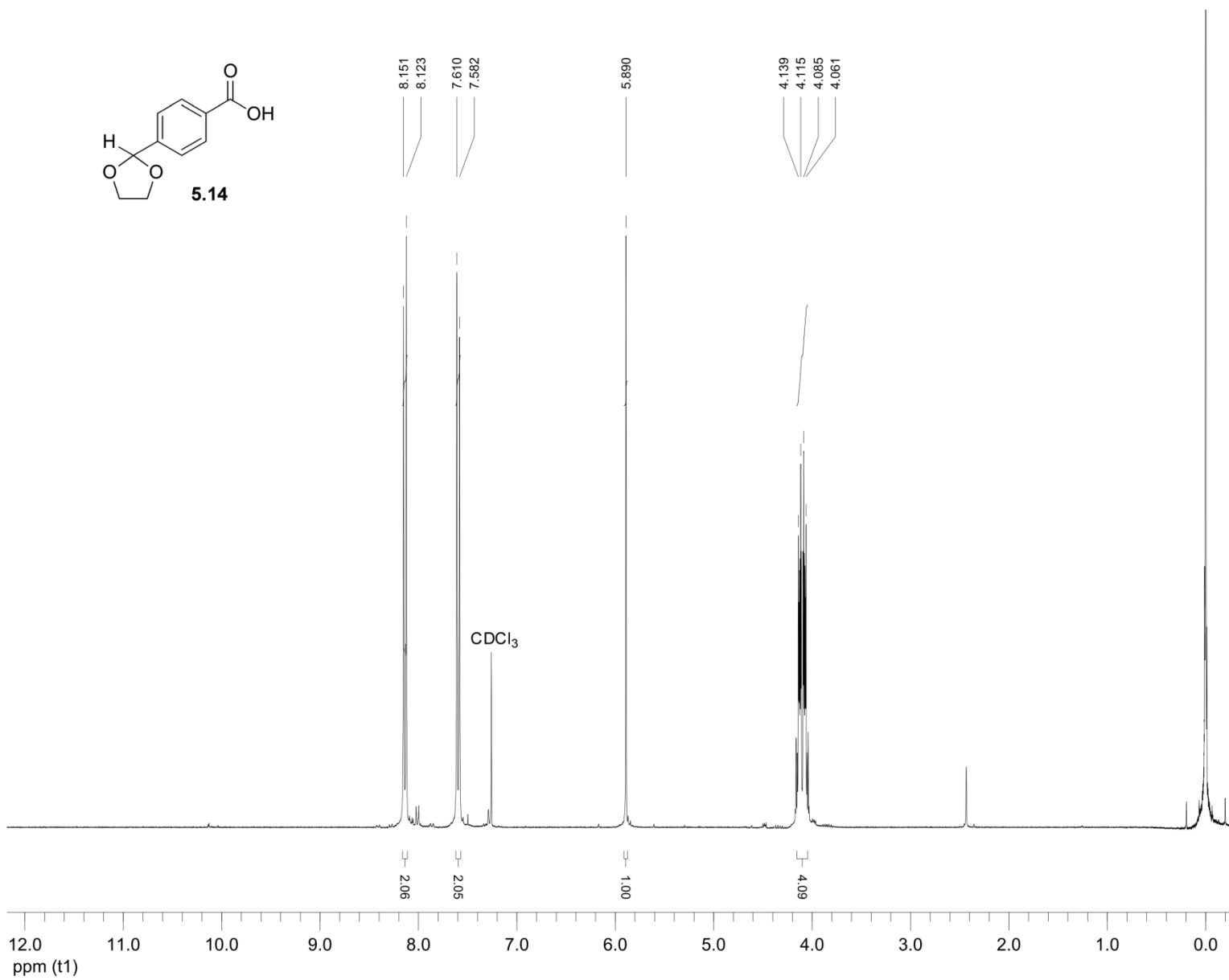
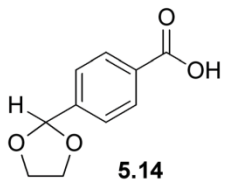


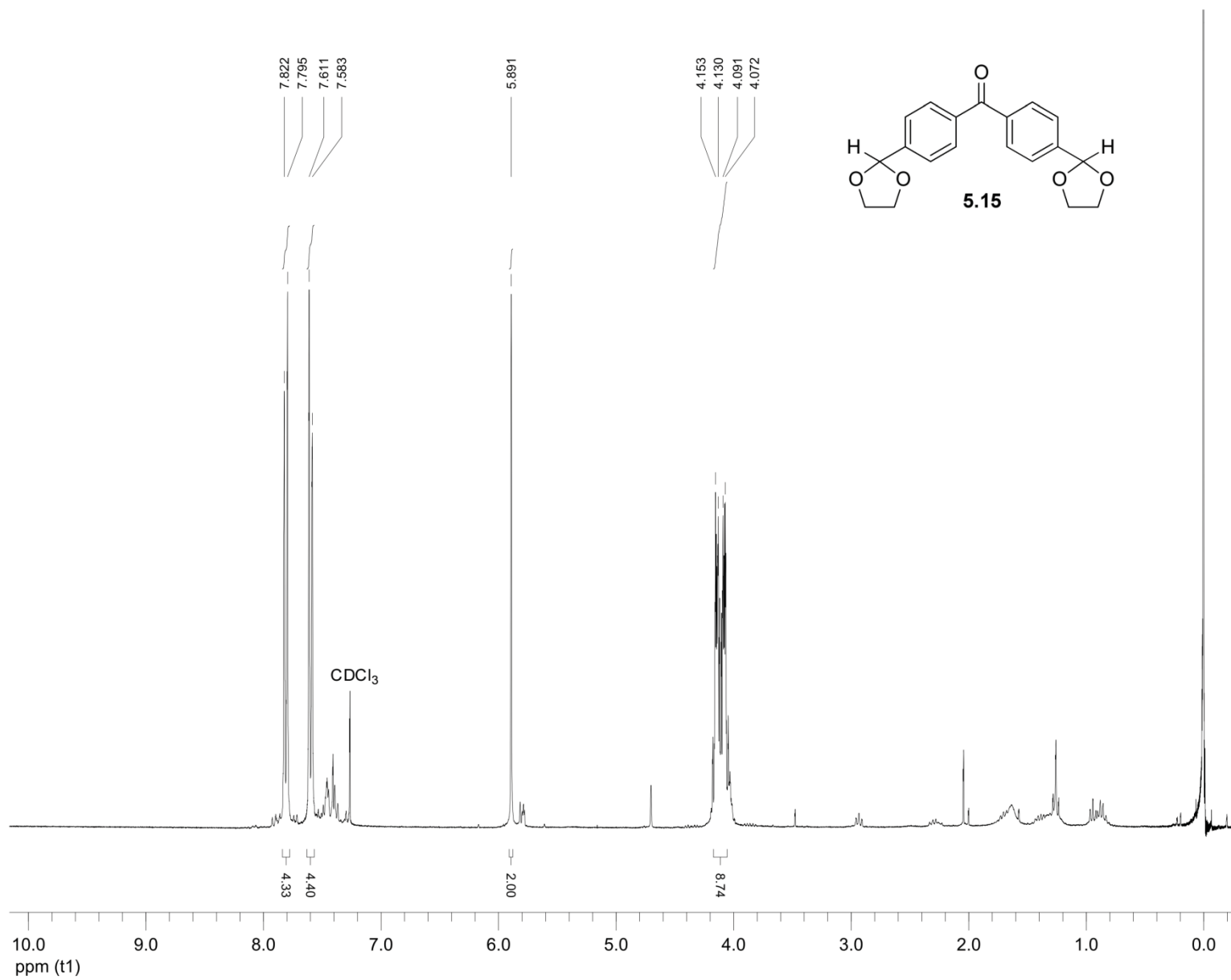
243



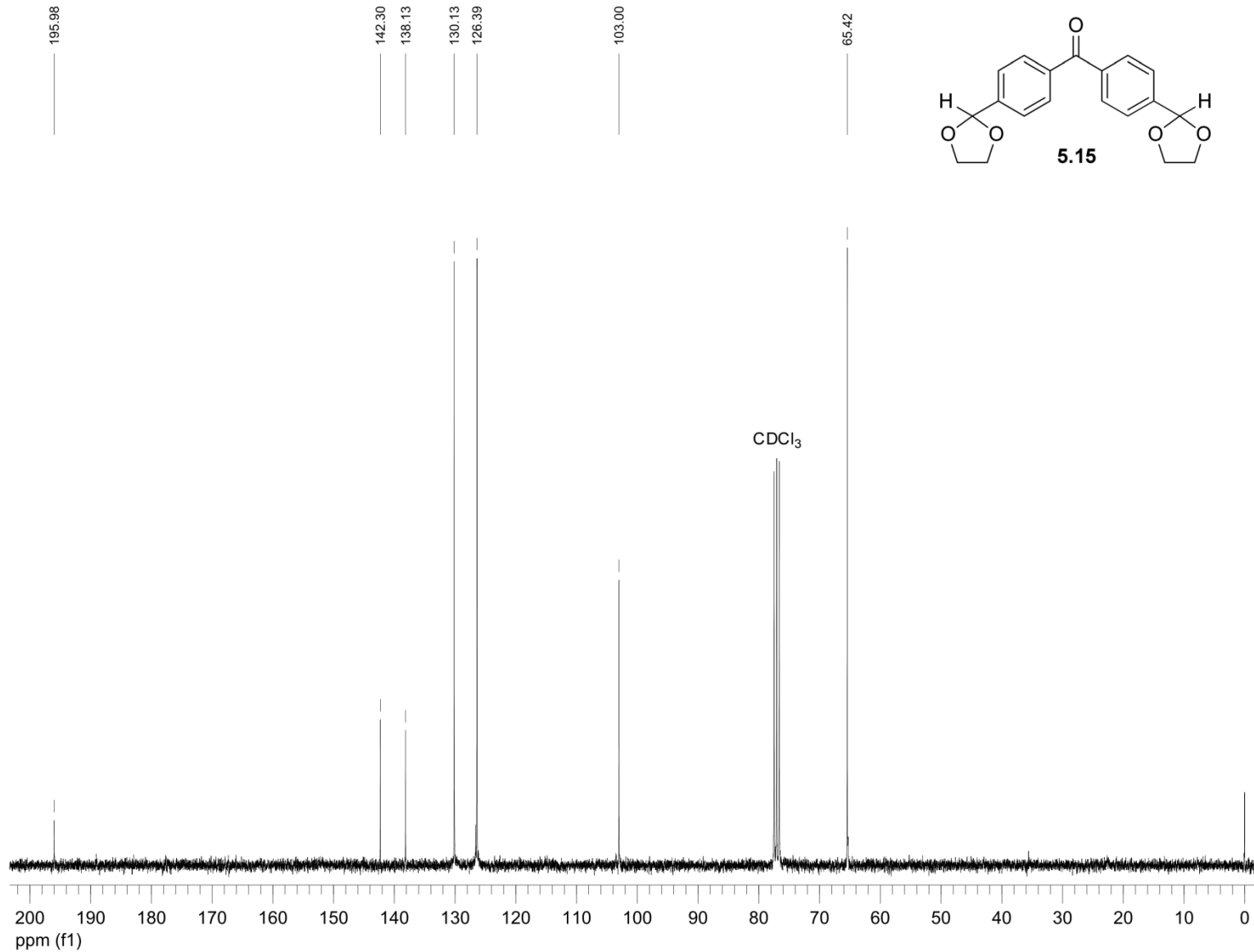


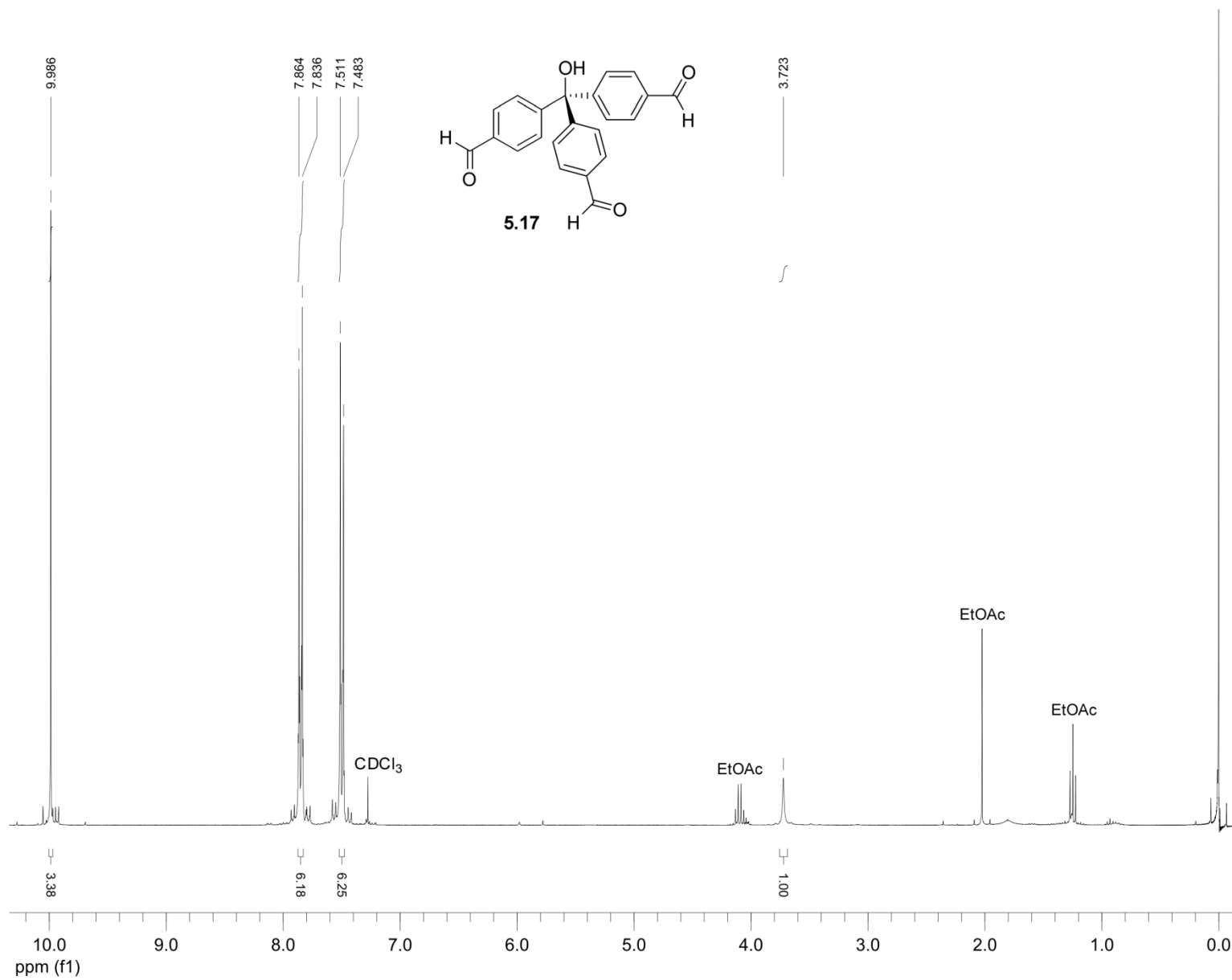
245

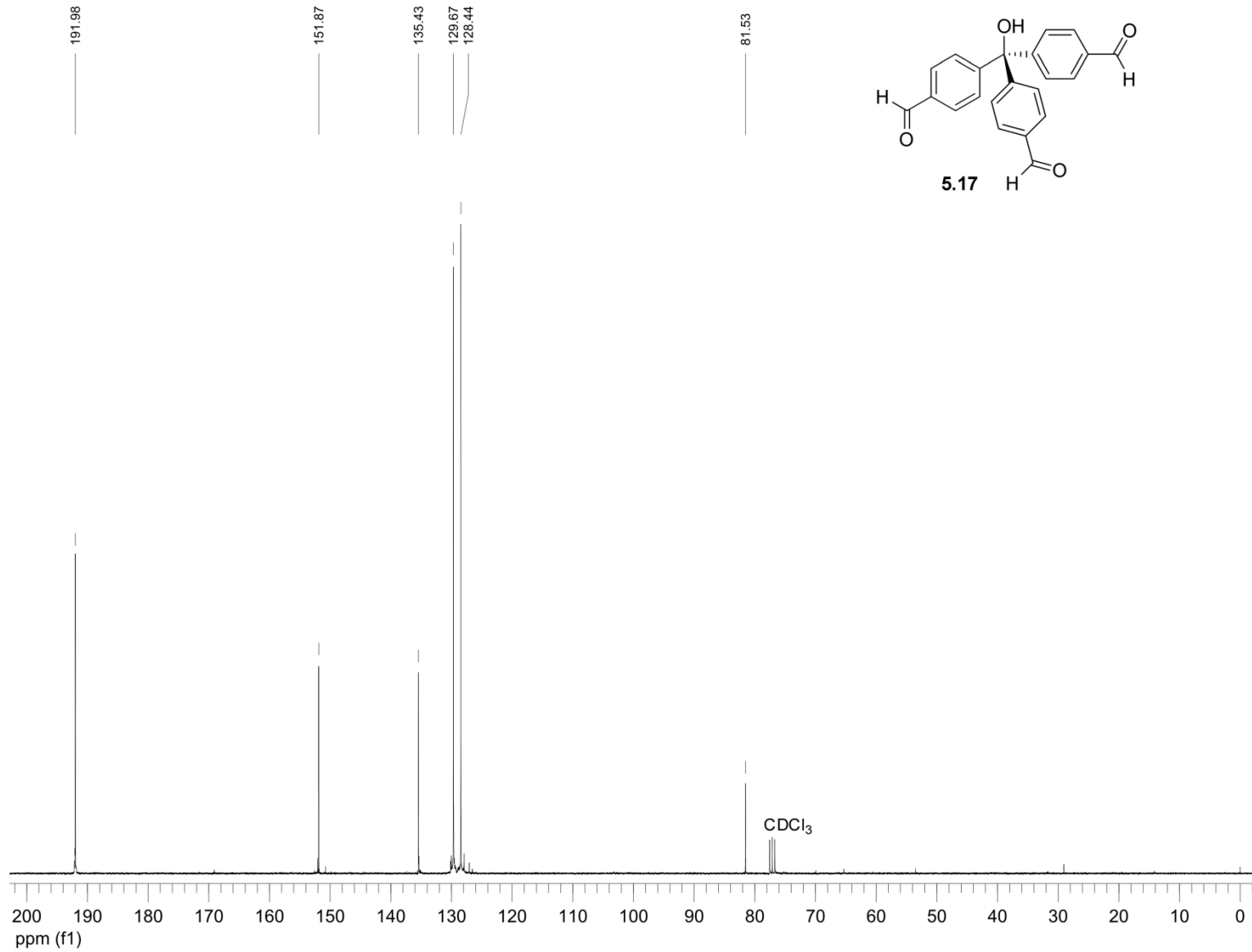




247







250

List of References

1. Anslyn, E. V.; Dougherty, D. A., *Modern Physical Organic Chemistry*. University Science Books: Mill Valley, CA, 2006.
2. Steed, J. W.; Atwood, J. L., *Supramolecular chemistry*. 2nd ed.; Wiley: Chichester, UK, 2009.
3. Inoue, Y.; Hakushi, T.; Liu, Y.; Tong, L.; Shen, B.; Jin, D., Thermodynamics of Molecular Recognition by Cyclodextrins. 1. Calorimetric Titration of Inclusion Complexation of Naphthalenesulfonates with α -, β -, and γ -Cyclodextrins: Enthalpy–Entropy Compensation. *J. Am. Chem. Soc.* **1993**, *115* (2), 475–481.
4. Peterson, B. R.; Wallimann, P.; Carcanague, D. R.; Diederich, F., Steroid complexation by cyclophane receptors in aqueous solution: Substrate selectivity, enthalpic driving force for cavity inclusion, and enthalpy–entropy compensation. *Tetrahedron* **1995**, *51* (2), 401–421.
5. (a) Linton, B.; Hamilton, A. D., Calorimetric investigation of guanidinium–carboxylate interactions. *Tetrahedron* **1999**, *55* (19), 6027–6038; (b) Haj-Zaroubi, M.; Mitzel, N. W.; Schmidtchen, F. P., The Rational Design of Anion Host Compounds: An Exercise in Subtle Energetics. *Angew. Chem. Int. Ed.* **2002**, *41* (1), 104–107.
6. Eaton, W. A.; Henry, E. R.; Hofrichter, J.; Mozzarelli, A., Is cooperative oxygen binding by hemoglobin really understood? *Nat. Struct. Mol. Biol.* **1999**, *6* (4), 351–358.
7. Badjić, J. D.; Nelson, A.; Cantrill, S. J.; Turnbull, W. B.; Stoddart, J. F., Multivalency and Cooperativity in Supramolecular Chemistry. *Acc. Chem. Res.* **2005**, *38* (9), 723–732.
8. Mammen, M.; Choi, S.-K.; Whitesides, G. M., Polyvalent Interactions in Biological Systems: Implications for Design and Use of Multivalent Ligands and Inhibitors. *Angew. Chem. Int. Ed.* **1998**, *37* (20), 2754–2794.
9. Fischer, E., Einfluss der Configuration auf die Wirkung der Enzyme (Influence of Configuration on the Activity of Enzymes). *Ber. Dtsch. Chem. Ges.* **1894**, *27* (3), 2985–2993.
10. Cram, D. J., Preorganization—From Solvents to Spherands. *Angew. Chem. Int. Ed. Engl.* **1986**, *25* (12), 1039–1057.
11. Koshland, D. E., Application of a Theory of Enzyme Specificity to Protein Synthesis. *Proc. Natl. Acad. Sci. U. S. A.* **1958**, *44* (2), 98–104.
12. (a) Pai, E. F.; Krengel, U.; Petsko, G. A.; Goody, R. S.; Kabsch, W.; Wittinghofer, A., Refined Crystal Structure of the Triphosphate Conformation of H-ras p21 at 1.35 Å Resolution: Implications for the Mechanism of GTP Hydrolysis. *EMBO J.* **1990**, *9* (8), 2351–2359; (b) Shi, W.; Munagala, N. R.; Wang, C. C.; Li, C. M.; Tyler, P. C.; Furneaux, R. H.; Grubmeyer, C.; Schramm, V. L.; Almo, S. C., Crystal Structures of *Giardia lamblia* Guanine Phosphoribosyltransferase at 1.75 Å. *Biochemistry* **2000**, *39* (23), 6781–6790; (c) Hirsch, A. K. H.; Fischer, F. R.; Diederich, F., Phosphate recognition in structural biology. *Angew. Chem. Int. Ed.* **2007**, *46* (3), 338–352; (d) Bazzicalupi, C.; Bencini, A.; Lippolis, V., Tailoring cyclic polyamines for inorganic/organic phosphate binding. *Chem. Soc. Rev.* **2010**, *39* (10), 3709–3728.

13. (a) Andres, A.; Arago, J.; Bencini, A.; Bianchi, A.; Domenech, A.; Fusi, V.; García-España, E.; Paoletti, P.; Ramirez, J. A., Interaction of Hexaazaalkanes with Phosphate Type Anions - Thermodynamic, Kinetic, and Electrochemical Considerations. *Inorg. Chem.* **1993**, *32* (16), 3418–3424; (b) Andres, A.; Bazzicalupi, C.; Bencini, A.; Bianchi, A.; Fusi, V.; García-España, E.; Giorgi, C.; Nardi, N.; Paoletti, P.; Ramirez, J. A.; Valtancoli, B., 1,10-Dimethyl-1,4,7,10,13,16-Hexaazacyclooctadecane L and 1,4,7-Trimethyl-1,4,7,10,13,16,19-Heptaazacyclohenicosane L1: Two New Macrocyclic Receptors for ATP Binding. Synthesis, Solution Equilibria and the Crystal Structure of (H₄L)(ClO₄)₄. *J. Chem. Soc., Perkin Trans. 2* **1994**, (11), 2367–2373; (c) Bencini, A.; Bianchi, A.; Giorgi, C.; Paoletti, P.; Valtancoli, B.; Fusi, V.; García-España, E.; Llinares, J. M.; Ramirez, J. A., Effect of nitrogen methylation on cation and anion coordination by hexa- and heptaazamacrocycles. Catalytic properties of these ligands in ATP dephosphorylation. *Inorg. Chem.* **1996**, *35* (5), 1114–1120; (d) Bazzicalupi, C.; Bencini, A.; Bianchi, A.; Cecchi, M.; Escuder, B.; Fusi, V.; García-España, E.; Giorgi, C.; Luis, S. V.; Maccagni, G.; Marcelino, V.; Paoletti, P.; Valtancoli, B., Thermodynamics of phosphate and pyrophosphate anions binding by polyammonium receptors. *J. Am. Chem. Soc.* **1999**, *121* (29), 6807–6815.
14. Arranz, P.; Bencini, A.; Bianchi, A.; Diaz, P.; García-España, E.; Giorgi, C.; Luis, S. V.; Querol, M.; Valtancoli, B., Thermodynamics of sulfate anion binding by macrocyclic polyammonium receptors. *J. Chem. Soc., Perkin Trans. 2* **2001**, (9), 1765–1770.
15. Matthews, S. E.; Beer, P. D., Calixarene-based anion receptors. *Supramol. Chem.* **2005**, *17* (6), 411–435.
16. Chen, Q. Y.; Chen, C. F., A highly selective fluorescent chemosensor for H₂PO₄⁻ based on a calix[4]arene tetraamide derivative. *Eur. J. Org. Chem.* **2005**, (12), 2468–2472.
17. Miao, R.; Zheng, Q. Y.; Chen, C. F.; Huang, Z. T., A novel calix[4]arene fluorescent receptor for selective recognition of acetate anion. *Tetrahedron Lett.* **2005**, *46* (12), 2155–2158.
18. Sessler, J. L.; Camiolo, S.; Gale, P. A., Pyrrolic and polypyrrolic anion binding agents. *Coord. Chem. Rev.* **2003**, *240* (1-2), 17–55.
19. Yoon, D. W.; Gross, D. E.; Lynch, V. M.; Sessler, J. L.; Hay, B. P.; Lee, C. H., Benzene-, pyrrole-, and furan-containing diametrically strapped calix[4]pyrroles - An experimental and theoretical study of hydrogen-bonding effects in chloride anion recognition. *Angew. Chem. Int. Ed.* **2008**, *47* (27), 5038–5042.
20. Yoon, D. W.; Gross, D. E.; Lynch, V. M.; Lee, C. H.; Bennett, P. C.; Sessler, J. L., Real-time determination of chloride anion concentration in aqueous-DMSO using a pyrrole-strapped calixpyrrole anion receptor. *Chem. Commun.* **2009**, (9), 1109–1111.
21. Wintergerst, M. P.; Levitskaia, T. G.; Moyer, B. A.; Sessler, J. L.; Delmau, L. H., Calix[4]pyrrole: A new ion-pair receptor as demonstrated by liquid–liquid extraction. *J. Am. Chem. Soc.* **2008**, *130* (12), 4129–4139.

22. Li, Y. J.; Flood, A. H., Pure C–H hydrogen bonding to chloride ions: A preorganized and rigid macrocyclic receptor. *Angew. Chem. Int. Ed.* **2008**, *47* (14), 2649–2652.
23. Li, Y.; Flood, A. H., Strong, Size-Selective, and Electronically Tunable C–H···Halide Binding with Steric Control over Aggregation from Synthetically Modular, Shape-Persistent [3₄]Triazolophanes. *J. Am. Chem. Soc.* **2008**, *130* (36), 12111–12122.
24. Hennrich, G.; Anslyn, E. V., 1,3,5-2,4,6-functionalized, facially segregated benzenes - Exploitation of sterically predisposed systems in supramolecular chemistry. *Chem. Eur. J.* **2002**, *8* (10), 2219–2224.
25. Schmuck, C.; Schwegmann, M., A molecular flytrap for the selective binding of citrate and other tricarboxylates in water. *J. Am. Chem. Soc.* **2005**, *127* (10), 3373–3379.
26. Brotherhood, P. R.; Davis, A. P., Steroid-based anion receptors and transporters. *Chem. Soc. Rev.* **2010**, *39* (10), 3633–3647.
27. Clare, J. P.; Ayling, A. J.; Joos, J. B.; Sisson, A. L.; Magro, G.; Perez-Payan, M. N.; Lambert, T. N.; Shukla, R.; Smith, B. D.; Davis, A. P., Substrate discrimination by cholapod anion receptors: Geometric effects and the "affinity-selectivity principle". *J. Am. Chem. Soc.* **2005**, *127* (30), 10739–10746.
28. O'Neil, E. J.; Smith, B. D., Anion recognition using dimetallic coordination complexes. *Coord. Chem. Rev.* **2006**, *250* (23-24), 3068–3080.
29. Lee, J. H.; Jeong, A. R.; Jung, J.-H.; Park, C.-M.; Hong, J.-I., A Highly Selective and Sensitive Fluorescence Sensing System for Distinction between Diphosphate and Nucleoside Triphosphates. *J. Org. Chem.* **2011**, *76* (2), 417–423.
30. Fabbrizzi, L.; Poggi, A., Sensors and switches from supramolecular chemistry. *Chem. Soc. Rev.* **1995**, *24* (3), 197–202.
31. de Silva, A. P.; Fox, D. B.; Huxley, A. J. M.; Moody, T. S., Combining luminescence, coordination and electron transfer for signalling purposes. *Coord. Chem. Rev.* **2000**, *205* (1), 41–57.
32. Cooper, C. R.; James, T. D., Selective D-glucosamine hydrochloride fluorescence signalling based on ammonium cation and diol recognition. *Chem. Commun.* **1997**, (15), 1419–1420.
33. Deetz, M. J.; Smith, B. D., Heteroditopic ruthenium(II) bipyridyl receptor with adjacent saccharide and phosphate binding sites. *Tetrahedron Lett.* **1998**, *39* (38), 6841–6844.
34. Nguyen, B. T.; Anslyn, E. V., Indicator–displacement assays. *Coord. Chem. Rev.* **2006**, *250* (23-24), 3118–3127.
35. Nonaka, A.; Horie, S.; James, T. D.; Kubo, Y., Pyrophosphate-induced reorganization of a reporter-receptor assembly via boronate esterification; a new strategy for the turn-on fluorescent detection of multi-phosphates in aqueous solution. *Org. Biomol. Chem.* **2008**, *6* (19), 3621–3625.
36. Connors, K. A., *Binding Constants: The Measurement of Molecular Complex Stability*. John Wiley & Sons: New York, NY, 1987.

37. Benesi, H. A.; Hildebrand, J. H., A Spectrophotometric Investigation of the Interaction of Iodine with Aromatic Hydrocarbons. *J. Am. Chem. Soc.* **1949**, *71* (8), 2703–2707.
38. Job, P., Studies on the formation of complex minerals in solution and on their stability. *Ann. Chim.* **1928**, *9*, 113–203.
39. Chakrabarti, P., Anion Binding Sites in Protein Structures. *J. Mol. Biol.* **1993**, *234* (2), 463–482.
40. Duxbury, A. C.; Duxbury, A. B., *An Introduction to the World's Oceans*. 5th ed.; William C. Brown Publishers: Dubuque, IA, 1997.
41. Huete, A. R.; Mccoll, J. G., Soil Cation Leaching by Acid-Rain with Varying Nitrate-to-Sulfate Ratios. *J. Environ. Qual.* **1984**, *13* (3), 366–371.
42. Porter, S. M., Seawater Chemistry and Early Carbonate Biomineralization. *Science* **2007**, *316* (5829), 1302.
43. Carpenter, S. R.; Caraco, N. F.; Correll, D. L.; Howarth, R. W.; Sharpley, A. N.; Smith, V. H., Nonpoint Pollution of Surface Waters with Phosphorus and Nitrogen. *Ecol. Appl.* **1998**, *8* (3), 559–568.
44. Katayev, E. A.; Kolesnikov, G. V.; Sessler, J. L., Molecular recognition of pertechnetate and perrhenate. *Chem. Soc. Rev.* **2009**, *38* (6), 1572–1586.
45. Simon, D. B.; Bindra, R. S.; Mansfield, T. A.; Nelson-Williams, C.; Mendonca, E.; Stone, R.; Schurman, S.; Nayir, A.; Alpay, H.; Bakkaloglu, A.; Rodriguez-Soriano, J.; Morales, J. M.; Sanjad, S. A.; Taylor, C. M.; Pilz, D.; Brem, A.; Trachtman, H.; Griswold, W.; Richard, G. A.; John, E.; Lifton, R. P., Mutations in the chloride channel gene, CLCNKB, cause Bartter's syndrome type III. *Nat. Genet.* **1997**, *17* (2), 171–178.
46. Anderson, M. P.; Gregory, R. J.; Thompson, S.; Souza, D. W.; Paul, S.; Mulligan, R. C.; Smith, A. E.; Welsh, M. J., Demonstration That CFTR Is a Chloride Channel by Alteration of Its Anion Selectivity. *Science* **1991**, *253* (5016), 202–205.
47. Devuyst, O.; Christie, P. T.; Courtoy, P. J.; Beauwens, R.; Thakker, R. V., Intra-renal and subcellular distribution of the human chloride channel, CLC-5, reveals a pathophysiological basis for Dent's disease. *Hum. Mol. Genet.* **1999**, *8* (2), 247–257.
48. (a) Scott, D. A.; Wang, R.; Kreman, T. M.; Sheffield, V. C.; Karniski, L. P., The Pendred syndrome gene encodes a chloride-iodide transport protein. *Nat. Genet.* **1999**, *21* (4), 440–443; (b) Yoshida, A.; Taniguchi, S.; Hisatome, I.; Royaux, I. E.; Green, E. D.; Kohn, L. D.; Suzuki, K., Pendrin is an iodide-specific apical porter responsible for iodide efflux from thyroid cells. *J. Clin. Endocrinol. Metab.* **2002**, *87* (7), 3356–3361.
49. Kornak, U.; Kasper, D.; Bosl, M. R.; Kaiser, E.; Schweizer, M.; Schulz, A.; Friedrich, W.; Delling, G.; Jentsch, T. J., Loss of the ClC-7 chloride channel leads to osteopetrosis in mice and man. *Cell* **2001**, *104* (2), 205–215.
50. Kaplan, R. S., Structure and function of mitochondrial anion transport proteins. *J. Membr. Biol.* **2001**, *179* (3), 165–183.
51. (a) Schneider, H. J., Binding Mechanisms in Supramolecular Complexes. *Angew. Chem. Int. Ed.* **2009**, *48* (22), 3924–3977; (b) Schneider, H. J.; Yatsimirsky, A. K.,

- Selectivity in supramolecular host–guest complexes. *Chem. Soc. Rev.* **2008**, *37* (2), 263–277.
52. (a) de Silva, A. P.; Gunaratne, H. Q. N.; Gunnlaugsson, T.; Huxley, A. J. M.; McCoy, C. P.; Rademacher, J. T.; Rice, T. E., Signaling recognition events with fluorescent sensors and switches. *Chem. Rev.* **1997**, *97* (5), 1515–1566; (b) Basabe-Desmonts, L.; Reinhoudt, D. N.; Crego-Calama, M., Design of fluorescent materials for chemical sensing. *Chem. Soc. Rev.* **2007**, *36* (6), 993–1017; (c) Gunnlaugsson, T.; Glynn, M.; Tocci, G. M.; Kruger, P. E.; Pfeffer, F. M., Anion recognition and sensing in organic and aqueous media using luminescent and colorimetric sensors. *Coord. Chem. Rev.* **2006**, *250* (23–24), 3094–3117.
 53. (a) Arnendola, V.; Bonizzoni, M.; Esteban-Gomez, D.; Fabbrizzi, L.; Licchelli, M.; Sancenon, F.; Taglietti, A., Some guidelines for the design of anion receptors. *Coord. Chem. Rev.* **2006**, *250* (11–12), 1451–1470; (b) Lankshear, M. D.; Beer, P. D., Interweaving anion templation. *Acc. Chem. Res.* **2007**, *40* (8), 657–668; (c) Schmidtchen, F. P., Artificial Host Molecules for the Sensing of Anions. In *Anion Sensing*, Stibor, I., Ed. Springer Berlin / Heidelberg: 2005; Vol. 255, pp 379–390.
 54. (a) Llinares, J. M.; Powell, D.; Bowman-James, K., Ammonium based anion receptors. *Coord. Chem. Rev.* **2003**, *240* (1–2), 57–75; (b) García-España, E.; Díaz, P.; Llinares, J. M.; Bianchi, A., Anion coordination chemistry in aqueous solution of polyammonium receptors. *Coord. Chem. Rev.* **2006**, *250* (23–24), 2952–2986.
 55. Davis, A. P.; Joos, J. B., Steroids as organising elements in anion receptors. *Coord. Chem. Rev.* **2003**, *240* (1–2), 143–156.
 56. Tamaru, S.; Hamachi, I., Recent Progress of Phosphate Derivatives Recognition Utilizing Artificial Small Molecular Receptors in Aqueous Media. In *Recognition of Anions*, Vilar, R., Ed. Springer Berlin / Heidelberg: 2008; Vol. 129, pp 95–125.
 57. (a) Conway, S. J.; Miller, G. J., Biology-enabling inositol phosphates, phosphatidylinositol phosphates and derivatives. *Nat. Prod. Rep.* **2007**, *24* (4), 687–707; (b) Irvine, R. F.; Schell, M. J., Back in the water: The return of the inositol phosphates. *Nat. Rev. Mol. Cell Biol.* **2001**, *2* (5), 327–338; (c) Best, M. D.; Zhang, H. L.; Prestwich, G. D., Inositol polyphosphates, diphosphoinositol polyphosphates and phosphatidylinositol polyphosphate lipids: Structure, synthesis, and development of probes for studying biological activity. *Nat. Prod. Rep.* **2010**, *27* (10), 1403–1430.
 58. Streb, H.; Irvine, R. F.; Berridge, M. J.; Schulz, I., Release of Ca²⁺ from a Nonmitochondrial Intracellular Store in Pancreatic Acinar-Cells by Inositol-1,4,5-Trisphosphate. *Nature* **1983**, *306* (5938), 67–69.
 59. (a) Carrasco, S.; Merida, I., Diacylglycerol, when simplicity becomes complex. *Trends Biochem. Sci.* **2007**, *32* (1), 27–36; (b) Gomez-Fernandez, J. C.; Corbalan-Garcia, S., Diacylglycerols, multivalent membrane modulators. *Chem. Phys. Lipids* **2007**, *148* (1), 1–25; (c) Sakane, F.; Imai, S.; Kai, M.; Yasuda, S.; Kanoh, H., Diacylglycerol kinases: Why so many of them? *Biochim. Biophys. Acta, Mol. Cell Biol. Lipids* **2007**, *1771* (7), 793–806.

60. (a) Berridge, M. J., Inositol Trisphosphate and Calcium Signaling. *Nature* **1993**, *361* (6410), 315–325; (b) Foskett, J. K.; White, C.; Cheung, K. H.; Mak, D. O. D., Inositol Trisphosphate Receptor Ca^{2+} Release Channels. *Physiol. Rev.* **2007**, *87* (2), 593–658; (c) Joseph, S. K., The inositol triphosphate receptor family. *Cell. Signalling* **1996**, *8* (1), 1–7; (d) Mikoshiba, K., IP_3 receptor/ Ca^{2+} channel: from discovery to new signaling concepts. *J. Neurochem.* **2007**, *102* (5), 1426–1446.
61. Niikura, K.; Metzger, A.; Anslyn, E. V., Chemosensor ensemble with selectivity for inositol-trisphosphate. *J. Am. Chem. Soc.* **1998**, *120* (33), 8533–8534.
62. Aoki, S.; Zulkefeli, M.; Shiro, M.; Kohsako, M.; Takeda, K.; Kimura, E., A Luminescence Sensor of Inositol 1,4,5-Triphosphate and Its Model Compound by Ruthenium-Templated Assembly of a Bis(Zn^{2+} -Cyclen) Complex Having a 2,2'-Bipyridyl Linker. *J. Am. Chem. Soc.* **2005**, *127* (25), 9129–9139.
63. Oh, D. J.; Ahn, K. H., Fluorescent sensing of IP_3 with a trifurcate Zn(II)-containing chemosensing ensemble system. *Org. Lett.* **2008**, *10* (16), 3539–3542.
64. Butterfield, S. M.; Tran, D. H.; Zhang, H.; Prestwich, G. D.; Matile, S., Fluorometric detection of inositol phosphates and the activity of their enzymes with synthetic pores: Discrimination of IP_7 and IP_6 and phytate sensing in complex matrices. *J. Am. Chem. Soc.* **2008**, *130* (11), 3270–3271.
65. (a) Cheley, S.; Gu, L. Q.; Bayley, H., Stochastic sensing of nanomolar inositol 1,4,5-trisphosphate with an engineered pore. *Chem. Biol.* **2002**, *9* (7), 829–838; (b) Luzzi, V.; Murtazina, D.; Allbritton, N. L., Characterization of a biological detector cell for quantitation of inositol 1,4,5-trisphosphate. *Anal. Biochem.* **2000**, *277* (2), 221–227; (c) Morii, T.; Sugimoto, K.; Makino, K.; Otsuka, M.; Imoto, K.; Mori, Y., A new fluorescent biosensor for inositol trisphosphate. *J. Am. Chem. Soc.* **2002**, *124* (7), 1138–1139.
66. (a) Morey, J.; Orell, M.; Barcelo, M. A.; Deya, P. M.; Costa, A.; Ballester, P., A 'naked-eye' chemosensor system for phytate. *Tetrahedron Lett.* **2004**, *45* (6), 1261–1265; (b) Oh, D. J.; Han, M. S.; Ahn, K. H., Metal-containing trifurcate chemosensing ensemble for phytate. *Supramol. Chem.* **2007**, *19* (4-5), 315–320.
67. (a) Bencini, A.; Bianchi, A.; Burguete, M. I.; García-España, E.; Luis, S. V.; Ramirez, J. A., Remarkable Shape Selectivity in the Molecular Recognition of Carboxylate Anions in Aqueous-Solution. *J. Am. Chem. Soc.* **1992**, *114* (5), 1919–1920; (b) Bencini, A.; Bianchi, A.; Burguete, M. I.; Dapporto, P.; Domenech, A.; García-España, E.; Luis, S. V.; Paoli, P.; Ramirez, J. A., Selective Recognition of Carboxylate Anions by Polyammonium Receptors in Aqueous-Solution - Criteria for Selectivity in Molecular Recognition. *J. Chem. Soc., Perkin Trans. 2* **1994**, (3), 569–577.
68. (a) Lewis, W. G.; Green, L. G.; Grynszpan, F.; Radic, Z.; Carlier, P. R.; Taylor, P.; Finn, M. G.; Sharpless, K. B., Click chemistry in situ: Acetylcholinesterase as a reaction vessel for the selective assembly of a femtomolar inhibitor from an array of building blocks. *Angew. Chem. Int. Ed.* **2002**, *41* (6), 1053–1057; (b) Kolb, H. C.; Finn, M. G.; Sharpless, K. B., Click chemistry: Diverse chemical function from a few good reactions. *Angew. Chem. Int. Ed.* **2001**, *40* (11), 2004–2021; (c) Rostovtsev, V. V.; Green, L. G.; Fokin, V. V.; Sharpless, K. B., A stepwise Huisgen

- cycloaddition process: Copper(I)-catalyzed regioselective "ligation" of azides and terminal alkynes. *Angew. Chem. Int. Ed.* **2002**, *41* (14), 2596–2599.
69. Prasuhn Jr., D. E.; Yeh, R. M.; Obenaus, A.; Manchester, M.; Finn, M. G., Viral MRI contrast agents: coordination of Gd by native virions and attachment of Gd complexes by azide–alkyne cycloaddition. *Chem. Commun.* **2007**, (12), 1269–1271.
 70. Wolfbeis, O. S., The click reaction in the luminescent probing of metal ions, and its implications on biolabeling techniques. *Angew. Chem. Int. Ed.* **2007**, *46* (17), 2980–2982.
 71. Hua, Y. R.; Flood, A. H., Click chemistry generates privileged CH hydrogen-bonding triazoles: the latest addition to anion supramolecular chemistry. *Chem. Soc. Rev.* **2010**, *39* (4), 1262–1271.
 72. Kim, S. K.; Seo, D.; Han, S. J.; Son, G.; Lee, I. J.; Lee, C.; Lee, K. D.; Yoon, J., A new imidazolium acridine derivative as fluorescent chemosensor for pyrophosphate and dihydrogen phosphate. *Tetrahedron* **2008**, *64* (27), 6402–6405.
 73. Fenniri, H.; Hosseini, M. W.; Lehn, J. M., Molecular recognition of NADP(H) and ATP by macrocyclic polyamines bearing acridine groups. *Helv. Chim. Acta* **1997**, *80* (3), 786–803.
 74. Carole, D. G.; Michel, D. M.; Julien, C.; Florence, D.; Anna, N.; Séverine, J.; Gérard, D.; Pierre, T.-D.; Jean-Pierre, G., Synthesis and antileishmanial activities of 4,5-di-substituted acridines as compared to their 4-mono-substituted homologues. *Bioorg. Med. Chem.* **2005**, *13* (19), 5560–5568.
 75. Chiron, J.; Galy, J.-P., Reactivity of the Acridine Ring: One-Pot Regioselective Single and Double Bromomethylation of Acridine and Some Derivatives. *Synlett* **2003**, (15), 2349–2350.
 76. Hwang, S.; Cha, W.; Meyerhoff, M. E., Polymethacrylates with a Covalently Linked Cu^{II}–Cyclen Complex for the In Situ Generation of Nitric Oxide from Nitrosothiols in Blood. *Angew. Chem. Int. Ed.* **2006**, *45* (17), 2745–2748.
 77. Pokorski, J. K.; Miller Jenkins, L. M.; Feng, H.; Durell, S. R.; Bai, Y.; Appella, D. H., Introduction of a Triazole Amino Acid into a Peptoid Oligomer Induces Turn Formation in Aqueous Solution. *Org. Lett.* **2007**, *9* (12), 2381–2383.
 78. (a) Gong, D. H.; Bostic, H. E.; Smith, M. D.; Best, M. D., Synthesis of Modular Headgroup Conjugates Corresponding to All Seven Phosphatidylinositol Polyphosphate Isomers for Convenient Probe Generation. *Eur. J. Org. Chem.* **2009**, (24), 4170–4179; (b) Gong, D. H.; Smith, M. D.; Manna, D.; Bostic, H. E.; Cho, W. H.; Best, M. D., Microplate-Based Characterization of Protein–Phosphoinositide Binding Interactions Using a Synthetic Biotinylated Headgroup Analogue. *Bioconjugate Chem.* **2009**, *20* (2), 310–316.
 79. Ziegler, T.; Hermann, C., Synthesis of novel multidentate carbohydrate–triazole ligands. *Tetrahedron Lett.* **2008**, *49* (13), 2166–2169.
 80. (a) Saxon, E.; Armstrong, J. I.; Bertozzi, C. R., A "traceless" Staudinger ligation for the chemoselective synthesis of amide bonds. *Org. Lett.* **2000**, *2* (14), 2141–2143; (b) Saxon, E.; Bertozzi, C. R., Cell surface engineering by a modified Staudinger

- reaction. *Science* **2000**, *287* (5460), 2007–2010; (c) Kohn, M.; Breinbauer, R., The Staudinger ligation - A gift to chemical biology. *Angew. Chem. Int. Ed.* **2004**, *43* (24), 3106–3116.
81. Spencer, T. A.; Wang, P. Z.; Li, D. S.; Russel, J. S.; Blank, D. H.; Huuskonen, J.; Fielding, P. E.; Fielding, C. J., Benzophenone-containing cholesterol surrogates: synthesis and biological evaluation. *J. Lipid Res.* **2004**, *45* (8), 1510–1518.
 82. (a) Golden, R.; Stock, L. M., Dissociation constants of 8-substituted 9,10-ethanoanthracene-1-carboxylic acids and related compounds. Evidence for the field model for the polar effect. *J. Am. Chem. Soc.* **1972**, *94* (9), 3080–3088; (b) Guillard, R.; Lopez, M. A.; Tabard, A.; Richard, P.; Lecomte, C.; Brandes, S.; Hutchison, J. E.; Collman, J. P., Synthesis and Characterization of Novel Cobalt Aluminum Cofacial Porphyrins - 1st Crystal and Molecular-Structure of a Heterobimetallic Biphenylene Pillared Cofacial Diporphyrin. *J. Am. Chem. Soc.* **1992**, *114* (25), 9877–9889.
 83. (a) Katz, H. E., 1,8-Anthracenediethynylbis(catechol boronate): A Bidentate Lewis Acid on a Novel Framework. *J. Org. Chem.* **1989**, *54* (9), 2179–2183; (b) Vögtle, F.; Koch, H.; Rissanen, K., Pinzettenförmige Kohlenwasserstoffe (Tweezer-Shaped Hydrocarbons). *Chem. Ber.* **1992**, *125* (9), 2129–2135.
 84. Pauvert, M.; Laine, P.; Jonas, M.; Wiest, O., Toward an artificial oxidative DNA photolyase. *J. Org. Chem.* **2004**, *69* (2), 543–548.
 85. (a) Atkins, T. J.; Richman, J. E.; Oettle, W. F., Macrocyclic Polyamines - 1,4,7,10,13,16-Hexaazacyclooctadecane. *Org. Synth.* **1988**, *50-9*, 652–662; (b) Micheloni, M.; Paoletti, P.; Bianchi, A., 1,4,7,10,13,16,19-Heptaazacycloheneicosane. A large, potentially dinucleating polyazacycloalkane. Synthesis and equilibria between hydrogen and copper(II) ions. *Inorg. Chem.* **1985**, *24* (22), 3702–3704; (c) Stones, G.; Tripoli, R.; McDavid, C. L.; Roux-Duplatre, K.; Kennedy, A. R.; Sherrington, D. C.; Gibson, C. L., Investigation of macrocyclisation routes to 1,4,7-triazacyclononanes: efficient syntheses from 1,2-ditosylamides. *Org. Biomol. Chem.* **2008**, *6* (2), 374–384.
 86. (a) Fukuyama, T.; Jow, C. K.; Cheung, M., 2-Nitrobenzenesulfonamides and 4-Nitrobenzenesulfonamides - Exceptionally Versatile Means for Preparation of Secondary-Amines and Protection of Amines. *Tetrahedron Lett.* **1995**, *36* (36), 6373–6374; (b) Siaugue, J. M.; Segat-Dioury, F.; Favre-Reguillon, A.; Madic, C.; Foos, J.; Guy, A., An efficient synthesis of pyridine containing triaza-macrocyclic triacetate ligand and luminescence properties of its europium(III) complex. *Tetrahedron Lett.* **2000**, *41* (39), 7443–7446; (c) Siaugue, J. M.; Segat-Dioury, F.; Sylvestre, I.; Favre-Reguillon, A.; Foos, J.; Madic, C.; Guy, A., Regioselective synthesis of *N*-functionalized 12-membered azapyridinomacrocycles bearing trialkylcarboxylic acid side chains. *Tetrahedron* **2001**, *57* (22), 4713–4718; (d) Kim, B. M.; So, S. M.; Choi, H. J., A concise, modular synthesis of chiral peraza-macrocycles using chiral aziridines. *Org. Lett.* **2002**, *4* (6), 949–952; (e) Burguete, M. I.; Escuder, B.; García-España, E.; Luis, S. V.; Miravet, J. F., Polyaza[*n*](1,4)naphthalenophanes and polyaza[*n*](9,10)anthracenophanes. *Tetrahedron* **2002**, *58* (14), 2839–2846.

87. Richman, J. E.; Atkins, T. J., Nitrogen Analogs of Crown Ethers. *J. Am. Chem. Soc.* **1974**, *96* (7), 2268–2270.
88. Zhang, Z. B.; Mikkola, S.; Lonnberg, H., Preparation of hexaaza and heptaaza macrocycles functionalized with a single aminoalkyl pendant arm. *Org. Biomol. Chem.* **2003**, *1* (5), 854–858.
89. Skerlj, R. T.; Nan, S. Q.; Zhou, Y. X.; Bridger, G. J., Facile synthesis of a selectively protected triazamacrocycle. *Tetrahedron Lett.* **2002**, *43* (42), 7569–7571.
90. Herges, R.; Dikmans, A.; Jana, U.; Kohler, F.; Jones, P. G.; Dix, I.; Fricke, T.; Konig, B., Design of a neutral macrocyclic ionophore: Synthesis and binding properties for nitrate and bromide anions. *Eur. J. Org. Chem.* **2002**, (17), 3004–3014.
91. Desroches, C.; Lopes, C.; Kessler, V.; Parola, S., Design and synthesis of multifunctional thiacalixarenes and related metal derivatives for the preparation of sol–gel hybrid materials with non-linear optical properties. *Dalton Trans.* **2003**, (10), 2085–2092.
92. Aucagne, V.; Leigh, D. A.; Lock, J. S.; Thomson, A. R., Rotaxanes of Cyclic Peptides. *J. Am. Chem. Soc.* **2006**, *128* (6), 1784–1785.
93. Taveras, A. G.; Remiszewski, S. W.; Doll, R. J.; Cesarz, D.; Huang, E. C.; Kirschmeier, P.; Pramanik, B. N.; Snow, M. E.; Wang, Y. S.; del Rosario, J. D.; Vibulbhan, B.; Bauer, B. B.; Brown, J. E.; Carr, D.; Catino, J.; Evans, C. A.; Girijavallabhan, V.; Heimark, L.; James, L.; Liberles, S.; Nash, C.; Perkins, L.; Senior, M. M.; Tzarbopoulos, A.; Ganguly, A. K.; Aust, R.; Brown, E.; Delisle, D.; Fuhrman, S.; Hendrickson, T.; Kissinger, C.; Love, R.; Sisson, W.; Villafranca, E.; Webber, S. E., Ras Oncoprotein Inhibitors: The Discovery of Potent, Ras Nucleotide Exchange Inhibitors and the Structural Determination of a Drug–Protein Complex. *Bioorg. Med. Chem.* **1997**, *5* (1), 125–133.
94. Lipton, M. F.; Sorensen, C. M.; Sadler, A. C.; Shapiro, R. H., Convenient Method for the Accurate Estimation of Concentrations of Alkylolithium Reagents. *J. Organomet. Chem.* **1980**, *186* (2), 155–158.
95. Burchat, A. F.; Chong, J. M.; Nielsen, N., Titration of alkylolithiums with a simple reagent to a blue endpoint. *J. Organomet. Chem.* **1997**, *542* (2), 281–283.
96. Xu, Y.; Smith, M. D.; Geer, M. F.; Pellechia, P. J.; Brown, J. C.; Wibowo, A. C.; Shimizu, L. S., Thermal Reaction of a Columnar Assembled Diacetylene Macrocycle. *J. Am. Chem. Soc.* **2010**, *132* (15), 5334–5335.
97. House, H. O.; Koepsell, D.; Jaeger, W., Derivatives of 1,8-Diphenylanthracene. *J. Org. Chem.* **1973**, *38* (6), 1167–1173.
98. (a) Mattingly, P. G., Mono-Protected Diamines - N^{α} -*tert*-Butoxycarbonyl α,ω -Alkanediamine Hydrochlorides from Amino-Alcohols. *Synthesis* **1990**, (4), 366–368; (b) Isomura, S.; Wirsching, P.; Janda, K. D., An immunotherapeutic program for the treatment of nicotine addiction: Hapten design and synthesis. *J. Org. Chem.* **2001**, *66* (12), 4115–4121; (c) Forbes, C. C.; DiVittorio, K. M.; Smith, B. D., Bolaamphiphiles promote phospholipid translocation across vesicle membranes. *J. Am. Chem. Soc.* **2006**, *128* (28), 9211–9218; (d) Bergbreiter, D. E.; Osburn, P. L.;

- Li, C. M., Soluble polymer-supported catalysts containing azo dyes. *Org. Lett.* **2002**, *4* (5), 737–740; (e) Vera, M.; Almontassir, A.; Rodriguez-Galan, A.; Puiggali, J., Synthesis and characterization of a new degradable poly(ester amide) derived from 6-amino-1-hexanol and glutaric acid. *Macromolecules* **2003**, *36* (26), 9784–9796; (f) Dutton, J. K.; Knox, J. H.; Radisson, X.; Ritchie, H. J.; Ramage, R., Synthesis of 17*H*-tetrabenz[*a,c,g,i*]fluorene derivatives as chiral selectors for enantiomeric separation by HPLC on porous graphitised carbon. *J. Chem. Soc., Perkin Trans. 1* **1995**, (20), 2581–2587.
99. (a) Kuykendall, D. W.; Anderson, C. A.; Zimmerman, S. C., Hydrogen-Bonded DeUG·DAN Heterocomplex: Structure and Stability and a Scalable Synthesis of DeUG with Reactive Functionality. *Org. Lett.* **2009**, *11* (1), 61–64; (b) Srinivasan, R.; Tan, L. P.; Wu, H.; Yang, P.-Y.; Kalesh, K. A.; Yao, S. Q., High-throughput synthesis of azide libraries suitable for direct "click" chemistry and in situ screening. *Org. Biomol. Chem.* **2009**, *7* (9), 1821–1828; (c) Coutrot, F.; Busseron, E., Controlling the Chair Conformation of a Mannopyranose in a Large-Amplitude [2]Rotaxane Molecular Machine. *Chem. Eur. J.* **2009**, *15* (21), 5186–5190.
100. (a) Heslin, J. C.; Moody, C. J., Rhodium Carbenoid Mediated Cyclisations. Part 2. Synthesis of Cyclic Ethers. *J. Chem. Soc., Perkin Trans. 1* **1988**, (6), 1417–1423; (b) Man, H.-W.; Hiscox, W. C.; Matteson, D. S., A Highly Enantioselective and Diastereoselective Synthesis of Cyclobutanes via Boronic Esters. *Org. Lett.* **1999**, *1* (3), 379–382; (c) Vicker, N.; Burgess, L.; Chuckowree, I. S.; Dodd, R.; Folkes, A. J.; Hardick, D. J.; Hancox, T. C.; Miller, W.; Milton, J.; Sohal, S.; Wang, S.; Wren, S. P.; Charlton, P. A.; Dangerfield, W.; Liddle, C.; Mistry, P.; Stewart, A. J.; Denny, W. A., Novel Angular Benzophenazines: Dual Topoisomerase I and Topoisomerase II Inhibitors as Potential Anticancer Agents. *J. Med. Chem.* **2002**, *45* (3), 721–739.
101. Garrett, R.; Grisham, C. M., *Biochemistry*. 3rd ed.; Thomson Brooks/Cole: Belmont, CA, 2005.
102. Dwek, R. A.; Butters, T. D., Introduction: Glycobiology-understanding the language and meaning of carbohydrates. *Chem. Rev.* **2002**, *102* (2), 283–284.
103. Yamamoto, T.; Seino, Y.; Fukumoto, H.; Koh, G.; Yano, H.; Inagaki, N.; Yamada, Y.; Inoue, K.; Manabe, T.; Imura, H., Over-Expression of Facilitative Glucose Transporter Genes in Human Cancer. *Biochem. Biophys. Res. Commun.* **1990**, *170* (1), 223–230.
104. Baxter, P.; Goldhill, J.; Hardcastle, J.; Hardcastle, P. T.; Taylor, C. J., Enhanced Intestinal Glucose and Alanine Transport in Cystic Fibrosis. *Gut* **1990**, *31* (7), 817–820.
105. (a) de Marchi, S.; Cecchin, E.; Basile, A.; Proto, G.; Donadon, W.; Jengo, A.; Schinella, D.; Jus, A.; Villalta, D.; Depaoli, P.; Santini, G.; Tesio, F., Close Genetic-Linkage between Hla and Renal Glycosuria. *Am. J. Nephrol.* **1984**, *4* (5), 280–286; (b) Elsas, L. J.; Rosenberg, L. E., Familial Renal Glycosuria - a Genetic Reappraisal of Hexose Transport by Kidney and Intestine. *J. Clin. Invest.* **1969**, *48* (10), 1845–1854.

106. Fedorak, R. N.; Gershon, M. D.; Field, M., Induction of Intestinal Glucose Carriers in Streptozocin-Treated Chronically Diabetic Rats. *Gastroenterology* **1989**, *96* (1), 37–44.
107. Peracaula, R.; Tabares, G.; Royle, L.; Harvey, D. J.; Dwek, R. A.; Rudd, P. M.; de Llorens, R., Altered glycosylation pattern allows the distinction between prostate-specific antigen (PSA) from normal and tumor origins. *Glycobiology* **2003**, *13* (6), 457–470.
108. (a) Tabares, G.; Radcliffe, C. M.; Barrabes, S.; Ramirez, M.; Aleixandre, R. N.; Hoesel, W.; Dwek, R. A.; Rudd, P. M.; Peracaula, R.; de Llorens, R., Different glycan structures in prostate-specific antigen from prostate cancer sera in relation to seminal plasma PSA. *Glycobiology* **2006**, *16* (2), 132–145; (b) Tabares, G.; Jung, K.; Reiche, J.; Stephan, C.; Lein, M.; Peracaula, R.; de Llorens, R.; Hoesel, W., Free PSA forms in prostatic tissue and sera of prostate cancer patients: Analysis by 2-DE and western blotting of immunopurified samples. *Clin. Biochem.* **2007**, *40* (5-6), 343–350.
109. Lorand, J. P.; Edwards, J. O., Polyol Complexes and Structure of the Benzeneboronate Ion. *J. Org. Chem.* **1959**, *24* (6), 769–774.
110. Martell, A. E.; Smith, R. M., *Critical Stability Constants*. Plenum Press: New York, NY, 1974.
111. Hartley, J. H.; Phillips, M. D.; James, T. D., Saccharide-accelerated hydrolysis of boronic acid imines. *New J. Chem.* **2002**, *26* (9), 1228–1237.
112. Bosch, L. I.; Fyles, T. M.; James, T. D., Binary and ternary phenylboronic acid complexes with saccharides and Lewis bases. *Tetrahedron* **2004**, *60* (49), 11175–11190.
113. (a) Branch, G. E. K.; Yabroff, D. L.; Bettman, B., The dissociation constants of the chlorophenyl and phenetyl boric acid. *J. Am. Chem. Soc.* **1934**, *56*, 937–941; (b) Soundararajan, S.; Badawi, M.; Kohlrust, C. M.; Hageman, J. H., Boronic Acids for Affinity-Chromatography - Spectral Methods for Determinations of Ionization and Diol-Binding Constants. *Anal. Biochem.* **1989**, *178* (1), 125–134; (c) Juillard, J.; Gueguen, N., Sur la Dissociation de Quelques Acides Arylboriques en Solvants Mixtes Eau–Methanol (On the Dissociation of Some Arylboronic Acids in Water–Methanol Solvent Mixtures). *Comp. Rend. Acad. Sci. C.* **1967**, *264* (3), 259–261.
114. Wulff, G., Selective Binding to Polymers Via Covalent Bonds - the Construction of Chiral Cavities as Specific Receptor-Sites. *Pure Appl. Chem.* **1982**, *54* (11), 2093–2102.
115. Wiskur, S. L.; Lavigne, J. J.; Ait-Haddou, H.; Lynch, V.; Chiu, Y. H.; Canary, J. W.; Anslyn, E. V., pK_a values and geometries of secondary and tertiary amines complexed to boronic acids - Implications for sensor design. *Org. Lett.* **2001**, *3* (9), 1311–1314.
116. (a) Zhu, L.; Shabbir, S. H.; Gray, M.; Lynch, V. M.; Sorey, S.; Anslyn, E. V., A structural investigation of the N–B interaction in an *o*-(*N,N*-dialkylaminomethyl)arylboronate system. *J. Am. Chem. Soc.* **2006**, *128* (4), 1222–1232; (b) Yang, W.; He, H.; Drueckhammer, D. G., Computer-guided design in

- molecular recognition: Design and synthesis of a glucopyranose receptor. *Angew. Chem. Int. Ed.* **2001**, *40* (9), 1714–1718.
117. (a) Matteson, D. S., α -Amido boronic acids: A synthetic challenge and their properties as serine protease inhibitors. *Med. Res. Rev.* **2008**, *28* (2), 233–246; (b) Snow, R. J.; Bachovchin, W. W.; Barton, R. W.; Campbell, S. J.; Coutts, S. J.; Freeman, D. M.; Gutheil, W. G.; Kelly, T. A.; Kennedy, C. A.; Krolikowski, D. A.; Leonard, S. F.; Pargellis, C. A.; Tong, L.; Adams, J., Studies on Proline Boronic Acid Dipeptide Inhibitors of Dipeptidyl Peptidase IV: Identification of a Cyclic Species Containing a B–N Bond. *J. Am. Chem. Soc.* **1994**, *116* (24), 10860–10869.
118. (a) Halamek, J.; Wollenberger, U.; Stocklein, W.; Scheller, F. W., Development of a biosensor for glycated hemoglobin. *Electrochim. Acta* **2007**, *53* (3), 1127–1133; (b) Liu, S. Q.; Wollenberger, U.; Katterle, M.; Scheller, F. W., Ferroceneboronic acid-based amperometric biosensor for glycated hemoglobin. *Sens. Actuators, B* **2006**, *113* (2), 623–629; (c) Adamczyk, M.; Chen, Y. Y.; Johnson, D. D.; Mattingly, P. G.; Moore, J. A.; Pan, Y.; Reddy, R. E., Chemiluminescent acridinium-9-carboxamide boronic acid probes: Application to a homogenous glycated hemoglobin assay. *Bioorg. Med. Chem. Lett.* **2006**, *16* (5), 1324–1328.
119. Halamek, J.; Wollenberger, U.; Stocklein, W. F. M.; Warsinke, A.; Scheller, F. W., Signal amplification in Immunoassays using Labeling via boronic acid binding to the sugar moiety of immunoglobulin G: Proof of concept for glycated hemoglobin. *Anal. Lett.* **2007**, *40* (7), 1434–1444.
120. Dowlut, M.; Hall, D. G., An improved class of sugar-binding boronic acids, soluble and capable of complexing glycosides in neutral water. *J. Am. Chem. Soc.* **2006**, *128* (13), 4226–4227.
121. (a) Springsteen, G.; Wang, B. H., Alizarin Red S as a general optical reporter for studying the binding of boronic acids with carbohydrates. *Chem. Commun.* **2001**, (17), 1608–1609; (b) Springsteen, G.; Wang, B. H., A detailed examination of boronic acid–diol complexation. *Tetrahedron* **2002**, *58* (26), 5291–5300.
122. Sørensen, M. D.; Martins, R.; Hindsgaul, O., Assessing the terminal glycosylation of a glycoprotein by the naked eye. *Angew. Chem. Int. Ed.* **2007**, *46* (14), 2403–2407.
123. Wilson, G. S.; Hu, Y. B., Enzyme based biosensors for in vivo measurements. *Chem. Rev.* **2000**, *100* (7), 2693–2704.
124. Takahashi, S.; Anzai, J., Phenylboronic Acid Monolayer-Modified Electrodes Sensitive to Sugars. *Langmuir* **2005**, *21* (11), 5102–5107.
125. (a) Hanzal-Bayer, M. F.; Hancock, J. F., Lipid rafts and membrane traffic. *FEBS Lett.* **2007**, *581* (11), 2098–2104; (b) Jacobson, K.; Mouritsen, O. G.; Anderson, R. G. W., Lipid rafts: at a crossroad between cell biology and physics. *Nat. Cell Biol.* **2007**, *9* (1), 7–14; (c) Zaas, D. W.; Duncan, M.; Rae Wright, J.; Abraham, S. N., The role of lipid rafts in the pathogenesis of bacterial infections. *Biochim. Biophys. Acta, Mol. Cell Res.* **2005**, *1746* (3), 305–313.
126. (a) Wu, P. G.; Brand, L., Resonance Energy Transfer: Methods and Applications. *Anal. Biochem.* **1994**, *218* (1), 1–13; (b) Clegg, R. M., Fluorescence resonance

- energy transfer. *Curr. Opin. Biotechnol.* **1995**, *6* (1), 103–110; (c) Jares-Erijman, E. A.; Jovin, T. M., FRET imaging. *Nat. Biotechnol.* **2003**, *21* (11), 1387–1395; (d) Sapsford, K. E.; Berti, L.; Medintz, I. L., Materials for fluorescence resonance energy transfer analysis: Beyond traditional donor-acceptor combinations. *Angew. Chem. Int. Ed.* **2006**, *45* (28), 4562–4588.
127. Rao, M.; Mayor, S., Use of Forster's resonance energy transfer microscopy to study lipid rafts. *Biochim. Biophys. Acta, Mol. Cell Res.* **2005**, *1746* (3), 221–233.
 128. Taliani, S.; Simorini, F.; Sergianni, V.; La Motta, C.; Da Settimo, F.; Cosimelli, B.; Abignente, E.; Greco, G.; Novellino, E.; Rossi, L.; Gremigni, V.; Spinetti, F.; Chelli, B.; Martini, C., New Fluorescent 2-Phenylindolglyoxylamide Derivatives as Probes Targeting the Peripheral-Type Benzodiazepine Receptor: Design, Synthesis, and Biological Evaluation. *J. Med. Chem.* **2006**, *50* (2), 404–407.
 129. Yang, H.; Vasudevan, S.; Oriakhi, C. O.; Shields, J.; Carter, R. G., Scalable Synthesis of Lissamine Rhodamine B Sulfonyl Chloride and Incorporation of Xanthene Derivatives onto Polymer Supports. *Synthesis* **2008**, (6), 957–961.
 130. Huh, Y.; Chung, A.; Erickson, D., Surface enhanced Raman spectroscopy and its application to molecular and cellular analysis. *Microfluid Nanofluid* **2009**, *6* (3), 285–297.
 131. Nie, S. M.; Emery, S. R., Probing single molecules and single nanoparticles by surface-enhanced Raman scattering. *Science* **1997**, *275* (5303), 1102–1106.
 132. (a) Kanayama, N.; Kitano, H., Interfacial recognition of sugars by boronic acid-carrying self-assembled monolayer. *Langmuir* **2000**, *16* (2), 577–583; (b) Chen, H. X.; Lee, M.; Lee, J.; Kim, J. H.; Gal, Y. S.; Hwang, Y. H.; An, W. G.; Koh, K., Formation and characterization of self-assembled phenylboronic acid derivative monolayers toward developing monosaccharide sensing-interface. *Sensors* **2007**, *7* (8), 1480–1495.
 133. Han, C.-C.; Balakumar, R., Mild and efficient methods for the conversion of benzylic bromides to benzylic thiols. *Tetrahedron Lett.* **2006**, *47* (47), 8255–8258.
 134. Banfield, S. C.; Omori, A. T.; Leisch, H.; Hudlicky, T., Unexpected Reactivity of the Burgess Reagent with Thiols: Synthesis of Symmetrical Disulfides. *J. Org. Chem.* **2007**, *72* (13), 4989–4992.
 135. (a) Kneeland, D. M.; Ariga, K.; Lynch, V. M.; Huang, C. Y.; Anslyn, E. V., Bis(alkylguanidinium) receptors for phosphodiester: effect of counterions, solvent mixtures, and cavity flexibility on complexation. *J. Am. Chem. Soc.* **1993**, *115* (22), 10042–10055; (b) Guy, J.; Caron, K.; Dufresne, S.; Michnick, S. W.; Skene; Keillor, J. W., Convergent Preparation and Photophysical Characterization of Dimaleimide Dansyl Fluorogens: Elucidation of the Maleimide Fluorescence Quenching Mechanism. *J. Am. Chem. Soc.* **2007**, *129* (39), 11969–11977.
 136. Simon, S.; Petrásek, J., Why plants need more than one type of auxin. *Plant Science* **2011**, *180* (3), 454–460.
 137. Ross, J. J.; O'Neill, D. P.; Wolbang, C. M.; Symons, G. M.; Reid, J. B., Auxin–Gibberellin Interactions and Their Role in Plant Growth. *J. Plant Growth Regul.* **2001**, *20* (4), 336–353.

138. Grossmann, K., Auxin herbicides: current status of mechanism and mode of action. *Pest Manage. Sci.* **2010**, *66* (2), 113–120.
139. Woodward, A. W.; Bartel, B., Auxin: Regulation, Action, and Interaction. *Ann. Bot.* **2005**, *95* (5), 707–735.
140. Dayan, F. E.; Duke, S. O.; Grossmann, K., Herbicides as Probes in Plant Biology. *Weed Sci.* **2010**, *58* (3), 340–350.
141. Grossmann, K., Mediation of Herbicide Effects by Hormone Interactions. *J. Plant Growth Regul.* **2003**, *22* (1), 109–122.
142. Grossmann, K., News from Old Compounds: The Mode of Action of Auxin Herbicides. In *Chemistry of Crop Protection*, Wiley-VCH Verlag GmbH & Co. KGaA: Weinheim, Germany, 2004; pp 131–142.
143. Gianfagna, T. J., Natural and synthetic growth regulators and their use in horticultural and agronomic crops. In *Plant Hormones: Physiology, Biochemistry and Molecular Biology*, 2nd ed.; Davies, P. J., Ed. Kluwer Academic Publishers: Dordrecht, Netherlands, 1995; pp 751–773.
144. Krikorian, A. D., Hormones in tissue culture and micropropagation. In *Plant Hormones: Physiology, Biochemistry, and Molecular Biology*, 2nd ed.; Davies, P. J., Ed. Kluwer Academic Publishers: Dordrecht, Netherlands, 1995; pp 774–796.
145. Farrimond, J. A.; Elliott, M. C.; Clack, D. W., Charge separation as a component of the structural requirements for hormone activity. *Nature* **1978**, *274* (5669), 401–402.
146. Romano, C. P.; Cooper, M. L.; Klee, H. J., Uncoupling Auxin and Ethylene Effects in Transgenic Tobacco and Arabidopsis Plants. *Plant Cell* **1993**, *5* (2), 181–189.
147. Strachan, S. D.; Casini, M. S.; Heldreth, K. M.; Scocas, J. A.; Nissen, S. J.; Bukun, B.; Lindenmayer, R. B.; Shaner, D. L.; Westra, P.; Brunk, G., Vapor Movement of Synthetic Auxin Herbicides: Aminocyclopyrachlor, Aminocyclopyrachlor-Methyl Ester, Dicamba, and Aminopyralid. *Weed Sci.* **2010**, *58* (2), 103–108.
148. Behrens, M. R.; Mutlu, N.; Chakraborty, S.; Dumitru, R.; Jiang, W. Z.; LaVallee, B. J.; Herman, P. L.; Clemente, T. E.; Weeks, D. P., Dicamba Resistance: Enlarging and Preserving Biotechnology-Based Weed Management Strategies. *Science* **2007**, *316* (5828), 1185–1188.
149. Grossmann, K., Quinclorac belongs to a New Class of Highly Selective Auxin Herbicides. *Weed Sci.* **1998**, *46* (6), 707–716.
150. Miyaura, N.; Yanagi, T.; Suzuki, A., The Palladium-Catalyzed Cross-Coupling Reaction of Phenylboronic Acid with Haloarenes in the Presence of Bases. *Synth. Commun.* **1981**, *11* (7), 513–519.
151. (a) Patrick, D. A.; Bakunov, S. A.; Bakunova, S. M.; Kumar, E. V. K. S.; Lombardy, R. J.; Jones, S. K.; Bridges, A. S.; Zhirnov, O.; Hall, J. E.; Wenzler, T.; Brun, R.; Tidwell, R. R., Synthesis and in Vitro Antiprotozoal Activities of Dicationic 3,5-Diphenylisoxazoles. *J. Med. Chem.* **2007**, *50* (10), 2468–2485; (b) Lim, S.; Harris, K. J.; Stefany, D.; Gardner, C. J.; Cao, B.; Boffey, R.; Gillespy, T. A.; Aguiar, J. C.; Hunt, H. J.; Dechaux, E. A. 2,6-Substituted-4-Monosubstituted Amino-Pyrimidine as Prostaglandin D2 Receptor Antagonists. World Patent WO/2006/044732, Apr 27, 2006.

152. Agejas-Chicharro, F. J.; Dressman, B. A.; Sonia, G. S.; Henry, S. S.; Martinez Perez, J. A.; Massey, S. M.; Monn, J. A.; Zia-Ebrahimi, M. S. Pyridyl Derivatives and Their Use as mGlu5 Receptor Antagonists. World Patent WO/2005/094822, Oct 13, 2005.
153. (a) Thompson, W. J.; Gaudino, J., A general synthesis of 5-arylNicotines. *J. Org. Chem.* **1984**, *49* (26), 5237–5243; (b) Potter, B. V. L.; Dowden, J.; Galione, A.; Guse, A. H.; Flügel, A. Therapeutics Comprising Pyridinium Derivatives. World Patent WO/2007/132179, Nov 22, 2007.
154. (a) Kiran, Y. B.; Ikeda, R.; Sakai, N.; Konakahara, T., Single-Step Conversion of Electron-Deficient Aldehydes into the Corresponding Esters in Aqueous Alcohols in the Presence of Iodine and Sodium Nitrite. *Synthesis* **2010**, *2010* (2), 276–282; (b) Collantes, E. M.; Schwarz, J. B. Pyridinyl Amides for the Treatment of CNS and Metabolic Disorders. World Patent WO/2009/098576, Aug 13, 2009; (c) Giblin, G. M. P.; Hall, A.; Hurst, D. N.; Kilford, I. R.; Lewell, X. Q.; Naylor, A.; Novelli, R. (2-((2-Alkoxy)-phenyl)-cyclopent-1-enyl) Aromatic Carbo and Heterocyclic Acid and Derivatives. World Patent WO/2003/084917, Oct 16, 2003.
155. Bossenmaier, B.; Friess, T.; Juchem, R.; Kling, L.; Kolm, I.; Krell, H.-W.; Von Hirschheydt, T.; Voss, E. Phenylpyridine Derivatives. U.S. Patent 7429605, Sep 30, 2008.
156. Oxford, A. W.; Davis, R. J.; Coleman, R. A.; Clark, K. L.; Clark, D. E.; Harris, N. V.; Fenton, G.; Hynd, G.; Stuttle, K. A. J.; Sutton, J. M.; Ashton, M. R.; Boyd, E. A.; Brunton, S. A. EP2 Receptor Agonists. World Patent WO/2005/080367, Sep 1, 2005.
157. Setliff, F. L.; Huie, W. R., Some Methyl 2,5-Dihalonicotines and 5,6-Dihalonicotines. *J. Chem. Eng. Data* **1981**, *26* (3), 332–333.
158. (a) Khan, F. A.; Choudhury, S., An Efficient Synthesis of Substituted meta-Halophenols and Their Methyl Ethers: Insight into the Reaction Mechanism. *Eur. J. Org. Chem.* **2010**, *2010* (15), 2954–2970; (b) Lee, Y.; Kelly, M. J., Solid-phase synthesis of phenols and pyridinones via arylboronation/oxidation protocol using aryl bromides. *Tetrahedron Lett.* **2006**, *47* (28), 4897–4901.
159. (a) Tullberg, E.; Schacher, F.; Peters, D.; Frejd, T., Solvent-Free Heck–Jeffery Reactions under Ball-Milling Conditions Applied to the Synthesis of Unnatural Amino Acids Precursors and Indoles. *Synthesis* **2006**, *2006* (7), 1183–1189; (b) Brown, A. D.; Bunnage, M. E.; Butcher, K. J.; Glossop, P. A.; James, K.; Lane, C. A. L.; Lewthwaite, R. A.; Price, D. A. Compounds Having beta-Agonist Activity. World Patent WO/2005/092841, Oct 6, 2005.
160. Noar, J. B.; Banaszczyk, M. G.; Millan, V.; Valkirs, G.; Buechler, K. F.; Noland, B. Reactive Heterocyclic Derivatives and Methods for Their Synthesis and Use. World Patent WO/2007/075931, Jul 5, 2007.
161. Thompson III, L. A.; Shi, J.; Zusi, C. F.; Dee, M. F.; Macor, J. E. Indole Acetic Acid Acyl Guanidines as beta-Secretase Inhibitors. U.S. Patent 7601751, Oct 13, 2009.
162. Wardman, P.; Folkes, L. K.; Dachs, G. U.; Rossiter, S.; Greco, O. Use of Indole-3-Acetic Acid Derivatives in Medicine. World Patent WO/2002/002110, Jan 10, 2002.

163. (a) Sestanjan, K. *N*[(2-Naphthalenyl)thioxomethyl]glycine Derivatives. U.S. Patent 4447452, May 8, 1984; (b) Dawson, M. I.; Hobbs, P. D.; Derdzinski, K. A. Naphthyl or Tetrahydronaphthyl-Substituted Naphthoic Acid and Derivatives. U.S. Patent 4454341, Jun 12, 1984; (c) Klein, E. S.; Johnson, A. T.; Standeven, A. M.; Beard, R. L.; Gillett, S. J.; Duong, T. T.; Nagpal, S.; Vuligonda, V.; Teng, M.; Chandraratna, R. A. Synthesis and Use of Retinoid Compounds Having Negative Hormone and/or Antagonist Activities. U.S. Patent 5958954, Sep 28, 1999; (d) Shishido, Y.; Nakao, K.; Nagayama, S.; Tanaka, H.; Duncton, M. A. J.; Cox, M.; Kincaid, J.; Sahasrabudhe, K.; Estiarte-Martinez, M. d. L. A. Amide Derivatives as Ion-Channel Ligands and Pharmaceutical Compositions And Methods of Using the Same. World Patent WO/2007/133637, Nov 22, 2007.
164. Wright, W. B.; Brabander, H. J., The Preparation of 3-Chlorobenzo[*b*]thiophene Derivatives from Cinnamic Acids. *J. Heterocycl. Chem.* **1971**, *8* (5), 711–714.
165. (a) Kato, T.; Mizoshita, N.; Kishimoto, K., Functional liquid-crystalline assemblies: Self-organized soft materials. *Angew. Chem. Int. Ed.* **2006**, *45* (1), 38–68; (b) Oshovsky, G. V.; Reinhoudt, D. N.; Verboom, W., Supramolecular chemistry in water. *Angew. Chem. Int. Ed.* **2007**, *46* (14), 2366–2393.
166. (a) El-Kaderi, H. M.; Hunt, J. R.; Mendoza-Cortes, J. L.; Cote, A. P.; Taylor, R. E.; O'Keeffe, M.; Yaghi, O. M., Designed synthesis of 3D covalent organic frameworks. *Science* **2007**, *316* (5822), 268–272; (b) Tranchemontagne, D. J.; Ni, N.; O'Keeffe, M. O.; Yaghi, O. M., Reticular chemistry of metal-organic polyhedra. *Angew. Chem. Int. Ed.* **2008**, *47*, 5136–5147; (c) Eddaoudi, M.; Moler, D. B.; Li, H. L.; Chen, B. L.; Reineke, T. M.; O'Keeffe, M.; Yaghi, O. M., Modular chemistry: Secondary building units as a basis for the design of highly porous and robust metal-organic carboxylate frameworks. *Acc. Chem. Res.* **2001**, *34* (4), 319–330; (d) Leininger, S.; Olenyuk, B.; Stang, P. J., Self-assembly of discrete cyclic nanostructures mediated by transition metals. *Chem. Rev.* **2000**, *100* (3), 853–907; (e) Seidel, S. R.; Stang, P. J., High-symmetry coordination cages via self-assembly. *Acc. Chem. Res.* **2002**, *35* (11), 972–983; (f) Yaghi, O. M.; O'Keeffe, M.; Ockwig, N. W.; Chae, H. K.; Eddaoudi, M.; Kim, J., Reticular synthesis and the design of new materials. *Nature* **2003**, *423* (6941), 705–714.
167. Beeren, S. R.; Sanders, J. K. M., History and Principles of Dynamic Combinatorial Chemistry. In *Dynamic Combinatorial Chemistry*, Wiley-VCH Verlag GmbH & Co. KGaA: Weinheim, Germany, 2010; pp 1–22.
168. Corbett, P. T.; Leclaire, J.; Vial, L.; West, K. R.; Wietor, J. L.; Sanders, J. K. M.; Otto, S., Dynamic combinatorial chemistry. *Chem. Rev.* **2006**, *106* (9), 3652–3711.
169. Meyer, C. D.; Joiner, C. S.; Stoddart, J. F., Template-directed synthesis employing reversible imine bond formation. *Chem. Soc. Rev.* **2007**, *36* (11), 1705–1723.
170. (a) Hwang, J.-J.; Tour, J. M., Combinatorial synthesis of oligo(phenylene ethynylene)s. *Tetrahedron* **2002**, *58* (52), 10387–10405; (b) Serwinski, P. R.; Lahti, P. M., Limits of Delocalization in Through-Conjugated Dinitrenes: Aromatization or Bond Formation? *Org. Lett.* **2003**, *5* (12), 2099–2102.
171. Wuts, P. G. M.; Greene, T. W., *Greene's protective groups in organic synthesis*. 4th ed.; Wiley-Interscience: Hoboken, N.J., 2007.

172. Djuric, S.; Venit, J.; Magnus, P., Silicon in Synthesis - Stabase Adducts - a New Primary Amine Protecting Group - Alkylation of Ethyl Glycinate. *Tetrahedron Lett.* **1981**, 22 (19), 1787–1790.
173. Balasubramaniam, S.; Aidhen, I. S., The Growing Synthetic Utility of the Weinreb Amide. *Synthesis* **2008**, (23), 3707–3738.
174. Fukuzaki, E.; Takahashi, N.; Imai, S.; Nishide, H.; Rajca, A., Synthesis of Dendritic, Non-Kekulé-, and Nondisjoint-type Triphenylmethanes Terminated with Galvinoxyl Radicals. *Polym. J.* **2005**, 37 (4), 284–293.
175. (a) Liu, X.; Liu, Y.; Li, G.; Warmuth, R., One-Pot, 18-Component Synthesis of an Octahedral Nanocontainer Molecule. *Angew. Chem. Int. Ed.* **2006**, 45 (6), 901–904; (b) Liu, X.; Warmuth, R., A simple one-pot multicomponent synthesis of an octahedral nanocontainer molecule. *Nat. Protoc.* **2007**, 2 (5), 1288–1296.
176. (a) Flavin, K.; Chaur, M. N.; Echegoyen, L.; Giordani, S., Functionalization of Multilayer Fullerenes (Carbon Nano-Onions) using Diazonium Compounds and “Click” Chemistry. *Org. Lett.* **2010**, 12 (4), 840–843; (b) Chui, C. H.; Wang, Q.; Chow, W. C.; Yuen, M. C. W.; Wong, K. L.; Kwok, W. M.; Cheng, G. Y. M.; Wong, R. S. M.; Tong, S. W.; Chan, K. W.; Lau, F. Y.; Lai, P. B. S.; Lam, K. H.; Fabbri, E.; Tao, X. M.; Gambari, R.; Wong, W. Y., 5-(Dimethylamino)-*N*-(4-ethynylphenyl)-1-naphthalenesulfonamide as a novel bifunctional antitumor agent and two-photon induced bio-imaging probe. *Chem. Commun.* **2010**, 46 (20), 3538–3540; (c) Gottardo, C.; Kraft, T. M.; Hossain, M. S.; Zawada, P. V.; Muchall, H. M., Linear free-energy correlation analysis of the electronic effects of the substituents in the Sonogashira coupling reaction. *Can. J. Chem.* **2008**, 86 (5), 410–415; (d) Aujard, I.; Baltaze, J.-P.; Baudin, J.-B.; Cogné, E.; Ferrage, F.; Jullien, L.; Perez, É.; Prévost, V.; Qian, L. M.; Ruel, O., Tetrahedral Onsager Crosses for Solubility Improvement and Crystallization Bypass. *J. Am. Chem. Soc.* **2001**, 123 (34), 8177–8188; (e) Hortholary, C.; Coudret, C., An Approach to Long and Unsubstituted Molecular Wires: Synthesis of Redox-Active, Cationic Phenylethynyl Oligomers Designed for Self-Assembled Monolayers. *J. Org. Chem.* **2003**, 68 (6), 2167–2174; (f) Erdélyi, M.; Gogoll, A., Rapid Homogeneous-Phase Sonogashira Coupling Reactions Using Controlled Microwave Heating. *J. Org. Chem.* **2001**, 66 (12), 4165–4169; (g) Anderson, S., Phenylene Ethynylene Pentamers for Organic Electroluminescence. *Chem. Eur. J.* **2001**, 7 (21), 4706–4714; (h) Tour, J. M.; Rawlett, A. M.; Kozaki, M.; Yao, Y.; Jagessar, R. C.; Dirk, S. M.; Price, D. W.; Reed, M. A.; Zhou, C.-W.; Chen, J.; Wang, W.; Campbell, I., Synthesis and Preliminary Testing of Molecular Wires and Devices. *Chem. Eur. J.* **2001**, 7 (23), 5118–5134; (i) Ishizaki, M.; Hoshino, O., Unprecedented Cesium and Potassium Fluorides Catalyzed Trialkylsilylation and Tributylstannylation of Terminal Alkynes with Trifluoromethyl-Trialkylsilanes and -Tributylstannane. *Tetrahedron* **2000**, 56 (45), 8813–8819.
177. (a) Flatt, A. K.; Yao, Y.; Maya, F.; Tour, J. M., Orthogonally Functionalized Oligomers for Controlled Self-Assembly. *J. Org. Chem.* **2004**, 69 (5), 1752–1755; (b) Tripiet, R.; Hollenstein, M.; Elhabiri, M.; Chauvin, A.-S.; Zucchi, G.; Piguet, C.; Bünzli, J.-C. G., Self-Assembled Triple-Stranded Lanthanide Dimetallic Helicates

- with a Ditopic Ligand Derived from Bis(benzimidazole)pyridine and Featuring an (4-Isothiocyanatophenyl)ethynyl Substituent. *Helv. Chim. Acta* **2002**, *85* (7), 1915–1929; (c) Kosynkin, D. V.; Tour, J. M., Phenylene Ethynylene Diazonium Salts as Potential Self-Assembling Molecular Devices. *Org. Lett.* **2001**, *3* (7), 993–995; (d) Melissaris, A. P.; Litt, M. H., A Simple and Economical Synthetic Route to p-Ethynylaniline and Ethynyl-Terminated Substrates. *J. Org. Chem.* **1994**, *59* (19), 5818–5821; (e) Grob, C. A.; Pfaendler, H. R., Solvolysis of α -Bromo-p-aminostyrene. Mesomeric vinyl cations, Part IV. *Helv. Chim. Acta* **1971**, *54* (7), 2060–2068.
178. (a) Soomro, S. A.; Schulz, A.; Meier, H., Dendrimers with peripheral stilbene chromophores. *Tetrahedron* **2006**, *62* (34), 8089–8094; (b) Worlikar, S. A.; Larock, R. C., Palladium-Catalyzed One-Step Synthesis of Isoindole-1,3-diones by Carbonylative Cyclization of o-Halobenzoates and Primary Amines. *J. Org. Chem.* **2008**, *73* (18), 7175–7180.
179. Leonard, K. A.; Hall, J. P.; Nelen, M. I.; Davies, S. R.; Gollnick, S. O.; Camacho, S.; Oseroff, A. R.; Gibson, S. L.; Hilf, R.; Detty, M. R., A Selenopyrylium Photosensitizer for Photodynamic Therapy Related in Structure to the Antitumor Agent AA1 with Potent in Vivo Activity and No Long-Term Skin Photosensitization. *J. Med. Chem.* **2000**, *43* (23), 4488–4498.
180. (a) Yamamoto, Y., The First General and Selective Palladium(II)-Catalyzed Alkoxyacylation of Arylboronates: Interplay among Benzoquinone-Ligated Palladium(0) Complex, Organoboron, and Alcohol Solvent. *Adv. Synth. Catal.* **2010**, *352* (2-3), 478–492; (b) Pardin, C.; Pelletier, J. N.; Lubell, W. D.; Keillor, J. W., Cinnamoyl Inhibitors of Tissue Transglutaminase. *J. Org. Chem.* **2008**, *73* (15), 5766–5775; (c) Sharma, S. K.; Tandon, M.; Lown, J. W., Synthesis of Geometrically Constrained Unsymmetrical Bis(polyamides) Related to the Antiviral Distamycin. *Eur. J. Org. Chem.* **2000**, *2000* (11), 2095–2103; (d) Gooßen, L. J.; Khan, B. A.; Fett, T.; Treu, M., Low-Pressure Hydrogenation of Arenecarboxylic Acids to Aryl Aldehydes. *Adv. Synth. Catal.* **2010**, *352* (13), 2166–2170; (e) Pelletier, G.; Bechara, W. S.; Charette, A. B., Controlled and Chemoselective Reduction of Secondary Amides. *J. Am. Chem. Soc.* **2010**, *132* (37), 12817–12819; (f) Srogl, J.; Voltrova, S., Copper/Ascorbic Acid Dyad as a Catalytic System for Selective Aerobic Oxidation of Amines. *Org. Lett.* **2009**, *11* (4), 843–845; (g) Tang, H.; Zhang, Z.; Cong, C.; Zhang, K., Synthesis of a novel β -diketone containing carbazole and 2,5-diphenyl-1,3,4-oxadiazole fragments. *Russ. J. Org. Chem.* **2009**, *45* (4), 559–563; (h) Grigorjeva, A.; Jirgensons, A.; Domracheva, I.; Yashchenko, E.; Shestakova, I.; Andrianov, V.; Kalvinsh, I., Synthesis of novel [1-aziridinyl-(hydroxyimino)methyl]arenes and their cytotoxic activity. *Chem. Heterocycl. Compd.* **2009**, *45* (2), 161–168; (i) Giménez, R.; Oriol, L.; Piñol, M.; Serrano, J. L.; Viñuales, A. I.; Fisher, T.; Stumpe, J., Synthesis and Properties of 2-Phenylbenzoxazole-Based Luminophores for in situ Photopolymerized Liquid-Crystal Films. *Helv. Chim. Acta* **2006**, *89* (2), 304–319; (j) Baillargeon, V. P.; Stille, J. K., Palladium-catalyzed formylation of organic halides with carbon monoxide and tin hydride. *J. Am. Chem. Soc.* **1986**, *108* (3), 452–461.

181. Nakatani, K.; Shirai, J.; Sando, S.; Saito, I., Guanine Specific DNA Cleavage by Photoirradiation of Dibenzoyldiazomethane–Oligonucleotide Conjugates. *J. Am. Chem. Soc.* **1997**, *119* (33), 7626–7635.
182. (a) Cousin, D.; Mann, J.; Nieuwenhuyzen, M.; van den Berg, H., A new approach to combretastatin D2. *Org. Biomol. Chem.* **2006**, *4* (1), 54–62; (b) Hon, Y.-S.; Lee, C.-F.; Chen, R.-J.; Szu, P.-H., Acetyltriphenylphosphonium bromide and its polymer-supported analogues as catalysts in protection and deprotection of alcohols as alkyl vinyl ethers. *Tetrahedron* **2001**, *57* (28), 5991–6001; (c) Kuramochi, Y.; Sandanayaka, A. S. D.; Satake, A.; Araki, Y.; Ogawa, K.; Ito, O.; Kobuke, Y., Energy Transfer Followed by Electron Transfer in a Porphyrin Macrocycle and Central Acceptor Ligand: A Model for a Photosynthetic Composite of the Light-Harvesting Complex and Reaction Center. *Chem. Eur. J.* **2009**, *15* (10), 2317–2327; (d) van der Linden, M.; Borsboom, J.; Kaspersen, F.; Kemperman, G., Asymmetric Synthesis of (*S*)-Mirtazapine: Unexpected Racemization through an Aromatic *ipso*-Attack Mechanism. *Eur. J. Org. Chem.* **2008**, *2008* (17), 2989–2997; (e) Wöll, D.; Smirnova, J.; Galetskaya, M.; Prykota, T.; Buhler, J.; Stengele, K. P.; Pfeleiderer, W.; Steiner, U. E., Intramolecular sensitization of photocleavage of the photolabile 2-(2-nitrophenyl)propoxycarbonyl (NPPOC) protecting group: Photoproducts and photokinetics of the release of nucleosides. *Chem. Eur. J.* **2008**, *14* (21), 6490–6497; (f) Barbasiewicz, M.; Małkosza, M., Intermolecular Reactions of Chlorohydrine Anions: Acetalization of Carbonyl Compounds under Basic Conditions. *Org. Lett.* **2006**, *8* (17), 3745–3748; (g) Chen, C.-T.; Weng, S.-S.; Kao, J.-Q.; Lin, C.-C.; Jan, M.-D., Stripping off Water at Ambient Temperature: Direct Atom-Efficient Acetal Formation between Aldehydes and Diols Catalyzed by Water-Tolerant and Recoverable Vanadyl Triflate. *Org. Lett.* **2005**, *7* (15), 3343–3346; (h) Lee, Y.; Silverman, R. B., Traceless Solid-Phase Synthesis of Chiral 3-Aryl β -Amino Acid Containing Peptides Using a Side-Chain-Tethered β -Amino Acid Building Block. *Org. Lett.* **2000**, *2* (3), 303–306.
183. (a) Deuss, P. J.; Popa, G.; Botting, C. H.; Laan, W.; Kamer, P. C. J., Highly Efficient and Site-Selective Phosphane Modification of Proteins through Hydrazone Linkage: Development of Artificial Metalloenzymes. *Angew. Chem. Int. Ed.* **2010**, *49* (31), 5315–5317; (b) Anderson, E.; Capon, B., Intramolecular nucleophilic assistance in reactions of acetals. *J. Chem. Soc., Perkin Trans. 2* **1972**, (5), 515–522.
184. Azzena, U.; Dettori, G.; Pisano, L.; Siotto, I., Reductive lithiation of 1,3-dimethyl-2-arylimidazolidines. *Tetrahedron* **2005**, *61* (13), 3177–3182.

Vita

Chi-Linh Do-Thanh (Đỗ Thanh, Chí Linh) was born in Aachen, West Germany, now Germany, in 1983. After growing up in Munich, the journey continued across the Atlantic to Richmond, Virginia, in 1997. He went on to attend the University of Virginia in Charlottesville, Virginia, where he obtained his B.S. in chemistry in 2005 despite speaking four languages and having absolute pitch hearing. He then enrolled in graduate studies at the University of Tennessee, Knoxville where he obtained his Ph.D. in organic chemistry under the guidance of Dr. Michael D. Best in May 2011 with zero sick days, and at the time of this writing, has yet to break a flask in his life.